The University of Nottingham
UNITED KINGDOM · CHINA · MALAYSIA
SCHOOL OF PHARMACY

SYNTHESIS AND BIOLOGICAL ACTIVITY OF NOVEL AND SELECTIVE MERCAPTOPYRUVATE SULFUR TRANSFERASE INHIBITORS

STUDENT

MAHA NASSER ALMEHAIZE

14341847

SUPERVISORS

DR BARRIE KELLAM

DR RICHARD ROBERTS

DR STEVE ALEXANDER

Abstract

Background

Hydrogen sulfide (H_2S) is now recognised as an endogenous gasotransmitter that regulates vascular, metabolic and inflammatory processes. One of its principal biosynthetic enzymes is 3-mercaptopyruvate sulfurtransferase (3MST), which generates H_2S and reactive persulfides in both mitochondria and cytosol. Dysregulation of the 3MST-H_2S pathway has been implicated in cancer, metabolic disease and redox signalling. The discovery of selective inhibitors of 3MST is therefore essential to enable pharmacological dissection of H_2S biology, in a manner analogous to the use of nitric oxide synthase inhibitors in defining the physiological roles of nitric oxide. Although the first selective 3MST inhibitors were reported in 2017, progress has been limited by the small number of available chemical tools and by issues of selectivity, reactivity and assay interference, which continue to complicate interpretation of biological data.

Aim

The aim of this thesis was to design, synthesise and biologically evaluate a focused library of novel 3MST inhibitors. A structure-guided approach was employed, in which commercially available chemical fragments were screened in silico against the 3MST active site using molecular docking to prioritise candidates with favourable predicted binding and synthetic tractability. Selected fragments were incorporated into a pyrimidinone-based scaffold to generate a series of mercaptoacetyl and mercaptoacetamide derivatives.

The resulting compounds were synthesised and evaluated using a fluorescence-based biochemical assay that measures enzymatic H_2S production. Comparative analysis with known inhibitors and reference compounds was used to assess inhibitory potency and selectivity.

Results

A total of 20 compounds were synthesised and evaluated for 3MST inhibition. A previous fluorescence-based screen in our laboratory had identified CDS004892 as a 3MST inhibitor, with an average IC_{50} of 7.92 µM, and this compound was used as a lead scaffold for the present study. In parallel, screening of commercially available compounds identified two additional 3MST inhibitors, NCC-00043864 and NCC-00065766, with IC_{50} values of 4.5 µM and 9.7 µM, respectively. From the newly synthesised series, four compounds, MNA1, MNA13, MNA20 and MNA23, displayed inhibitory activity with potencies comparable to those reported for the best literature 3MST inhibitors, which typically exhibit IC_{50} values in the range of 1.7 to 6.3 µM. Notably, MNA1 and MNA23 also showed selectivity profiles comparable to reference compounds, indicating preferential inhibition of 3MST over related enzymes.

Conclusion

These findings demonstrate that rational, structure-guided design combined with biochemical screening can yield novel, potent and selective 3MST inhibitors. The identification of both newly synthesised and commercially available inhibitors expands the currently limited repertoire of chemical tools available to investigate the 3MST–H_2S pathway. In particular, the discovery of selective inhibitors within the MNA series provides valuable starting points for the development of improved pharmacological tools. The compounds developed here provide a platform for further optimisation and biological evaluation, particularly in cell-based assays and mitochondria-specific contexts.

Publication arising from this work

Almaheize M, Alharthi S, Hemp P, Mattos J, van Leer M, Garle M, Alexander S, Roberts R. Effect of 3-mercaptopyruvate sulfurtransferase (3-MST) inhibitors on contractile responses in porcine coronary artery. Br J Pharmacol. 2025 Nov;182(22):5453-5468. doi: 10.1111/bph.70141. Epub 2025 Jul 18. PMID: 40682254.

Acknowledgements

I would like to express my deepest gratitude to my supervisors for their guidance, patience, and unwavering support throughout this PhD. Their expertise, encouragement, and belief in my work have been fundamental to the completion of this thesis, especially during the most challenging periods of my doctoral journey.

I am profoundly grateful to the Government of Saudi Arabia, through PSA University, for generously funding this PhD and making it possible for me to pursue my studies abroad. This support has not only enabled my academic training, but also allowed me to grow personally and professionally while undertaking this work far from home.

I owe heartfelt thanks to my family, whose love, trust, and encouragement gave me the confidence to follow this path. Their belief in my decision to study overseas sustained me through moments of doubt and distance, and I carry their support with me in everything I have achieved.

To my friends across the sea, who checked in on me daily and reminded me that I was never alone despite the distance, I am deeply thankful. Your messages, care, and constant presence provided comfort and strength when I needed it most. To my friends in Nottingham, thank you for making life brighter and more joyful during this journey. Your kindness, laughter, and companionship turned a demanding chapter of my life into one filled with warmth and unforgettable memories.

This thesis is not only the product of scientific work, but also of the many people who supported, believed in, and stood by me throughout this journey. To all of you, thank you.

Table of Contents

1. Chapter I General Introduction 9
1.1 Endogenous production of H_2S 11
1.2 3-Mercaptopyruvate sulfur transferase (3MST) 14
1.3 Mitochondria targeting agents 20
1.4 H_2S synthesising enzymes and cancer 23
1.5 H_2S producing enzymes and bacteria 24
1.6 Other indigenous sulfur species: sulphane sulfurs 26
1.7 Detection of H_2S 27
1.7.1 Signal Interference in Fluorescence-Based H_2S Assays 32
1.8 Inhibitors of H_2S producing enzymes 35
1.9 Crystal structure of 3MST 39
1.10 Aims of the Project 39
2. Chapter II Virtual Screening for 3MST Inhibitors 41
2.1 Background 41
2.1.1 DataWarrior 42
2.1.2 Fragment Fingerprint (FragFP) 43
2.1.3 AutoDock Vina 44
2.1.4 Specificity and Selectivity 45
2.1.5 Impact on Substrate Screening 46
2.1.6 Implications for Inhibitor Design 46
2.1.7 Structure-activity relationships (SAR) 48
2.2 Results 49
2.2.1 Screening for 3MST inhibitors via SF7-AM fluorescence probe 49
2.2.2 Virtual Screening and docking studies of 3MST inhibitors 55
2.2.3 Discussion 58
3. Chapter III 61
3.1 Synthesis and biological evaluation of novel 3MST Inhibitors 61
3.1.1 background 61
3.1.2 Design and synthesis rational 61
3.2 Chemistry 62
3.2.1 Synthesis of amide linker compounds 62
3.2.2 Synthesis of mercaptoacetyl-linker Compounds 63
3.2.3 Synthesis challenges and limitations 63
3.2.4 Suggested SAR 64

3.3 Biochemical investigations of 3MST Inhibitors 67
3.3.1 Background 67
3.3.2 Results and Discussion 67
4. Chapter IV: Discussion 89
4.1 High-Throughput Screening and Similarity Search Insights 90
4.2 Summary of Lead Compounds 90
4.3 Limitations and Future Directions 91
4.4 Sulphane sulfurs: Biochemical Relevance and Future Considerations 92
5. Experimental 94
5.1 Biological evaluation 94
5.1.1 Sources and preparation of drugs and reagents: 94
5.1.2 General principle of the biochemical assays used to evaluate H_2S enzyme inhibitors 95
5.1.3 General notes and optimisations 100
5.2 Chemistry Experimental Methods 109
5.2.1 General Experimental Information 109
5.2.2 Synthesis and Characterization of Target Compounds 112
5.3 Computational Studies 127
5.3.1 Source of Compounds for High-Throughput Screening and Computational Studies 127
5.3.2 Molecular Docking Studies 127
5.3.3 Analysis of Virtual Screening Results 128
5.3.4 Data warrior 128
6. References 129
7. Appendix 135

List of figures

Figure no.	page no.	Figure no.	page no.
Figure 1	19	Figure 34	86
Figure 2	20	Figure 35	87
Figure 3	25	Figure 36	88
Figure 4	37	Figure 37	89
Figure 5	39	Figure 38	90
Figure 6	40	Figure 39	90
Figure 7	42	Figure 40	91
Figure 8	43	Figure 41	91
Figure 9	44	Figure 42	92
Figure 10	45	Figure 43	93
Figure 11	53	Figure 44	93
Figure 12	55	Figure 45	94
Figure 13	55	Figure 46	94
Figure 14	56	Figure 47	101
Figure 15	57	Figure 48	102
Figure 16	59	Figure 49	103
Figure 17	60	Figure 50	103
Figure 18	61	Figure 51	107
Figure 19	62	Figure 52	108
Figure 20	63	Figure 53	109
Figure 21	69	Figure 54	109
Figure 22	72	Figure 55	110
Figure 23	74	Figure 56	110
Figure 24	75	Figure 57	111
Figure 25	75	Figure 58	111
Figure 26	76	Figure 59	112
Figure 27	76	Figure 60	112
Figure 28	77	Figure 61	114
Figure 29	78	Figure 62	116
Figure 30	79	Figure 63	117
Figure 31	83		
Figure 32	84		
Figure 33	85		

List of tables

Table 1 **Comparison of 3-MST Knockdown and Knockout Phenotypes**.....16
Table 2 Chemical structures of the MNA series and shows inhibitory effect on the enzymatic production of H2S via 3MST pathway in rat liver cytosol samples (n=3) using H_2S detection assay via SF7-AM fluorescence probe compared to control. Whereas 0% means complete inhibition. 74

Abbreviations

3MST: 3-mercaptopyruvate sulfur transferase

AOAA: aminooxyacetic acid

AVG: aminoethoxyvinylglycine

AzMC: 7-Azido-4-Methylcoumarin

BCA: b-cyano-L-alanine

CAT: cysteine aminotransferase

CBS: cystathionine β-synthase

CGL or CSE: cystathionine γ-lyase

CO: carbon monoxide

GSH: glutathione

H_2S: hydrogen sulfide

HA: hydroxylamine

LC: L-cysteine

MP: mercaptopyruvate

NaHS: sodium hydrosulfide

NO: nitric oxide

NOS: nitric oxide synthase

PAG propargylglycine

PLE: Pig liver esterase

PLP: pyridoxal-5'-phosphate

RLC: rat liver cytosol

TPP+: triphenylphosphonium

TUM1: tRNA thiouridin modification protein 1

VEGF: vascular endothelial growth factor

α-KG: α-ketoglutarate

1. Chapter I General Introduction

Historically, hydrogen sulfide (H_2S) has been known to be a highly toxic molecule and a dangerous environmental pollutant. It is a colourless and water-soluble gas with a distinguishable unpleasant odour of rotten eggs. The presence of H_2S in living organisms was perceived to be a mere metabolic by-product or a biomarker for enzymatic activity (Szabo, 2018). However, over two decades ago, it was discovered to be vital for the maintenance of normal physiological functions (Abe and Kimura, 1996). Currently, it is labelled as a 'gasotransmitter', the third recognised molecule of this kind following nitric oxide (NO) and carbon monoxide (CO)(Mustafa et al., 2009).

Similar to the other gasotransmitters, H_2S has the unique ability to travel through cell membranes without the aid of specific transporters (Riahi and Rowley, 2014). The amount of endogenous H_2S produced by a cell is estimated to have a sphere of action that involves more than 200 neighbouring cells (Cuevasanta et al., 2012). The effects of H_2S do not apply through a single receptor or pathway but are displayed upon several cell effectors in either a cell, tissue or a species dependent manner.

There is increasing literature regarding the beneficial effects of endogenous H_2S and its importance. An example of its earlier discovered effects is its action on vascular tone by regulating blood pressure and decreasing inflammation(Bhatia, 2005). Furthermore, H_2S was reported to prevent tissue oedema and inhibit the expression of leukocyte adhesion molecules. Cystathionine γ-lyase (one of H_2S producing enzymes) knockout mice showed a significant decrease in endothelial vasorelaxation and notable hypertension, supposedly due to decreased H_2S in those mice(Yang et al., 2008).

H_2S has also been shown to promote angiogenesis in vascular endothelial cells during chronic ischaemia, specifically by increasing extracellular kinase pathways that consequently induce vessel growth (Kimura, 2014a). Additionally, H_2S promotes development of primary or current endothelial cells causing induction of endothelial cell proliferation and migration, as well as being associated with signalling of vascular endothelial growth factor (VEGF) (Polhemus and Lefer, 2014).

The antioxidant effects of H_2S are considered to be of the most prominent beneficial cytoprotective mechanisms of this gasotransmitter (Whiteman et al., 2004); (Esechie et al., 2008). Antioxidation via H2S occurs through direct chemical reactions with oxidant molecules, or by stimulating intracellular antioxidant "master switches", or through activating *γ*-glutamylcysteine synthase and increasing glutathione levels in the cell (Xie et al., 2016).

H_2S modulates multiple signal transduction processes such as proinflammatory signal transduction mechanisms and intracellular calcium homeostasis (Nagai et al., 2004). Furthermore, H_2S activates the PI3K/Akt system, which promotes metabolism, proliferation , cell survival, growth and angiogenesis (Cai et al., 2007). H_2S also affects several other systems such as sirtuins, which are family of proteins that have a key role in regulating cellular homeostasis (Hu et al., 2015).

Persulphidation (also known as sulfhydration) is a H_2S-mediated process that modifies critical regulatory cysteines in ATP-sensitive potassium channels (K_{ATP} channels) and opens them (Zhao et al., 2001). H_2S-mediated persulphidation was also found to modulate an increasing number of enzymes and affects their catalytic activities (Nagy, 2015).

Transient receptor potential channels (TRP channels) in sensory neurons, urinary bladder, dorsal root ganglion, blood vessels, and other tissues, were reported to be activated by H_2S and consequently partakes in important functionalities (Hajna et al., 2016). Furthermore, H_2S was reported to inhibit the catalytic activity of cAMP and cGMP phosphodiesterases, and thereby increasing the levels of cAMP and cGMP in the cell and invoking all their biological functions (Andreadou et al., 2015).

The therapeutic benefits of hydrogen sulfide inhibition are multifaceted, encompassing its effects on oxidative stress, metabolic regulation, inflammatory responses, neuroprotection, and cardiovascular health. The ability to manipulate hydrogen sulfide levels presents a promising avenue for therapeutic interventions across a range of diseases. As research continues to elucidate the complex roles of hydrogen sulfide in human physiology, it is likely that new therapeutic strategies will emerge, harnessing the potential of hydrogen sulfide inhibition to improve health outcomes.

Oxidative stress is a condition characterized by excessive reactive oxygen species (ROS) that can lead to cellular damage and contribute to various diseases, including cardiovascular disorders and neurodegenerative diseases. Studies have shown that hydrogen sulfide can exert protective effects against oxidative stress by modulating mitochondrial function and enhancing antioxidant defences. For instance, moderate doses of hydrogen sulfide have been linked to improved mitochondrial respiration, which is crucial for maintaining cellular energy homeostasis and reducing oxidative damage (Carter & Morton, 2015). This protective mechanism is particularly relevant in conditions such as ischemia-reperfusion injury, where the restoration of blood flow can lead to a surge in ROS production (Bos et al., 2012).

In addition to its antioxidant properties, hydrogen sulfide inhibition has been associated with beneficial effects on metabolic regulation. Research indicates that hydrogen sulfide plays a role in the regulation of glucose metabolism and lipid homeostasis. In particular, it has been shown to influence insulin secretion and sensitivity, making it a potential target for therapeutic interventions in metabolic disorders such as type 2 diabetes (Carter & Morton, 2015). The modulation of hydrogen sulfide levels can therefore have significant implications for managing metabolic diseases, as it may help to restore normal metabolic function and prevent the progression of insulin resistance.

Furthermore, hydrogen sulfide inhibition has been explored in the context of inflammatory responses. The body produces hydrogen sulfide as part of its physiological processes, and its manipulation can have therapeutic implications for conditions characterized by systemic inflammation, such as sepsis. Inflammatory responses are often accompanied by an imbalance between pro-inflammatory and anti-inflammatory mediators, leading to tissue damage and organ dysfunction. By inhibiting hydrogen sulfide production, it may be possible to modulate these inflammatory pathways and promote a more balanced response, thereby

improving outcomes in patients suffering from inflammatory conditions (Rivers-Auty & Bhatia, 2013).

The therapeutic potential of hydrogen sulfide inhibition extends to its role in neuroprotection. Neurodegenerative diseases, such as Alzheimer's and Parkinson's, are characterized by oxidative stress and inflammation, both of which can be exacerbated by elevated levels of hydrogen sulfide. Inhibiting hydrogen sulfide production may help to alleviate these pathological processes, thereby offering a novel approach to neuroprotection. Studies have suggested that targeting hydrogen sulfide pathways could enhance neuronal survival and function, particularly in the context of neuroinflammatory conditions (Carter & Morton, 2015).

Moreover, the therapeutic benefits of hydrogen sulfide inhibition are not limited to metabolic and inflammatory disorders. There is growing evidence to suggest that it may also play a role in cardiovascular health. Hydrogen sulfide has been implicated in the regulation of vascular tone and blood pressure, and its inhibition may help to prevent or treat conditions such as hypertension and atherosclerosis. By modulating hydrogen sulfide levels, it may be possible to improve endothelial function and reduce the risk of cardiovascular events (Carter & Morton, 2015).

Following the description of all the important physiological effects of H_2S and its vital role in the human body, researchers and pharmaceutical companies started investigating mechanisms to enhance H_2S production. H_2S-releasing prodrugs are currently being developed as novel therapeutics, which is not surprising, considering all the known wide-ranging effects of H_2S, which could be exploited in multiple pathological systems (Zheng et al., 2015). Said effects include potent antioxidation, antiapoptotic, anti-inflammatory, metabolic, vasoactive, and cytoprotective actions (Módis et al., 2014). Generally, the potent anti-oxidant effects of H_2S production is especially attractive. Consequently, manipulating H_2S enzymatic production by developing H_2S prodrugs could be exploited in various pathological conditions such as acute myocardial infarction, stroke, diabetes, arthritis, peripheral artery disease and metabolic syndrome (Caliendo et al., 2010).

1.1 Endogenous production of H_2S

H_2S production in mammalian cells follows both enzymatic and non-enzymatic pathways. Glycolysis and reduction of elemental sulfur, thiosulphate or glutathione are examples of non-enzymatic mechanisms for H_2S production (Kolluru et al., 2013). Initially, two enzymes were reported to produce H_2S in the cytosol, cystathionine β-synthase (CBS) and cystathionine γ-lyase (CGL or CSE), which are not expressed ubiquitously, rather, each enzyme is unique in some of the locations as reported so far (Bełtowski, 2015). For instance, CBS was reported to be expressed in the brain, liver, pancreas, kidney, ileum, uterus and placenta (Kimura, 2014b). H_2S is synthesised in the CBS pathway via the β-elimination reaction of cysteine or β-replacement reaction of condensed cysteine with homocysteine (Chen et al., 2004). CBS is allosterically activated by S-adenoxylmethionine, enhancing the production of H_2S, while CO and NO decrease its activity and subsequent H_2S production (Kimura, 2014a). CBS and CSE are

both haemoproteins located in the cytoplasm. Regarding CSE expression in the body, it was reported to be expressed in the liver, kidney, portal vein, ileum, uterus and placenta (Kimura, 2011). Notably, CSE is not expressed in the brain. Cysteine is also a substrate of CSE, undergoing α,β-elimination to produce H_2S (Aitken and Kirsch, 2005). In homocysteinemia, when homocysteine is higher than the normal physiological levels, H_2S is mainly produced by a,c-elimination and c-replacement reactions of homocysteine (Kimura, 2015).

It was previously thought that CSE and CBS are the sole enzymatic producers of H_2S in the body, until brains of CBS knockout mice were reported to produce H_2S, which lead to the discovery of the third enzyme 3-mercaptopyruvate sulfur transferase (3MST) and cysteine aminotransferase (CAT) soon after (see Figure 1) (Shibuya et al., 2009a). CAT is responsible for the production of 3-mercaptopyruvate (3MP) by catalysing both L-cysteine and α-ketoglutarate, 3MP then produces H_2S via 3MST. In addition to L-cysteine, D-cysteine undergoes peroxisomal D-amino acid oxidase production of 3MP (Shibuya et al., 2009b).

Rhodanese, also known as thiosulphate sulfur transferase (TST), is an enzyme located in the mitochondria of various mammalian species (Saidu, 2004). It performs essential functions and is mostly known for its cyanide detoxification (Wróbel et al., 2004). It also detoxifies H_2S through trans-sulfuration and shares high amino acid sequence identity (58%) with 3MST, with both belonging to the rhodanese/Cdc25 phosphatase superfamily (Bordo and Bork, 2002). Thus, many compounds that exert their actions on 3MST are also likely to affect rhodanese, for example, tetrathionate, which raises concerns regarding selectivity of 3MST inhibitors.

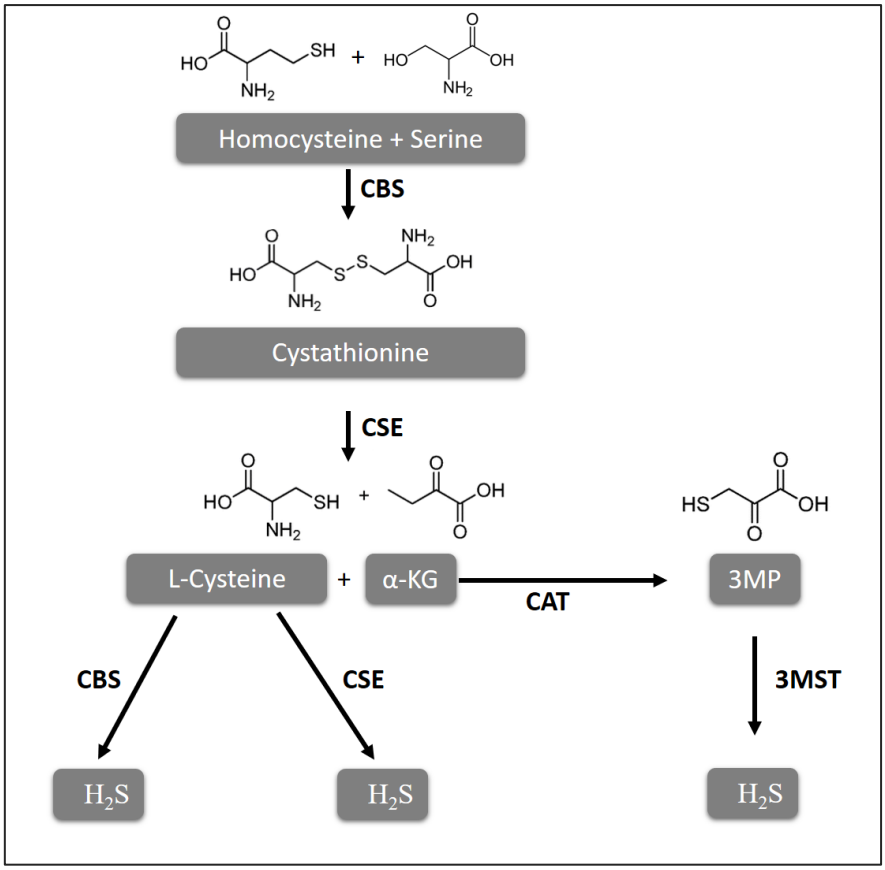


Figure 1 ***Enzymatic Synthesis of Hydrogen Sulfide****. Hydrogen sulfide (H2S) is generated endogenously in mammals via enzymatic mechanisms, three main enzymes are responsible for H2S generation throughout the body: cystathionine β-synthase (CBS), cystathionine γ-lyase (CGL or CSE) and 3-mercaptopyruvate sulfurtransferase (3MST). (3MST) produces H2S through via generating 3-mercaptopyruvate (3MP) from α-ketoglutarate (α-KG) by cysteine aminotransferase (CAT). (CBS) produces H2S via generating cystathionine from homocysteine and L-cysteine from cystathione. (CSE) produces H2S through a reaction involving the generation of L-cysteine from cystathionine. (Source: Personal collection)*

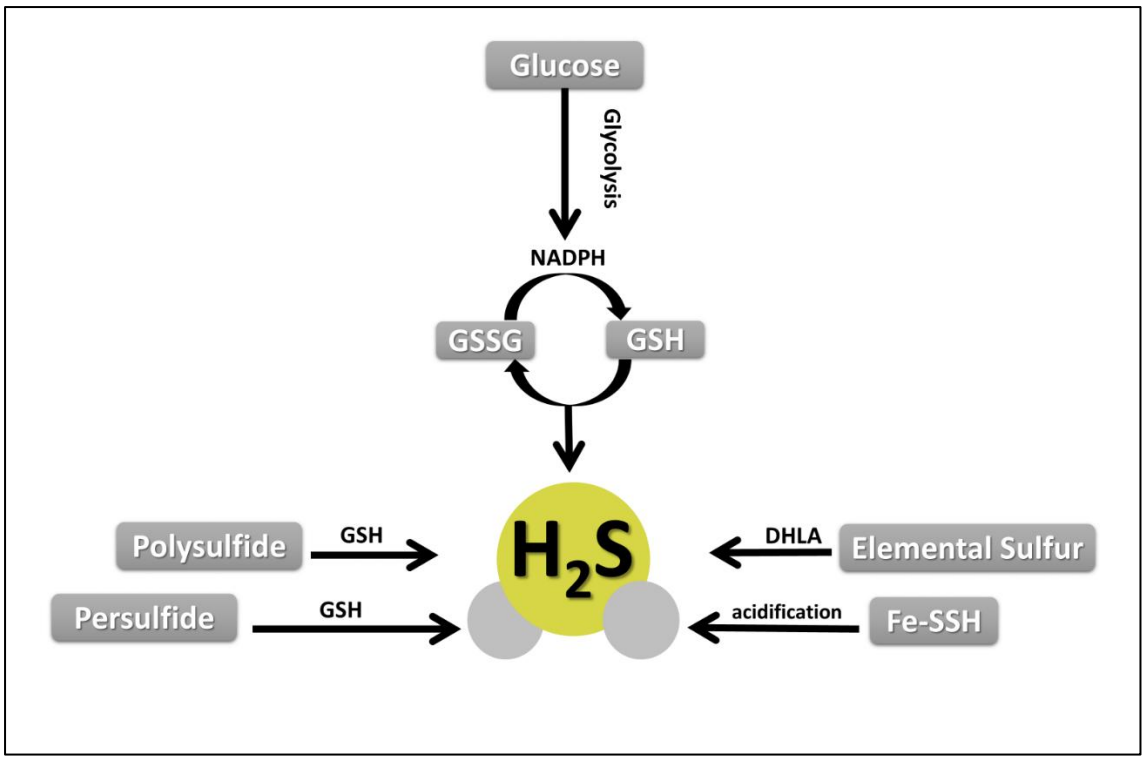


Figure 2 **Non-enzymatic pathways of hydrogen sulfide (H_2S) production in vivo.**
Reduced glutathione (GSH) can convert polysulfides and persulfides back to free H_2S through thiol-mediated transpersulfidation. Dihydrolipoate (DHLA), reduces elemental sulfur to H_2S. Acidic environments promote the release of H_2S from acid-labile iron–sulfur clusters. In erythrocytes, glycolytic metabolism generates NADH, which provides reducing equivalents that facilitate the non-enzymatic conversion of elemental sulfur to H_2S.

1.2 3-Mercaptopyruvate sulfur transferase (3MST)

3MST is a zinc dependant enzyme localised in the cytoplasm and cysteine-rich mitochondria. It is a 33 kDa protein reported to exist in a monomer-dimer equilibrium, with the active form being the monomer protein (Nagahara, 2018). There are two splice variants of 3MST that have similar enzymatic activity, TUM1-(tRNA thiouridin modification protein 1) Iso1 and TUM1-Iso2. TUM1-Iso 2 is found in the cytoplasm and mitochondria, while TUM1-Iso1 was reported to exist only in the cytoplasm (Fräsdorf et al., 2014). The cytoprotective effect against oxidative stress and maintenance of mitochondrial function were rationally linked to the presence of 3MST in the mitochondria and its production of copious amounts of H_2S(Kimura, 2013a). Additionally, studies found that D-cysteine, which ultimately results in the production of H_2S via the 3MST pathway, decreases oxidative stress in neurons and reduces ischaemia–reperfusion damage in kidneys (Shibuya et al., 2013). This is a further evidence pointing at the relationship between decreased oxidative stress and abundance of H_2S in the mitochondria.

The generation of H_2S by 3MST occurs via a mechanism involving a persulfurated enzyme intermediate. In the first step, the sulfur atom from the substrate 3-mercaptopyruvate (3-MP), which is itself derived from cysteine and α-ketoglutarate via cysteine aminotransferase

(CAT), is transferred to the catalytic cysteine residue (Cys247 in humans) of 3MST (Takano et al., 2017). This reaction forms a cysteine persulfide (Cys-SSH) intermediate on the enzyme and releases pyruvate (Zhao et al., 2001). In the second step, this bound persulfurated sulfur can follow one of two fates: (1) it can be reduced by physiological thiols (e.g., thioredoxin or dihydrolipoic acid) to release free H_2S as a diffusible gasotransmitter, or (2) it can be transferred directly to a target protein, creating a protein persulfide (Protein-SSH) in a post-translational modification known as persulfidation. Reduction of the resulting persulfurated protein via reducing agents, such as thioredoxin, yield H_2S. This dual output allows 3MST to function not only as a source of H_2S but also as a direct regulator of protein function, positioning it as a central node in reactive sulfur species signalling (Shibuya et al., 2009; Kimura et al., 2017).

3MST is ubiquitously distributed throughout mammalian cells, although some cell types express higher levels, such as the kidney, liver, brain, testes, large intestine and endocrine organs (Bełtowski, 2015). It was confirmed that 3MST is also expressed in various cancer cells (Jurkowska et al., 2011). The levels of 3MST were significantly higher than CSE in some cancerous cell lines, such as the U373 astrocytoma line, the SH-SY5Y neuroblastoma line and two melanoma cell lines, A375 and WM35, suggesting that 3MST is the dominant source of H_2S in these cells(Wróbel et al., 2017). In addition, 3MST was reported to be upregulated in multidrug-resistant cell lines and cell lines that show stem-like properties upon recovery from cytotoxic stimulus, indicating that 3MST could be specifically upregulated in these cell lines and may be responsible for their tumour cytoprotective properties.

Most previous studies on 3MST were dependant on using 3MST knockout organisms to observe the consequences of its deletion, mainly due to absence of potent and selective 3MST inhibitors, until Hanaoka et al. presented several inhibitors (Hanaoka et al., 2017). 3MST silencing resulted in distinguishing many of its now known properties, such as regulation of cellular bioenergetics, cytoprotection, induction of cellular proliferation and antioxidation, which were also exhibited in primary tumour cells (Szabo et al., 2014). However, as 3MST is an enzyme, its role may extend beyond the H_2S system alone. As with many proteins, genetic deletion may obscure certain enzymatic interactions or redox-related functions, raising the possibility that some aspects of its activity could be overlooked unless studies using selective inhibitors are considered alongside knockout models.

Studies using both knockdown and knockout models of 3-mercaptopyruvate sulfurtransferase (3-MST) demonstrate that partial and complete loss of the enzyme lead to distinct biological outcomes. In knockdown systems, reduced 3-MST expression produces pronounced effects on cellular metabolism and bioenergetics, including altered lipid handling, impaired glycolysis and oxidative phosphorylation, and reduced ATP production. These changes are particularly evident in cancer cell models, where 3-MST knockdown suppresses cell proliferation and migration, indicating a role for 3-MST-derived hydrogen sulfide in supporting tumour cell metabolism and growth (Loiselle *et al.*, 2018; Katsouda *et al.*, 2020; Casili *et al.*, 2022; Santos *et al.*, 2023).

By contrast, complete genetic deletion of 3-MST results in comparatively mild baseline phenotypes in vivo, with knockout mice and zebrafish showing normal development and gross morphology, suggesting the presence of compensatory sulfur-metabolic or redox pathways (Nagahara *et al.*, 2013; Katsouda *et al.*, 2020). Nevertheless, 3-MST knockout animals exhibit reduced production of H_2S and polysulfide species, altered neurotransmitter

regulation, and context-dependent metabolic effects, including changes in lipid metabolism and improved hepatic steatosis under high-fat diet conditions (Loiselle *et al.*, 2018; Sun *et al.*, 2021). Together, these findings indicate that while knockdown models reveal strong cell-autonomous roles for 3-MST in energy metabolism and proliferation, whole-animal knockout models may partially mask these functions through long-term adaptation and compensatory mechanisms. A comparison between 3-MST knockdown and knockout phenotypes is shown in Table 1.

Table 1 ***Comparison of 3-MST Knockdown and Knockout Phenotypes***

Category	**3MST Knockdown (KD)**	**3MST Knockout (KO)**
Model type	Partial reduction of 3-MST expression (e.g. siRNA/shRNA or targeted KD approaches) *(Santos et al., 2023; Katsouda et al., 2020)*	Complete genetic deletion of 3-MST in animal models *(Nagahara et al., 2013; Katsouda et al., 2020)*
Development and Behaviour	No major developmental defects reported *(Santos et al., 2023)*	Normal gross morphology observed in mice and zebrafish under physiological conditions *(Nagahara et al., 2013; Katsouda et al., 2020; Rao et al., 2023)* Increased anxiety-like behaviour and altered neurotransmitter regulation *(Nagahara et al., 2013)*
H_2S / sulfur signalling	Reduced H_2S production leading to altered redox balance and sulfur signalling *(Santos et al., 2023; Augsburger and Szabó, 2020)*	Markedly reduced enzymatic H_2S and polysulfide production from 2MST *(Nagahara et al., 2013; Rao et al., 2023)*
Metabolic effects	Dysregulation of lipid metabolism; increased lipid uptake and accumulation in adipocytes; altered glycolysis and oxidative phosphorylation *(Casili et al., 2022; Santos et al., 2023)*	Minimal phenotype under normal diet, but altered lipid metabolism under high-fat diet conditions; improved hepatic steatosis reported *(Loiselle et al., 2018; Sun et al., 2021)*
Energy metabolism	Decreased basal ATP production in metabolically active and cancer cells, linked to reduced H_2S signalling *(Loiselle et al., 2018; Santos et al., 2023)*	Alterations in energy metabolism suggested, though often compensated under basal conditions *(Casili et al., 2022)*

Cell proliferation and migration	Suppression of tumour growth-associated bioenergetics and migration in vitro (Katsouda et al., 2020; Loiselle et al., 2018)	Proliferative phenotypes less prominent; systemic compensation may mask cell-specific effects *(Loiselle et al., 2018)*

Moreover, 3MST localization in both neurons and glial cells suggests that it plays a multifaceted role in the brain's response to stress and injury (Furuie, 2023). The enzyme's activity is not only essential for maintaining normal physiological functions but also for modulating pathological processes. For example, the inhibition of H_2S synthesis through 3MST has been linked to increased tumour progression and immunosuppression in cancer models, highlighting its potential as a therapeutic target (Dawoud, 2024).

In addition to its role in the brain, 3MST is also implicated in vascular health. The enzyme contributes to endothelial function by enhancing nitric oxide bioavailability, which is vital for maintaining vascular tone and preventing hypertension (Lavier et al., 2021). The interplay between H_2S and nitric oxide signalling pathways underscores the importance of 3MST in cardiovascular physiology. Furthermore, the enzyme's involvement in the regulation of calcium homeostasis in smooth muscle cells suggests that it may influence vascular contractility and relaxation (Bartman et al., 2020).

The cytoprotective effect against oxidative stress and maintenance of mitochondrial function were rationally linked to the presence of 3MST in the mitochondria and its production of copious amounts of H_2S (Kimura, 2013a). Additionally, studies found that D-cysteine, which ultimately results in the production of H_2S via the 3MST pathway, decreases oxidative stress in neurons and reduces ischaemia–reperfusion damage in kidneys (Shibuya et al., 2013). This is a further evidence pointing at the relationship between decreased oxidative stress and the abundance of H_2S in the mitochondria.

The significance of 3MST is further emphasized by its potential therapeutic applications. Given its role in H_2S production, targeting 3MST could provide novel strategies for treating conditions associated with oxidative stress, inflammation, and vascular dysfunction. For instance, enhancing 3MST activity may offer protective effects against ischemic injuries and neurodegenerative diseases, while inhibiting its function could be explored in cancer therapies (Dawoud, 2024).

Until 2017, there were few known compounds that inhibited 3MST. Those chemical entities included substrate mimics such as pyruvate, oxobutyrate, oxoglutamate, phenylpyruvate, 2-mercaptopropionic acid, 3-mercaptopropionic acid and other chemicals like hypotaurine and methanesulfinic acid (Wróbel and Jurkowska, 2007). Those compounds were neither potent (IC50 values in millimolar range) nor selective, rendering them impractical for pharmacological studies.

As for selective 3MST inhibitors, none were identified until 2017, when a research group performed high throughput screening of 174,118 compounds and discovered novel 3MST inhibitors (Hanaoka et al., 2017). Compound "3" in their study (2-4-hydroxy-6-methylpyrimidin2-yl-sulfanyl-1-naphthalen-1-yl-ethan-1-one), showed selectivity compared to the other H_2S producing enzymes, while compound "1" showed the lowest IC_{50} value at 1.7 µM.

In a previous study carried out in our laboratory, a florescence based screen of commercially available compounds identified 1-(3,4-Dihydroxyphenyl)-2-[(4-hydroxy-6-methyl-2-pyrimidinyl)sulfanyl]ethanone (CDS004892) as an inhibitor of 3MST (Almehaize, 2017). CDS004892 is structurally similar to the compounds discovered by Hanaoka's research group (Hanaoka et al., 2017).The calculated IC_{50} of CDS004892 is 7.92 µM, which is comparable to Hanaoka et al.'s compounds 1–3 and 5 that displayed IC_{50} values between 1.7–6.3 µM (figure 2). Additionally, results from a previous project in our laboratory showed that another compound, tetrathionate, is a 3MST inhibitor with an IC_{50} of 6 µM but was not selective as it also inhibits rhodanese with an IC_{50} of 10 µM.

As a consequence of the relatively recent discovery of selective inhibitors for H_2S-producing enzymes and the expanding recognition of their physiological roles, the development of potent and enzyme-specific inhibitors remains at an early stage. In addition, the later appreciation of the therapeutic relevance of modulating H_2S biosynthesis has further slowed progress in this area. The discovery of new, selective inhibitors will be crucial for advancing pharmacological investigations, providing much-needed insight into the specific biological functions of H_2S—much as nitric oxide synthase inhibitors such as NG-monomethyl-L-arginine (an L-arginine analogue) were instrumental in elucidating the roles of nitric oxide (Gillespie et al., 1989).

Selective 3MST inhibitors have great potential not only as pharmacological agents, but also as compounds with valuable therapeutic benefits. Many disease models have been reported to display increased levels of 3MST, including several tumour types such as lung cancer, glioma, melanoma (Szczesny et al., 2016a) and polycythemia vera (Frendo and Wróbel, 1997).

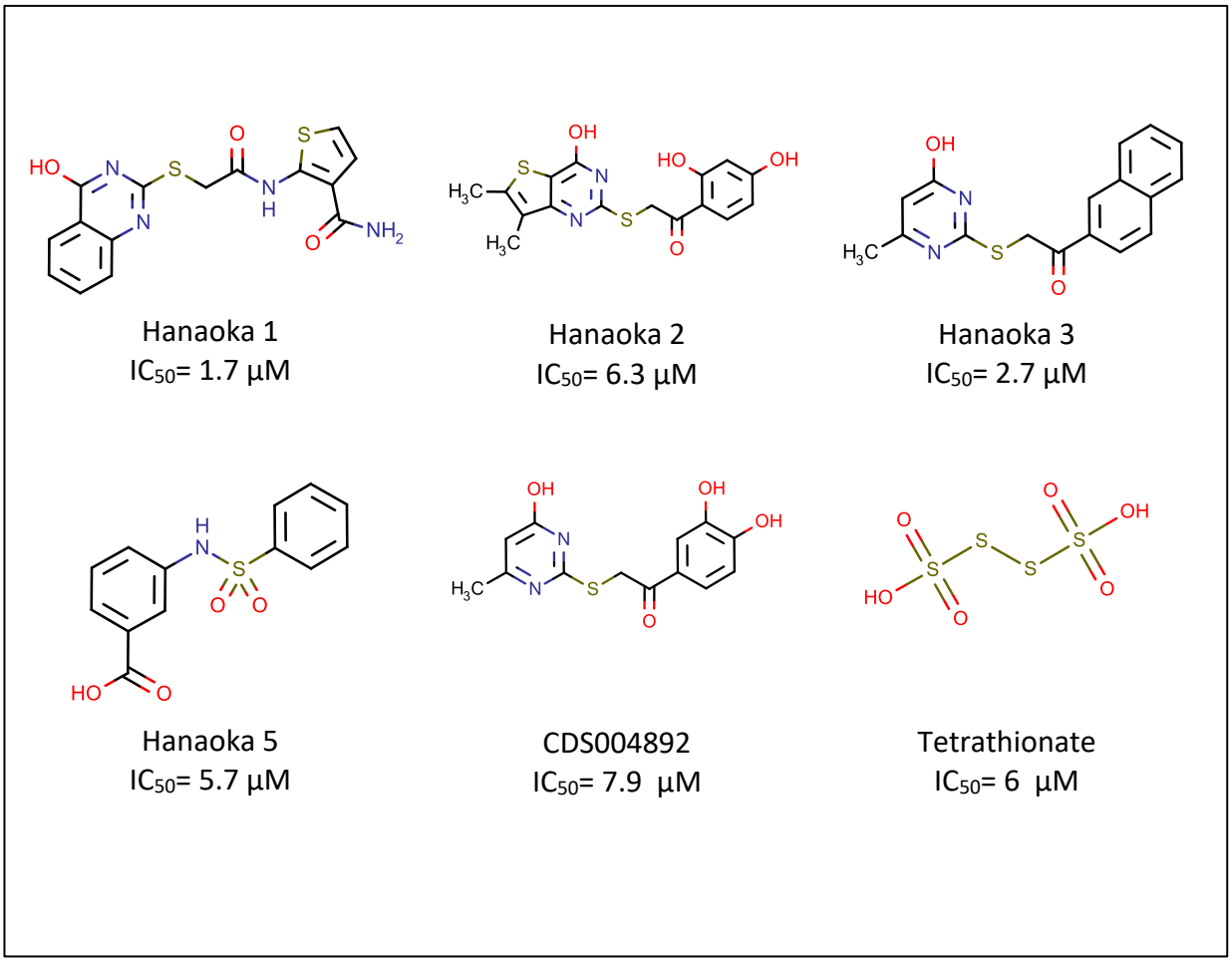


Figure 3 Chemical structures of 3MST inhibitors, 1-(3,4-Dihydroxyphenyl)-2-[(4-hydroxy-6-methyl-2-pyrimidinyl)sulfanyl]ethanone (CDS004892) from a previous study (Almehaize, 2017). As seen in the graph, CDS004892 is structurally similar to the compounds discovered by Hanaoka's research group (Hanaoka et al., 2017)

1.3 Mitochondria targeting agents

The cytoprotective effects against oxidative stress and the preservation of mitochondrial function have been logically attributed to the mitochondrial localization of 3MST and its substantial production of hydrogen sulfide (H_2S) (Kimura, 2013). Low concentrations of H_2S affects the mitochondrial enzyme sulfide quinone oxidoreductase and directly donates electrons into the mitochondrial electron transport chain (Szabo et al., 2014). In addition, H_2S inhibits mitochondrial cAMP phosphodiesterases and stimulates mitochondrial antioxidation, thus supporting the functionalities of the mitochondria (Suzuki et al., 2011). Furthermore, H_2S interacts directly with mitochondrial DNA repair enzymes (e.g. endo/exonuclease) and consequently stimulates repair of mitochondrial DNA (Szczesny et al., 2016b). H_2S also enhances mitochondrial ATP synthase (complex V) activity via persulphidation (Módis et al., 2016). However, at high concentrations H_2S was reported to interact with the copper centres of mitochondrial complex IV (i.e., cytochrome c oxidase) and thereby it inhibits cellular respiration (Nicholls et al., 2013). Inhibition of an essential enzyme such as mitochondrial complex IV will affects the regular intercellular phosphorylation mechanisms that bind oxygen, thus compromising mitochondrial electron transport and ATP generation.

Such inhibitory effects of H_2S have always been associated with its toxicity as an environmental pollutant. However, there are interesting attempts to investigate the therapeutic value of such inhibitory effects. The exploration into the reversible inhibition of complex IV via H_2S is considered advantageous in comparison to the irreversible inhibition of cyanide. An example of such experimentation involves triggering reversible metabolic suppression as a coping mechanism to instances of oxygen deprivation in the tissues, which occurs following severe blood loss or lethal hypoxia (Aslami et al., 2009). Interestingly, reversible metabolic suppression could also be applied by the same concept to extend the shelf life of stored organs (Lobb et al., 2017).

Mitochondria are important intracellular organelles that control cellular energetics and critical oxidative processes. Naturally, compounds that target the mitochondria to alter its critical functions have attracted much attention. Specifically targeting H_2S delivery and production in the mitochondria is an interesting pharmacological approach, especially because of all the aforementioned physiological and cytoprotective effects exerted by low concentrations of H_2S on the mitochondria, and the amounts of ROS species produced by the mitochondria that can cause decreased levels of physiological H_2S. H_2S donors that specifically target the mitochondria have been synthesised and investigated *in vitro*. Szczensy research group synthesised the H_2S donor prodrug (10-oxo-10-(4-(3-thioxo-3H-1,2-dithiol5yl)-phenoxy)decyl) triphenylphosphonium bromide, also known as AP39, providing an example of H_2S inducing compounds. AP39 comprises two parts, a H_2S generation moiety dithiolethione (ADT-OH) and triphenylphophinium (TPP), the mitochondria-targeting moiety (Szczesny et al., 2014b). Lipophilic cation compounds such as triphenylphosphonium (TPP+) and its derivatives are used as chemical tags to specifically target the mitochondria. The inner

mitochondrial negative membrane potential facilitates uptake of those TPP+ cations in vivo, leading to accumulation of TTP+ in the mitochondria. The lipophilic TPP+ establishes covalent bonds making a decent delivery method to insert small bioactive entities specifically into the mitochondria in vivo. AP39 and another related compound AP123 were able to successfully increase H_2S levels selectively in the mitochondria (Montoya and Pluth, 2016). Therefore, these compounds were able to demonstrate cytoprotective effects in concentrations ranging from high nanomaolar to low micromolar against oxidative stress in vitro in different cell types such as endothelial cells, epithelial cells, platelets, neurons and cardiac myocytes (Chatzianastasiou et al., 2016). Upon further investigations, AP39 showed superior ability to release H_2S compared to AP123 (Gerő et al., 2016), and consequently accumulated the larger number of studies. In accordance with the bell shaped effects of H_2S on mitochondrial functions, and the positive effect of H2S on cellular bioenergetics at low concentrations, low concentrations of AP39 (25–100 nM) caused increased mitochondrial basal respiration and maximal respiration in endothelial cells and neurons (Zhao et al., 2016). On the other hand, increasing AP39 concentrations to 250-300 nM did not cause any apparent positive effects on basal mitochondrial activity (Szczesny et al., 2014a). In cells suffering from oxidative stress, AP39 decreased ROS levels by delivering H_2S into the mitochondria. Furthermore, in oxidatively stressed cells, both AP39 and AP123 induced mitochondrial DNA repair (Karwi et al., 2017). This effect was deduced to be caused by mitochondrial H_2S, which was specifically promoting assembly and activation of DNA repair complexes in the mitochondria. Notably, the mitochondrial functionalities and signalling processes exerted by AP39 were distinguished from other none-targeted H_2S donors, due to distinctive localization of H_2S cellular targets (Szabo and Papapetropoulos, 2017).
Upon investigation, AP39 showed that it could maintain mitochondrial integrity, reduce the release of mitochondrial death signals, and attenuate mitochondrially-regulated cell death responses. Following initial investigations, AP39 was considered a potential candidate for disease-modifying therapy for Alzheimer's disease and acute renal injury (Ahmad et al., 2016b)

Specifically targeting the mitochondria has some promising advantages, such as independence from the NO system and the cGMP/protein kinase G system (Tomasova et al., 2015). AP39 has shown interesting pharmacological effects when the compound accumulates in the sinoatrial nodes because of the difference between the positive charge of AP39 and the high negative resting potential of the nodal cells, which may eventually result in activating Ca_V3, RyR2, and Cl^- cardiac membrane channels (Tomasova et al., 2015). In addition, AP39 is speculated to block permeability pores and desensitise permeability transition pores in the mitochondria (Chatzianastasiou et al., 2016).

Application of AP39 *in vivo* mimics the distinguished physiological effects of H_2S and H_2S donors, such as decreasing blood pressure and heart rate (Tomasova et al., 2015). In addition, AP39 exerts cytoprotective effects at very low doses in several disease models such as neurodegeneration (Ahmad and Szabo, 2016), myocardial ischemia-reperfusion (Chatzianastasiou et al., 2016), burn injury and renal ischemia-reperfusion (Ahmad et al., 2016a). Despite the focus on cytoprotective effects of mitochondrially targeted H_2S donors in therapeutic approaches, other studies discovered that those compounds could also be

utilised in antitumor therapeutics, such as combination with methyl aminolevulinate to induce photodynamic therapy (Ferguson et al., 2014).

Specific targeting of H_2S to the mitochondria is seemingly a graceful approach with multiple advantages, yet there are certain possible concerns that should be addressed. Firstly, as mentioned earlier, delivery of large concentration of H_2S to the mitochondria is speculated to cause decreased aerobic respiration and ATP generation, which is the main toxic effect of H_2S on the electron transport chain in the mitochondria. This effect is apparent from the bell-shaped effect of H_2S delivery by AP39 (Szczesny et al., 2014a). Therefore, further extensive studies on the therapeutic index of those compounds, including the elucidation of the tight balance between the minimum toxic dose and minimum effective concentration should be conducted. The mitochondria-targeting moiety (TPP) is also known to cause cytotoxic effects upon overdosing (Guzman-Villanueva and Weissig, 2017). Secondly, although AP39 is designed to target the mitochondria, it eventually loses its selectivity and also causes increased H_2S levels in the cytoplasm when delivered at high concentrations (Szczesny et al., 2014a).

Finally, dependence on the positively charged lipophilic mitochondria targeting moieties to accomplish accumulation of the desired compound/donor may have its own limitations. As the delivery mechanism depends mainly on the membrane potential in the mitochondria, any pathological condition affecting mitochondrial membranes or malfunctioning of the mitochondria may compromise this method of delivery. This theory was tested by adding mitochondrial uncoupler carbonyl cyanide-4-phenylhydrazone to cells with AP39; the results show the disconcerting inability of AP39 to specifically increase mitochondrial H_2S in fluorescence studies (Szczesny et al., 2014a). Those results may indicate that using such methods of targeted delivery is unreliable in disease models that display mitochondrial dysfunctions. Despite these concerns, targeting the mitochondria by using lipophilic cations has produced many useful pharmacological tools in delivering antioxidants and H_2S donors; some clinical trials are underway (e.g., with mito-Q (Frantz and Wipf, 2010). Using this methodology to specifically deliver H_2S inhibitors instead of donors, may bypass some of the concerns and disadvantage of this technique. Furthermore, the currently available inhibitors have large IC_{50} values and lack potency, and in some cases selectivity. Thus, using targeted delivery systems and accumulating these inhibitors in the mitochondria may accomplish greater inhibitory effects compared to regular delivery methods. In addition, targeted delivery could improve selectivity for 3MST inhibitors as CBS and CSE are mainly localised in the cytoplasm, while 3MST is localised in both the mitochondria and cytoplasm. Coupling inhibitors such as CDS004892 to the lipophilic TPP moiety to specifically target the mitochondria and inhibit 3MST is a technique that may aid with attaining superior inhibitory effects, which is hampered by the current difficulty with discovering potent novel inhibitors.

1.4 H_2S synthesising enzymes and cancer

The role of hydrogen sulfide in cancer treatment has garnered significant attention in recent years, primarily due to its dual nature as both a signalling molecule and a potential therapeutic agent. H_2S is recognized for its involvement in various physiological processes, including vasodilation, anti-inflammatory responses, and modulation of cellular metabolism. However, its role in cancer is complex, as it can exhibit both tumour-promoting and tumour-inhibiting effects depending on the context and concentration.

One of the critical aspects of H_2S in cancer biology is its ability to influence cellular proliferation and apoptosis. For instance, studies have shown that H_2S can promote the proliferation of cancer cells through the activation of specific signalling pathways. It was emonstrated that H_2S enhances cell proliferation in oral cancer by activating the COX2/AKT/ERK1/2 signalling axis, indicating that H_2S can act as a growth factor in certain malignancies (Zhang et al., 2016). This finding suggests that while H_2S may have therapeutic potential, its role as a promoter of tumour growth in specific contexts cannot be overlooked.

Conversely, H_2S has also been implicated in the inhibition of cancer cell growth. For example, the use of hydrogen sulfide-releasing aspirin has shown promise in inhibiting the growth of leukemic cells, suggesting that H_2S can modulate pathways involved in cell cycle regulation and apoptosis (Chattopadhyay et al., 2013). This duality highlights the necessity for a nuanced understanding of H_2S's role in cancer, as its effects can vary significantly based on the tumour type and microenvironment.

Moreover, the modulation of inflammatory responses by H_2S is another critical factor in cancer treatment. Inflammation is a well-known contributor to tumorigenesis, and H_2S has been shown to exert anti-inflammatory effects. It was noted that H_2S is generated as an anti-inflammatory agent in the host, which may lead to its elevation in tumour samples due to the tissue's reaction to tumour-induced inflammation (Hale et al., 2018). This supports how H_2S is harnessed to mitigate the inflammatory microenvironment that often supports tumour growth. It has been shown that H_2S can affect the behaviour of immune cells within the tumour milieu, potentially influencing the anti-tumour immune response. For instance, H_2S has been suggested to inhibit leukocyte adhesion, which may alter the infiltration of immune cells into tumours, thereby impacting tumour progression and response to therapy (Lin et al., 2018). This aspect of H_2S biology highlights the importance of considering the immune context when evaluating its therapeutic potential.

In addition to its direct effects on cancer cells, H_2S has been explored for its potential in enhancing the efficacy of other therapeutic modalities. For instance, there is a nanoplatform

that utilizes H_2S-triggered multimodal cascade therapy for colon cancer, combining photothermal therapy with H_2S-mediated respiration inhibition (Yang et al., 2022). This innovative approach underscores the potential of H_2S in synergistic therapies, where it can enhance the effectiveness of existing treatments.

The mechanisms by which H_2S exerts its effects are also of great interest. Research has indicated that H_2S can influence the expression of various genes involved in cancer progression. For example, the upregulation of cystathionine-β-synthase (CBS) and cystathionine gamma-lyase (CSE) has been observed in several cancer types, leading to increased H_2S production (Untereiner et al., 2017). This suggests that targeting the enzymes responsible for H_2S synthesis could be a viable strategy in cancer therapy, either by inhibiting their activity to reduce H_2S levels in tumour-promoting contexts or by enhancing their activity to exploit H_2S's potential anti-cancer properties.

The therapeutic applications of H_2S are not limited to its direct effects on cancer cells. The development of H_2S-releasing nanoparticles for targeted delivery in cancer therapy represents a promising avenue for enhancing treatment specificity and reducing systemic toxicity (Ma et al., 2017). These innovative delivery systems can provide controlled release of H_2S in the tumour microenvironment, potentially maximizing its therapeutic effects while minimizing adverse effects on healthy tissues.

In summary, the role of hydrogen sulfide in cancer treatment is multifaceted, encompassing both tumour-promoting and tumour-inhibiting properties. Its ability to modulate cellular signalling pathways, influence inflammatory responses, and interact with the tumour microenvironment positions H_2S as a potential therapeutic target. However, the complexity of its effects necessitates a careful and context-dependent approach to harness its full potential in cancer therapy. Future research should focus on elucidating the precise mechanisms by which H_2S influences cancer biology and exploring its applications in combination with existing treatment modalities.

1.5 H_2S producing enzymes and bacteria

Another interesting therapeutic target that involves H_2S producing enzymes is pathogenic bacteria. H_2S is known to be produced in bacterial cells but was initially thought to be a metabolic by-product (Szabo, 2018). Upon further investigation, CBS, CSE and 3MST were all detected and found to be expressed in those prokaryotes and promptly, consequences of chemical inhibition of those enzymes was investigated (Flannigan et al., 2011). Interestingly, increased sensitivity to antibiotics upon inhibition of H_2S synthesising enzymes was discovered, which led to interest in using inhibitors as therapeutic agents in synergy with antibiotics (Kimura, 2013b). However, such an approach must used with caution, as it was

reported that increased resistance to antibiotics was also associated with inhibition of H_2S synthesis (Shatalin et al., 2011). Another gasotransmitter, NO, is also associated with cyto-protectant effects in bacterial cells. Incidentally, bacteria artificially deficient in both NO synthase and CBS/CSE are unable to form colonies, suggesting the importance of both NO and H_2S in bacterial survival. Moreover, when either NO or H_2S is deficient, the other will be over-produced, suggesting at a compensation to assure survival (Kimura, 2014b). H_2S synthesising enzymes were found in almost all types of bacteria to date, whereas NO synthase is only expressed in certain types of gram-negative bacteria. Bacterial CBS, CSE and 3MST have unique qualities differentiating them from their mammalian counterparts, which introduces the opportunity to explore targeting bacterial enzymes as a synergistic therapy with antibiotics (Shatalin et al., 2011).

The role of hydrogen sulfide (H_2S) inhibition in antibacterial treatment is increasingly recognized as a promising strategy to combat antibiotic resistance. H_2S is produced by various bacteria and has been implicated in mechanisms that confer resistance to antibiotics. This phenomenon is particularly evident in pathogens such as Staphylococcus aureus and Pseudomonas aeruginosa, where H_2S production has been shown to protect these organisms from the effects of aminoglycoside antibiotics and other antimicrobial agents (Weikum et al., 2018; Shatalin et al., 2021).

Research indicates that H_2S acts as a defence mechanism for bacteria, allowing them to survive antibiotic treatment. For instance, H_2S production in Staphylococcus aureus provides a protective effect against aminoglycosides, suggesting that targeting H_2S synthesis could enhance the efficacy of existing antibiotics (Weikum et al., 2018). Similarly, it was reported that inhibiting bacterial H_2S biogenesis can restore antibiotic susceptibility in resistant strains, highlighting the potential of H_2S inhibitors as adjuvants in antibiotic therapy (Shatalin et al., 2021).

Moreover, the enhancement of bactericidal effects of antibiotics through the inhibition of H_2S-producing enzymes has been documented. In one study, small molecules that inhibit H_2S production were shown to potentiate the effects of various antibiotics, including beta-lactams and quinolones, in both in vitro and in vivo models (Серегина et al., 2022). This suggests that the strategic inhibition of H_2S production could be a viable approach to overcoming bacterial resistance.

The biochemical pathways involving H_2S also play a critical role in the development of antibiotic resistance. For example, H_2S has been implicated in the modification of bacterial responses to oxidative stress, which is a common mechanism of action for many antibiotics (Shukla et al., 2017). By inhibiting H_2S production, it may be possible to sensitize bacteria to oxidative stress, thereby enhancing the effectiveness of antibiotic treatments.

In addition to its protective role, H_2S has been shown to interfere with the action of certain antibiotics by modifying their chemical structure. It was found that H_2S can inactivate beta-lactam antibiotics through the formation of ring-opened products, which further complicates the treatment landscape for infections caused by H_2S-producing bacteria (Ono et al., 2021).

Overall, the inhibition of hydrogen sulfide production presents a multifaceted approach to enhancing antibacterial treatment. By targeting the mechanisms through which H_2S confers resistance, researchers are paving the way for novel therapeutic strategies that could significantly improve outcomes in the fight against antibiotic-resistant infections.

1.6 Other indigenous sulfur species: sulphane sulfurs

Sulphane sulfurs represent a distinct class of reactive sulfur species (RSS), characterised by the presence of chains or networks of sulfur atoms. These include molecular species such as polysulfides and persulfides, often represented as H_2S_x, where x is greater than or equal to 2. Unlike hydrogen sulfide, which predominantly exists in its gaseous form under physiological conditions and is rapidly metabolised or oxidised, sulphane sulfurs are typically more stable and persist longer in biological systems. This chemical distinction makes them particularly relevant in the context of cellular signalling and redox biology (Jacob & Anwar, 2008; Schneider et al., 2000).

The term "sulphane" has historically been used interchangeably with terms such as bound sulfur or zero-valent sulfur, but in modern biochemical contexts, it refers more specifically to sulfur atoms that are in an oxidation state capable of being transferred or incorporated into biomolecules. Unlike free H_2S, which often undergoes rapid oxidation or enzymatic degradation, sulphane sulfurs exhibit enhanced reactivity toward biological nucleophiles, such as protein thiols and low-molecular-weight thiols like glutathione. Through these interactions, they form persulfides (R–SSH), which are now recognised as important post-translational modifications capable of altering protein conformation, activity, and stability. One of the most significant roles of sulphane sulfurs lies in their participation in redox regulation and intracellular signalling pathways. Their ability to act as sulfur donors in redox reactions enables them to modulate oxidative stress responses and influence cellular fate decisions, including apoptosis and autophagy. The process of protein persulphidation, also referred to as S-sulfhydration, has emerged as a major mechanism by which sulphane sulfurs exert their biological effects. This modification can enhance or inhibit protein function and has been implicated in diverse processes such as mitochondrial function, inflammation, and metabolic regulation (Singh et al., 2023; Chalmers et al., 2024).

From a metabolic perspective, sulphane sulfurs often arise as byproducts or intermediates in amino acid catabolism, particularly in the degradation of cysteine via the transsulfuration pathway. Enzymes such as cystathionine γ-lyase (CSE), cystathionine β-synthase (CBS), and 3-mercaptopyruvate sulfurtransferase (3MST) contribute to the generation of various sulfur species, including both H_2S and sulphane sulfurs. The balance and interconversion between

these sulfur pools are thought to play a critical role in maintaining cellular redox homeostasis and mitochondrial health. Moreover, sulphane sulfurs have been implicated in modulating the activity of several enzymes and transcription factors via thiol modification, positioning them as important regulators of gene expression and signal transduction. Recent studies have also linked sulphane sulfur species to pathological conditions, particularly in the context of inflammation, cardiovascular disease, and cancer. Altered sulphane sulfur levels have been associated with enhanced tumorigenicity and poor prognosis in various cancer types, suggesting that these species may influence cell proliferation, angiogenesis, or immune evasion (Linden et al., 2012; Adánez-Rubio et al., 2020). The exact mechanisms remain under investigation, but their impact on redox-sensitive pathways and mitochondrial dynamics is believed to be central.

Given their unique chemical and biological properties, sulphane sulfurs are emerging as potential therapeutic agents and targets in drug discovery. Their prolonged reactivity, selectivity toward thiol-containing biomolecules, and involvement in redox-sensitive processes make them attractive candidates for diseases characterised by oxidative stress or metabolic dysregulation. Current medicinal chemistry efforts are increasingly focusing on the development of synthetic sulphane sulfur donors, modulators of sulfur metabolism, or inhibitors that specifically influence sulphane-related signalling pathways (Bonifácio et al., 2020). These approaches may prove particularly valuable in the treatment of neurodegenerative disorders, cardiovascular disease, and certain cancers.

As such, sulphane sulfurs represent a versatile and biologically significant class of sulfur species with roles that extend well beyond those of hydrogen sulfide. Their capacity to modulate protein function, participate in redox signalling, and influence disease states highlights their potential as both biomarkers and therapeutic targets. As research into the sulfur metabolome expands, a deeper understanding of sulphane sulfur biology is likely to reveal novel insights into cellular regulation and open new avenues for therapeutic intervention.

1.7 Detection of H_2S

With the increased interest in H_2S over the last two decades, several methods were developed to measure its production. It is essential to accurately measure the levels of H_2S, or at least elucidate acceptable estimates to validate experimental analysis when investigating the inhibition of enzymatic production or inducing it by administering donors or substrates.

Methods to measure H_2S levels include fluorimetric, spectrophotometric, chemiluminescent and chromatographic investigations. Measuring enzymatic activity of CBS/CSE and their production of H_2S was seldom used and reported as reliable means of estimating H_2S levels. Measuring H_2S metabolites, in a manner akin to the measurement of nitrite/nitrate to estimate NO levels, was suggested but awaits validation (Takano et al., 2017).

The volatile and transient state of H_2S makes it one of the more challenging moieties to measure accurately in biological samples (Kabil and Banerjee, 2010). Moreover, H_2S is also notoriously labile to redox reactions and has a low steady state concentration (Olson, 2009).

Those challenges resulted in different measuring techniques with different abilities to measure H_2S in concentration scaling between three digits of micromolars down to few nanomolars.

Detection methods include

- Colorimetric assays (methylene blue).
- Using a sulfide ion-selective electrode or a polarographic electrode.
- Gas chromatography (GC)
- Ion chromatography.
- Sulfide-sensitive fluorescent dyes.
- HPLC analysis of the monobromobimane derivative of sulfide with fluorescence detection.

According to Papapetropoulos, 'reproducibility, sensitivity and ease of application' are the three most important aspects of an experiment to be favoured and used by researchers. However, no 'perfect' universal method has been established to date. For instance, H_2S produced by donors in aqueous buffers can be measured with relative accuracy, however it is still challenging to measure in biological samples containing endogenous thiols and other cellular substances that may compromise results (Papapetropoulos et al., 2015).

One of the earliest and most commonly used techniques for hydrogen sulfide detection is the methylene blue assay—a straightforward colorimetric method based on spectrophotometric analysis of optical density, first reported by Emil Fischer in 1886 (Chen and Mortenson, 1977). This assay remains popular among researchers due to its ability to clearly differentiate H_2S concentrations between control and experimental samples. Its continued relevance is attributed to its simplicity, selectivity, and sensitivity. The assay functions by reacting sulfides in aqueous solutions with N,N-dimethyl-p-phenylenediamine in the presence of trace ferric ions, forming a blue-coloured heterocyclic thiazine dye. The intensity of this blue colour is measured using UV-visible spectroscopy, with a detection threshold of 0.01 ppm. Despite being a "classic" method, it has notable limitations, including an inability to measure H_2S in vivo, a relatively high detection limit (above 1 µM), and susceptibility to interference from other sulfides in biological samples—especially due to the reagent acidity affecting iron-sulfur clusters. Additionally, this method is not suitable for real-time, continuous monitoring and is too labour-intensive for high-throughput applications.

To address the need for greater sensitivity, gas chromatography (GC) coupled with sulfur chemiluminescence detection has been employed to measure H_2S at nanomolar concentrations in biological matrices (Furne et al., 2008; Kabil et al., 2011; Levitt et al., 2011; Vitvitsky et al., 2012). In this approach, H_2S equilibrates between the liquid and gas phases in a sealed chamber. It is then separated from other sulfur-containing compounds via GC and

subsequently detected by sulfur chemiluminescence. During detection, H_2S is combusted to form sulfur monoxide, which reacts with ozone to produce light-emitting sulfur dioxide. A photomultiplier tube measures the emitted light, which correlates linearly with H_2S concentration (Vitvitsky et al., 2012). However, this technique has its own drawbacks—sensitivity is highly dependent on multiple variables such as the column type and injection mode, all of which must be carefully optimized before analysis. Furthermore, when samples contain only trace levels of H_2S, larger sample volumes are required, but GC capillaries typically cannot handle gas injections greater than 1 mL (Vitvitsky and Banerjee, 2015).

Electrochemical sensors and gas chromatography methods have been applied to detect H_2S in homogenized tissues, cell lysates, and blood. Nonetheless, these approaches fall short in enabling rapid and real-time detection of H_2S in living cells. Molecular imaging, particularly using fluorescent probes, has emerged to fill this gap. Over the past two decades, the development of H_2S-sensitive fluorescent probes has significantly outpaced other detection technologies such as colorimetric, chromatographic, and ion-selective methods. Despite their non-invasive nature and growing popularity, challenges remain. These include the naturally low levels of endogenous H_2S and the presence of other abundant thiols that can cause interference. In vivo imaging also faces hurdles such as poor tissue penetration by fluorophores and their instability under high excitation wavelengths. Although many fluorogenic sensors demonstrate good selectivity for H_2S, they can still be affected by other biological thiols like cysteine and glutathione, especially when present in high concentrations. Consequently, ongoing research efforts aim to develop highly selective and sensitive probes.

Common issues with fluorescent probes include low imaging resolution (typically under 200 nm), which hampers accurate intracellular localization and detection of H_2S. Additionally, many probes are prone to photobleaching during prolonged use, highlighting the need for improved photostability and resistance to bleaching. Ideal fluorescent probes should be water-soluble, highly selective for H_2S, photostable in the near-infrared (NIR) region, fast-responding, sensitive, and exhibit low cytotoxicity (Liang et al., 2023).

Three key chemical mechanisms underpin most modern fluorescent imaging strategies: reduction of azides to amines, nucleophilic reactions, and copper sulfide precipitation. Research continues to optimize these mechanisms for better probe design. For example, Xiang and colleagues introduced a novel BODIPY-based ratiometric probe that selectively detects intracellular H_2S in live cells. This probe is noted for its low cytotoxicity and high selectivity (Liu et al., 2011). Lin and Wang also utilized selective H_2S-mediated reduction of azides and sulphonylazides to develop sensitive probes (Lin et al., 2013a). Wang (2014) and Xian designed probes featuring adjacent electrophilic sites to effectively trap H_2S (Liu et al., 2011), while other groups, such as Nagano (Sasakura et al., 2011), Zeng, and Bai (Hou et al., 2012), explored copper sulfide-based detection strategies. Numerous other techniques have emerged, making H_2S probing a rapidly growing research area (Xu et al., 2012; Wang et al., 2012).

However, most of these tools are limited to detecting exogenously added H_2S in cell systems or in vitro enzyme assays. In a notable advancement, Lin and colleagues reported a series of imaging probes that utilize the biocompatible, H_2S-specific reduction of azides to amines for live-cell detection (Lin et al., 2013b). Their compounds—SF4, SF5-AM, and SF7-AM—are highly selective for H_2S over other reactive sulfur, nitrogen, and oxygen species, and offer strong fluorescence "turn-on" signals compatible with standard microscopy filters. SF7-AM stands out for its enhanced sensitivity, improved glutathione selectivity, and decent photostability when excited with low-power visible lasers. Crucially, it enables real-time tracking of endogenous H_2S fluctuations in living cells. (Lin et al., 2013).

For the purposes of this study, fluorescent probes with rapid activity and high selectivity for low concentration of biological H_2S were selected, and assays were modified until satisfactory reproducibility was obtained. Furthermore, probes had to be compatible with commercial 96-well plates and plate readers, and generate strong detectable signals in commonly used assay buffers and with mixtures of different concentrations of biological thiols tissue components. Commercially available and well-priced probes would facilitate conduction of high-throughput screening assays. Thus, Sf7-AM, an elegant, selective, sensitive, non-invasive and commercially available probe was mainly used in this report.

In this study, florescence probe (SF7-AM) is used to measure the production of hydrogen sulfide. As seen in Figure 4, chemo-selective reduction of azides to amines in the fluorogenic SF7-AM occurs in the presence of H_2S, causing fluorescence. The amount of fluorescence is directly proportional to the amount of H2S production and is measured by using a fluorimeter. It is assumed that when an inhibitor binds to an enzyme, less H_2S will be produced and detected compared to the standard (negative control) levels.

7-Azido-4-Methylcoumarin (AzMC) is popular and readily available small coumarinyl moiety, was used alongside SF7-AM in this study, the probe was designed and synthesised by MK Thorson (Thorson, 2014). Exploiting the reducing property of H2S, they synthesised the azido derivative as a probe which is readily reduced to fluorogenic amine in the presence of H_2S. The aforementioned reduction produces strong fluorescence signal, which is used to detect either exogenous or endogenous cellular H_2S in samples. This probe is commercially available because it is easily synthesised and relatively stable, with good sensitivity to H2S and selectivity over other biological species such as RNS, RSS, ROS and anions. In addition, successful real-time visualization of H_2S in tissues was reported. A well established linear relationship between concentration of H_2S and fluorescence intensity was observed. The probe was stable in degassed PBS buffers within the pH range (5.9–7.9) and produced intense fluorescence when H_2S was added. Finally, this probe is easy to procure and cost effective in detection and high-throughput screening assays related to biological H_2S.

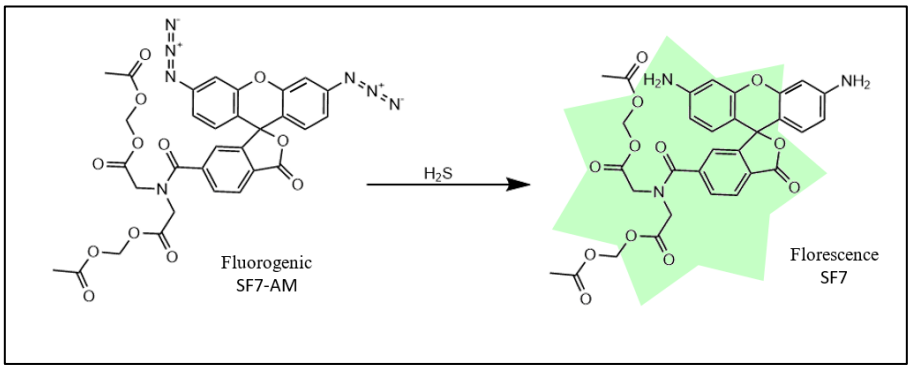


Figure 4 Chemoselective reduction of azides to amines in the fluorogenic SF7-AM occurs in the presence of H2S, causing fluorescence. (Source: Personal collection)

1.7.1 Signal Interference in Fluorescence-Based H_2S Assays

In H_2S fluorescence detection assays, reduced fluorescence can arise from two fundamentally different mechanisms: quenching of the fluorescent signal or scavenging of H_2S itself. Although both lead to lower measured fluorescence, they reflect very different underlying processes.

1.7.1.1. Mechanisms of Quenching

In the context of biological assays, quenching refers to any process that reduces or inhibits a detectable signal, such as fluorescence, luminescence, or colorimetric readouts, without necessarily affecting the biological activity itself. Failure to account for quenching can lead to false conclusions, such as misidentifying a compound as an enzyme inhibitor when it is actually interfering with the detection signal (Chen et al., 1999).

1.7.1.2. Scavenging (Analyte-Level Interference)

An H_2S scavenger is a chemical substance or compound that could remove or neutralize H_2S from a particular environment. In biological assays, an H_2S scavenger chemically reacts with free H_2S, removing it from solution. As H_2S availability has been artificially reduced, scavenging leads to biologically misleading conclusions. In case of fluorescence based screening, less H_2S is available to react with the fluorescent probe, which leads to reduced fluorescence. Notably, in the case of scavenging, the fluorescent readout remains accurate because the probe itself is not directly interfered with, in contrast to quenching (Battin & Brumaghim, 2009).

1.7.1.3. Relevance to Fluorescence-based H_2S detection assays

Compounds tested for enzyme inhibition may sometimes interact directly with fluorescent probes, resulting in reduced signals that are independent of any actual enzymatic inhibition (Möller & Denicola, 2002). In H_2S detection assays, for instance, a quenching compound can decrease fluorescence even when H_2S production is unaffected, either by absorbing emitted light from the fluorophore or by interacting with its excited state (Bantzi et al., 2021). Such effects can potentially mislead the interpretation of enzyme inhibitor screens. Therefore, it is essential to distinguish true enzymatic inhibition from probe quenching. This concept is illustrated schematically in Figure 5.

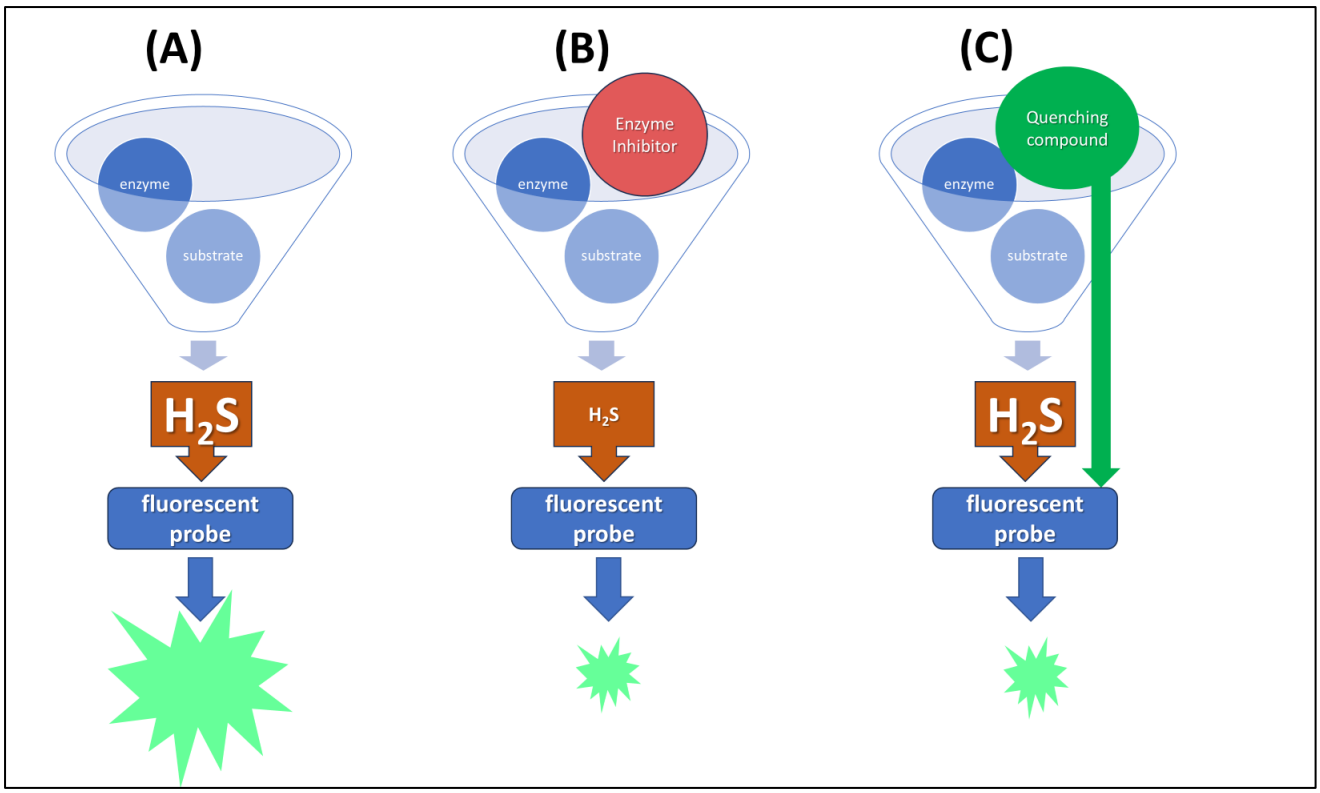


Figure 5 Schematic illustration of quenching versus enzyme inhibition in H_2S fluorescence assays.

(A) In the absence of inhibitors, the enzyme produces H_2S, which reacts with the fluorescent probe to produce fluorescence. (B) In the presence of a true enzyme inhibitor, H_2S production is reduced, resulting in decreased fluorescence. (C) When a quenching compound is present, H_2S production remains unchanged, but the compound interacts directly with the probe, reducing the fluorescent signal independently of enzyme activity.

Accordingly, appropriate control experiments are essential. Comparing fluorescence signals generated from an H_2S donor in the presence and absence of the test compound provides a straightforward means of assessing whether reduced signal intensity arises from direct interaction with the fluorescent probe or from scavenging of H_2S in solution. If no change in fluorescence is observed under enzyme-free conditions, the likelihood of direct signal interference is considered low.

Mercaptopyruvate, the physiological substrate of 3-MST, non-enzymatically and spontaneously releases a measurable amount of H_2S in solution (Augsburger and Szabo, 2018) and can therefore serve as a suitable H_2S donor surrogate in fluorescence-based detection assays. Its use offers two advantages: first, it is already an integral component of the assay system and thus represents an appropriate internal control; second, it generates H_2S rapidly compared with many exogenous H_2S-releasing compounds, facilitating efficient assessment of potential quenching or scavenging effects.

GYY4137 is a novel H_2S donor, recognized for its ability to release H_2S in a controlled and sustained manner. This compound is classified as a phosphorodithioate derivative and is designed to provide a slower release of hydrogen sulfide compared to traditional donors such as sodium hydrosulfide (NaHS) and is used as a marker for quenching effects (Raggio et al., 2018; Whiteman et al., 2015). In Figure 6 GYY4137 structure is shown and compared with 3MST substrate mercaptopyruvate, which is used in our own assay setup as a replacement quenching assessor.

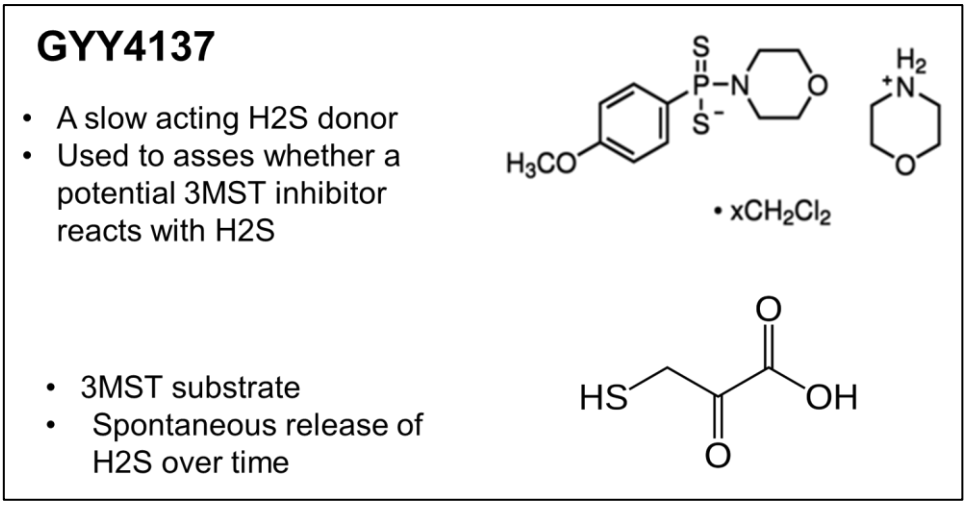


Figure 6 Chemical structure of GYY4137 and 3MST substrate mercaptopyruvate

1.8 Inhibitors of H_2S producing enzymes

As a consequence of the relatively recent discovery of H_2S enzymatic production and its myriad of physiological functions, the identification of potent and selective inhibitors for each enzyme is in its early stages. Furthermore, the later discovery of the therapeutic significance of inhibiting H_2S production delayed the process further. Discovery of novel inhibitors will aid the pharmacological investigations, providing much needed insights on the specific actions of H_2S, similar to how NO synthase inhibitors, such as NG-monomethyl-l-arginine (an analogue of l-arginine), aided the understanding of the functionalities of NO (Gillespie et al., 1989).

Several inhibitors of H_2S synthesising enzymes have been reported (Asimakopoulou et al., 2013). Due to the belated discovery of 3MST, CBS and CSE inhibitors were, naturally, discovered and researched first, including aminooxyacetic acid (AOAA), β-cyano-L-alanine (BCA) and propargylglycine (PAG) (Whiteman et al., 2011). PAG has been established to inhibit CSE via irreversible suicide inactivation. It is an antibiotic produced by Streptomyces sp. and the crystal structure of the enzyme-inhibitor complex was captured with PLP as the cofactor. It was elucidated that only the L-isoform acts as an inhibitor, while the D-isoform is toxic when metabolised (Asimakopoulou et al., 2013). In earlier studies, it was not reported which racemic form was used and the IC50 fluctuated between studies, which could be attributed to the use of purified enzyme or intact cells as PAG has limited cell membrane permeability. The IC50 of the isolated L-isoform was reported to be 40 µM, with PAG showing selectivity for recombinant human CSE versus CBS. Unfortunately, there are a few disadvantages to using this compound, chiefly its inhibition of other enzymes when administered in millimolar concentrations. PAG was reported to inhibit aspartate aminotransferase and alanine aminotransferase (Asimakopoulou et al., 2013).

BCA is another compound used to inhibit CSE/CBS (Whiteman et al., 2011). It is more potent than PAG against CSE, with a lower IC50, but is not as selective as PAG, showing inhibitory actions on CBS in millimolar concentrations. Similar to PAG, BCA has the drawback of inhibiting other enzymes like aspartate b-decarboxylase and alanine aminotransferase, but unlike PAG, it binds reversibly to the enzymes (Asimakopoulou et al., 2013).

AOAA is commonly used in CBS inhibition experiments. Initially, AOAA was used as a CBS selective inhibitor . However, when tested on recombinant CBS and CSE enzymes, it was reported that AOAA in fact inhibits both enzymes with higher potency in relation to CSE. In vivo studies supported the biochemical findings, as AOAA inhibited stimulated vasodilation of rat aortic rings, which do not contain detectable amounts of CBS (Asimakopoulou et al., 2013).

The irreversible inhibitor trifluoroalanine acts on several PLP dependant enzymes, including CBS and CSE. It was suggested that the mode of inhibition was via covalent modification of the enzyme (Singh et al., 2009). When compared with CSE, trifluoroalanine was four times more selective for CBS.

Aminoethoxyvinylglycine (AVG) is another inhibitor of H_2S synthesising enzymes, although not as commonly tested as the other compounds. Initially, AVG was known to inhibit enzymes of the transsulfuration pathway, including PLP dependant enzymes (Clausen et al., 1997). Notably, it has shown high potency in inhibiting CSE, with an IC50 of only 1 µM. AVG was also reported to produce no effects on CBS under 1 mM, however, it has the disadvantage of

affecting other enzymes, which must be taken under consideration despite its high potency for CSE (Asimakopoulou et al., 2013).

A final example of CSE/CBS inhibitors is hydroxylamine (HA), which has been used to inhibit many haem-containing enzymes (Spooren and Evelo, 1997). Interestingly, HA releases NO, an inhibitor that tightly binds to CBS. CBS, being a haem protein, is inhibited by both NO and CO by binding to the haem moiety. However, it has been determined that the actions of HA are direct and independent of NO production, with HA inhibiting both CBS and CSE but 60-times more selective towards CSE (Asimakopoulou et al., 2013).

Regarding selective 3MST inhibitors, none were identified until 2017, when Hanaoka et al. performed high throughput screening and discovered novel 3MST inhibitors (Hanaoka et al., 2017). (see Figure 7) The high-throughput screening was performed using the H_2S-selective fluorescent probe HSip-1 to monitor enzymatic H_2S production. Four structurally related hit compounds (1, 2, 3, and 5) exhibited dose-dependent inhibition of 3MST activity, with IC_{50} values of approximately 2–7 μM. Selectivity profiling suggested that these compounds preferentially inhibit 3MST compared with other H_2S-producing enzymes, CBS and CSE, with compound 3 appearing to show the greatest relative selectivity.

In my previous study (Almehaize,2017), a florescence-based screen of commercially available compounds identified 1-(3,4-Dihydroxyphenyl)-2-[(4-hydroxy-6-methyl-2-pyrimidinyl)sulfanyl]ethanone (CDS004892) as an inhibitor of 3MST. As seen in Figure 8, CDS004892 is structurally similar to the compounds discovered by Hanaoka's research group. Time constrictions prevented further investigations regarding selectivity and potency of CDS004892.

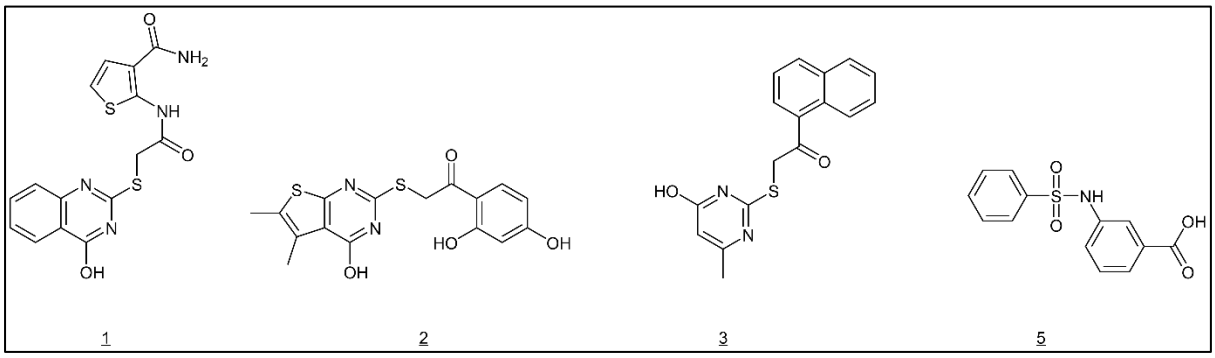


Figure 7 ***Chemical structures of hit compounds that showed dose-dependent inhibitory activity against 3MST in the third screening conducted by Hanaoka et al., 2017.***

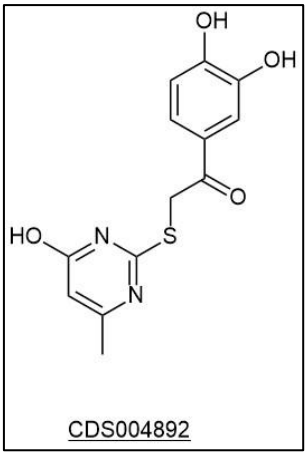


Figure 8 Structure of 1-(3,4-Dihydroxyphenyl)-2-[(4-hydroxy-6-methyl-2-pyrimidinyl)sulfanyl]ethanone (CDS004892)

In a subsequent study, Bantzi et al. (2021) reported the synthesis of a focused library of 63 novel aryl-substituted pyrimidone derivatives, using compound 1a (Hanaoka compound 3) from the literature as the lead scaffold. This compound had previously been identified as a potent and selective 3-MST inhibitor with micromolar IC_{50} values, and therefore served as the structural starting point for analogue development. The primary aim of this work was to enhance 3MST inhibitory potency and selectivity while also exploring potential anticancer activity, particularly against colon cancer cell lines (Bantzi et al., 2021). Biological evaluation of the compound library identified six analogues (1b, 2b, 13a, 13b, 21a, and 26a Figure 9) as the most selective 3MST inhibitors. These compounds demonstrated effective inhibition of 3MST without measurable activity against the other H_2S-producing enzymes CBS or CSE, and none exhibited significant H_2S-scavenging behaviour. Notably, despite comparable in vitro enzyme inhibition, only compound 1b produced a significant reduction in tumour growth in an in vivo MC38 colon cancer model, whereas the parent compound 1a and analogue 2b did not, highlighting the importance of factors beyond enzyme inhibition alone in determining antitumour efficacy.

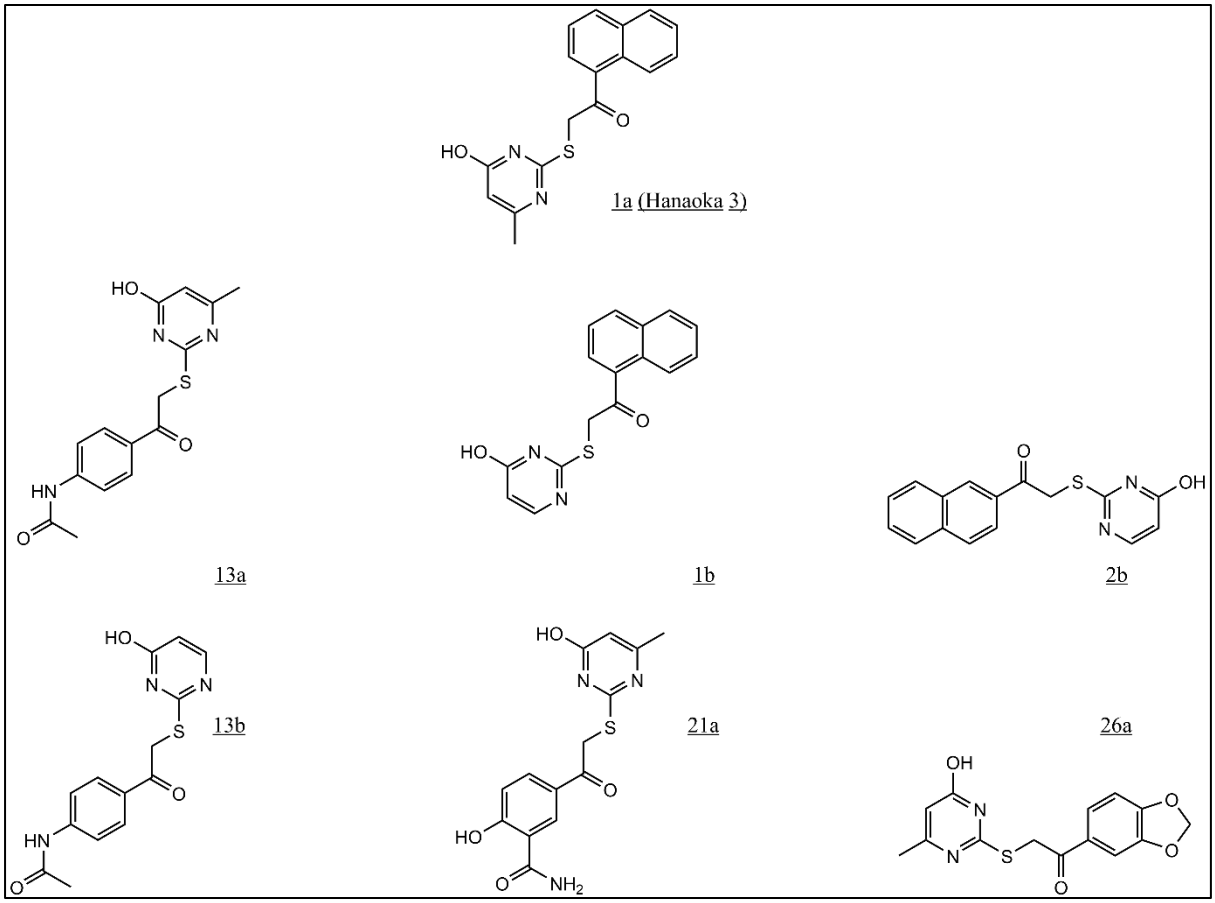


Figure 9 ***Chemical structures of novel 3MST inhibitors identified by Bantzi et al., 2021.***

1.9 Crystal structure of 3MST

The crystal structure of 3MST from *Mus musculus* in complex with a small-molecule inhibitor (PDB ID 5WQJ) provided a major breakthrough in understanding enzymatic H_2S production and inhibitor selectivity. This structure, solved by X-ray crystallography at 1.20 Å resolution, captured the enzyme bound to the inhibitor 7N3 (compound 1), chemically defined as *2-[2-[(4-oxidanylidene-3~{H}-quinazolin-2-yl)sulfanyl]ethanoylamino]thiophene-3-carboxamide* (Hanaoka *et al*., 2017; PMID: 28079151) see Figure 10. Importantly, it provided the first direct experimental evidence that 3MST forms a persulfurated catalytic cysteine intermediate (Cys-SSH) during turnover, confirming a ping-pong sulfur-transfer mechanism.

The structure revealed that inhibitor binding is driven by a long-range electrostatic interaction between the pyrimidone moiety of 7N3 and the negatively charged sulfur atom of the persulfurated catalytic cysteine (Cys247-SSH). This interaction is chemically unique to 3MST and does not occur in related sulfurtransferases, explaining the high selectivity of these inhibitors, which specifically target the persulfide chemistry of the 3MST active site rather than the thiol chemistry used by CBS, CSE, or rhodanese. The exceptional resolution of the structure allowed visualization of the precise hydrogen-bonding and electrostatic networks that stabilise this interaction, providing a detailed blueprint for rational inhibitor design.

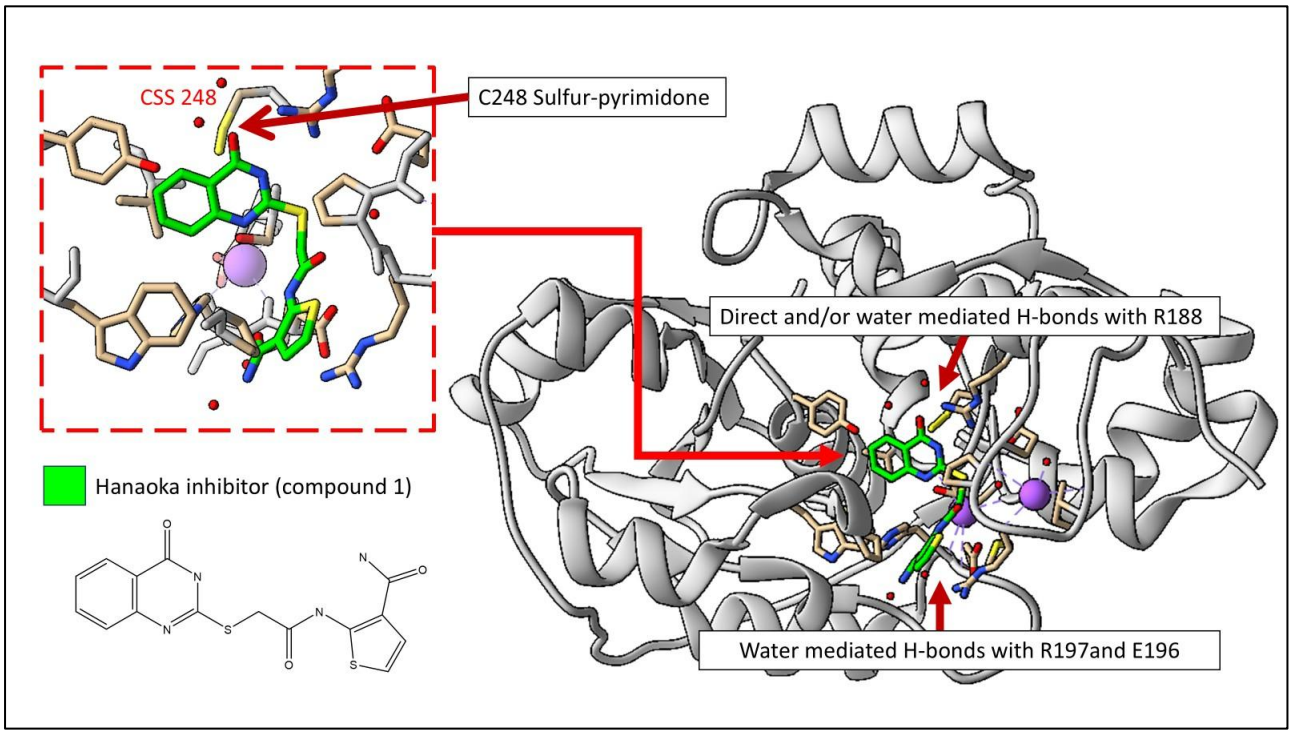


Figure 10 Crystal structure of 3-mercaptopyruvate sulfurtransferase (3MST) from Mus musculus (PDB ID: 5WQJ) in complex with compound 1 (7N3). The structure reveals binding of the inhibitor within the active site via a key electrostatic interaction between its pyrimidone moiety and the persulfurated catalytic cysteine (Cys-SSH), providing a structural basis for selective 3MST inhibition (Hanaoka et al., 2017).

1.10 Aims of the Project

The discovery and development of small-molecule inhibitors of H_2S-producing enzymes has advanced considerably in recent years, highlighting the critical regulatory roles of H_2S in metabolism, redox signalling and disease. Among these enzymes, 3MST has emerged as a major contributor to intracellular H_2S and persulfide production, particularly within

mitochondria. However, the pharmacological investigation of 3MST has been hindered by the limited availability of selective and well-characterised inhibitors, as well as by the chemical reactivity and assay interference associated with many existing tools. Although the first selective 3MST inhibitors were reported in 2017, their small number and restricted chemical diversity continue to limit mechanistic and translational studies of this pathway.

The identification of novel, selective and chemically tractable 3MST inhibitors therefore represents a critical step toward enabling rigorous pharmacological interrogation of the 3MST-H_2S pathway, in a manner analogous to how nitric oxide synthase inhibitors enabled the functional dissection of nitric oxide biology.

Accordingly, in the present study, we aimed to design, synthesise and pharmacologically characterise a focused library of novel 3MST inhibitors using a structure-guided approach. By combining in silico screening of commercially accessible compound libraries with biochemical H_2S detection assays, this work sought to identify new inhibitory scaffolds and to define structure-activity relationships governing 3MST inhibition. In addition, selected lead compounds were synthesised and optimised in order to improve potency and selectivity, with the ultimate goal of generating new chemical tools suitable for future cellular and mechanistic studies of the 3MST-H_2S pathway.

2. Chapter II Virtual Screening for 3MST Inhibitors

2.1 Background

High-throughput docking (HTD) is an advanced computational technique employed in drug design that integrates molecular docking with high-throughput screening methodologies. This approach allows researchers to rapidly evaluate a vast array of compounds against specific biological targets, significantly accelerating the drug discovery process. The primary objective of HTD is to identify potential lead compounds that exhibit favourable binding affinities and specific interactions with target proteins.

The process of high-throughput docking involves the use of sophisticated algorithms to simulate the binding of numerous small molecules to a target protein's active site. Molecular docking has evolved to become a cornerstone of structure-based drug discovery, enabling the identification of novel compounds while reducing the time and costs associated with traditional experimental methods (Pinzi & Rastelli, 2019). The scalability of HTD is particularly advantageous, as it allows for the screening of thousands of compounds in a relatively short timeframe, which is essential in the context of modern drug discovery where large chemical libraries are often utilized. This approach allows researchers to rapidly evaluate a vast array of compounds against specific biological targets, significantly accelerating the drug discovery process. The primary objective of HTD is to identify potential lead compounds that exhibit favorable binding affinities and specific interactions with target proteins.

One of the critical challenges in high-throughput docking is the accuracy of docking scoring functions. While molecular docking methods are cost-effective and fast, they can sometimes struggle to reliably distinguish between active compounds and decoys, as well as to accurately predict binding modes (Guterres et al., 2022). To address these limitations, researchers have developed various enhancements, including the integration of molecular dynamics simulations to refine docking results and improve the discrimination of active from inactive compounds (Guterres & Im, 2020).

Additionally, the application of high-throughput docking is not limited to traditional small-molecule libraries. This method is gaining traction in the context of fragment-based drug discovery (FBDD), where smaller, low-affinity ligands are screened and subsequently optimized into higher-affinity compounds (Fang et al., 2016). This approach allows for the identification of novel ligands that may not be apparent in larger compound libraries, thereby expanding the potential for discovering effective therapeutics.

The advancements in computational power and algorithms have also facilitated the implementation of machine learning techniques in high-throughput docking. For instance, studies demonstrate how machine learning can enhance the efficiency and accuracy of virtual

screening processes, thereby improving the overall hit rates in drug discovery campaigns (Masters et al., 2023). These innovations are crucial as they enable researchers to sift through extensive datasets more effectively, identifying promising candidates for further experimental validation.

To put it briefly, high-throughput docking represents a pivotal advancement in drug design, combining the principles of molecular docking with high-throughput screening to facilitate the rapid identification of potential drug candidates. By leveraging computational techniques and addressing the challenges associated with docking accuracy, HTD enhances the efficiency of the drug discovery process, ultimately leading to the development of novel therapeutics. Docking has evolved to become a cornerstone of structure-based drug discovery, enabling the identification of novel compounds while reducing the time and costs associated with traditional experimental methods (Pinzi & Rastelli, 2019).

One of the critical challenges in high-throughput docking is the accuracy of docking scoring functions. While molecular docking methods are cost-effective and fast, they can sometimes struggle to reliably distinguish between active compounds and decoys, as well as to accurately predict binding modes (Guterres et al., 2022). To address these limitations, researchers have developed various enhancements, including the integration of molecular dynamics simulations to refine docking results and improve the discrimination of active from inactive compounds (Guterres & Im, 2020).

The advancements in computational power and algorithms have also facilitated the implementation of machine learning techniques in high-throughput docking. For instance, studies by demonstrate how machine learning can enhance the efficiency and accuracy of virtual screening processes, thereby improving the overall hit rates in drug discovery campaigns (Masters et al., 2023). These innovations are crucial as they enable researchers to sift through extensive datasets more effectively, identifying promising candidates for further experimental validation.

High-throughput docking represents a pivotal advancement in drug design, combining the principles of molecular docking with high-throughput screening to facilitate the rapid identification of potential drug candidates. By leveraging computational techniques and addressing the challenges associated with docking accuracy, HTD enhances the efficiency of the drug discovery process, ultimately leading to the development of novel therapeutics.

2.1.1 DataWarrior

DataWarrior is a versatile software tool designed for data visualization and analysis, particularly in the field of chemistry. It allows users to perform exploratory data visualizations, enabling rapid graphical inspection of patterns within datasets. The software is particularly noted for its ability to calculate chemical descriptors, which are essential for assessing various properties of chemical compounds, including their potential toxicity and biological activity (Sander et al., 2015).

The accuracy of DataWarrior can be inferred from its widespread use in various research studies, where it has been employed to generate visual representations of chemical spaces and to analyze complex datasets. For instance, it has been utilized to create Bemis-Murcko scaffolds, which are crucial for understanding the structural features of chemical compounds (Ion et al., 2020). Additionally, the software has been integrated into studies assessing the activity landscapes of drug candidates, indicating its reliability in providing meaningful insights into chemical interactions and properties (Naveja & Medina-Franco, 2015).

Furthermore, DataWarrior's open-source nature allows for continuous improvement and validation by the scientific community, which enhances its credibility and accuracy. The software has been cited in numerous peer-reviewed articles, demonstrating its acceptance and trustworthiness among researchers (Sander et al., 2015; Silva et al., 2023).

DataWarrior is a powerful tool for data analysis in chemistry, with a proven track record of accuracy and reliability as evidenced by its application in various scientific studies. Its ability to facilitate complex data visualizations and analyses makes it an invaluable resource for researchers in the field.

2.1.2 Fragment Fingerprint (FragFP)

FragFP, or Fragment Fingerprint, is a computational tool utilized in cheminformatics for the representation of molecular structures. It is based on a substructure fragment dictionary that consists of 512 predefined structural fragments, which allows for the generation of binary fingerprints that can be used to characterize and compare chemical compounds effectively (Yu, 2023; Sander et al., 2015; Korff et al., 2009). This descriptor is particularly useful in various applications, including virtual screening, similarity searching, and clustering of chemical libraries.

The FragFP descriptor operates by encoding the presence or absence of specific structural fragments within a molecule into a binary format. Each bit in the fingerprint corresponds to a particular fragment, where a '1' indicates the presence of that fragment and a '0' indicates its absence. This method of representation facilitates the rapid comparison of large sets of compounds, making it a valuable tool in drug discovery and development (Egieyeh et al., 2016; Korff et al., 2009; Ertl et al., 2015).

In practical applications, FragFP has been employed in software such as DataWarrior, which is designed for data visualization and analysis in chemistry. Researchers have utilized FragFP to perform principal component analysis (PCA) and to visualize chemical spaces covered by various libraries of compounds (Lagarde et al., 2018; Handa, 2023; Montoya-Inzunza et al., 2023). Additionally, it has been instrumental in identifying structural similarities among compounds, aiding in the discovery of new drug candidates and the repositioning of existing drugs for new therapeutic targets (Kaur et al., 2022; Moreira et al., 2023).

The utility of FragFP extends beyond mere structural comparison; it also plays a role in machine learning applications where it can be used to cluster compounds based on their chemical similarity, thereby enhancing the efficiency of virtual screening processes (Tsebriy,

2023; Goldwaser et al., 2022). This capability is particularly important in the context of identifying potential inhibitors for various biological targets, as demonstrated in studies focusing on antimalarial and antimicrobial agents (Kaur et al., 2022; Moreira et al., 2023; Whiteland et al., 2020).

2.1.3 AutoDock Vina

AutoDock Vina is a widely utilized molecular docking software that serves as a successor to the original AutoDock program. It was developed to enhance the accuracy and efficiency of predicting the binding modes of small molecules to macromolecular targets, such as proteins. The software employs a sophisticated scoring function and a search algorithm that significantly improves the prediction of binding poses and affinities compared to its predecessor, AutoDock 4 (Wang et al., 2016; Li et al., 2014; Gaillard, 2018).

The accuracy of AutoDock Vina has been extensively evaluated in various studies. For instance, it has been shown to outperform AutoDock 4 in terms of binding pose prediction accuracy, with improvements attributed to its novel scoring function and enhanced sampling methods (Wang et al., 2016; Lin & Siu, 2018). In comparative studies, AutoDock Vina has demonstrated a high scoring power, making it a preferred choice for high-throughput screening (HTS) applications in drug discovery (Kamerlin et al., 2020; Hassan et al., 2017).

Additionally, research indicates that AutoDock Vina achieves a significant reduction in computational time while maintaining a high level of accuracy, which is crucial for large-scale virtual screening efforts (Shidi et al., 2022). The software's ability to handle complex docking scenarios, including the modeling of specific features such as macrocycles and explicit water molecules, further contributes to its robustness and versatility (Ding et al., 2023; Eberhardt et al., 2021).

The accuracy of binding affinity predictions in AutoDock Vina has been a subject of research, with studies indicating that while Vina often provides more accurate binding poses compared to its predecessor, AutoDock4, it may not always correlate well with experimental binding affinities (Nguyen et al., 2019; Lin & Siu, 2018). For instance, a study highlighted that AutoDock Vina achieved a high docking success rate but exhibited a low correlation coefficient for binding affinity when compared to experimental data (Pham et al., 2021). This discrepancy suggests that while Vina is effective for pose prediction, further refinement of its scoring function may be necessary to enhance its predictive accuracy for binding affinities (Pham et al., 2021).

In practical applications, AutoDock Vina has been utilized in various studies to predict binding affinities of different compounds against specific targets. For example, in a study investigating potential MAO-B inhibitors, the binding affinities of several natural compounds were evaluated using AutoDock Vina, demonstrating its utility in drug discovery (Ferrari, 2024). Similarly, another study reported binding affinities for a positive control compound using multiple docking programs, including AutoDock Vina, which provided comparative insights into the performance of different docking tools (Shukla et al., 2023).

The binding affinity predictions from AutoDock Vina have been validated against experimental results in several cases. For instance, a study on phytochemicals showed that the binding affinities predicted by AutoDock Vina were consistent with experimental findings, reinforcing the reliability of the software in virtual screening applications (Ahmed & Alkali, 2018). Additionally, the program's ability to predict binding affinities has been leveraged in the identification of novel inhibitors for various diseases, including SARS-CoV-2, where it was used to assess the interaction of phytochemicals with viral proteins (Hiremath et al., 2020).

Predicted binding affinities in AutoDock Vina are a crucial aspect of molecular docking studies, as they provide insights into the strength of interaction between ligands and their target proteins. AutoDock Vina employs a scoring function that estimates binding affinities based on the conformational energy of the ligand-receptor complex, which is influenced by various factors including the ligand's shape, size, and the nature of interactions with the binding site.

AutoDock Vina serves as a powerful tool for predicting binding affinities in molecular docking studies, although its predictions should be interpreted with caution due to potential discrepancies with experimental data. Continuous improvements in its scoring algorithms and validation against experimental results are essential for enhancing its predictive capabilities in drug discovery.

The characteristics of a small and rigid substrate binding pocket in enzymes significantly influence substrate screening and the overall enzyme functionality. Such structural features can dictate the specificity, efficiency, and selectivity of enzyme-substrate interactions, which are crucial for both natural enzymatic processes and biotechnological applications.

2.1.4 Specificity and Selectivity

A small and rigid binding pocket typically indicates that the enzyme is highly selective for its substrates. This specificity arises because the pocket can only accommodate substrates that fit precisely within its confines. For example, describe a "gourd" shaped substrate-binding pocket that can accommodate both bulky and small groups of a substrate, which allows for selective binding and anti-Prelog selectivity in their dehydrogenase/reductase enzymes (Su et al., 2019). This specificity is essential for ensuring that the enzyme catalyses the correct reaction without interference from similar molecules.

The rigidity of the binding pocket further enhances this selectivity by limiting the conformational flexibility that could otherwise allow for the accommodation of non-specific substrates. et al. emphasize that the dynamical properties of substrate binding pockets can significantly influence binding affinity and specificity, suggesting that rigid pockets may restrict the binding of substrates that do not precisely match the enzyme's active site (Yang, 2024). This characteristic can be advantageous in drug design, as it allows for the development of inhibitors that can effectively block the active site without affecting similar enzymes.

A small and rigid binding pocket, as seen in 3MST, typically indicates that the enzyme is highly selective for its substrates. This specificity arises because the pocket can only accommodate substrates that fit precisely within its confines This specificity is essential for ensuring that the enzyme catalyses the correct reaction without interference from similar molecules.

The rigidity of the binding pocket further enhances this selectivity by limiting the conformational flexibility that could otherwise allow for the accommodation of non-specific substrates. The dynamical properties of substrate binding pockets can significantly influence binding affinity and specificity, suggesting that rigid pockets may restrict the binding of substrates that do not precisely match the enzyme's active site (Yang, 2024). This characteristic can be advantageous in drug design, as it allows for the development of inhibitors that can effectively block the active site without affecting similar enzymes, such as CBS/CSE.

2.1.5 Impact on Substrate Screening

The small size of the binding pocket can complicate substrate screening efforts. When screening for potential substrates or inhibitors, a rigid and small binding pocket may limit the range of compounds that can be tested effectively. For instance, discuss how the substrate-binding pocket of trypsin is formed by specific residues that create a defined space for substrate interaction, which can restrict the types of substrates that can be evaluated (Chi et al., 2011). This limitation necessitates careful selection of substrates during screening to ensure that only those that can fit into the binding pocket are considered.

Moreover, the rigidity of the binding pocket can lead to a lack of induced fit, where the enzyme does not undergo significant conformational changes upon substrate binding. et al. note that increased rigidity in the active pocket can enhance the enzyme's ability to bind substrates effectively, but it may also reduce the enzyme's adaptability to accommodate different substrates (Wang, 2024). This rigidity can hinder the discovery of novel substrates or inhibitors, as the screening process may overlook compounds that do not fit the predefined structural criteria.

2.1.6 Implications for Inhibitor Design

The structural characteristics of a small and rigid binding pocket also have significant implications for inhibitor design. Inhibitors that mimic the substrate's structure can be designed to fit snugly within the binding pocket, effectively blocking substrate access and inhibiting enzyme activity. highlight that the specificity pockets of enzymes like trypsin are finely tuned for their natural substrates, which can be exploited in designing selective inhibitors (Gráf et al., 1987). However, the challenge lies in ensuring that the inhibitors are sufficiently similar to the substrate to fit into the binding pocket while also being distinct enough to prevent substrate binding.

Furthermore, the limited space within a small binding pocket can lead to competitive inhibition scenarios, where the binding of an inhibitor directly competes with substrate binding. discuss how the rigidity of a binding pocket can influence the binding dynamics of both substrates and inhibitors, which is critical for understanding how to design effective inhibitors that can outcompete natural substrates (Baron & Vellore, 2012). This competitive aspect is particularly important in drug development, where the goal is often to create inhibitors that can effectively block enzyme activity in the presence of physiological concentrations of substrates.

A small and rigid substrate binding pocket, such as 3MST ligand binding site, significantly affects substrate screening by enhancing specificity and selectivity while limiting the range of substrates that can be effectively evaluated. This structural characteristic can complicate the discovery of new substrates and inhibitors, necessitating careful consideration during screening processes. Additionally, the implications for inhibitor design are profound, as the rigidity and size of the binding pocket dictate the types of compounds that can be developed as effective inhibitors. Understanding these dynamics is crucial for advancing enzyme-related research. The characteristics of a small and rigid substrate binding pocket in enzymes significantly influence substrate screening and the overall enzyme functionality. Such structural features can dictate the specificity, efficiency, and selectivity of enzyme-substrate interactions, which are crucial for both natural enzymatic processes and biotechnological applications. As seen below in Figure 11, the binding pocket of 3MST is very narrow.

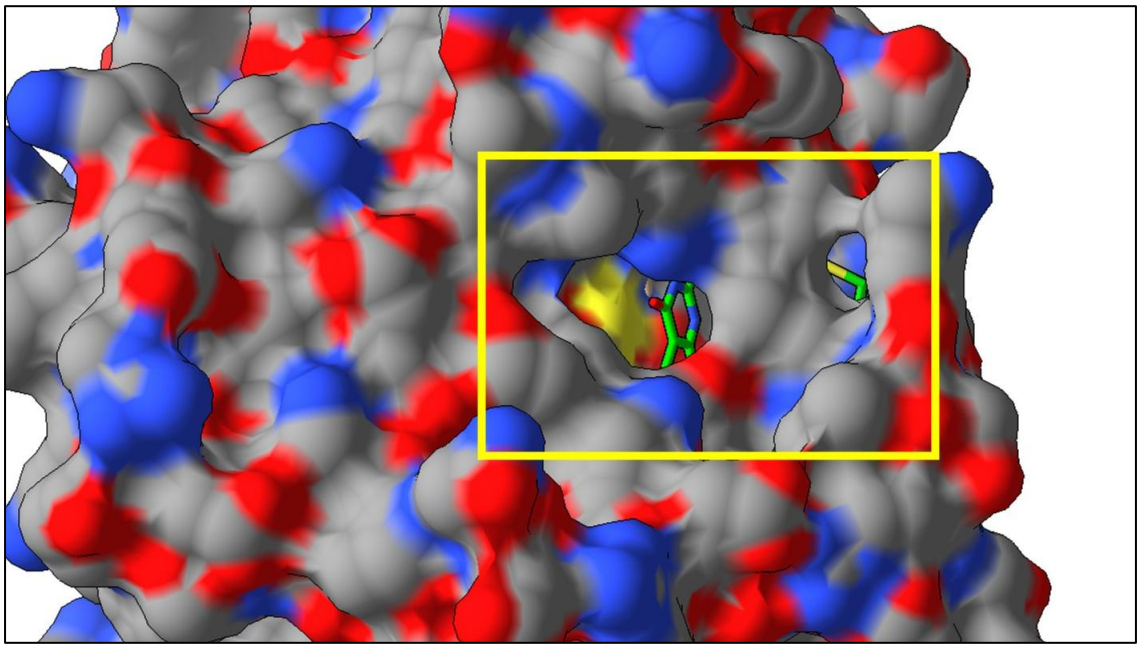


Figure 11 Crystal structure of 3MST showing the narrow ligand-binding pocket. The enzyme is displayed as a surface representation, highlighting the confined binding cavity. Ligand compound 1 is shown bound within this narrow active-site pocket, illustrating how the inhibitor is accommodated within the 3MST binding site (PDB ID: 5WQJ).

3MST has a small and rigid substrate binding pocket, that significantly affects substrate screening by enhancing specificity and selectivity while limiting the range of substrates that can be effectively evaluated. This structural characteristic can complicate the discovery of new substrates and inhibitors, necessitating careful consideration during screening processes. Additionally, the implications for inhibitor design are profound, as the rigidity and size of the binding pocket dictate the types of compounds that can be developed as effective inhibitors.

2.1.7 Structure-activity relationships (SAR)

The determination of structure-activity relationships (SAR) of compounds is a critical aspect of medicinal chemistry, as it provides insights into how the chemical structure of a compound influences its biological activity. This process involved a systematic analysis of various chemical entities to identify structural features that correlate with specific biological effects.

Our first and foundational approaches to SAR analysis was the use of computational tools and data mining techniques. Using Autodock vina and Datawarrior in tandem facilitated the extraction of SAR information from compound datasets in the UON library, thereby aiding in the optimization of lead compounds for biochemical evaluation (Lounkine et al., 2010). The application of network-like similarity graphs in Datawarrior was used to analyze SAR, which played a major role in lead optimization. These computational approaches allowed us to visualize and quantify the relationships between the library's chemical structures and their corresponding biological activities.

Determining the structure-activity relationship of compounds involves a multifaceted approach that integrates computational analysis, molecular descriptor quantification, and advanced machine learning techniques. These methodologies collectively enhance the understanding of how structural variations influence biological activity, ultimately guiding the design and optimization of new therapeutic agents.

2.2 Results

2.2.1 Screening for 3MST inhibitors via SF7-AM fluorescence probe

The University of Nottingham's chemical compound library contains more than 85,000 compounds, which were virtually screened for 3MST inhibitors. Additionally, a similarity test for compounds containing either a pyrimidone ring or 3-benzenesulfonamide as seen in inhibitors from literature was conducted. For the biochemical assays, 222 compounds with the best profiles were selected at 10µM final concentration and tested for 3MST inhibition using SF7-AM fluorescence probe to detect H_2S. Four compounds showed more than 20% inhibition (Figure 12). The two compounds that showed superior inhibition, NCC-00043864 and NCC-00065766, were further investigated in SF7-AM assays to calculate IC_{50} values and confirm activity using counter assays with AzMC fluorescence probe Figure 13, Figure 14). The calculated IC_{50} values of NCC-00065766 and NCC-00043864 are 4.5 µM and 9.7 µM respectively. A full description of the methodology is given in the Experimental chapter.

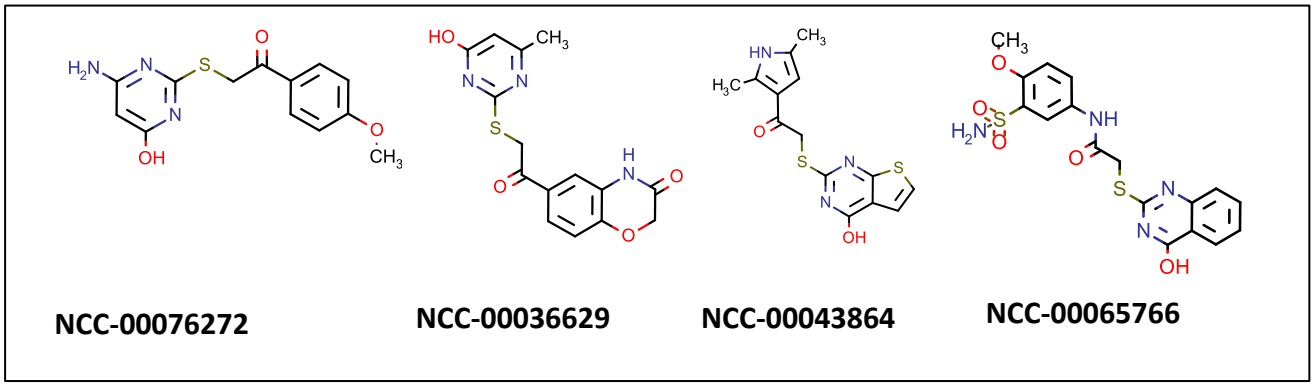


Figure 12 Chemical structures of four hit compounds, which showed more than 20% inhibition in the screening assays

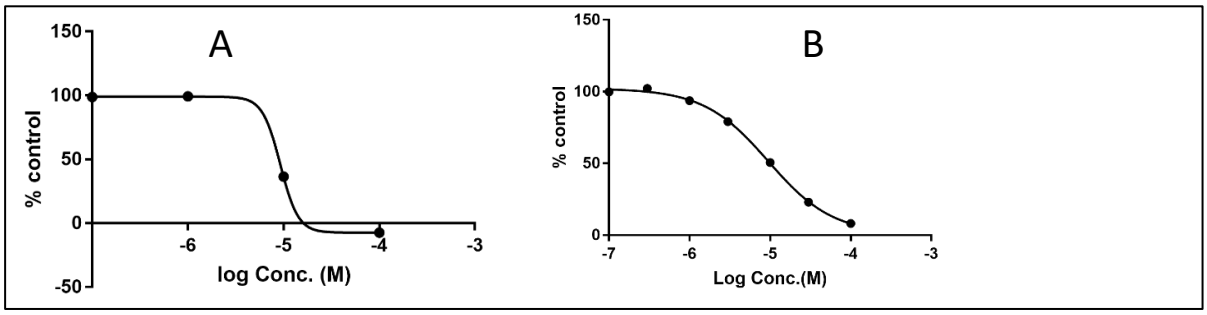


Figure 13 Assay of the inhibitory effect of NCC-00043864 on the enzymatic production of H_2S via the 3mst pathway in rat liver cytosol (RLC) samples (n=3) using H_2S detection assay via AzMC (A) and SF7-AM (B) at 37°C. Data sets represent mean ± SEM.

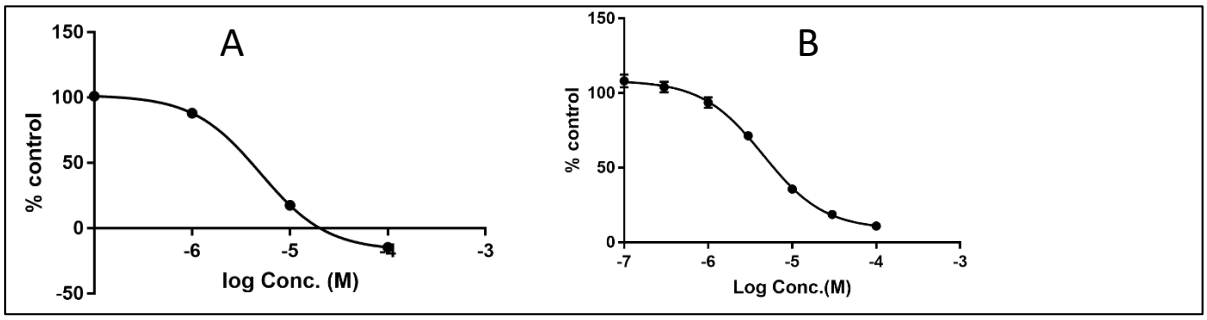


Figure 14 Assay of the inhibitory effect of NCC-00065766 on the enzymatic production of H_2S via the 3mst pathway in rat liver cytosol (RLC) samples (n=3) using H_2S detection assay via AzMC (A) and SF7-AM (B) at 37°C. Data sets represent mean ± SEM.

The physiochemical properties of the screened compounds were calculated using DataWarrior software as shown in Figure 15. Actives from literature (Hanaoka compounds 1, 2, 3 and 5) were added in the software list for calculation. The chart shows that all actives have at least one hydrogen bond donor and at least 5 acceptors. Additionally, cLogP values range between 1-3.5 and molecular weight is less than 450 g/mol. Many inactive compounds in the screening had the same properties, and as seen in Figure 16, most of the screened compounds share structural similarity with inhibitors from literature. Figure 16-B shows that all compounds with high structural similarity (0.6<) to Hanaoka 1 are inactive at 10 µM. Figure 17 shows that only two of the compounds structurally similar to CDS004892 were active, while all others are inactive at 10 µM.

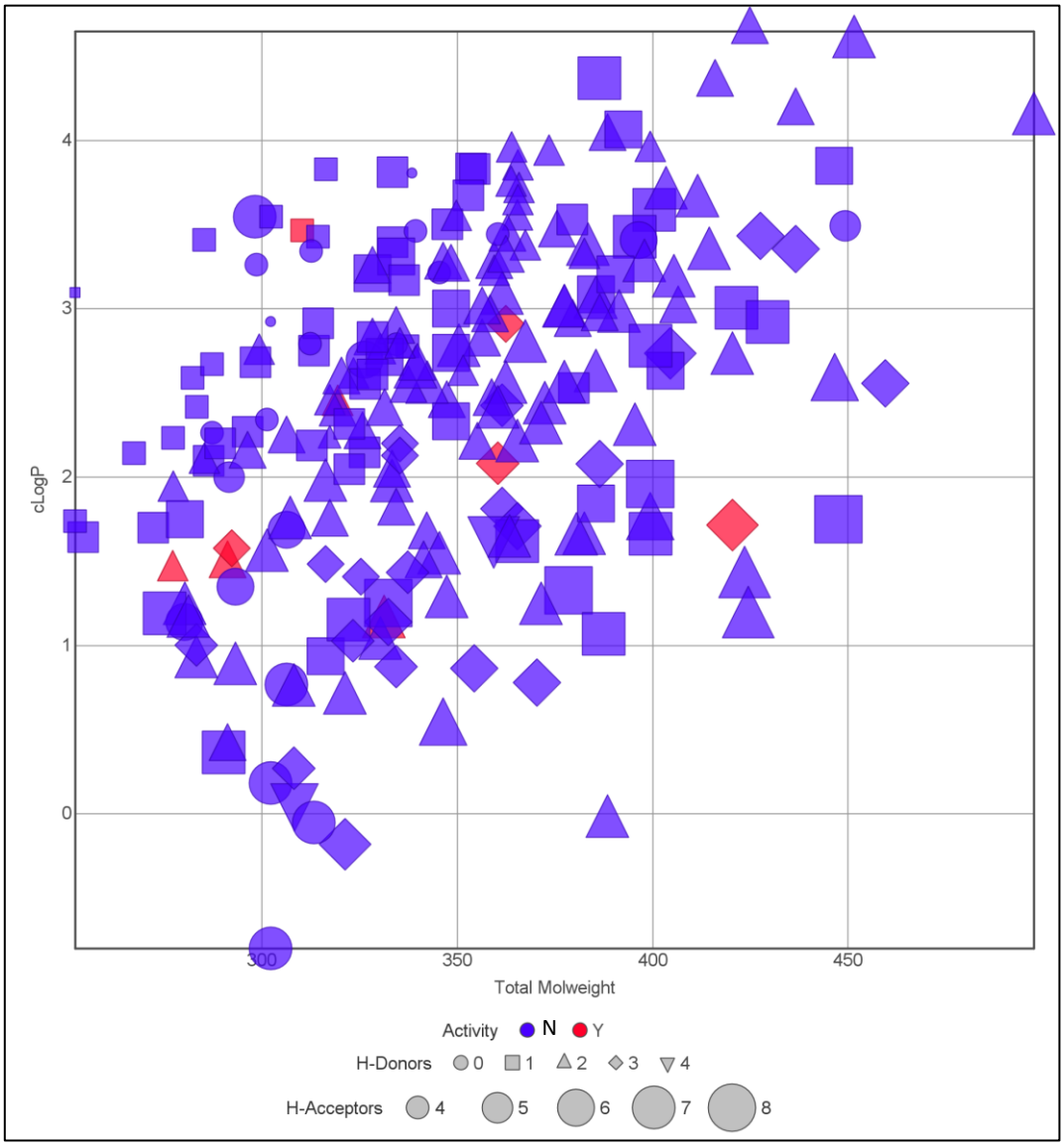


Figure 15 Scatter plot of compounds screened for 3MST inhibitory activity via SF7-AM fluorescence probe. The figure shows biological activity status at 10 µM dubbed (N: not active(blue), Y: yes, active(red)). The size of each shapes indicates the number of H-bond acceptors. The shape itself indicates the number of H-bond doners. The X axis indicates

molecular weight and Y axis ClogP. This plot shows that 'actives' are scattered across the plot with minimal clustering, indicating diversity of physiochemical properties.

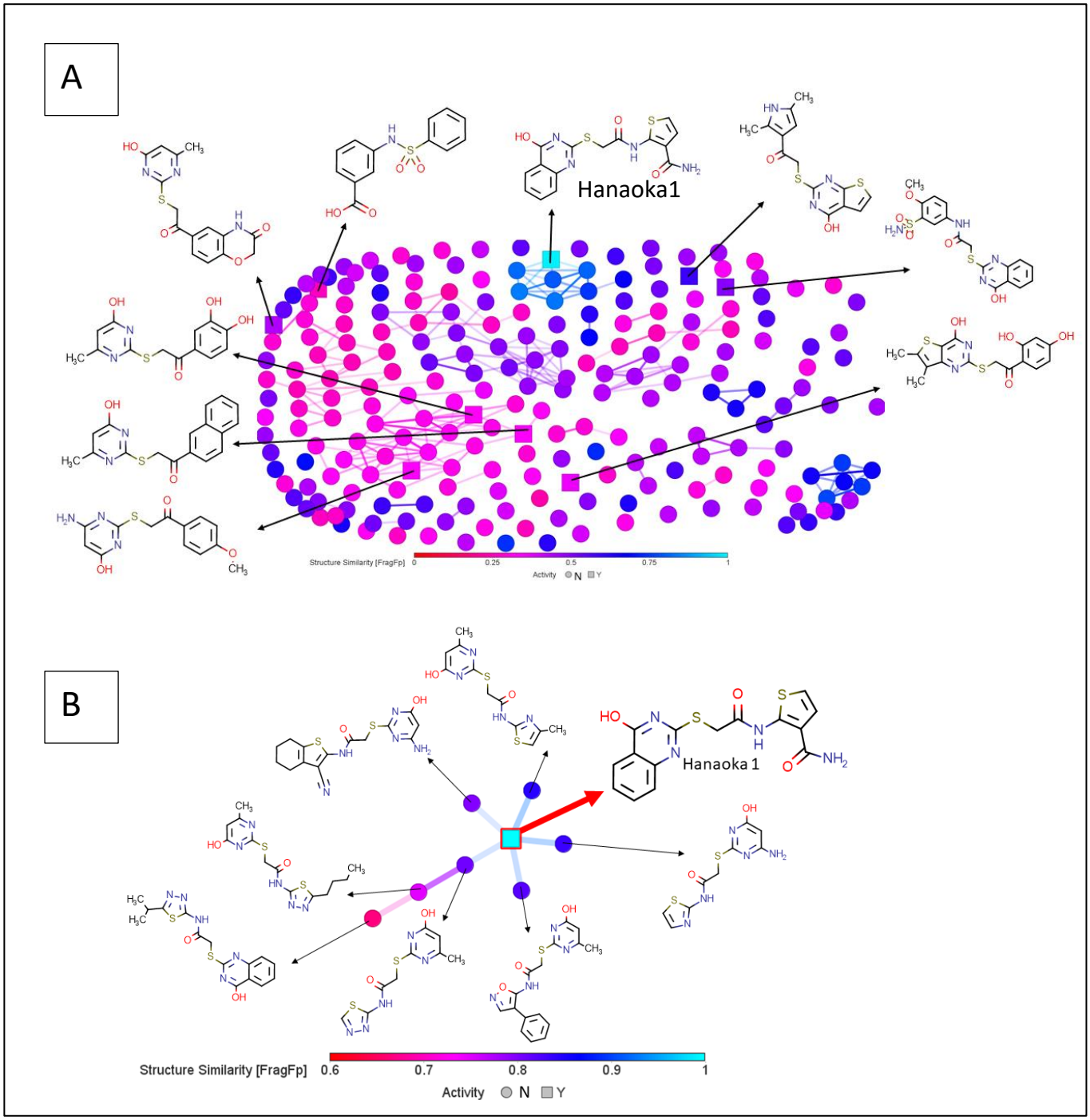


Figure 16 ***Structure similarity tree of screened compounds relative to Hanaoka compound 1.***
(A) shows all screened compounds, with the chemical structures of active compounds displayed, and (B) shows a magnified view of the region surrounding Hanaoka compound 1. Biological activity at 10 µM is indicated by node shape (N = inactive, circles; Y = active, squares). Compounds are clustered in two-dimensional space based on FragFP chemical fingerprints, such that spatial proximity reflects structural similarity to the lead compound Hanaoka 1. Node colour represents the degree of structural similarity (FragFP), with blue indicating higher similarity and red indicating lower similarity. Although many compounds exhibit high structural similarity to Hanaoka 1, none were found to be active in the biochemical assay.

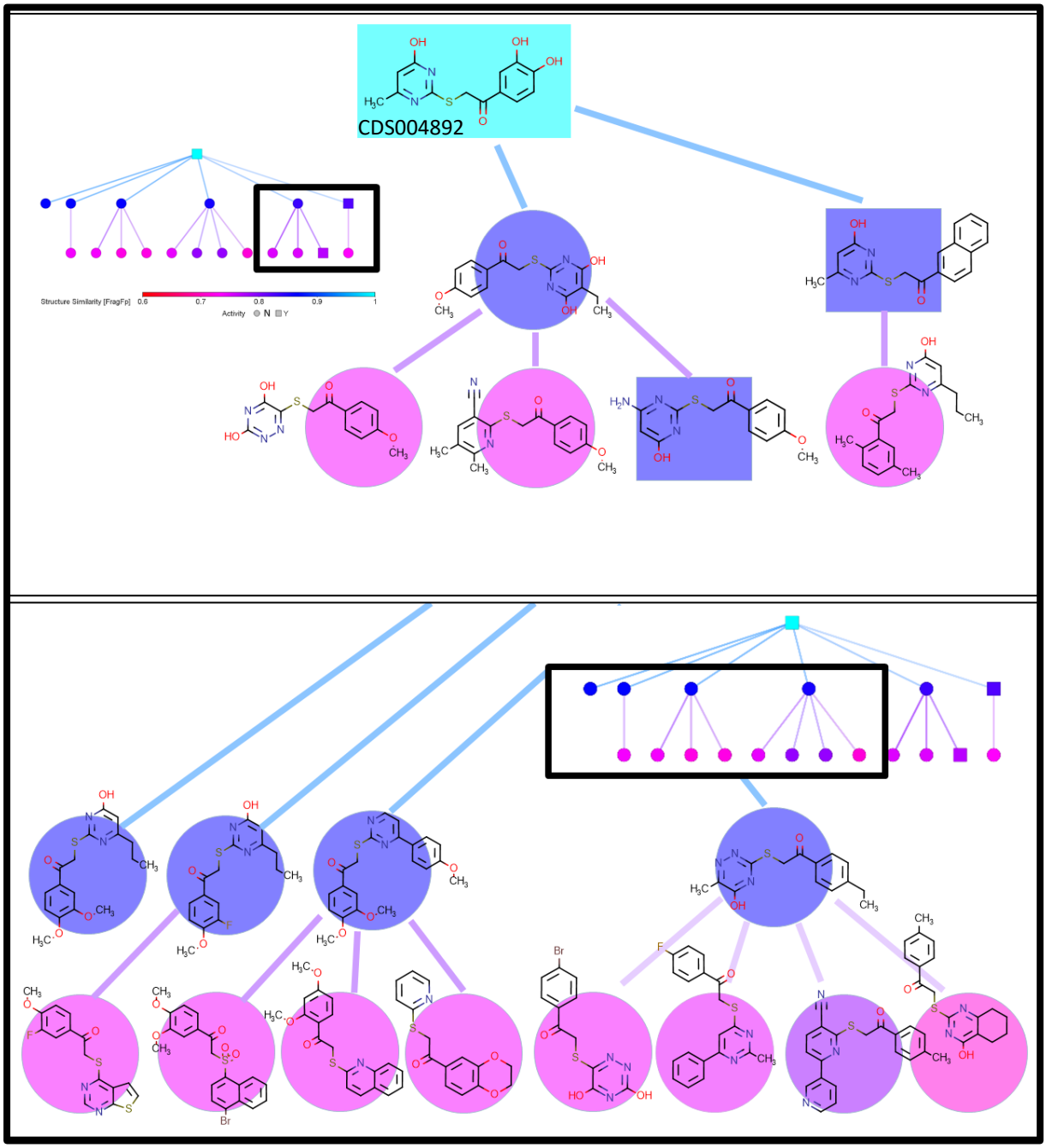


Figure 17 ***Structure similarity tree focused on CDS004892 and neighbouring compounds.***
A magnified view of the region surrounding CDS004892 within the DataWarrior similarity tree is shown. Compounds are positioned according to FragFP chemical fingerprints, such that spatial proximity reflects structural similarity. Biological activity at 10 µM is indicated by node shape (circles = inactive; squares = active). Only two compounds within this structurally related cluster were identified as active in the biochemical assay, highlighting a narrow structure–activity relationship around CDS004892.

2.2.2 Virtual Screening and docking studies of 3MST inhibitors

Docking studies of over 1800 compounds were conducted using UCSF Chimera software. The compounds were selected from the University of Nottingham's chemical library using substructure and similarity search of 3-benzenesulfonamidobenzoic acid (Hanaoka compound 5) and 3-benzenesulfonamide. Compounds were scored by their predicted affinity and categorized into fit and no fit groups. The best score was -10.7 and the poorest was -5.4. Only 350 compounds fit the binding site in the protein. The compounds used in the sulphonamide screen and the corresponding AutoDock Vina results are provided in the Appendix.

"Fit" definition

- Cysteine 248 Sulfur-pyrimidone interaction
- Direct and water mediated hydrogen bonds with Arginine 188
- Water mediated hydrogen bonds with Arginine 197 and Glutamic acid 196

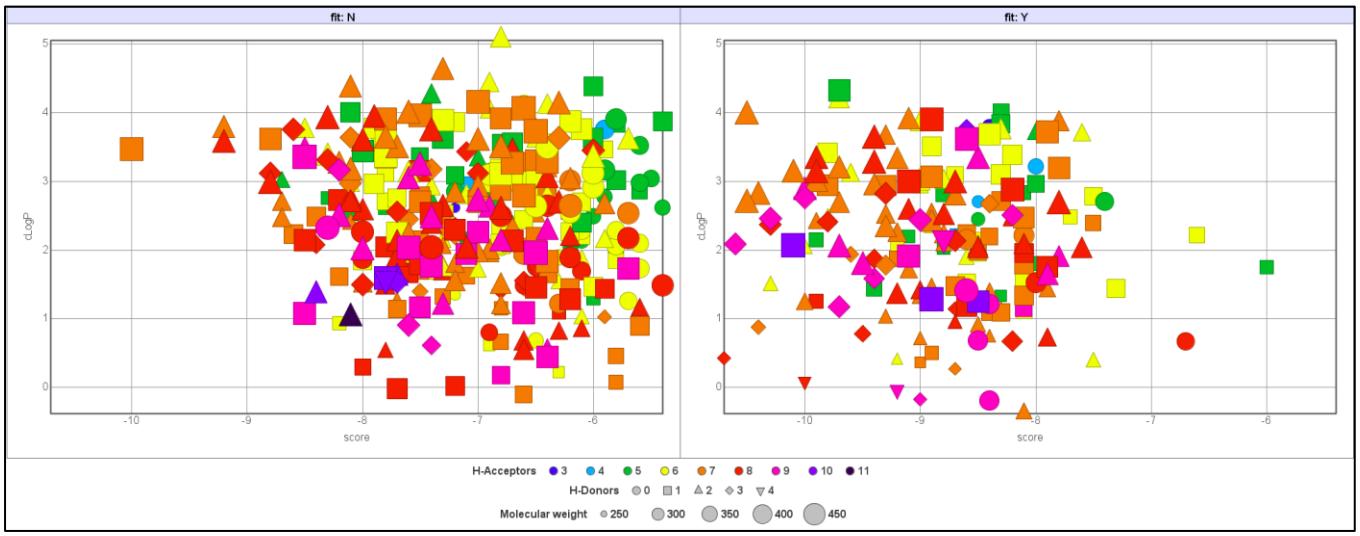


Figure 18 Scatter plot of a representative subset of 523 sulphonamides virtually screened for 3MST inhibition. Compounds are plotted according to docking score (x-axis) and calculated clogP (y-axis), and separated by their predicted binding "fit" classification (left: non-fit, N; right: fit, Y). Point size represents molecular weight, colour indicates the number of hydrogen-bond acceptors, and symbol shape denotes the number of hydrogen-bond donors. This visualization illustrates the physicochemical diversity of the sulphonamide library and the distribution of compounds selected by the fit criteria following virtual screening against 3MST.

As seen in Figure 18, there is an apparent correlation between good binding scores and the probability of fitting into the binding site. All compounds with scores between -10 and -10.7 have at least one hydrogen bond donor (HBD) and six hydrogen bond acceptors (HBA). Other properties like cLogP, polar surface area and molecular weight do not appear to affect binding scores. However, no compounds with a bromine substituent fit the binding site. Also, compounds containing 2,6-Dimethylbenzenesulfonamide showed poor binding scores. Furthermore, branching at the nitrogen atom in the 3-benzenesulfonamide compounds

caused poor predicted binding as seen in Figure 19. Compounds that contain 3-benzenesulfonamidobenzoic acid or have high similarity (0.6<) to it have good binding scores and were most likely to fit the binding site as seen in Figure 20.

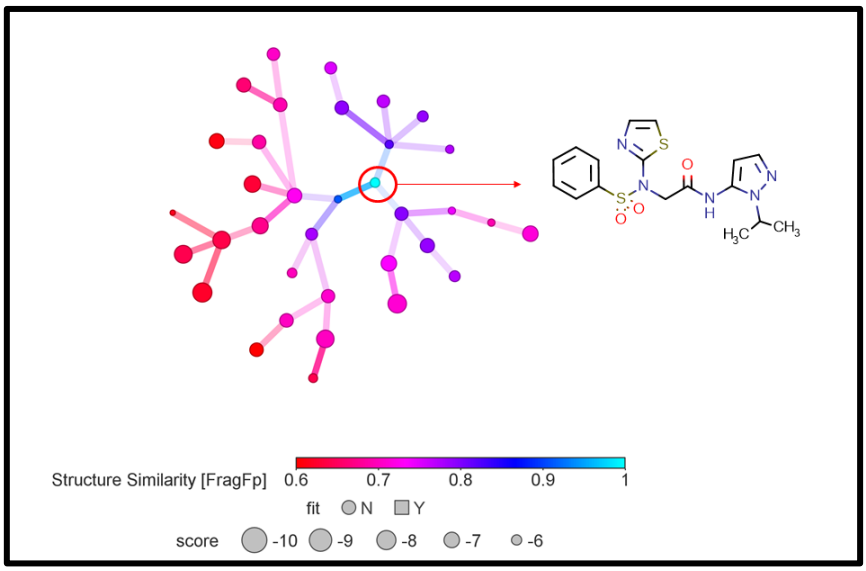


Figure 19 Structure similarity tree of screened compounds containing N-branching in the 3-benzenesulfonamide moiety.Compounds are arranged according to FragFP chemical fingerprints, such that spatial proximity reflects structural similarity within this subseries. Node colour indicates the degree of similarity (FragFP), with blue representing higher similarity and red lower similarity. Node size reflects docking score. The highlighted node (circled) corresponds to the reference compound shown on the right, illustrating its position within the local chemical space defined by N-substituted 3-benzenesulfonamides.

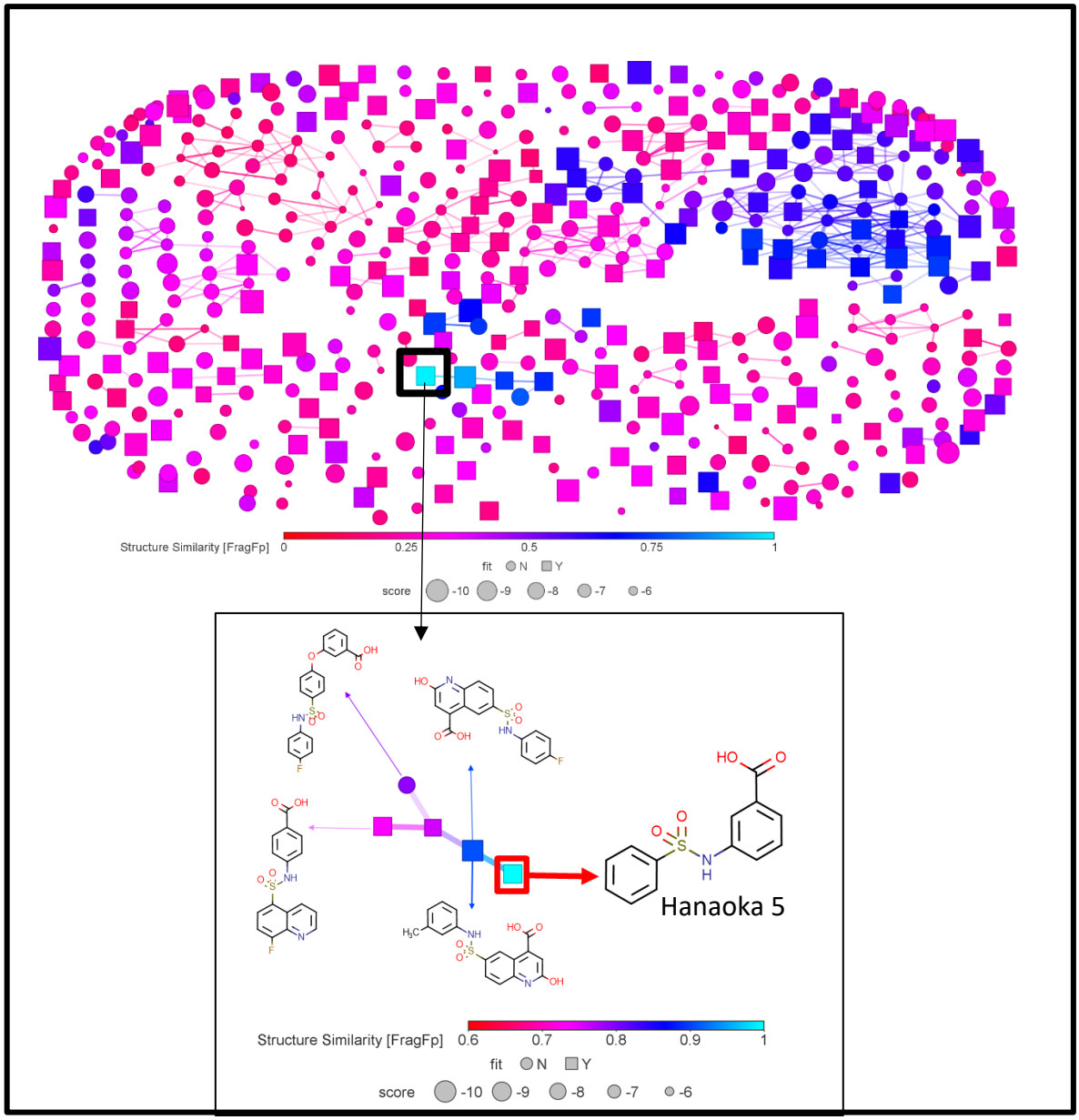


Figure 20 ***Structure similarity tree of screened compounds relative to Hanaoka compound 5.*** *Structure similarity analysis of screened N-branched 3-benzenesulfonamides. The DataWarrior similarity tree shows compounds containing N-substitution within the 3-benzenesulfonamide moiety, arranged according to FragFP chemical fingerprints such that spatial proximity reflects structural similarity. The full map illustrates the overall chemical space of this sub-library, while the magnified view highlights a local cluster centred on the reference compound (circled), whose chemical structure is shown. Node colour indicates the degree of structural similarity (FragFP; blue = high, red = low), node shape denotes predicted binding fit (circles = non-fit, squares = fit), and node size corresponds to docking score.*

2.2.3 Discussion

In this study, the unique University of Nottingham chemical compounds library were screened virtually using the crystal structure of mouse 3MST (PDB ID: 5WQJ)(Hanaoka et al., 2017). Initial hits were visually inspected and a selection of 222 compounds (screening was limited by experimental feasibility and budgetary considerations). The majority of these compounds shared a core pyrimidone ring and were predicted to imitate the literature inhibitors in their mode of action and binding to protein. Hanaoka group suggested that their inhibitors (1,2 and 3) form a novel long-range electrostatic interaction between the positively charged carbonyl moieties in the pyrimidone ring and the persulfurated cysteine (CSS 248) in the active site of 3MST. Inspection of 3-benzenesulfonamidobenzoic acid (Compound 5) in docking studies show similar interaction between the benzenesulphonamide and CSS 248. Most of the selected compounds were docked individually before physical testing to investigate docking poses, scores and proper fit into the active site pocket. Biochemical screening assays of H_2S production using SF7-AM fluorescence probe have proven to be a reliable method that is reproducible, sensitive, relatively inexpensive and easy to perform manually (first year report). Compound samples as small as 2µL (10mM) were sufficient to perform multiple repeats and detect activity in 96-well plates. Utilising state of the art virtual screening programs in combination with available screening methodology was the first step to discovering novel inhibitors and gaining better understanding of a suitable pharmacophore. Compounds that displayed more than 20% inhibition in the initial screening assays were selected for further investigation. Two hits, compound NCC-00065766 and NCC-00043864, showed superior inhibition and displayed activity independent on assay conditions by using a counter screen and a range of concentrations to determine their IC_{50} values. The compounds share a high structural similarity with the established inhibitors from literature and have IC_{50} values in the same micromolar range. Coincidentally, NCC-00065766 contains a benzenesulphonamide moiety, making a unique combination of the pyrimidine structure of compounds 1,2 and 3 and benzenesulphonamide in compound 5. Unfortunately, 218 compounds that also shared high structural similarities in the screen did not display any hint of inhibition at 10uM concentration. As the initial aim was to discover inhibitors with improved potency and selectivity profiles, application of 10uM of test samples in the assay was deemed a sufficient concentration. However, it is possible that these compounds have activity at higher concentrations.

The biochemical screening was separated into two batches, the first one focused on pyrimidones (171 compounds) and the second on benzenesulphonamides (51 compounds). Despite slight selectivity issue against CBS, 3-benzenesulfonamidobenzoic acid (Compound 5) could be considered a more attractive choice of inhibitor as it contains a sulphonamide moiety. Since the discovery of antibacterial sulphonamides, they have become important and favourable functional groups in medicinal chemistry with multiple applications in medicine. This electron-withdrawing motif has displayed many attractive properties, such as an inclination to undergo two-electron interactions over radical processes and resistance to hydrolysis and reduction at sulfur. Sulphonamides were not only used to treat pathogenic bacteria in biological systems, as they have been used as treatments in multiple disease models such as diabetes, cancer, fungal infections, inflammatory conditions, Alzheimer's,

malaria and many others (Zhao et al., 2019). Additionally, the FDA has approved over 150 drugs containing the sulfur moiety, and pharmaceutical companies are developing many more sulphonamides. The excellent biological and chemical profile of sulphonamides raises them to be the superior option in discovery of 3MST inhibitors if they are to be utilised therapeutically in the future, especially as an antibacterial or anticancer agent.

The University of Nottingham chemical library contains thousands of sulphonamides readily available for screening. To narrow down the candidates for screening, the first step was selecting all compounds that "contained" the exact chemical structure of compound 5, and only 52 compounds met this condition, of which 16 compounds fit the binding site with good scores. Compounds that contained branching at the sulphonamide nitrogen, more than three fused rings or extensive substitution on the benzene sulphonamide did not fit the pocket properly and gave poor scores. To test this theory, a second search for all compounds that contained a benzenesulphonamide without any substitution on the phenyl ring came up with 259 compounds, of which 71 fit the pocket with decent scores. Another search with the exact criteria, only with no branching on the sulphonamide nitrogen was carried out and 80 compounds, of which 28 gave good scores. Docking results supported the previous observations. Another apparent trend was that lipophilic compounds with bromine substitutions did not fit the pocket at all. All compounds with good scores (10->) had at least one hydrogen bond donor and at least six acceptors. In addition, a long chain of substituents spread in an elongated space is more tolerated than branched or bulky compounds.

Two searches of compounds that contained small para alkyl substitution (methyl, iso propyl and tertiary butyl) at the phenyl of the benzylsulfonamide, came up with 56 compounds and the substitution looked to be well tolerated unless more than two substituents were present on the ring (e.g. 2,4,6 tri substitution). Furthermore, a group of 24 naphthalene-2-sulfonamides were docked and 50% of them showed good scores. Another group of indane-5-sulfonamides showed similar results. Overall, the results show that all the docked sulphonamides have similar physiochemical profiles that do not significantly affect binding scores. Of the 522 sulphonamides docked, 164 gave scores of -8 and less and are to be tested for inhibitory activity in future studies.

To test compounds for 3MST inhibitory activity in biochemical assays, SF7-AM fluorescence probe and AzMC fluorescence probe were deemed suitable agents. However, for selectivity assays against CBS/CSE, only SF7-AM was reliable. CBS and CSE are PLP dependant enzymes, thus the expectation is that production of H_2S should not be detected in the absence of either PLP or the substrate L-cysteine. However, investigating the compatibility of AzMC with CBS/CSE substrate and the coenzyme PLP showed unexpected increase in RFU values despite addition of inhibitor and lack of substrate in the assays. Additionally, changing the concentration of AzMC from 10μM to 50μM showed different trends in the results. Such discrepancies indicate that some element is interfering with the assays and that the method is not reliable for H_2S detection produced by the CBS/CSE pathway.

The search for selective and potent 3MST inhibitors using a combination of virtual screening and biochemical HTS studies is underway. However, the results from the initial screen show that good binding scores in docking studies, high structural similarity and having identical

physiochemical properties do not guarantee inhibitory activity. Therefore, another approach of delivering existing inhibitors could provide an alternative to discovering potent novel inhibitors.

In the fluorescence based screen of 222 compounds tested for 3MST inhibition using SF7-AM fluorescence probe to detect H_2S, two hits were successfully discovered and validated. The two compounds NCC-00043864 and NCC-00065766 were further investigated in SF7-AM assays to calculate IC_{50} values and confirm activity using counter assays with AzMC fluorescence probe. The calculated IC_{50} values of NCC-00065766 and NCC-00043864 are 4.5 µM and 9.7 µM respectively. Both values are under 10 µM and within the range of the Hanaoka et al. compounds.

3. Chapter III

3.1 Synthesis and biological evaluation of novel 3MST Inhibitors

3.1.1 background

The design of the compounds synthesised in this work followed a systematic, structure-guided strategy aimed at identifying potential inhibitors of 3 MST. Initially, commercially available chemical fragments were surveyed using the BDI chemical library and the Sigma-Aldrich catalogue, with the pyrimidone ring selected as the core scaffold for all designs. A diverse set of suitable building blocks was assembled and each fragment was docked individually into the 3MST active site using computational modelling. This enabled ranking of fragments based on predicted binding affinity and synthetic feasibility. From this in silico prioritisation, 25 promising building blocks were identified; however, due to commercial availability constraints, only 16 could be obtained. These fragments were subsequently incorporated into the pyrimidone scaffold to generate a focused library of analogues, designed to probe structure–activity relationships around the 3MST binding site. This integrated computational and synthetic strategy produced a rationally designed compound set for subsequent biological evaluation.

3.1.2 Design and synthesis rational

Priority was given to starting materials that were readily available within the UK or EU and could be delivered within one month, with budgetary constraints further narrowing the selection. To ensure reliable supply and consistent quality, Sigma-Aldrich was used as the primary supplier due to its extensive catalogue and dependable logistics. An initial survey of their inventory yielded approximately 100 commercially available aryl bromides, which formed the starting pool for compound selection.

To refine this pool, molecular docking was performed using UCSF Chimera and AutoDock Vina to estimate predicted binding affinities within the 3MST active site. In parallel, structural similarity to known 3MST inhibitors, derived from both the literature and analogues from my previous work, was assessed using DataWarrior. This combined computational approach enabled prioritisation of candidates that were both predicted to bind favourably and were chemically tractable. Certain compounds, such as MNA07, were deliberately included to facilitate the exploration of structure activity relationships (SAR). The final set of approximately 20 compounds was selected based on these criteria together with physical availability, either through commercial suppliers or from the compound collection held in the Nottingham BDI building.

In designing the compound library, two linker motifs were explored, mercaptoacetyl and mercaptoacetamide. These were chosen on the basis of reported biological activity in the literature as well as positive trends observed in my prior screening of related analogues. A constant structural element retained throughout the series was the 6 mercapto 2 methyl 4(3H) pyrimidinone core, which constitutes the central pharmacophore and was not modified across the library.

The terminal groups were primarily aromatic moieties functionalized with hydrogen bond donors or acceptors, chosen based on their presence in known 3MST inhibitors or their bioequivalence to quinoline-containing compounds, such as (Hanaoka compound 3). For example, MNA23 includes a benzofuran group to mimic quinoline's spatial and electronic features, while MNA17 features a trifluoromethyl-substituted benzene ring, which is partially bioequivalent and occupies a similar region within the enzyme's binding pocket.

Other compounds were designed to explore specific structure–activity relationship (SAR) hypotheses. For instance, hydrophobic or lipophilic analogues were introduced to (1) assess the

contribution of π-stacking interactions, and (2) replace hydrogen-bonding catechol hydroxyl groups with halogens, as seen in MNA14, to test whether hydrogen donor/acceptor capacity is essential at these positions. In MNA21, the positions of the hydroxyl groups on the catechol moiety were modified relative to CDS, and in MNA1, MNA2, and related analogues, I varied hydroxy, methyl, and methoxy substitutions to further probe positional effects.

Additional structural variations were also explored. For example, MNA007 was designed to compare the effect of extending the aromatic system from benzene to naphthalene, thereby increasing the planar surface area and potential stacking interactions. MNA12 was intended to mimic Hanaoka compound 2, but it proved chemically unstable and could not be tested in biological assays. Comprehensive chemical methodologies are described in the Experimental chapter.

3.2 Chemistry

3.2.1 Synthesis of amide linker compounds

3.2.1.1.

For selected compounds, amide bond formation using conventional coupling reagents proved challenging. Optimal yields were achieved using a BEP/NMI-mediated coupling protocol in acetonitrile. The appropriate carboxylic acid and amine were dissolved in acetonitrile, followed by the addition of BEP (0.25 mmol, 1 equiv.) and N-methylimidazole (NMI) (0.87 mmol, 3.5 equiv.). The reaction mixture was stirred at room temperature until completion, as monitored by TLC. The reaction was then quenched, and the product was isolated by filtration or solvent extraction. Removal of the volatile solvent under reduced pressure afforded the crude amide, which was purified as required by flash chromatography.

3.2.2 Synthesis of mercaptoacetyl-linker Compounds

A suspension of the nucleophile (1.0 equivalent) in methanol (0.1 M) was prepared, and a solution of KOH (1.0 equivalent, 1 M in methanol) was added dropwise. The mixture was stirred at room temperature for 15 minutes, after which the electrophile (1.2 equivalents) was introduced. The reaction was allowed to proceed for 12 hours at room temperature. Afterward, water (in an amount equal to the volume of methanol used) was added to quench the reaction. The resulting product was collected by filtration, washed with diethyl ether, and dried under high vacuum. A suspension of the nucleophile (1.0 equivalent) in methanol (0.1 M) was prepared, and a solution of KOH (1.0 equivalent, 1 M in methanol) was added dropwise. The mixture was stirred at room temperature for 15 minutes, after which the electrophile (1.2 equivalents) was introduced. The reaction was allowed to proceed for 12 hours at room temperature. Afterward, water (in an amount equal to the volume of methanol used) was added to quench the reaction. The resulting product was collected by filtration, washed with diethyl ether, and dried under high vacuum (Figure 21).

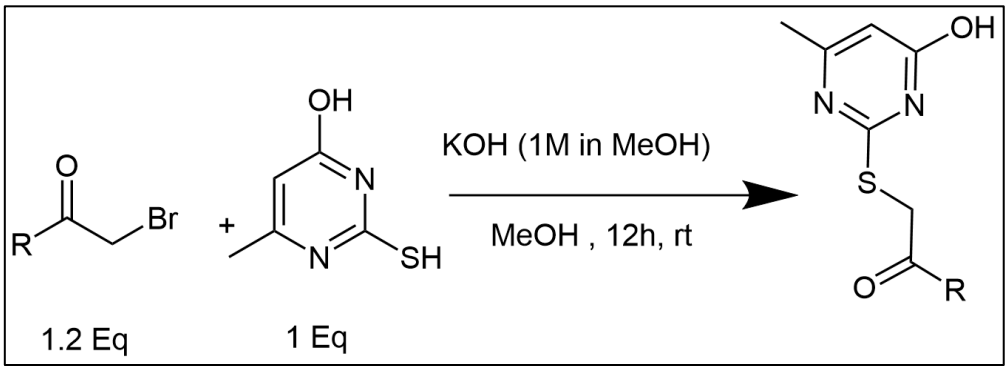


Figure 21 Simplified scheme of mercaptoacetyle linker compounds synthesis

3.2.3 Synthesis challenges and limitations

One of the earliest and most persistent synthetic challenges arose in forming amide linkers, particularly in compounds such as MNA001, MNA002, and MNA003. I initially employed EDCI and HOBt in DMF, expecting a straightforward coupling. However, this method failed to generate clean products, even with increased starting material (≥100 mg). The reactions frequently stalled or yielded only trace amounts of poorly defined product. Manual silica gel column chromatography using 5% methanol in DMF was attempted for purification, but co-elution with HOBt and low recovery made this impractical. In these cases, reaction mixtures often turned brown, possibly due to oxidation or degradation of unstable intermediates under prolonged reaction times.

To troubleshoot these issues, I turned to a COMU/DIPEA-mediated amide coupling strategy. In this protocol, 2-((4-hydroxy-6-methylpyrimidin-2-yl)thio)acetic acid was pre-activated with COMU in DMF, followed by the addition of DIPEA and the target amine. While the method showed some improvement over EDCI/HOBt, the reactions still gave low yields, and purification remained difficult

due to persistent brown residues and partial decomposition. Manual column chromatography proved inefficient, prompting a transition to reverse-phase flash chromatography, which significantly improved the separation of products from byproducts. Even so, yields remained modest, and certain substrates required repetition with increased reaction scale to obtain sufficient material.

Following persistent difficulties, especially with more sterically hindered or electron-rich amines, I trialled a modified protocol based on the method by Beutner et al., 2018.The amide bond was formed between 2-((4-hydroxy-6-methylpyrimidin-2-yl)thio)acetic acid and the relevant aromatic amine using BEP/NMI/MeCN which ensures high efficiency by preventing side reactions (e.g., protonation of intermediates). In my work, this strategy proved generally effective, but product yield and purity were highly dependent on the amine used. Electron-rich and sterically hindered amines, such as *5-amino-2-methoxyphenol*, were particularly problematic: reactions frequently developed a dark brown colouration and generated complex LC-MS spectra, likely indicating partial oxidation or decomposition of the intermediate or final product. In contrast, amines with less electron density and steric hindrance, such as *3-amino-5-methylphenol*, proceeded smoothly and reproducibly, yielding clean products in significantly higher yield and purity with minimal optimization.

In parallel, another class of compounds featuring a mercaptoacetyl linker was synthesized via base-mediated substitution reactions adapted from a protocol by Bantzi et al. (2021). These involved treating the appropriate thiol intermediate with potassium hydroxide in methanol. This method worked well for compounds such as MNA013 and MNA014, producing high yields under mild conditions. However, several analogues proved capricious and required multiple repetitions to generate usable material. The reactions were also highly sensitive to fluctuations in ambient temperature, with yields suffering during extreme weather conditions. Several syntheses had to be repeated on more stable days to obtain consistent and reproducible results.

3.2.4 Suggested SAR

Structure–activity relationship (SAR) analysis of the compound series highlighted several important trends. The 6-mercapto-2-methyl-4(3H)-pyrimidinone core appeared to be essential for activity, as nearly all compounds retaining this group exhibited more than 20% inhibition at 100 µM. Notably, only MNA8, MNA17, and MNA21 failed to meet this threshold. Among the structural variations, the position and nature of terminal aromatic substitutions played a key role in modulating both potency and selectivity. Para and meta substitutions on the benzene ring were generally more favorable, while ortho-substituted analogues such as MNA18 and MNA21 often displayed reduced activity, likely due to steric hindrance observed in docking studies—though MNA20 was an exception. Interestingly, halogen substitution on the terminal aromatic ring (e.g., in MNA20) appeared to decrease selectivity against off-target enzymes such as CBS and CSE. The mercaptoacetyl linker showed better performance across this batch compared to the mercaptoacetamide counterpart, suggesting that linker flexibility or geometry may contribute to binding efficacy.

The presence of hydrogen bond donors or acceptors on the terminal ring generally correlated with improved activity, but this was not always predictive of potency. A direct comparison between MNA13 (bearing a 3-methoxybenzene) and MNA16 (3-hydroxybenzene) showed that while the methoxy group increased potency, it also reduced selectivity, whereas the hydroxyl group offered better selectivity but slightly lower potency. Lipophilicity also played a nuanced role—compounds like MNA17 and MNA21 demonstrated that increasing lipophilicity without maintaining ring rigidity compromises π-stacking interactions, resulting in reduced activity. In contrast, MNA23, which

incorporates a benzofuran moiety bioequivalent to the naphthalene group in Hanaoka compound 3, showed excellent potency and binding characteristics, further supporting the importance of mimicking known bioactive scaffolds while preserving structural rigidity.

Several compounds demonstrated potent 3MST inhibition, with MNA1, MNA13, MNA20, and MNA23 each achieving nearly 100% inhibition at 100 µM. Among these, MNA20 stood out due to its unexpected off-target effects. While it inhibited 3MST effectively, it had no inhibitory effect on CBS or CSE, and instead strongly induced their activity, particularly CSE, which showed a 900% increase over control levels. This remarkable induction suggests that MNA20 may have potential utility as a CSE activator, opening up new directions for further investigation. A similar phenomenon was observed with MNA18, which induced CBS/CSE activity by approximately 300%, probably due to containing terminal halogen groups associated with off-target effects.

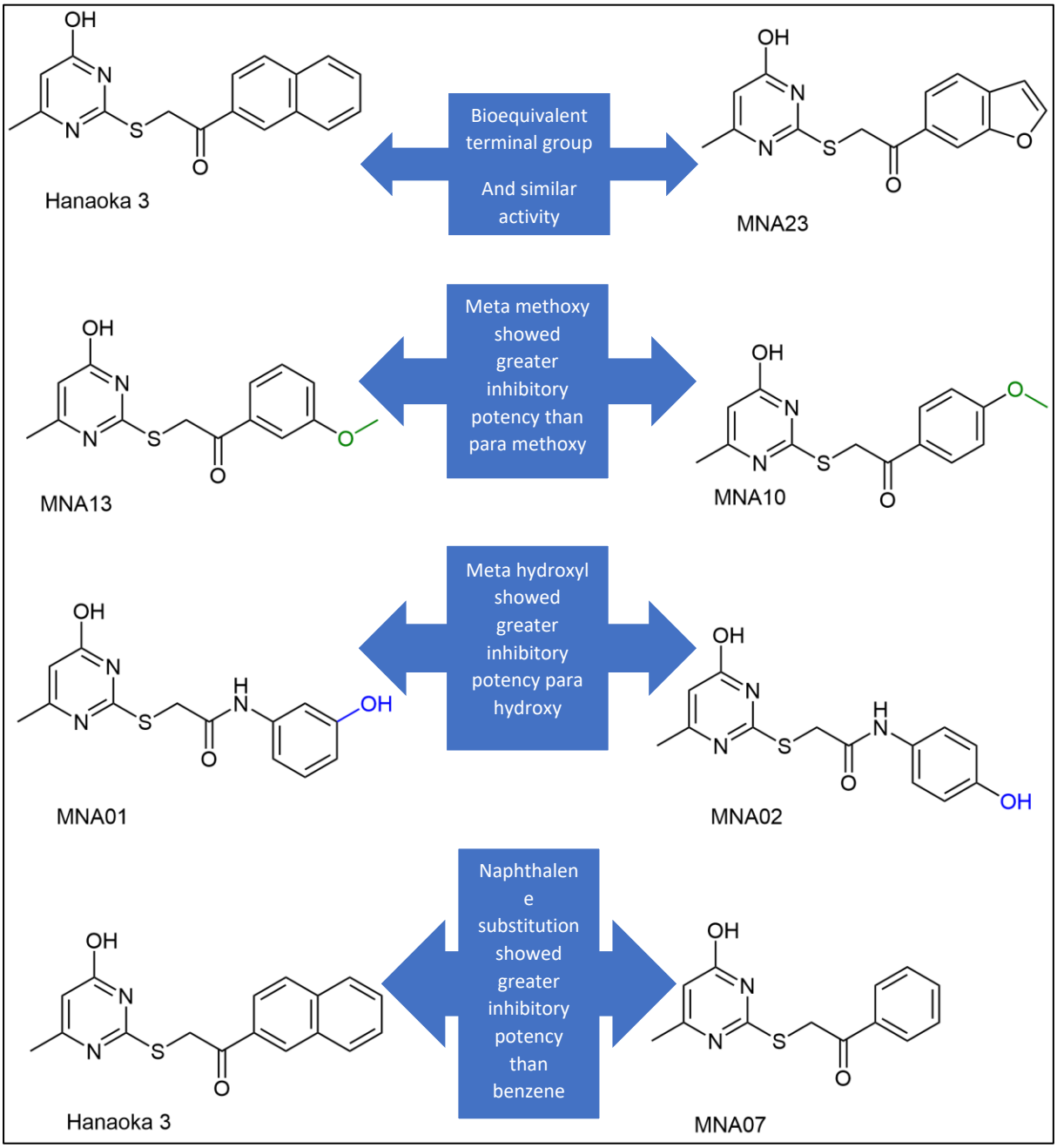


Figure 22 Notes on SAR, potency is associated with lower IC_{50} values

3.3 Biochemical investigations of 3MST Inhibitors

3.3.1 Background

To evaluate the inhibitory activity and selectivity of the designed compounds, a fluorescence-based biochemical screening platform was employed. Initial assay conditions were established through a pilot study using **CDS004892**, which served as a reference compound to optimise assay performance and validate the screening protocol. Two H_2S-sensitive fluorescent probes, SF7-AM and AzMC, were used to monitor enzymatic H_2S production, and methylene blue was also evaluated as a complementary detection method. Inhibition was assessed against 3MST and, for comparison, the related H_2S-producing enzymes cystathionine CBS and CSE. Rat liver cytosols were used as the enzyme source and assays were performed in 96-well plate format to enable medium-throughput screening. Compounds were tested over a concentration range of 1–100 µM to capture both weak and moderate inhibitory effects. Full experimental procedures are described in the Experimental chapter.

3.3.2 Results and Discussion

3.3.2.1. Pilot study of CDS004892

A previous fluorescence-based screen in our laboratory identified 1-(3,4-dihydroxyphenyl)-2-[(4-hydroxy-6-methyl-2-pyrimidinyl)sulfanyl]ethanone (CDS004892) as a 3MST inhibitor (Almehaize, 2017). This compound was subsequently used as a pilot molecule for initial biochemical investigations. CDS004892 is structurally related to the inhibitors reported by Hanaoka et al. (2017) and showed a comparable potency, with an average IC_{50} of 7.92 µM versus 1.7 to 6.3 µM for literature compounds 1,2,3 and 5. Both CDS004892 and literature compounds contained a pyrimidone like moiety and a terminal aromatic ring connected by a mercaptoacetyl linker. Hanaoka et al reported that their inhibitors form an electrostatic interaction with the persulferated cysteine residue of 3MST, preventing the production of H_2S. As CDS004892 is structurally similar to inhibitor 2 and 3, it is possible that it has formed the same kind of interaction with the persulferated 3MST.

CDS004892 has shown potent inhibitory effects on 3MST in two separate methods with varying IC_{50} values between male and female rat cytosol samples (3.5±0.29 µM in male and 7.14±0.34 in female). Both values are under 10 µM and within the range of the Hanaoka et al compounds and could be affected by the gender of the animals. Moreover, CDS004892 did not show any significant CBS/CSE inhibition in either SF7-AM fluorescence screen or methylene blue method, granting it a promising selectivity profile.

3.3.2.1.1.1. SF7-AM fluorescence assays

3.3.2.1.1.1.1. CSE/CBS pathway

Once assay conditions were deemed satisfactory, an assay was set up to test the selectivity of the candidate 3MST inhibitor, CDS004892, against CBS and CSE in three cytosol samples

(see Figure 23). The results indicate that CDS004892 displays no prominent inhibitory effects on CSE/CBS, therefore, the selectivity of CDS004892 is promising.

In comparison, the calculated mean IC50 of AOAA was 0.88±0.17 µM, which is comparable to the IC_{50} value of other groups (IC_{50} 1.1 ± 0.1 µM) for CSE inhibition.

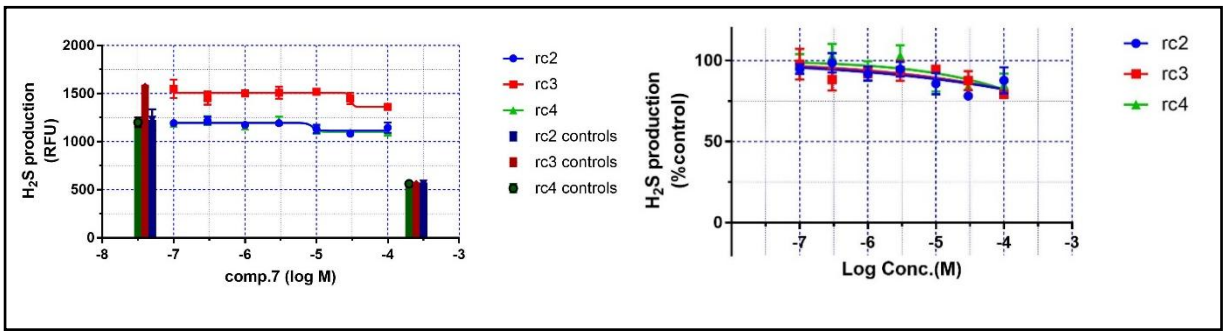
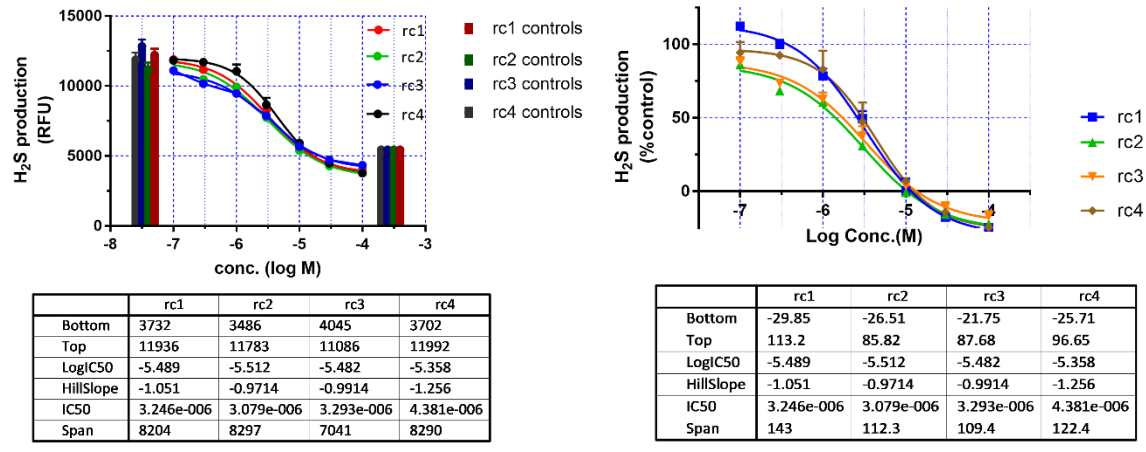


Figure 23 Concentration-inhibition curve of CDS004892 shows no significant effects on the enzymatic production of H_2S via CSE/CBS pathway in rat liver cytosol samples (n=3) using H_2S detection assay via SF7-AM fluorescence probe. Data on the right are expressed as a percentage of the negative control (no inhibitor); data on the left are expressed as RFU which correlates with H_2S production. Data sets represents mean ± SEM

3.3.2.1.1.1.2. 3MST pathway

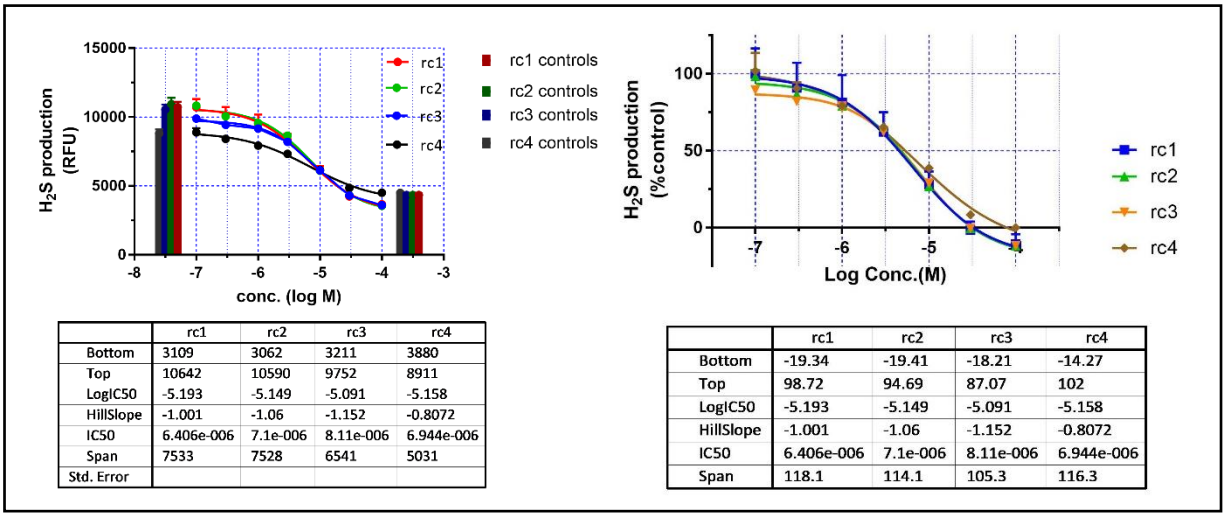
The inhibitory activity of CDS004892 on the production of H_2S via the 3MST pathway was tested on four male and four female rat cytosol samples (see Figure 24 and Figure 25). In these assays, the mean IC50 was 3.5±0.29 µM in male test samples and 7.14±0.34 µM in female samples, both values are within the range of the reported selective 3MST inhibitors values between (2–7 µM) (Hanaoka et al., 2017). The discrepancy between female and male samples could be related to the sex of the animal, as some studies indicated that oestrogen stimulates 3MST activity (Lechuga et al., 2015) and that DHT downregulates H2S enzymatic production (Brancaleone et al., 2015). Further investigations must be conducted to ascertain the reasons for the differences in IC_{50}.



	rc1	rc2	rc3	rc4
Bottom	3732	3486	4045	3702
Top	11936	11783	11086	11992
LogIC50	-5.489	-5.512	-5.482	-5.358
HillSlope	-1.051	-0.9714	-0.9914	-1.256
IC50	3.246e-006	3.079e-006	3.293e-006	4.381e-006
Span	8204	8297	7041	8290

	rc1	rc2	rc3	rc4
Bottom	-29.85	-26.51	-21.75	-25.71
Top	113.2	85.82	87.68	96.65
LogIC50	-5.489	-5.512	-5.482	-5.358
HillSlope	-1.051	-0.9714	-0.9914	-1.256
IC50	3.246e-006	3.079e-006	3.293e-006	4.381e-006
Span	143	112.3	109.4	122.4

Figure 24 Concentration-inhibition curve of CDS004892 shows an inhibitory effect on the enzymatic production of H_2S via 3MST pathway in male rat liver cytosol samples (n=4) using H_2S detection assay via SF7-AM fluorescence probe. Data on the right are expressed as a percentage of the negative control (no inhibitor; data on the left are expressed as RFU which correlates with H_2S production. Data sets represent mean ± SEM



	rc1	rc2	rc3	rc4
Bottom	3109	3062	3211	3880
Top	10642	10590	9752	8911
LogIC50	-5.193	-5.149	-5.091	-5.158
HillSlope	-1.001	-1.06	-1.152	-0.8072
IC50	6.406e-006	7.1e-006	8.11e-006	6.944e-006
Span	7533	7528	6541	5031
Std. Error				

	rc1	rc2	rc3	rc4
Bottom	-19.34	-19.41	-18.21	-14.27
Top	98.72	94.69	87.07	102
LogIC50	-5.193	-5.149	-5.091	-5.158
HillSlope	-1.001	-1.06	-1.152	-0.8072
IC50	6.406e-006	7.1e-006	8.11e-006	6.944e-006
Span	118.1	114.1	105.3	116.3

Figure 25 Concentration-inhibition curve of CDS004892 shows an inhibitory effect on the enzymatic production of H_2S via 3MST pathway in female rat liver cytosol samples (n=4) using H_2S detection assay via SF7-AM fluorescence probe. Data on the right are expressed as a percentage of the negative control (no inhibitor); data on the left are expressed as RFU which correlates with H_2S production. Data sets represent mean ± SEM

3.3.2.1.1.2. Methylene blue method

3.3.2.1.1.2.1. CSE/CBS pathway

Initial investigations of the effect of AOAA on H_2S production via the CBS/CSE pathway in four rat liver cytosol samples showed concentration-dependant inhibition in the methylene blue method (see Figure 26). As the results were uniform across all RLC samples, assay conditions were deemed satisfactory and no further optimisation was required.

The effects of CDS004892 on H_2S production via the CSE/CBS pathway was investigated in four rat liver cytosol samples using the methylene blue method, and the results showed no significant inhibition of H_2S (Figure 27), which corresponded to the previous results from the sf7-AM fluorescence assays. All in all, two separate and different methods were used to test

selectivity of CDS004892 and both showed no significant inhibition of CBS/CSE enzymes, which suggests that CDS004892 is a selective 3MST inhibitor.

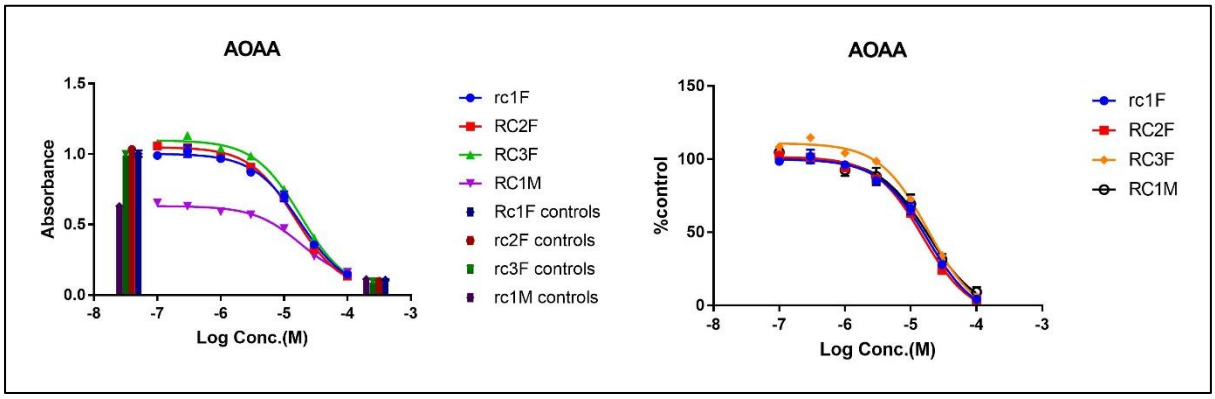


Figure 26 Concentration-inhibition curve of AOAA shows an inhibitory effect on the enzymatic production of H_2S via CBS/CSE pathway in rat liver cytosol samples (n=4) using the H_2S detection assay via methylene blue assay. Data on the right are expressed as a percentage of the negative control (no inhibitor); data on the left are expressed as absorbance which correlates with H_2S production. Data sets represent mean ± SEM

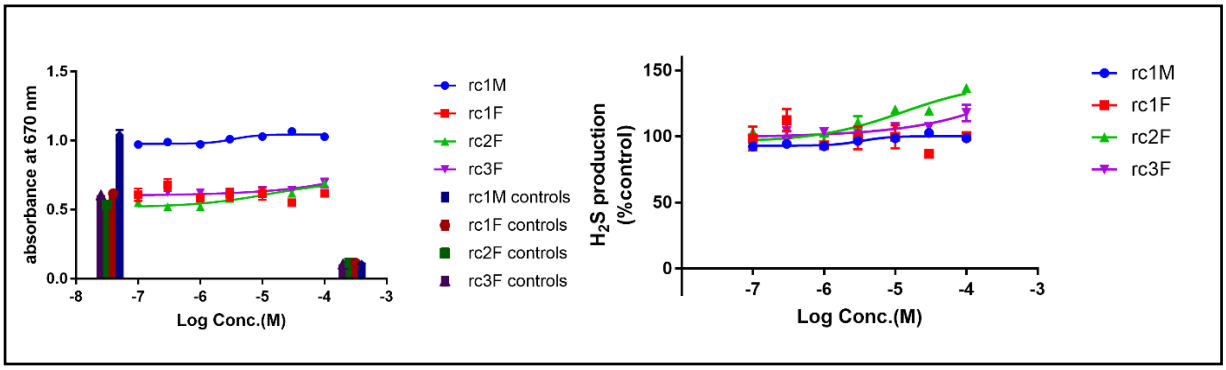


Figure 27 Concentration-inhibition curve of CDS004892 shows no significant effects on the enzymatic production of H_2S via CSE/CBS pathway in rat liver cytosol samples (n=4) using the H_2S detection assay via methylene blue method. Data on the right are expressed as a percentage of the negative control (no inhibitor); data on the left are expressed as absorbance which correlates with H_2S production. Data sets represent mean ± SEM

3.3.2.1.1.2.2. 3MST pathway

The inhibitory activity of CDS004892 on the production of H_2S via the 3MST pathway was tested on one male and three female rat cytosol samples. The average IC_{50} was 5.1 µM in the mixed population of male and female samples (Figure 28), confirming the previous fluorescence assays suggesting that CDS004892 displays inhibitory effects in the micromolar range.

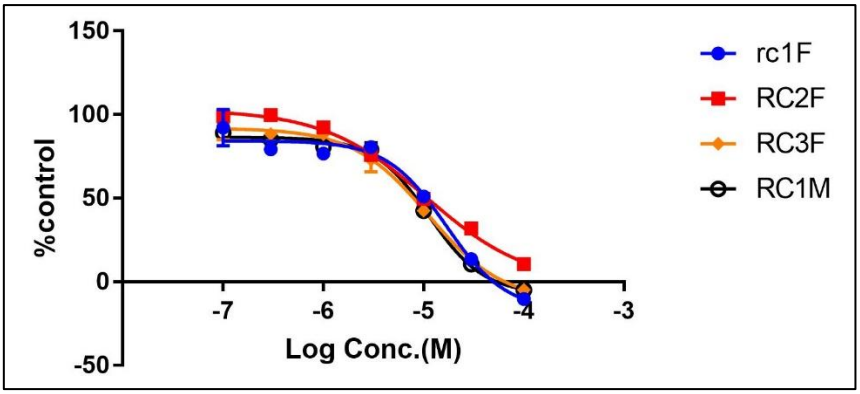


Figure 28 Concentration-inhibition curve of CDS004892 shows an inhibitory effect on the enzymatic production of H_2S via the 3MST pathway in mixed male and female rat liver cytosol samples (n=4) using H_2S detection assay via the methylene blue method. Data are expressed as a percentage of the control (cytosol and no inhibitor). Data sets represent mean ± SEM

3.3.2.2. Biological evaluation of synthesised compounds

In this study, we focused on investigating the biochemical properties and selectivity of a series of novel 3MST inhibitors. To explore this, we designed and synthesized 20 structurally similar inhibitors, which, despite sharing a common scaffold, featured various functional group modifications.

The primary goal was to assess how these structural variations influenced the inhibitors' ability to selectively target 3MST. The synthesized compounds were evaluated using fluorescence-based assays conducted on rat liver cytosol as the enzyme source. Two fluorogenic agents, SF7-AM and AzMC, were employed to detect hydrogen sulfide production, allowing us to quantify the inhibitory effects of the compounds in real-time. These assays provided detailed insights into each compound's efficacy in suppressing 3MST activity while also helping determine their selectivity over other related sulfurtransferases (CBS/CSE).

Through these assays, we systematically explored the structure-activity relationships (SARs) of the synthesized compounds, identifying key functional groups and chemical environments that significantly impacted binding affinity and inhibition potential.

Overall, this work provides a comprehensive understanding of how structural modifications influence the efficacy and selectivity of 3MST inhibitors. The insights gained from these fluorescence-based assays using SF7-AM and AzMC pave the way for further optimization of

these inhibitors, contributing to the development of potential therapeutic agents targeting dysregulated H_2S production.

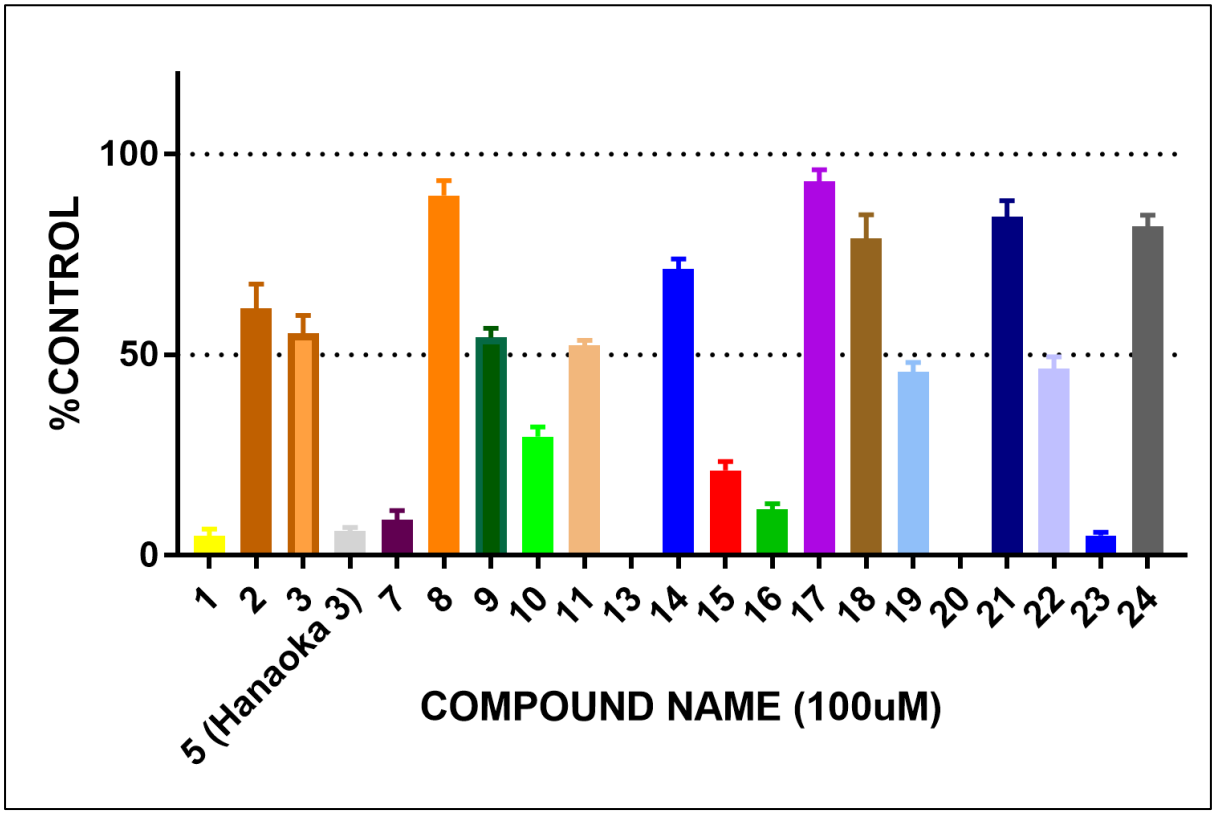


Figure 29 Graph shows inhibitory effect on the enzymatic production of H2S via 3MST pathway in rat liver cytosol samples (n=3) using H2S detection assay via AzMC fluorescence probe. Data sets represent mean ± SEM

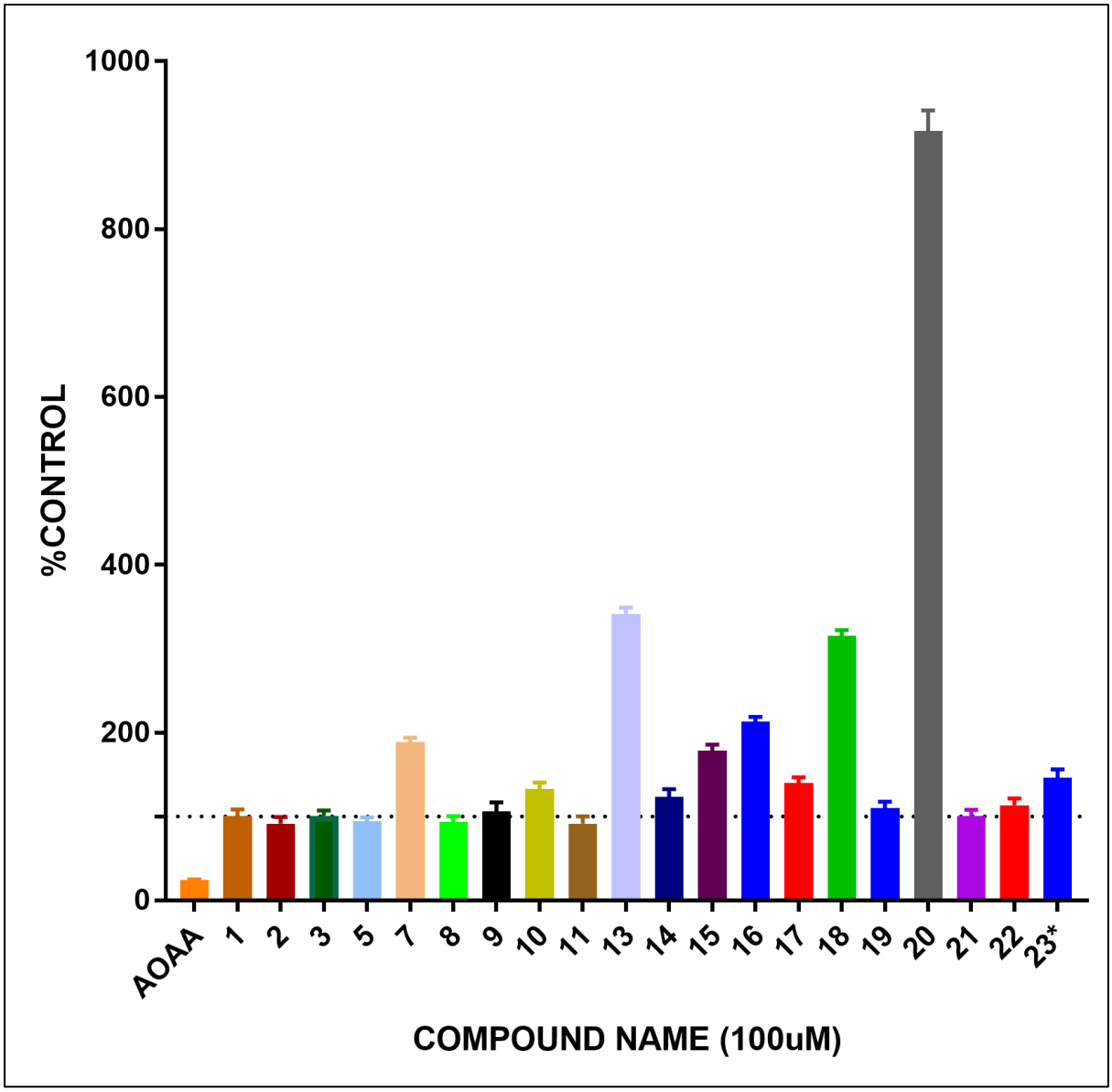
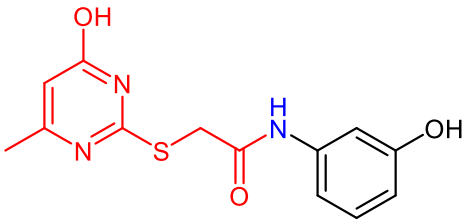
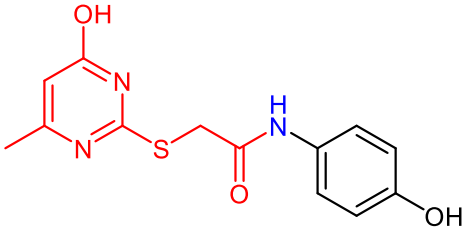
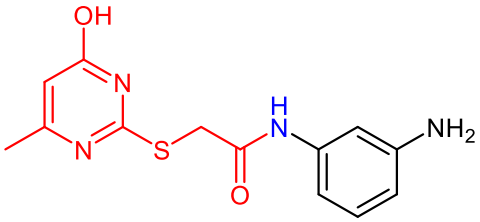
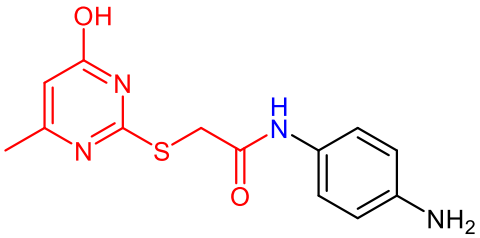
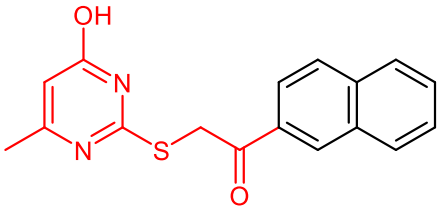
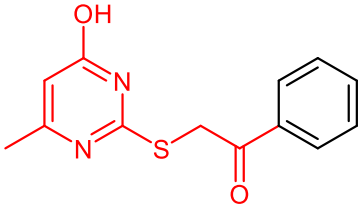


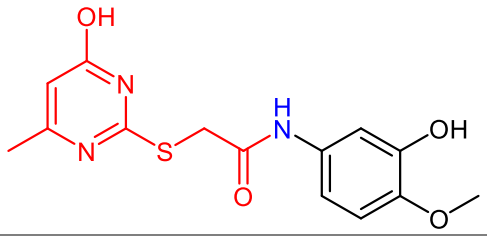
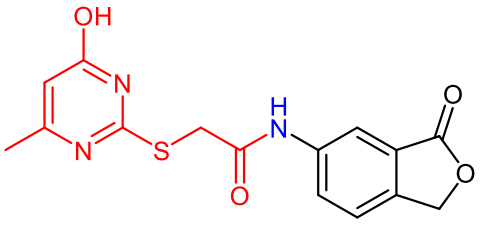
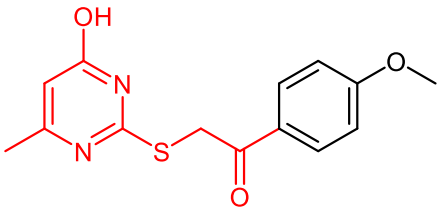
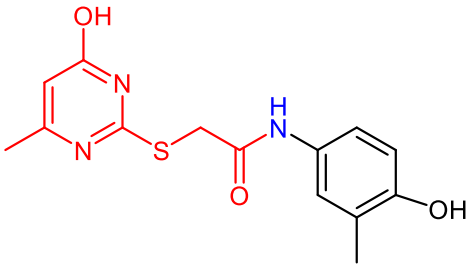
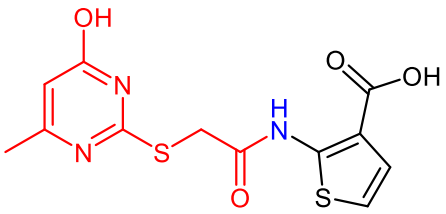
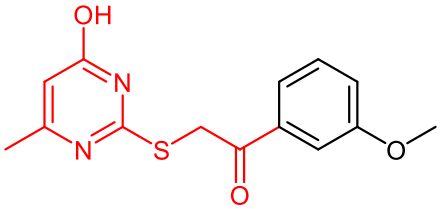
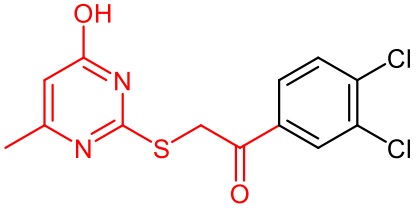
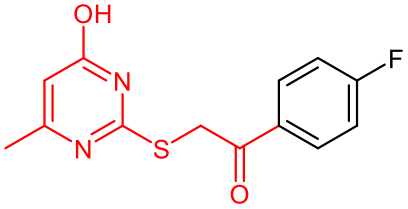
Figure 30Graph shows inhibitory effect on the enzymatic production of H2S via CBS CSE pathway in rat liver cytosol samples (n=3) using H2S detection assay via SF7-AM fluorescence probe. Data sets represent mean ± SEM

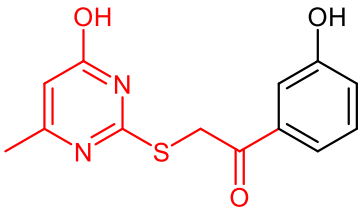
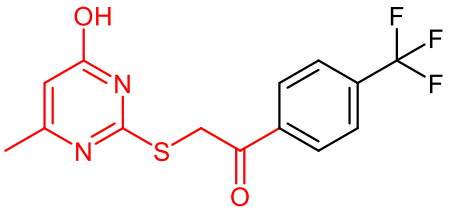
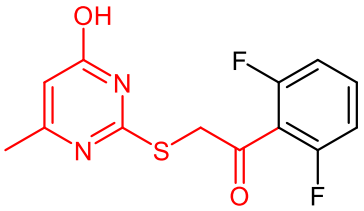
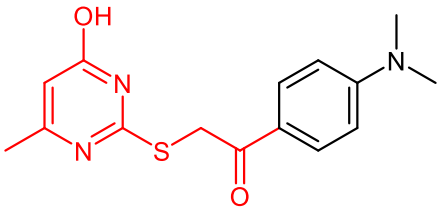
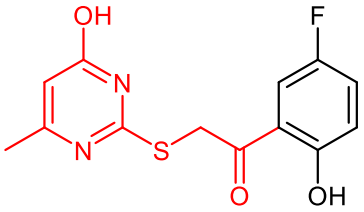
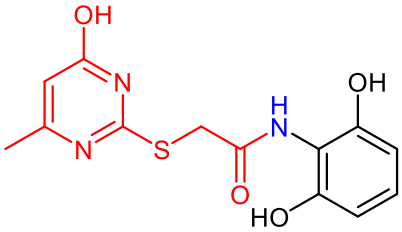
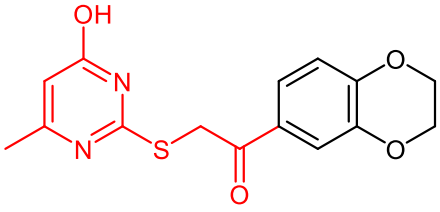
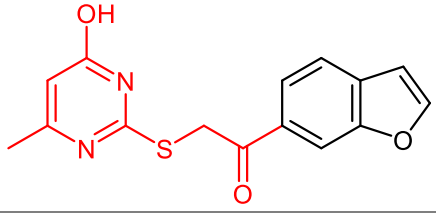
**Compounds 13, 18 and 20 have markedly increased SFU values compared to control, interestingly they show good 3MST inhibition*

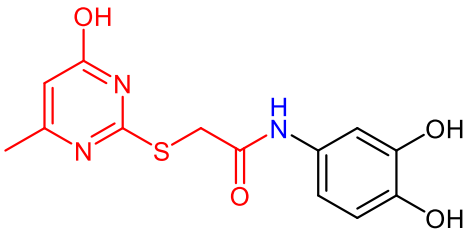
The dual nature of some compounds, both inhibiting and stimulating H_2S production depending on the enzyme, opens exciting opportunities for further exploration. These potential H_2S donors, which emerged during our investigation, could serve as valuable tools for modulating H_2S levels in biological systems, particularly in conditions where H_2S supplementation is beneficial. This discovery adds another layer of complexity to the structure-activity relationship study and highlights the versatility of these compounds.

Table 2 Chemical structures of the MNA series and shows inhibitory effect on the enzymatic production of H2S via 3MST pathway in rat liver cytosol samples (n=3) using H_2S detection assay via SF7-AM fluorescence probe compared to control. Whereas 0% means complete inhibition.

name	Structure	%control At 100µM final concentration
1		4.9
2		61.6
3		55.4
4		N/A
5		6.1
7		8.9

8		89.7
9		54.3
10		29.6
11		52.3
12		N/A
13		0
14		71.4
15		21.2

16		11.5
17		93.2
18		79
19		45.8
20		0
21		84.4
22		46.5
23		5

24		82

3.3.2.2.1.1. Investigating synthesised compounds inhibitory activity – 3MST pathway AzMC

To evaluate the inhibitory activity of the synthesized compounds against 3MST, we employed a fluorescence-based assay using 7-azido-4-methylcoumarin (AzMC), a selective probe for hydrogen sulfide (H_2S). Rat liver cytosol was incubated with each compound in the presence of its physiological substrate, 3-mercaptopyruvate (3-MP), and the resulting H_2S production was quantified based on fluorescence intensity generated by AzMC reduction.

Initial screening at a fixed compound concentration (typically 100 µM) allowed rapid identification of derivatives that significantly suppressed H_2S release compared to control. From this primary assessment, several promising candidates were shortlisted based on their ability to inhibit >80% of 3-MST activity.

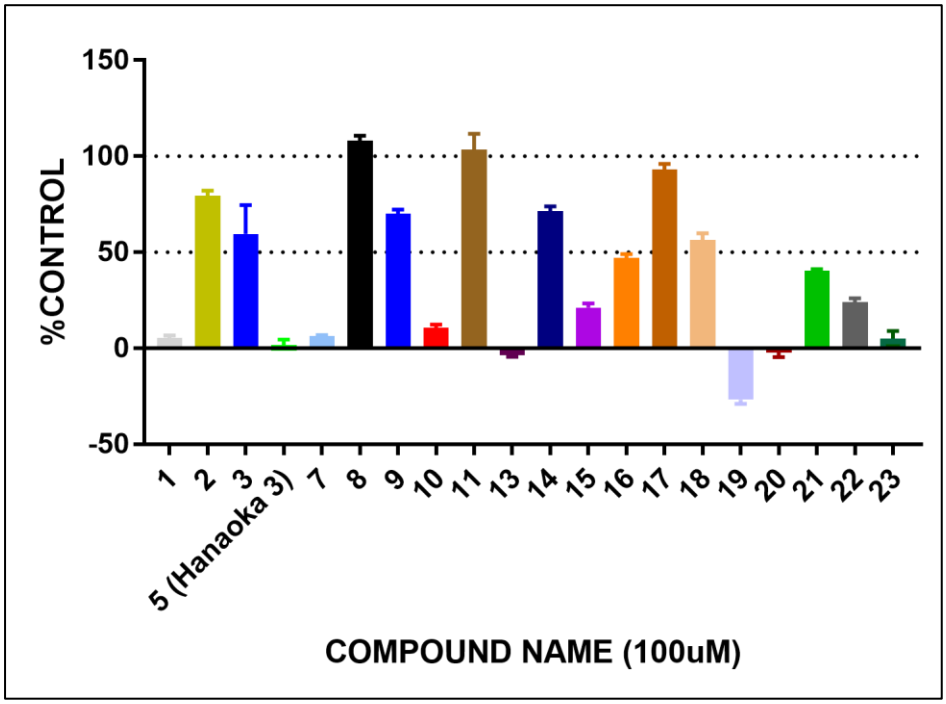
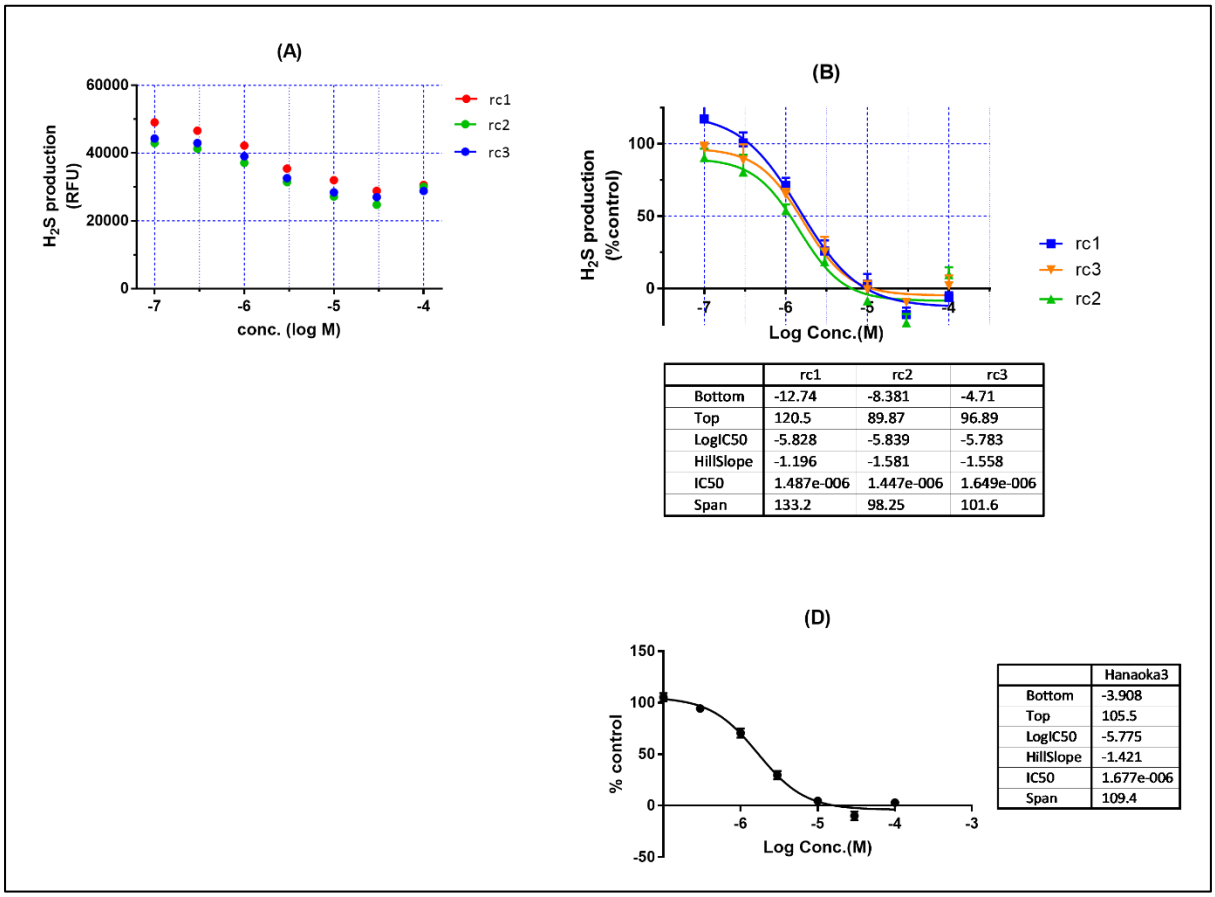


Figure 31 Screening of synthesised compounds in 3MST pathway in RLC (n-3) using H2S detection assay via AzMC at 37°C. Data sets represent mean ± SEM

Subsequent dose–response experiments were performed for these top-performing hits to determine their IC_{50} values. Detailed graphical analyses (Figure 32,Figure 33,Figure 34,Figure 35,Figure 36) highlight the concentration-dependent inhibition profiles of the most potent and selective compounds, illustrating clear suppression of 3-MST activity relative to the reference compound. The

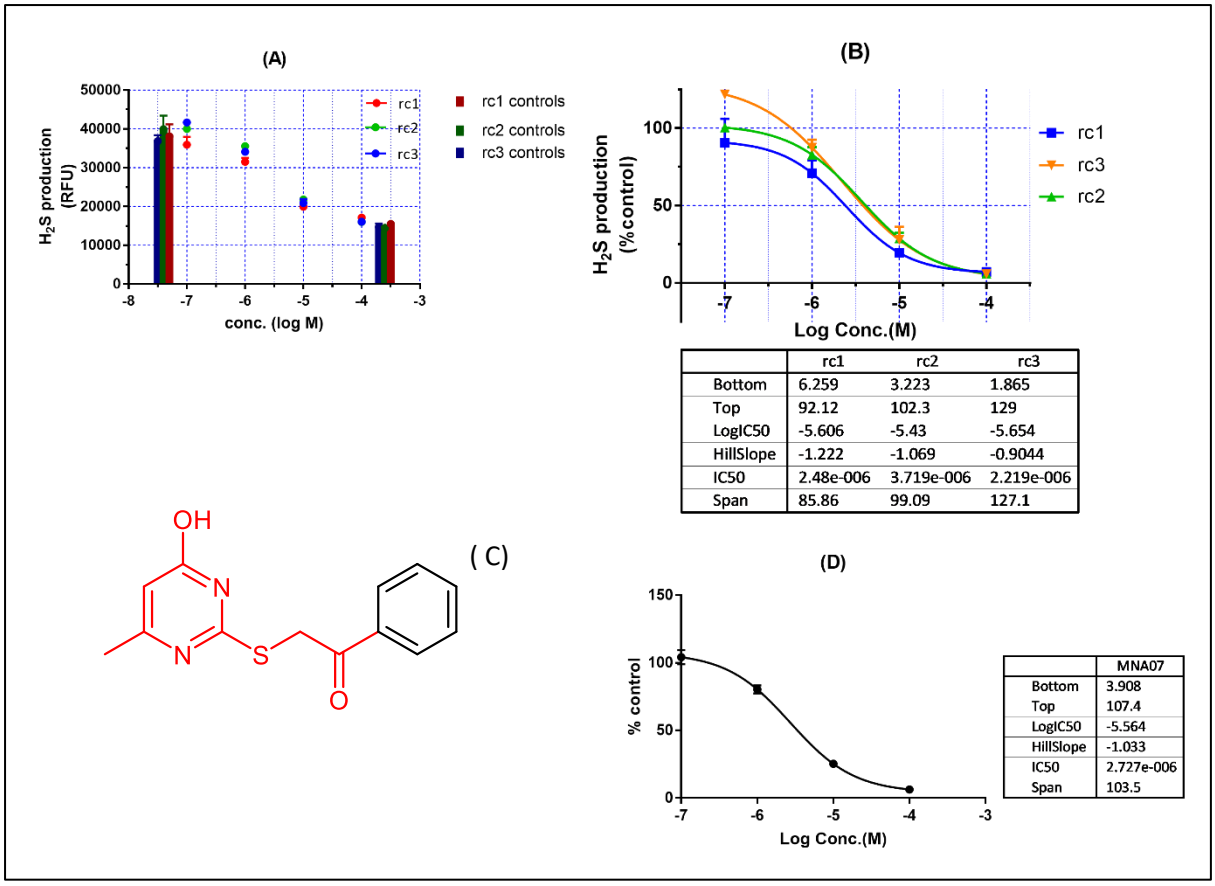
highest-performing compounds were subjected to SAR evaluation..



	rc1	rc2	rc3
Bottom	-12.74	-8.381	-4.71
Top	120.5	89.87	96.89
LogIC50	-5.828	-5.839	-5.783
HillSlope	-1.196	-1.581	-1.558
IC50	1.487e-006	1.447e-006	1.649e-006
Span	133.2	98.25	101.6

	Hanaoka3
Bottom	-3.908
Top	105.5
LogIC50	-5.775
HillSlope	-1.421
IC50	1.677e-006
Span	109.4

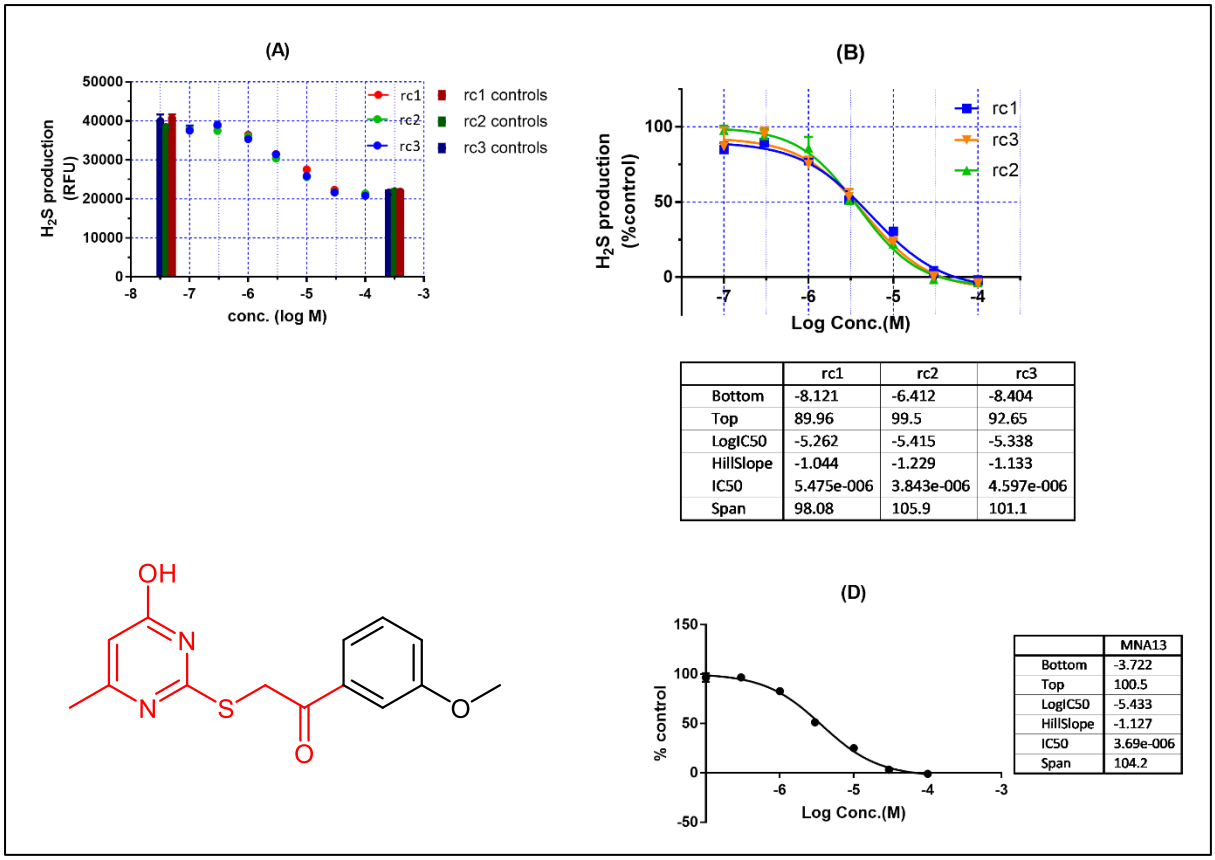
Figure 32 Assay of the inhibitory effect of Hanaoka 3 on the enzymatic production of H2S via the 3MST pathway in rat liver cytosol (RLC) samples (n=3) using H2S detection assay via AzMC at 37°C. (a) are raw data in RFU values. (b) are normalized data, 0 is tissue blank and 100 represents control. (d) is mean of b. Data sets represent mean ± SEM



	rc1	rc2	rc3
Bottom	6.259	3.223	1.865
Top	92.12	102.3	129
LogIC50	-5.606	-5.43	-5.654
HillSlope	-1.222	-1.069	-0.9044
IC50	2.48e-006	3.719e-006	2.219e-006
Span	85.86	99.09	127.1

	MNA07
Bottom	3.908
Top	107.4
LogIC50	-5.564
HillSlope	-1.033
IC50	2.727e-006
Span	103.5

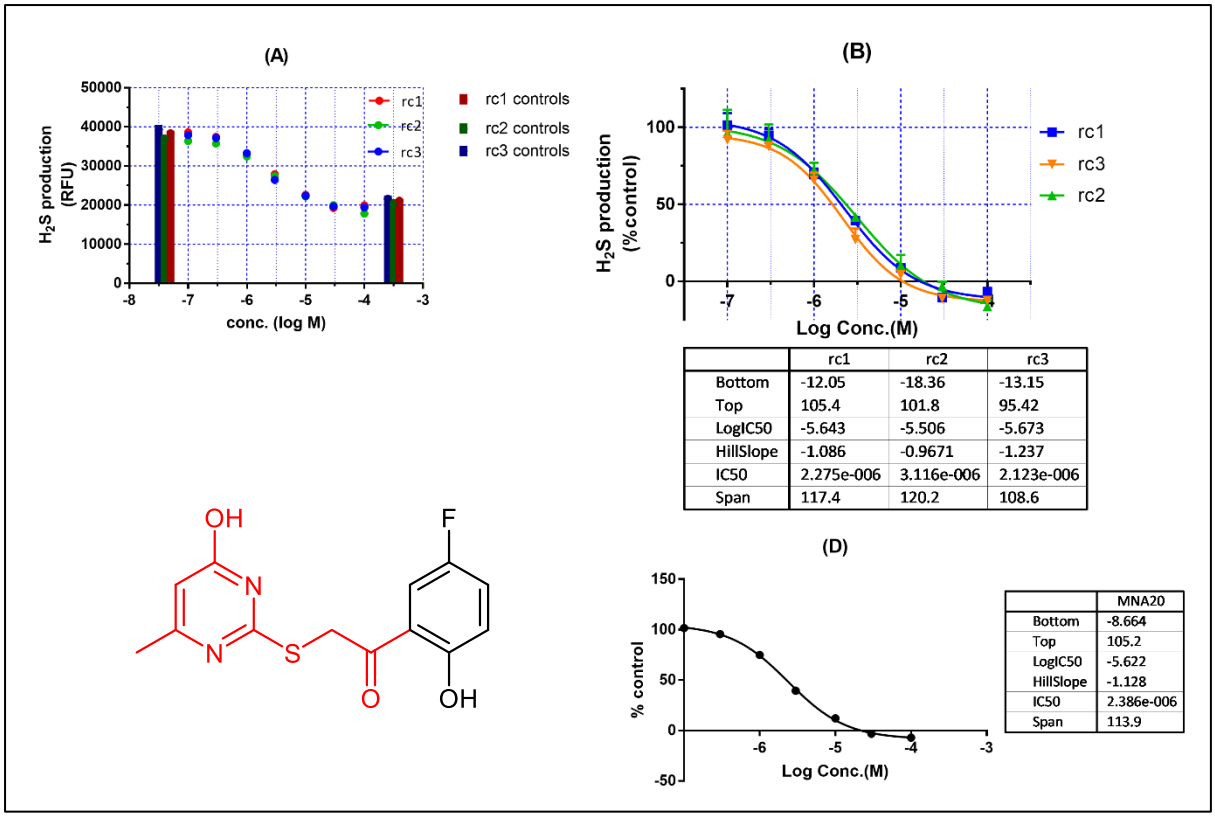
Figure 33 Assay of the inhibitory effect of MNA07 on the enzymatic production of H2S via the 3MST pathway in rat liver cytosol (RLC) samples (n=3) using H2S detection assay via AzMC at 37°C. (a) raw data in RFU values. (b) are normalized data, 0 is tissue blank and 100 represents control. (d) is mean of b. Data sets represent mean ±



	rc1	rc2	rc3
Bottom	-8.121	-6.412	-8.404
Top	89.96	99.5	92.65
LogIC50	-5.262	-5.415	-5.338
HillSlope	-1.044	-1.229	-1.133
IC50	5.475e-006	3.843e-006	4.597e-006
Span	98.08	105.9	101.1

	MNA13
Bottom	-3.722
Top	100.5
LogIC50	-5.433
HillSlope	-1.127
IC50	3.69e-006
Span	104.2

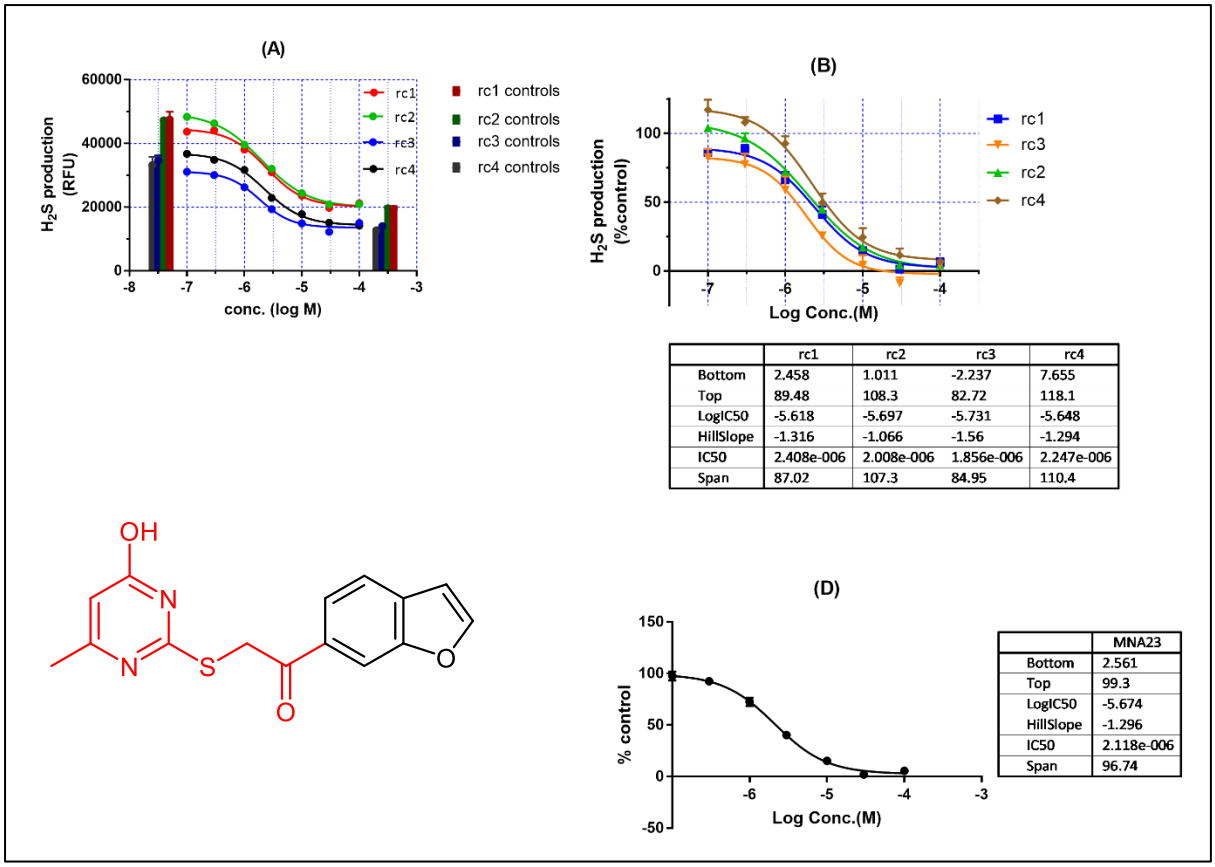
Figure 34 Assay of the inhibitory effect of MNA13 on the enzymatic production of H2S via the 3MST pathway in rat liver cytosol (RLC) samples (n=3) using H2S detection assay via AzMC at 37°C. (a) raw data in RFU values. (b) are normalized data, 0 is blank and 100 represents control. (d) is mean of b. Data sets represent mean ± SEM



	rc1	rc2	rc3
Bottom	-12.05	-18.36	-13.15
Top	105.4	101.8	95.42
LogIC50	-5.643	-5.506	-5.673
HillSlope	-1.086	-0.9671	-1.237
IC50	2.275e-006	3.116e-006	2.123e-006
Span	117.4	120.2	108.6

	MNA20
Bottom	-8.664
Top	105.2
LogIC50	-5.622
HillSlope	-1.128
IC50	2.386e-006
Span	113.9

Figure 35 Assay of the inhibitory effect of MNA20 on the enzymatic production of H2S via the 3MST pathway in rat liver cytosol (RLC) samples (n=3) using H2S detection assay via AzMC at 37°C. (a) raw data in RFU values. (b) are normalized data, 0 is blank and 100 represents control. (d) is mean of b. Data sets represent mean ± SEM



	rc1	rc2	rc3	rc4
Bottom	2.458	1.011	-2.237	7.655
Top	89.48	108.3	82.72	118.1
LogIC50	-5.618	-5.697	-5.731	-5.648
HillSlope	-1.316	-1.066	-1.56	-1.294
IC50	2.408e-006	2.008e-006	1.856e-006	2.247e-006
Span	87.02	107.3	84.95	110.4

	MNA23
Bottom	2.561
Top	99.3
LogIC50	-5.674
HillSlope	-1.296
IC50	2.118e-006
Span	96.74

Figure 36 Assay of the inhibitory effect of MNA23 on the enzymatic production of H2S via the 3MST pathway in rat liver cytosol (RLC) samples (n=4) using H2S detection assay via AzMC at 37°C. (a) raw data in RFU values. (b) are normalized data, 0 is blank and 100 represents control. (d) is mean of b. Data sets represent mean ± SEM

3.3.2.2.1.2. Investigating synthesised compounds inhibitory activity – 3MST pathway SF7-AM

To evaluate the inhibitory activity of the synthesized compounds against 3MST , we employed a fluorescence-based assay using SF7-. Rat liver cytosol was incubated with each compound in the presence of its physiological substrate, 3-mercaptopyruvate (3-MP), and the resulting H_2S production was quantified based on fluorescence intensity generated by AzMC reduction.

Initial screening at a fixed compound concentration (typically 100 µM) allowed rapid identification of derivatives that significantly suppressed H_2S release compared to control. From this primary assessment, several promising candidates were shortlisted based on their ability to inhibit >80% of 3-MST activity.

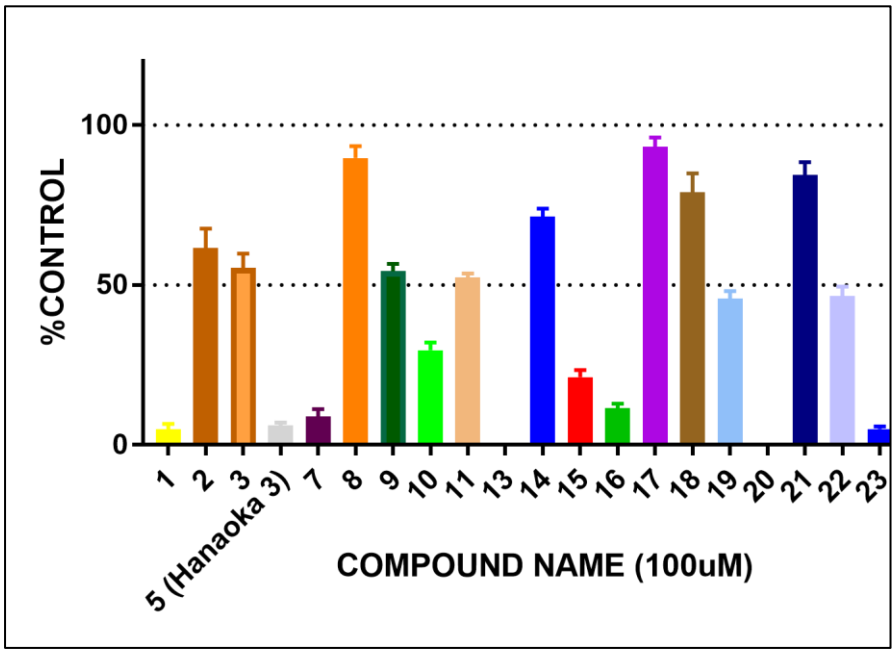
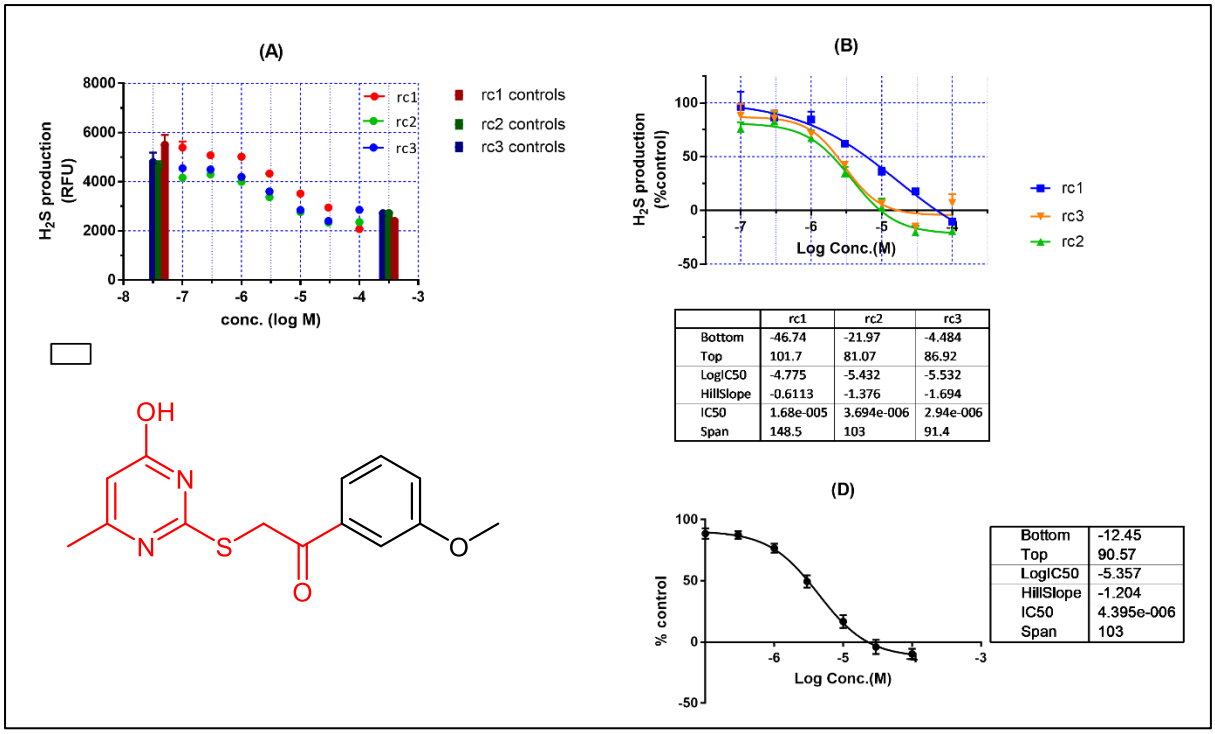


Figure 37 Screening of synthesised compounds in 3MST pathway in RLC (n-3) using H2S detection assay via SF7-AM at 37°C. Data sets represent mean ± SEM

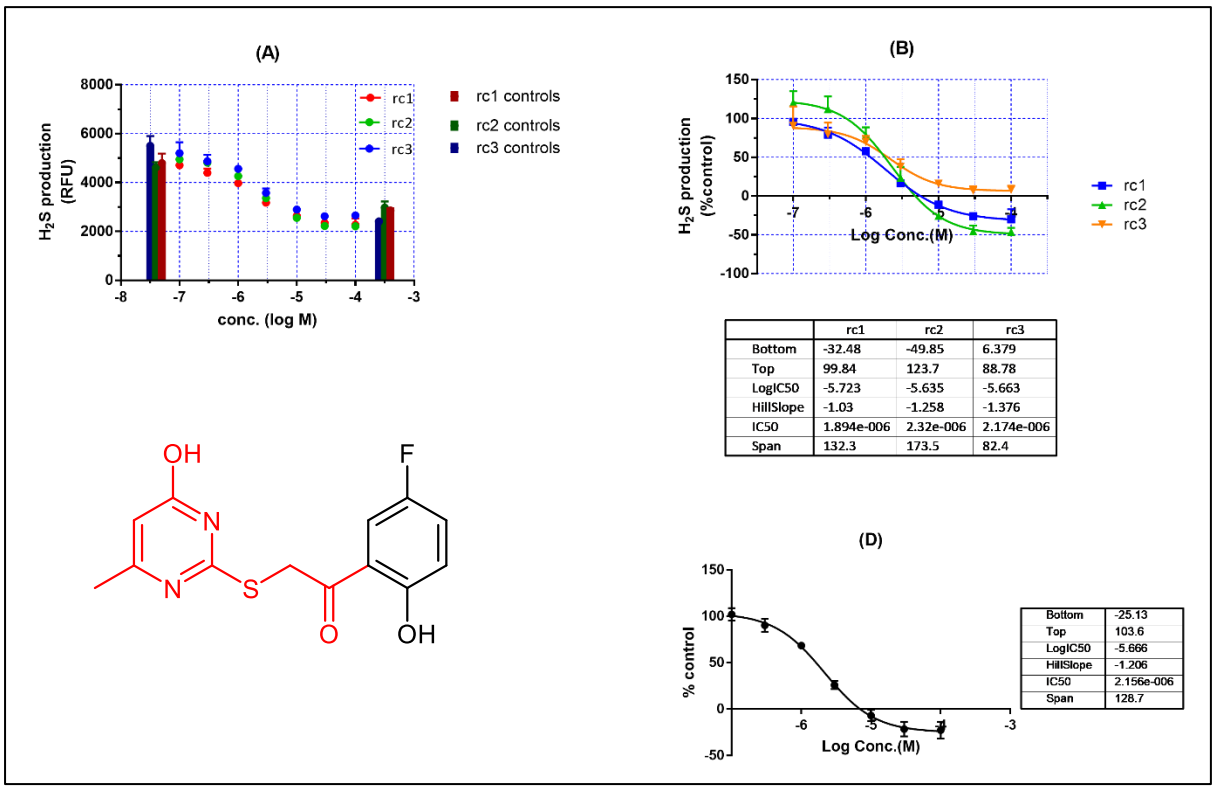
Subsequent dose–response experiments were performed for these top-performing hits to determine their IC_{50} values. Detailed graphical analyses (Figure 38,Figure 39,Figure 40) highlight the concentration-dependent inhibition profiles of the most potent and selective compounds, illustrating clear suppression of 3-MST activity relative to the reference compound. The best-performing inhibitors were investigated for SAR.



	rc1	rc2	rc3
Bottom	-46.74	-21.97	-4.484
Top	101.7	81.07	86.92
LogIC50	-4.775	-5.432	-5.532
HillSlope	-0.6113	-1.376	-1.694
IC50	1.68e-005	3.694e-006	2.94e-006
Span	148.5	103	91.4

Bottom	-12.45
Top	90.57
LogIC50	-5.357
HillSlope	-1.204
IC50	4.395e-006
Span	103

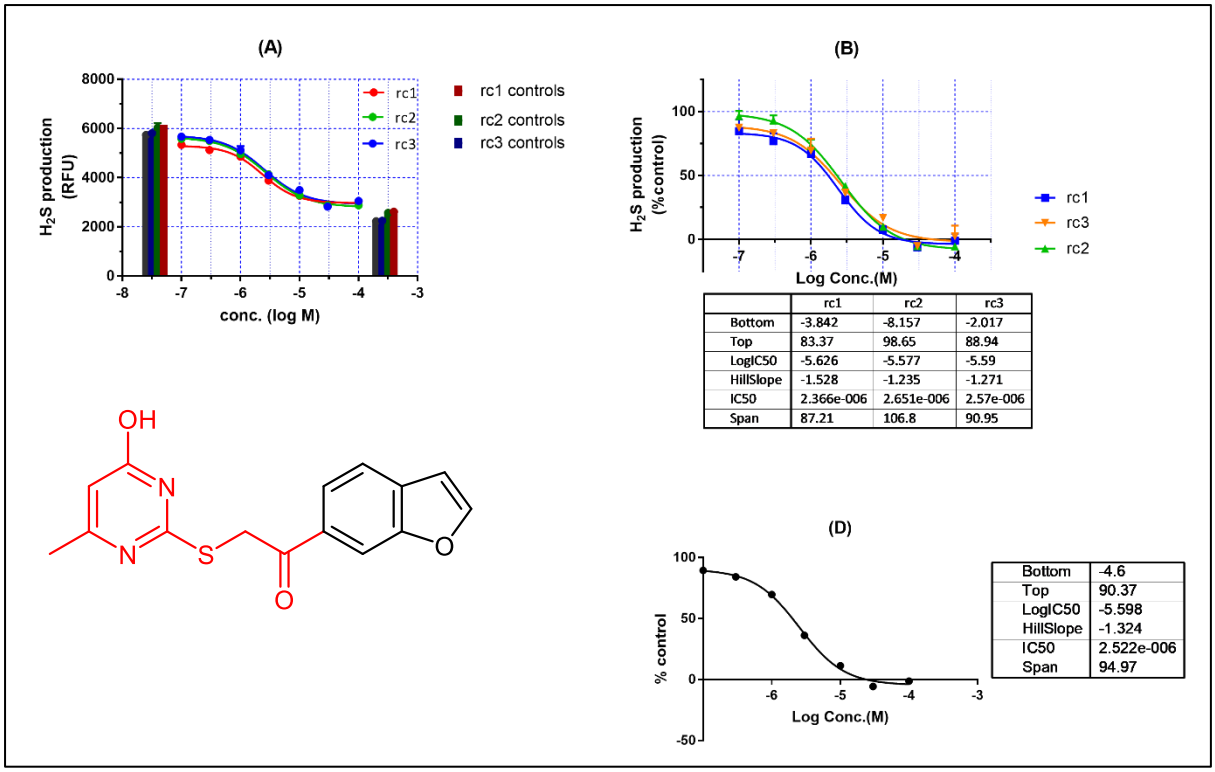
Figure 38 Assay of the inhibitory effect of MNA13 on the enzymatic production of H2S via the 3MST pathway in rat liver cytosol (RLC) samples (n=3) using H2S detection assay via SF7-AM at 37°C. (a) raw data in RFU values. (b) are normalized data, 0 is blank and 100 represents control. (d) is mean of b. Data sets represent mean ± SEM



	rc1	rc2	rc3
Bottom	-32.48	-49.85	6.379
Top	99.84	123.7	88.78
LogIC50	-5.723	-5.635	-5.663
HillSlope	-1.03	-1.258	-1.376
IC50	1.894e-006	2.32e-006	2.174e-006
Span	132.3	173.5	82.4

Bottom	-25.13
Top	103.6
LogIC50	-5.666
HillSlope	-1.206
IC50	2.156e-006
Span	128.7

Figure 39 Assay of the inhibitory effect of MNA20 on the enzymatic production of H2S via the 3MST pathway in rat liver cytosol (RLC) samples (n=3) using H2S detection assay via SF7-AM at 37°C. (a) raw data in RFU values. (b) are normalized data, 0 is blank and 100 represents control. (d) is mean of b. Data sets represent mean ± SEM



	rc1	rc2	rc3
Bottom	-3.842	-8.157	-2.017
Top	83.37	98.65	88.94
LogIC50	-5.626	-5.577	-5.59
HillSlope	-1.528	-1.235	-1.271
IC50	2.366e-006	2.651e-006	2.57e-006
Span	87.21	106.8	90.95

Bottom	-4.6
Top	90.37
LogIC50	-5.598
HillSlope	-1.324
IC50	2.522e-006
Span	94.97

Figure 40 Assay of the inhibitory effect of MNA23 on the enzymatic production of H2S via the 3MST pathway in rat liver cytosol (RLC) samples (n=3) using H2S detection assay via SF7-AM at 37°C. (a) raw data in RFU values. (b) are normalized data, 0 is blank and 100 represents control. (d) is mean of b. Data sets represent mean ± SEM

3.3.2.3. Investigating 3-benzenesulfonamidobenzoic acid (Hanaoka compound 5) inhibitory activity

3.3.2.3.1. 3MST pathway

The inhibitory activity of 3-benzenesulfonamidobenzoic acid on the production of H_2S via the 3MST pathway was tested on four rat cytosol samples in two fluorescence based assays using SF7-AM and AzMC fluorescence probes (see Figure 41). In these assays, the mean calculated IC_{50} was 5.6 µM in the SF7-AM assay and 3.8 µM in the AzMC assay, both values are within the range reported in literature (5.7 µM) (Hanaoka et al., 2017).

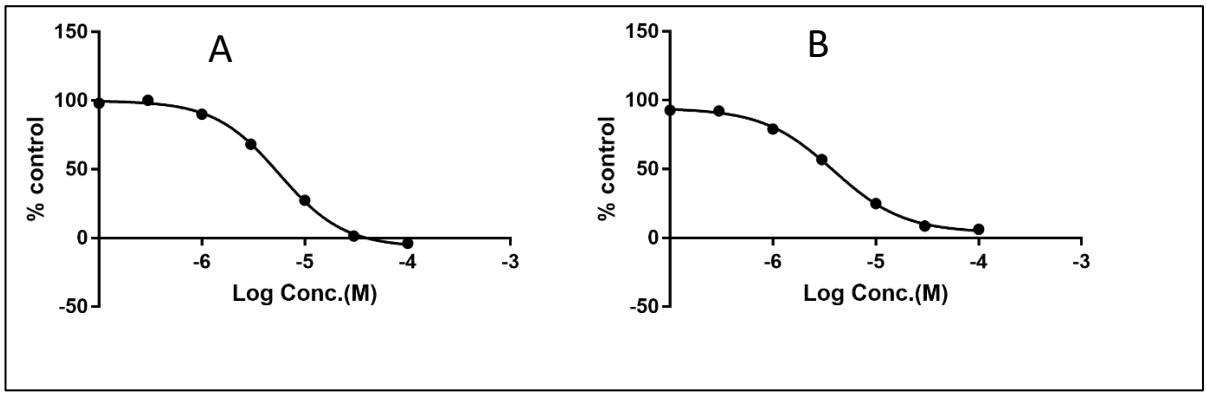


Figure 41 Assay of the inhibitory effect of 3-benzenesulfonamidobenzoic acid on the enzymatic production of H_2S via the 3MST pathway in rat liver cytosol (RLC) samples (n=4) using H_2S detection assay via AzMC (A) and SF7-AM (B) at 37°C. Data sets represent mean ± SEM.

3.3.2.3.2. CBS/CSE pathway

The selectivity of 3-benzenesulfonamidobenzoic acid for 3MST was assessed using SF7-AM fluorescence assay at three concentrations (1µM,10µM and 100 µM). The compound did not show any change in enzymatic H_2S production compared to control samples as seen in Figure 42.

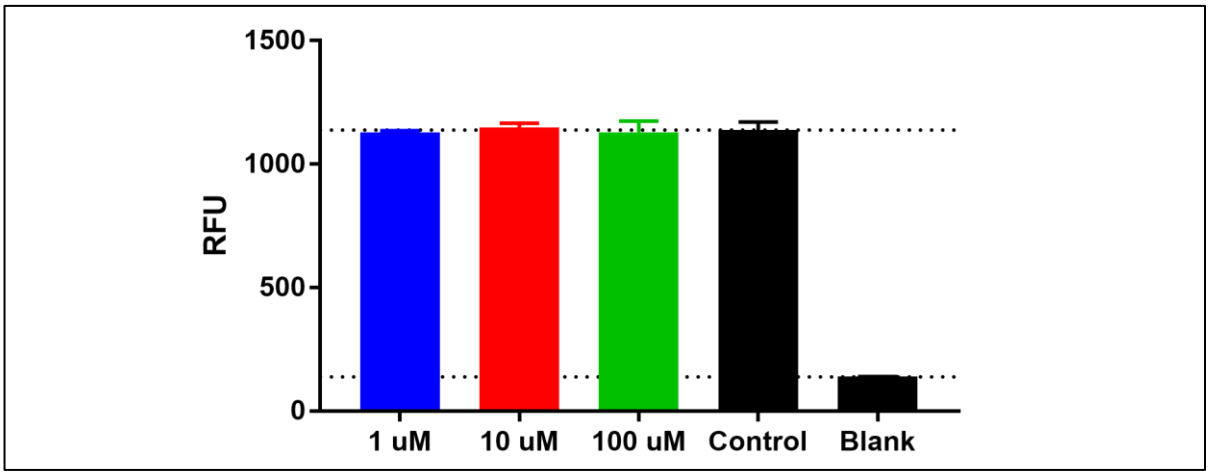


Figure 42 assay of the inhibitory effect of 3-benzenesulfonamidobenzoic acid on the enzymatic production of H_2S via the CBS/CSE pathway in rat liver cytosol (RLC) samples (n=3) using H_2S detection assay via SF7-AM at 37°C. Data sets represent mean ± SEM.

3.3.2.4. Mitochondria-Targeted Inhibitor Strategy and MNA006 Evaluation

As part of a parallel design strategy, a potential 3MST inhibitor, 2-[(1,6-dihydro-4-methyl-6-oxo-2-pyrimidinyl)thio]-N-(3-hydroxyphenyl)acetamide (MNA001), was synthesized. This compound was structurally similar to established 3MST inhibitors and was developed with two specific aims: (1) to further elucidate structure-activity relationships (SAR) within this chemical class, and (2) to serve as a conjugation partner for AP21967 (AP219), forming a mitochondria-targeted complex (MNA006). The rationale was that, by coupling MNA001 to AP219, the resulting conjugate would accumulate in the mitochondria and potentially exhibit enhanced inhibitory effects through targeted delivery.

The complex MNA006 was successfully synthesized and computationally docked into the 3MST binding site, where it showed a good fit and favourable binding scores. However, biochemical evaluation of MNA006 did not result in significant inhibitory activity in vitro. To investigate the lack of activity, an esterase cleavage assay was performed using porcine liver esterase (PLE) to test whether the bond between MNA001 and AP219 could be hydrolysed, thereby releasing free MNA001, which is known to be active. The complex was incubated with up to 4 mg of PLE for 24 hours prior to addition to the biochemical assay, but no increase in inhibition was observed. As a control, free MNA001 was also incubated under the same conditions to rule out potential degradation due to temperature or buffer conditions. Only a minor loss of activity was observed in MNA001 after incubation, confirming its relative stability under assay conditions.

MNA06 did not show the expected activity. Esterase at different concentrations (1,2,4, and 50mg per ml) was added to potentiate ester bond breakage but no effect was observed (Figure 46 ,Figure 45). Based on these results, it is hypothesized that the mitochondria-targeting mechanism

of AP219 may require the presence of intact organelles or whole cells to function properly. In the current biochemical assay setup, which lacks cellular context and mitochondrial membranes, the targeting ligand may not localize the compound effectively, and esterase activity may be insufficient or misdirected. As such, future experiments should test MNA006 in whole cells or isolated mitochondria to better assess the delivery and inhibitory potential of this targeted conjugate.

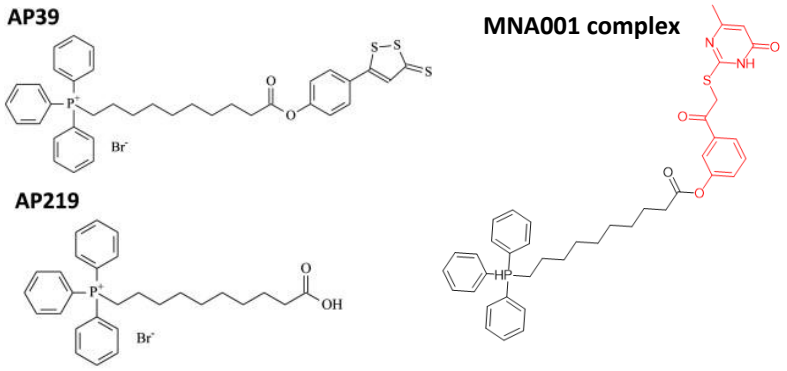


Figure 433 Chemical structure of AP39, AP 219 and MNA001 complex

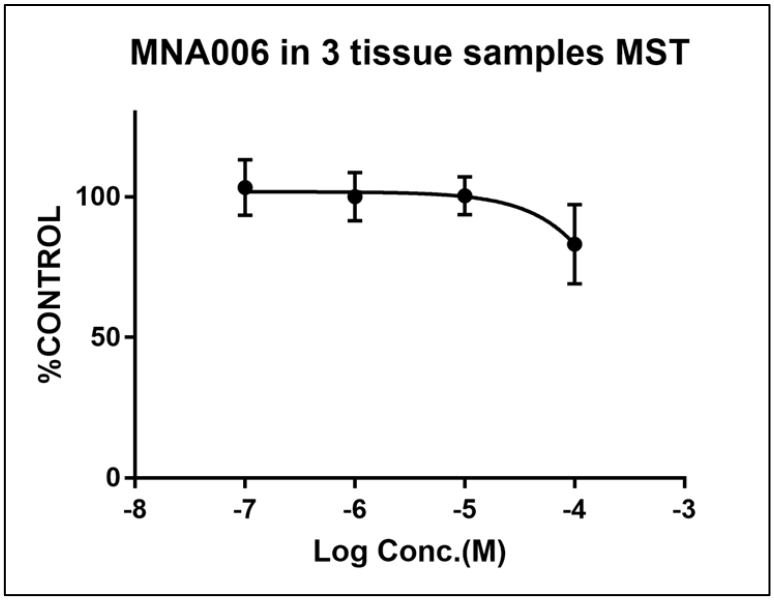


Figure 44 Assay of the inhibitory effect of MNA06 on the enzymatic production of H2S via the 3MST pathway in rat liver cytosol (RLC) samples (n=3) using H2S detection assay via SF7-AM at 37°C. normalized data, 0 is blank and 100 represents control. Data sets represent mean ± SEM

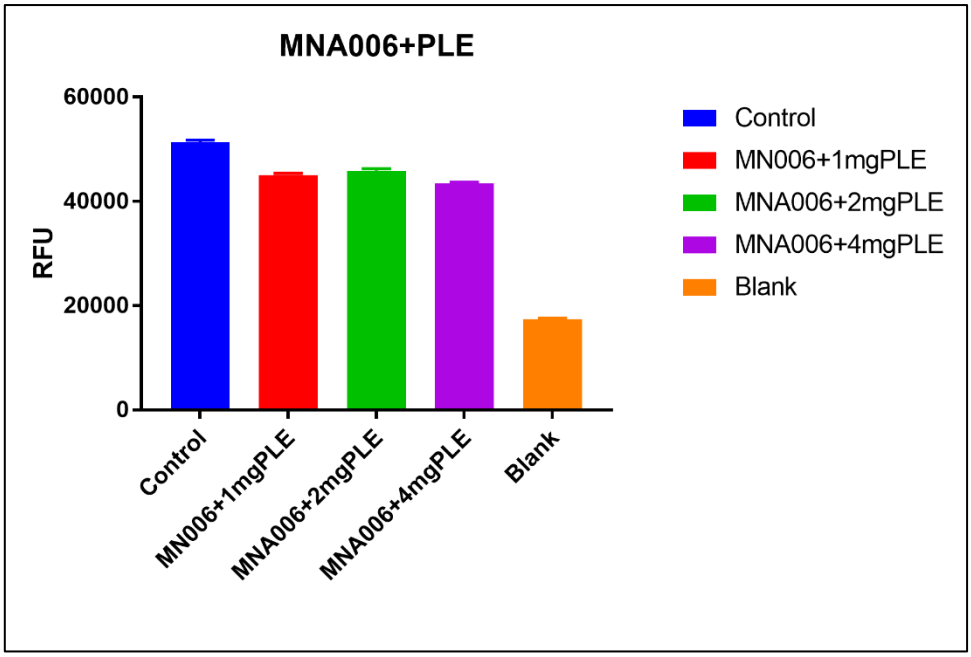


Figure 45 MNA06 with added porcine liver esterase (PLE) at varying concentrations. The inhibitory effect of MNA06 in the presence of porcine liver esterase was evaluated on H_2S production via the 3MST pathway in rat liver cytosol (RLC) samples (n = 3) using the SF7-AM fluorescence assay at 37 °C. Data are presented as raw fluorescence units (RFU). The control contains RLC without inhibitor, and the blank contains neither RLC nor inhibitor. Values represent mean ± SEM.

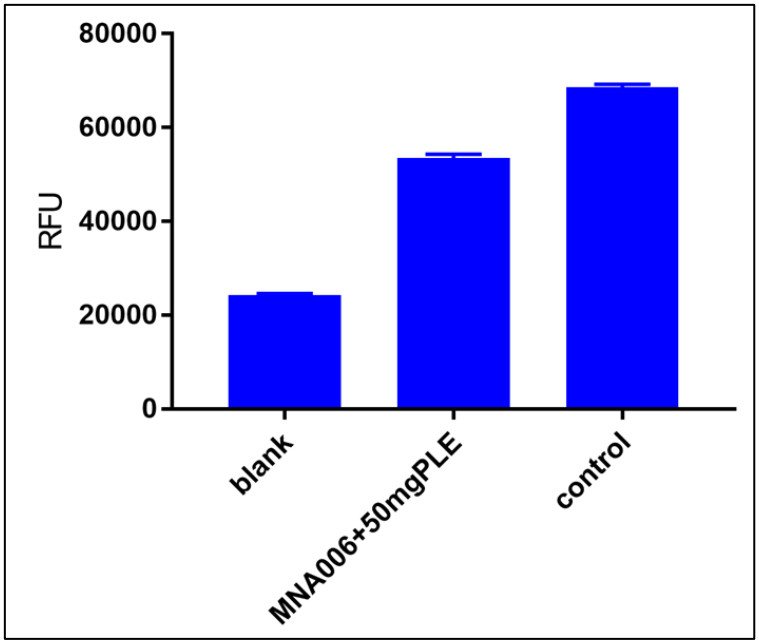


Figure 46 MNA06 with added porcine liver esterase (PLE) at 50mh/ml. The inhibitory effect of MNA06 in the presence of porcine liver esterase was evaluated on H_2S production via the 3MST pathway in rat liver cytosol (RLC) samples (n = 3) using the SF7-AM fluorescence assay at 37 °C. Data are presented as raw fluorescence units (RFU). The control contains RLC without inhibitor, and the blank contains neither RLC nor inhibitor. Up to 40% inhibition is seen. Values represent mean ± SEM.

4. Chapter IV: Discussion

This study aimed to identify novel, selective, and potent inhibitors of 3MST through rational design, synthesis, and biological evaluation of structurally diverse small molecules. In addition to discovering new inhibitory scaffolds, the work sought to clarify structure–activity relationships (SAR) and explore mitochondria-targeted delivery strategies. Despite increased interest, few structurally diverse and selective 3MST inhibitors have been reported to date. To address this, I designed a focused library of compounds based on literature-guided motifs and in silico screening.

3MST is emerging as a significant target in cancer research due to its relationship with H_2S production and its role in oncogenic processes. This enzyme contributes to maintaining intracellular redox balance and regulating various cellular signalling pathways that are crucial for cancer progression and survival. The endogenous production of H_2S by 3-MST and other enzymes has been implicated in creating an environment that supports tumour growth, invasiveness, and resistance to anticancer therapies (Augsburger et al., 2020; Dawoud et al., 2024).

Research shows that many cancer cells rely on H2S for their proliferation and metabolic needs, which varies based on cancer type (Dawoud et al., 2024). In colorectal cancer, for example, the activity of 3-MST is reportedly upregulated, indicating that tumors may exploit this pathway for their development (Dawoud et al., 2024). Evidence suggests that H2S produced via 3-MST influences essential processes, such as angiogenesis, which is often necessary for ensuring an adequate blood supply to tumour tissues (Dawoud et al., 2024)(Szabó et al., 2013; . High levels of H2S have also been correlated with increased tumorigenicity, pointing to the potential of inhibiting 3-MST as a means to restrict tumour growth significantly (Dawoud et al., 2024).

Moreover, the role of 3-MST in cancer extends beyond bioenergetics. It protects cancer cells from apoptosis (programmed cell death) by modulating cellular signalling pathways involved in cell survival (Augsburger & Szabó, 2020; . Specifically, H2S has been linked to the activation of pathways that promote cell proliferation, including phosphoinositide-3-kinase (PI3K) and protein kinase B (Akt) signalling, which inhibit apoptosis and support tumour progression (Szabó et al., 2013; (Augsburger & Szabó, 2020).

The importance of targeting 3-MST is highlighted by its dual role as both a contributor to tumour biology and a potential therapeutic candidate. Inhibiting this enzyme could reduce cancer cell proliferation and impede vital survival pathways, making it an attractive target for drug development (Augsburger et al., 2020; Majumder, 2023). Pharmacological inhibition of 3-MST has been shown to diminish cell migration and bioenergetic potential in various colon cancer models, supporting the notion that it may serve as a viable therapeutic target in cancer treatment (Majumder, 2023).

In addition to facilitating tumour growth, 3-MST may play a crucial role in the tumour microenvironment, influencing factors like inflammation and immune evasion, which are essential for tumour survival and growth (Dawoud et al., 2024; Augsburger & Szabó, 2020). This interaction with tumour cells and their surrounding stroma suggests that targeting 3-MST could have broad implications for cancer therapy—not only by directly impacting tumour cells but also by addressing the adaptive immune resistance commonly seen in malignancies (Dawoud et al., 2024).

In summary, the multifunctional roles of 3-MST in cancer—its involvement in metabolism, signal transduction, apoptosis avoidance, and interaction with the tumour microenvironment—underscore its significance as a meaningful target. Continued investigation into this area may lead to novel therapeutic interventions aimed at more effectively managing colorectal cancer and potentially other malignancies that utilize similar pathways (Augsburger & Szabó, 2020; Majumder, 2023).

4.1 High-Throughput Screening and Similarity Search Insights

To complement the rational design and synthesis of my core compound series, I conducted a high-throughput screening (HTS) of commercially available compounds selected based on structural similarity to known 3MST inhibitors. A similarity search using the DataWarrior program was carried out using compound 1 from the literature as the reference structure. Several hits with over 60% similarity were identified and screened at 10 µM. However, the results revealed a substantial disconnect between structural similarity and biological activity: although many compounds shared core features with known inhibitors, only a few showed measurable inhibition.

For example, compound NCC00076272, which contained a para-methoxy-substituted benzene ring, showed no inhibition at the screening concentration, despite resembling active analogues like MNA13. Similarly, compound NCC00036629, which featured a 3-methylene-3,4-dihydro-2H-benzo[1,4]oxazine scaffold, also failed to exhibit any activity. These outcomes underscore the limitations of ligand-based similarity metrics, which may not fully account for factors like functional group orientation, steric clashes, solubility, or cell permeability.

On the other hand, a few structurally related hits did yield positive results. Compound NCC00065766, which bears both a para-methoxy group and an ortho-sulfonamide, demonstrated significant 3MST inhibition. This structure closely resembles compound 5 from existing literature, which is known for its high potency, supporting the relevance of the sulfonamide motif in binding. Additionally, compound NCC00043864, featuring a 2,5-dimethyl-1H-pyrrole moiety, also showed inhibition, suggesting that rigid, heterocyclic terminal groups may be promising candidates in future designs. Collectively, these findings highlight the importance of complementing computational similarity and docking-based selection with experimental screening, as even minor differences in structure or substitution patterns can drastically affect biological outcomes.

4.2 Summary of Lead Compounds

Among the synthesized and screened compounds, several emerged as lead candidates based on their strong inhibition of 3MST and favourable selectivity profiles. MNA1, MNA13, MNA20, and MNA23 all exhibited ~100% inhibition at 100 µM, making them the most potent compounds in the series. MNA13, which features a meta-methoxy-substituted benzene ring, was particularly effective but showed reduced selectivity due to its ability to induce CBS and CSE activity (~300% of control). In contrast, MNA16, bearing a meta-hydroxy group, showed lower 3MST potency but greater selectivity, suggesting a potential trade-off between electronic features and target specificity.

MNA23, which incorporates a benzofuran moiety bioequivalent to the naphthalene group seen in Hanaoka compound 3, was among the most promising, exhibiting both high potency and minimal off-target effects. MNA20 demonstrated full 3MST inhibition but unexpectedly induced CSE activity to 900% of control, making it a unique candidate for potential CSE activation studies rather than inhibition. Similarly, MNA18, which also contains halogen substituents, induced CBS/CSE activity (~300%) instead of inhibiting them. This pattern highlights the influence of halogenation on off-target effects, suggesting such groups may compromise selectivity. Notably, the best-performing and most selective compounds tended to share mercaptoacetyl linkers, meta-substituted terminal aromatic rings, and non-halogenated, oxygen-containing functional groups.

Interestingly, MNA16 and MNA13 provided insight into how terminal substitution patterns affect selectivity. MNA16, which features a terminal phenol, exhibited only modest 3MST inhibition, but also induced CBS and CSE activity by 170–200%, suggesting off-target interactions. This is in contrast to

MNA13, which contains a methoxy-substituted aromatic ring and was highly potent against 3MST but showed less selectivity, inducing CBS/CSE activity by over 300%. On the other hand, MNA23, which incorporates a benzofuran group bioequivalent to literature-reported naphthalene scaffolds (e.g., Hanaoka compound 3), maintained both potency and selectivity, making it one of the most promising candidates in the series.

Several compounds yielded unexpected biological results, deviating from predictions based on structural similarity and docking studies. All compounds were initially selected based on high predicted binding affinity scores, calculated using UCSF Chimera and AutoDock Vina. Docking results consistently showed that the compounds fit well within the 3MST active site pocket, often forming plausible hydrogen bonds and hydrophobic interactions. However, despite strong computational predictions, several compounds underperformed in biological assays. For instance, MNA2, which contains a para-hydroxy substitution on the terminal phenol, was expected to behave similarly to MNA1 (meta-hydroxy), but this small positional change resulted in a dramatic drop in activity—from 100% inhibition in MNA1 to just 40% in MNA2. Likewise, MNA3, which combines meta-hydroxy and amine groups, also showed minimal inhibition (~10%). This pattern repeated in MNA10, a para-methoxy analogue of the highly potent MNA13 (meta-methoxy), which also displayed a marked reduction in activity. Poor performance of MNA8, MNA11, and MNA21, despite favorable docking, suggests that factors beyond static binding pose predictions, such as solubility, chemical stability, or dynamic enzyme–ligand interactions, may influence biological activity. Notably, MNA21, which includes ortho-dihydroxy substitutions, only achieved ~15% inhibition, likely due to steric hindrance or poor alignment within the catalytic pocket. These discrepancies underscore the complexity of predicting biological activity from docking data alone and suggest that further experimental probing and molecular dynamics studies may be needed to fully understand the determinants of 3MST inhibition.

Based on these findings, several design principles have emerged to guide the next generation of 3MST inhibitors. One priority will be to explore ortho-hydroxy substitutions on the terminal aromatic ring in a more controlled way; although such substitutions were attempted in this series (e.g., MNA21), synthetic limitations prevented a full evaluation of this motif. Given the consistent off-target activity observed in halogenated analogues, especially in compounds like MNA20 and MNA18, halogen substituents will be excluded in future designs to improve selectivity against CBS and CSE. Additionally, compounds with mercaptoacetyl linkers—particularly those lacking amide nitrogens—appeared to better maintain 3MST selectivity at 100 μM. Therefore, the mercaptoacetyl linker will be prioritized in future scaffold iterations. Conversely, terminal groups containing nitrogen atoms (e.g., amines or anilines) generally showed poor activity and will likely be avoided in subsequent compound series.

There is also a strong case for further bioisosteric exploration of the naphthalene moiety, as demonstrated by the high activity and selectivity of MNA23, which features a benzofuran group. This suggests that maintaining rigid, planar, π-stacking-capable aromatic systems may be a key factor in 3MST inhibition. As such, future designs may include more complex multi-ring systems, possibly incorporating three or more fused or linked aromatic rings to better probe the extent and orientation of π-stacking interactions within the binding pocket. Finally, there will be an intentional shift toward oxygen-containing terminal groups (e.g., hydroxyls, ethers, or furans) rather than nitrogen-based functionalities, which appeared less effective overall in this series.

4.3 Limitations and Future Directions

While this study successfully identified several promising 3MST inhibitors, there are important limitations that should be acknowledged. First, although docking studies using Chimera and AutoDock

Vina were valuable for initial selection, predicted binding affinities did not always correlate with experimental inhibition, particularly for compounds like MNA2, MNA3, and MNA10, which fit well in the active site but showed weak or no activity. This suggests that factors beyond static binding—such as solubility, metabolic stability, conformational flexibility, and redox behaviour may play critical roles in determining functional inhibition. Moreover, some compounds with favourable features were excluded from further testing due to chemical instability (e.g., MNA12), synthetic difficulties, or poor yield, limiting the scope of structure–activity relationship (SAR) analysis in certain regions of chemical space.

In future work, compound design will focus on building from the most selective and potent scaffolds, such as MNA23, and optimizing features shown to enhance activity; namely, mercaptoacetyl linkers, oxygen-based terminal groups (e.g., hydroxyl or methoxy), and rigid, π-stacking-capable aromatic systems like benzofurans. Substitutions with halogens will likely be avoided due to their association with off-target CBS and CSE activation. There is also strong interest in evaluating ortho-hydroxy substitution patterns, which could not be fully explored in this series due to synthetic constraints. Finally, the next generation of compounds may incorporate larger, fused aromatic systems to better probe π–π interactions, as well as metabolic profiling and cellular permeability assessments to guide future lead optimization.

4.4 Sulphane sulfurs: Biochemical Relevance and Future Considerations

Sulphane sulfurs, which are sulfur species with biological functions possessing more than one sulfur atom bonded together (e.g., polysulfides and persulfides), have emerged as more reliable indicators in biochemical assays compared H_2S for several reasons.

Sulphane sulfurs are significantly more stable than H_2S under physiological conditions. This stability allows sulphane sulfurs to better reflect the ongoing biochemical processes in the cellular environment over time. For instance, H_2S is prone to rapid oxidative conversion and can easily volatilize, which can lead to unreliable quantification in assay systems or misinterpretation of cellular environments (Czapla–Masztafiak et al., 2012; (Bonifácio et al., 2020; . In contrast, sulphane sulfurs possess a robust structure, allowing them to persist long enough to exert biological effects, such as modulating redox states and participating in signalling pathways (Wilk et al., 2024)(Czapla–Masztafiak et al., 2012).

Furthermore, sulphane sulfurs have distinct biochemical properties that enable them to interact with thiols and other biomolecules. This interaction capacity is crucial in several enzymatic processes, such as iron-sulfur cluster formation, which is critical for mitochondrial function and various metabolic pathways (Czapla–Masztafiak et al., 2012; O-Sánchez et al., 2023). The presence of polysulfides as regulatory molecules indicates that they may serve vital functions in cell signalling and metabolic regulation that are not fully replicated by H_2S. The ability to form persulfides upon reaction with thiols represents a unique biochemical mechanism through which sulphane sulfurs can regulate protein function and cellular responses, highlighting their importance as mediators of cellular homeostasis and signalling (Bonifácio et al., 2020; Wilk et al., 2024).

Moreover, studies have revealed that elevated levels of sulphane sulfurs correlate with certain pathological conditions, including malignancies, providing a more direct link to disease states than H_2S (Wilk et al., 2024). As cancer biology progresses, the role of these sulfur species in tumorigenicity and cellular stress responses has been investigated, resulting in a more nuanced understanding of their contribution to cellular and physiological functions (Wilk et al., 2024). This correlation may not exist

to the same degree with H_2S, which, due to its fluctuating levels, may not be as reliable as a biomarker in certain contexts.

In conclusion, sulphane sulfurs offer advantages in biochemical assays due to their stability, unique reactivity, and significance in fundamental cellular processes. Their involvement in various regulatory functions makes them superior candidates for studying biochemical pathways and disease states compared to H_2S, which may not provide an accurate or comprehensive picture of sulfur-related biochemical activities in living organisms.

This study successfully identified and characterized a series of novel small-molecule inhibitors targeting 3MST, an emerging enzymatic source of hydrogen sulfide and sulfane sulfur with therapeutic relevance. Through a structure-guided design strategy, a focused library of compounds was synthesized using a common 6-mercapto-2-methyl-4(3H)-pyrimidinone core, varying linker types and terminal aromatic groups to explore structure–activity relationships. Several compounds demonstrated potent inhibition in biochemical assays, with MNA1, MNA13, MNA20, and MNA23 achieving nearly complete inhibition at 100 µM. Among these, MNA23 emerged as a promising lead due to its combination of potency and selectivity, supported by its bioisosteric similarity to known active scaffolds.

Comprehensive SAR analysis revealed the importance of meta-substitution, oxygen-containing functional groups, and mercaptoacetyl linkers for activity and selectivity. The study also highlighted the limitations of docking predictions and similarity-based virtual screening, emphasizing the need for empirical testing. An exploratory approach using a mitochondria-targeted complex (MNA006) illustrated the potential for subcellular targeting but also revealed limitations of biochemical assay systems lacking cellular context.

Overall, this work contributes valuable new scaffolds, design principles, and biological insights into 3MST inhibition. The compounds developed here provide a platform for further optimization and biological evaluation, particularly in cell-based assays and mitochondria-specific contexts. Future directions will include expanding chemical diversity, enhancing selectivity, and probing the role of sulfane sulfur signalling, with the ultimate goal of advancing 3MST inhibitors toward therapeutic applications

5. Experimental

5.1 Biological evaluation

5.1.1 Sources and preparation of drugs and reagents:

5.1.1.1. Sources

- All the assays were conducted in sterile 96-well microplates (Thermo Scientific, Loughborough).
- All compounds and reagents were obtained from Sigma-Aldrich (Poole, Dorset, UK) unless otherwise indicated.
- Sodium mercaptopyruvate: Acquired from ChemCruz (Dallas, Texas USA).

5.1.1.2. Preparation of solutions

5.1.1.2.1. Preparation of SF7 -AM

5mM stock solutions of the fluorescence probe SF7-AM were prepared and stored at -20^{o}C. The stock reagents were originally dissolved in DMSO and prior to each assay, they were diluted with Tris-EDTA buffer (0.1 M Tris, 1mM EDTA [pH7.4]) to make 5 µM final concentration.

5.1.1.2.2. Preparation of AzMC

5mM stock solutions of the fluorescence probe AzMC were prepared and stored at -20^{o}C. The stock reagents were originally dissolved in DMSO and prior to each assay, they were diluted with HEPES buffer (1 M HEPES [pH8]) to make 10 µM final concentration.

5.1.1.2.3. Preparation of Rat Liver Cytosol (prepared by Michael Garle)

For these experiments, four male and four female Sprague Dawley rat livers were used after killing them by cervical dislocation. The liver was washed in ice-cold buffer (50 mM Tris HCl containing 1mM EDTA buffer at pH 7.4) then cut into pieces and homogenized using a Turax homogeniser for 30 seconds at full speed. Each one gram of liver was contained in 10 ml of homogenate. Afterwards, the homogenate was distributed into balanced centrifuge tubes and spun at 1000xg for 20 min at 4°C. Only the supernatant was removed and then spun at 30,000xg for 60 minutes. Again, the supernatant was removed and stored in 1.2 ml aliquots as the supernatant fraction and stored in a -80^{o}C freezer. Before each experiment, working stock solutions were freshly prepared by diluting rat liver cytosol in Tris-EDTA buffer.

5.1.2 General principle of the biochemical assays used to evaluate H_2S enzyme inhibitors

In this assay, rat liver cytosol is used as the enzyme source and dispensed after dilution into 96-well plates together with the corresponding substrate. The reaction produces H_2S, which subsequently reacts with a selective fluorescent probe. The resulting fluorescence is measured using a fluorometer. Addition of an enzyme inhibitor reduces H_2S production and consequently decreases the detected fluorescence signal. The difference in signal production is used to calculate percentage of inhibition. See Figure 47.

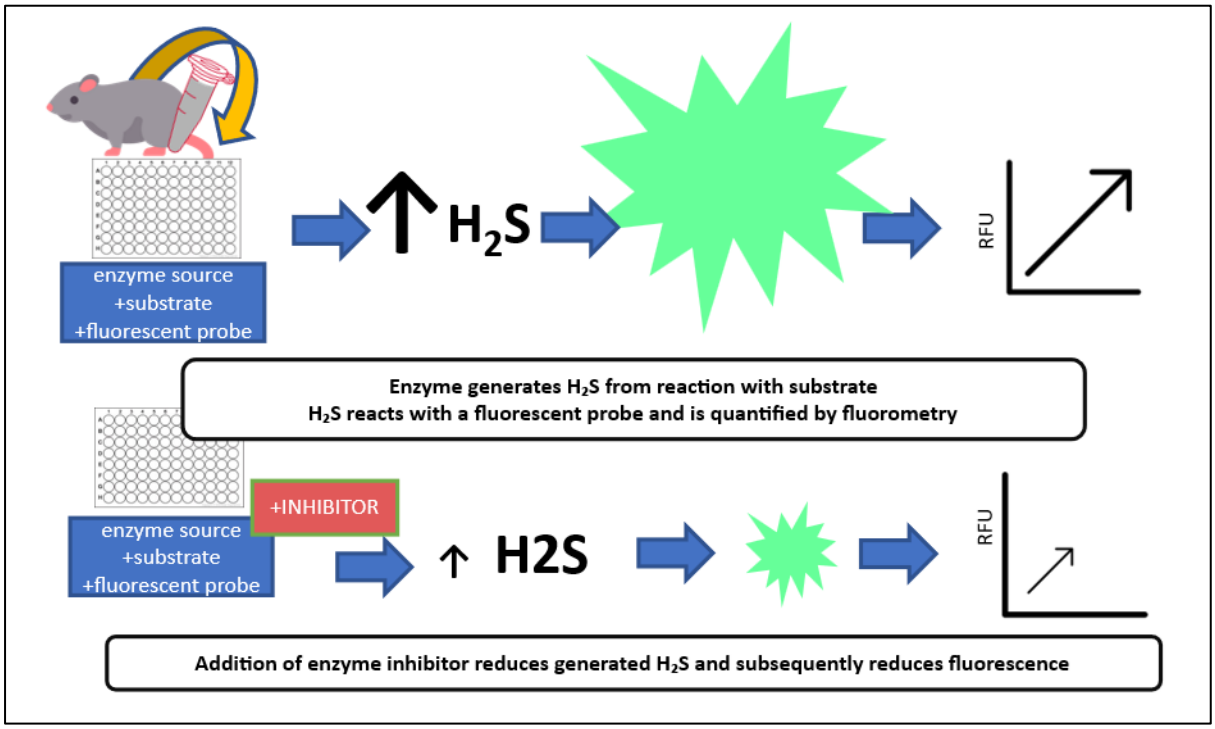


Figure 47 Schematic representation of the biochemical assay used to assess inhibition of enzymatic (H_2S) production.

Definition of assay controls see Figure 48

Sample: a well containing the compound/inhibitor to be investigated. Cytosol with fluorescent probe and substrate are added.

Control: a well containing cytosol with fluorescent probe and substrate. Test compound/inhibitor is replaced with buffer.

Blank: a well containing buffer instead of cytosol, with fluorescent probe and substrate. Test compound/inhibitor is replaced with buffer.

Positive control: a well containing a known inhibitor from literature to verify results. Cytosol with fluorescent probe and substrate are added.

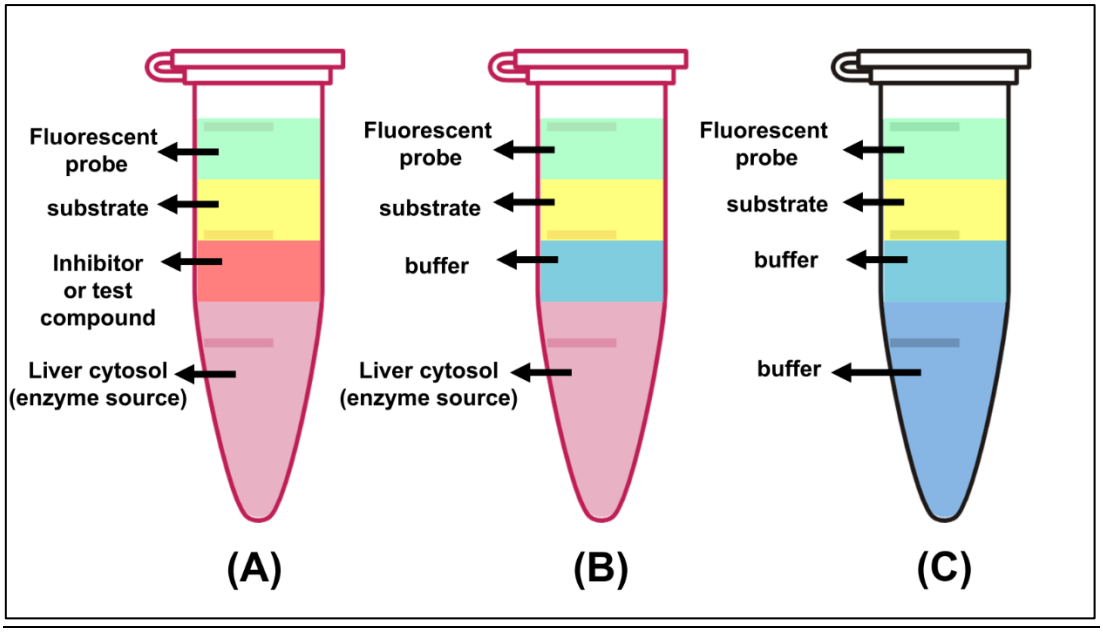


Figure 48 Differentiation between control and blank biochemical assays

(A) Sample, (B) Control, (C) Blank

5.1.2.1.1. H_2S production through 3MST using SF7-AM fluorescence probe.

In order to test the effect of compounds on the 3MST pathway, 10mM stock solutions were prepared in DMSO. Serial dilutions were then performed in Tris-EDTA buffer (0.1 M Tris, 1mM EDTA [pH7.4]) to test final concentrations ranging from 100nM to 100µM. 10 µL of the compound was added to 70 µL rat liver cytosol (1/10 dilution in Tris-EDTA buffer) in 96-well microplates and pre-incubated for 30 minutes at 37°C. After pre-incubation, 10 µL of 50µM SF7 reagent stock was added to the mixture. Hydrogen sulfide production was stimulated by the addition of 3MST substrate: mercaptopyruvate (10 µL of 100 mM stock solution). The plates were then incubated for a further 60 minutes at 37°C. After incubation, the fluorescence was measured by using a fluorimeter (excitation 485nm and emission at 538nm). The readings were normalized with tissue blanks where applicable.

SF7-AM and mercaptupyruvate were added to all wells. Negative control samples received rat liver cytosol but no test compounds. Tissue blanks contained Tris-EDTA buffer and no rat liver cytosol or compounds. Solutions containing Sodium mercaptopyruvate in Tris-EDTA buffer were freshly prepared before each experiment (10mM final concentration).

5.1.2.1.2. H_2S production through CBS/CSE pathway using SF7-AM fluorescence probe.

Detection of H_2S in the CBS/CSE pathway using SF7-AM is similar to the 3MST pathway. However, in this assay, CBS/CSE activity is stimulated by adding their common substrate L-cysteine instead of mercaptopyruvate. Both CBS and CSE are dependent on the co-enzyme pyridoxal phosphate (PLP), thus it was added to the reaction mixture. AOAA (see Figure 49) and PAG (see figure Figure 50) are

known CBS/CSE inhibitors and were incorporated into the investigations to be used as positive controls.

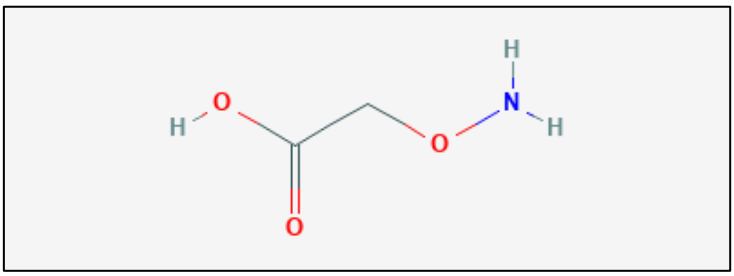


Figure 49 Chemical structure of AOAA (aminooxyacetic acid)

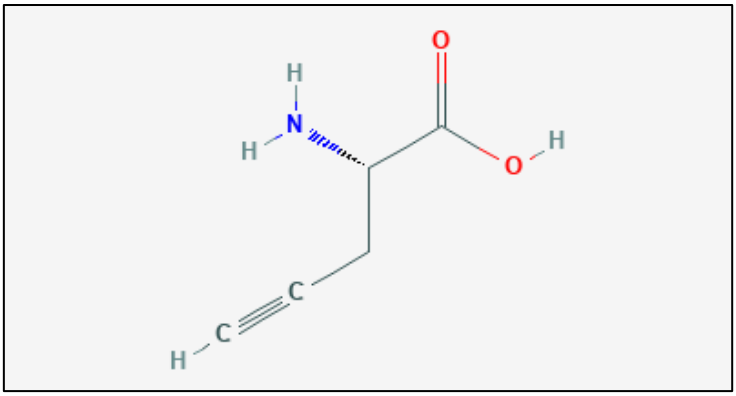


Figure 50 Chemical structure of PAG (Propargylglycine)

In this assay, serial dilutions ranging from 100nM to 100µM (final concentrations) of compounds (CDS004892, AOAA and PAG dissolved in either DMSO or Tris-EDTA were prepared. 10µL of each concentration was added to 96-well plates containing 80µL RLC (1/10 dilution in Tris EDTA buffer) and pre-incubated for 60 minutes at 37°C. After incubation, 10µL of a mixture containing 100mM L-cystiene, 50µM SF7-AM and 1 mM PLP, all dissolved in Tris-EDTA buffer, were added to all wells. The plates were further incubated for 90 minutes. After incubation, the fluorescence was measured by using a fluorimeter (excitation 485nm and emission at 538nm). The readings were normalized with tissue blanks where applicable. Negative control samples contained RLC and no compounds. Tissue blanks did not contain either RLC or compounds.

5.1.2.1.3. H_2S Detection via Methylene Blue Method

5.1.2.1.3.1. CBSE/CSE Pathway

Measurement of H_2S in this method is dependent on the production of methylene blue, which absorbs strongly at 670 nm. Methylene blue is the product of ferrous catalysed reaction of zinc trapped sulfide with dimethylphenylendiamine (DMPD) under acidic conditions.

In this method, RLC samples were diluted (1 to 4) in Tris-EDTA buffer containing 100µM PLP. Serial dilutions of test compounds (AOAA and CDS004892) were performed (ranging from 100nM to 100µM final concentration) and were added to test samples. Cytosols and cytosols containing test compounds were then incubated for 15 minutes at 37°C. After that, L-cysteine (10mM final concentration) was added to all samples except the blanks and the samples were further incubated for 120 minutes. The final volume was 300µL. L-cysteine was added to the blanks after incubation. At the end of the incubation period, 75µL 0.5M sodium hydroxide and 500µL 6% zinc acetate were added to all samples

to stop the reaction and trap H_2S. The mixture was left for 30 minutes at room temperature as zinc acetate precipitated the protein. After that, 300 µL of a mixture containing Dimethyl-phenylenediamine Sulphate (DMPD) 0.1%w/v and Ferric Chloride 50 mM was added to all samples, and blue colour developed over 30 minutes when appropriate. Samples were then centrifuged for five minutes at 3000xg. The supernatant was then pipetted into 96-well microplates and a Spectramax plate reader was used to measure absorbance at 670nm.

5.1.2.1.3.2. 3MST Pathway

To observe full activity, it is recommended to use a sulfur based reducing agent, such as DTT. Mercaptupyruvate is used as a substrate, and because of its spontaneous decomposition, enzymes were added to blanks only after the reaction was stopped using zinc acetate and NaOH.

RLC samples were diluted in Tris EDTA buffer which contained 0.5M DTT. Serial dilutions of the compound (CDS004892) were performed (ranging from 100nM to 100µM final concentration) and 3µL was added of each concentration. 3 µL of 100% v/v DMSO was added to the control and tissue blank. The compound was added in the beginning to allow binding via pre-incubation for 30 minutes at 37°C. After pre-incubation, 30µL of mercaptupyruvate (10mM final concentration) was added to all tubes, which were then incubated for 60 minutes at 37°C. At the end of the incubation period, 75µL of 0.5M sodium hydroxide and 500µL 6% w/v zinc acetate were added to all samples to stop the reaction and trap H_2S and RLC was added to the blanks. After that, 300 µL of a mixture containing Dimethyl-phenylenediamine Sulphate (DMPD) 0.1%w/v and Ferric Chloride 50 mM was added to all samples, and blue colour developed over 30 minutes when appropriate. Samples were then centrifuged for five minutes at 3000xg. The supernatant was then pipetted into 96-well microplates and a Spectramax plate reader was used to measure absorbance at 670nm.

5.1.2.1.4. H_2S production through 3MST using AzMC fluorescence probe

In order to test the effect of compounds on the 3MST pathway, 10mM stock solutions were prepared in DMSO. Serial dilutions were then performed in HEPES buffer [pH8] to test final concentrations ranging from 100nM to 100µM. 10 µL of the compound was added to 70 µL rat liver cytosol (1/10 dilution in HEPES buffer) in 96-well microplates and pre-incubated for 30 minutes at 37°C. After pre-incubation, 10 µL of 100µM AzMC reagent stock was added to the mixture. Hydrogen sulfide production was stimulated by the addition of 3MST substrate: mercaptopyruvate (10 µL of 100 mM stock solution). The plates were then incubated for a further 40 minutes at 37°C. After incubation, the fluorescence was measured by using a fluorimeter (excitation 365nm and emission at 450nm). The readings were normalized with tissue blanks where applicable.

AzMC and mercaptupyruvate were added to all wells. Control samples received rat liver cytosol but no test compounds. Tissue blanks contained Tris-EDTA buffer and no rat liver cytosol or compounds. Solutions containing Sodium mercaptopyruvate in HEPES buffer were freshly prepared before each experiment (10mM final concentration).

5.1.2.1.5. Data analysis and statistical procedures

All data are presented as means ± SEM. Statistical analysis included Two-way ANOVA and followed by Tukey's multiple comparisons test. Differences were considered statistically significant when P-value was less than 0.05. Statistical analysis was performed by using GraphPad Prism version 7.04 for Windows, GraphPad Software, La Jolla California USA, www.graphpad.com

5.1.2.1.5.1. Normalisation of results

Percent Activity (% control)

$$\% \text{ Activity} = \frac{S_{\text{sample}} - S_{\text{blank}}}{S_{\text{control}} - S_{\text{blank}}} \times 100$$

Where:

- S_{sample}= signal with cytosol and test compound
- S_{control}= signal with cytosol and vehicle (buffer) only (100% activity)
- S_{blank}= background signal (no enzyme) (0%)

5.1.3 General notes and optimisations

Several assay conditions were altered, investigated and tested to provide more reproducible and accurate results.

Changing the concentrations of some elements in the protocol, such as the concentration of the florescence probe SF7-AM (diluting to 0.5 µM concentration), produced almost undetectable signalling compared to initial 5 µM. It was also observed that fresh preparations of SF7-AM showed larger RFU values compared to stored (in -20° freezer) preparations, which led to the conclusion that fresh (no more than six months in storage) preparations should be used in the all assays. In addition, rat liver cytosol samples (stored in -80° freezer) must also be relatively fresh to produce uniform results. Another observation was that used samples in Eppendorf tubes when returned to freezer and then reused in other experiments retained enzymatic activity (but only in the CBS/CSE assays). Furthermore, as the activity of CSE/CBS are dependent on PLP, test assays without PLP produced almost undetectable signalling in the initial investigations. It is noteworthy that high concentrations of PLP tend to react rapidly with L-cysteine, thus the mixture must be pipetted rapidly to produce uniform results in the plate and between tissue samples. However, reducing the concentration of PLP (1 to 10) produced faint signalling and values of the negative controls and tissue blanks were not distinguished enough to qualify the use of lower concentrations. To overcome this issue, a repeater pipette (rapid addition of PLP/L-C/Sf7) was used with the recommended concentration (100 µM) of PLP in the protocol with positive results. Moreover, the compounds were tested down to 0.1 µM instead of 1 µM to obtain a broader range of results.

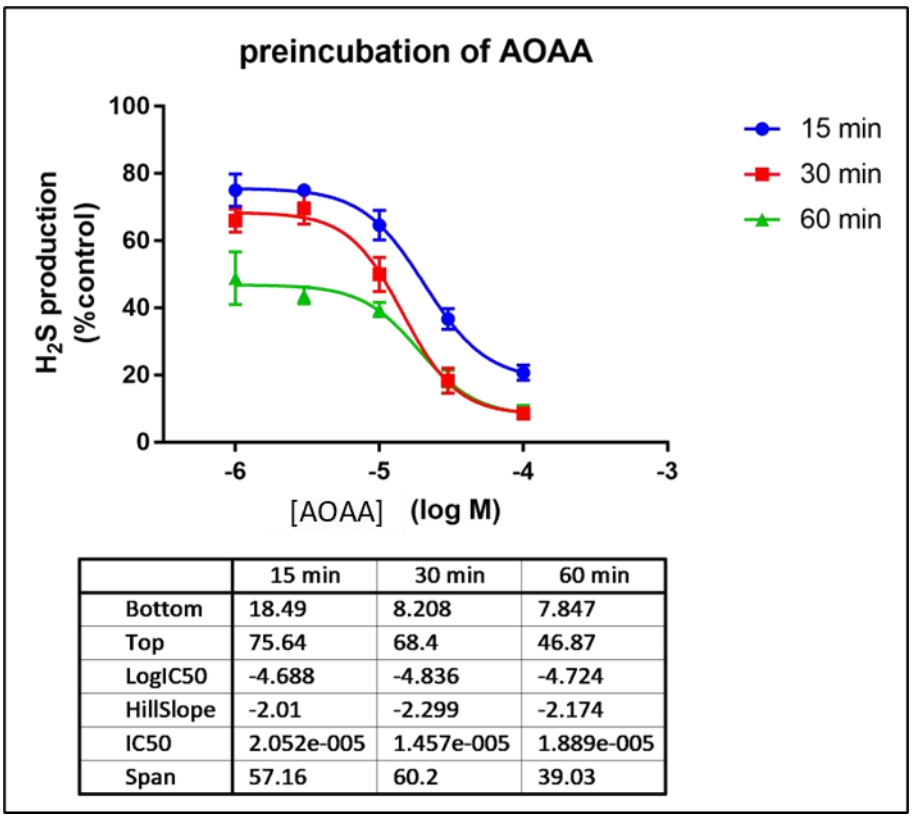
Initial investigations of the effect of AOAA and PAG on H_2S production via the CBS/CSE pathway in three rat liver cytosol samples showed concentration-dependant inhibition for both compounds. However, the results were not uniform or conclusive. Precise IC_{50} values in most RLC samples could not be calculated and each sample showed a different slope. In addition, some data sets showed high error bars. Based on these results, it was decided to optimise the assays to attain more uniform and accurate results.

Increased homogenisation of the reaction mixtures in each plate was attempted through several routes, including the simple altered pipetting sequence to maximise homogenisation and decrease use of tips, as well as shaking the plate during kinetic assays or by using a shaking incubator, which provided misleading results (see below). Investigating pre-incubation times (15, 30, 60 minutes) was also performed to maximise compound binding to enzymes. Moreover, suitable incubation times were investigated in kinetic assays.

It was observed that by randomly changing the location of compounds and controls in the plate, that some assays suffered from “edge effect”, a phenomenon where part of the plate, usually the perimeter, partially evaporates, causing previously unexplained errors in the results. Therefore, pipetting in perimeter wells was avoided when possible. Another investigation to identify the cause of errors was comparison of the experiments in regular transparent 96-well plates with replicate experiments using black opaque 96-well plates. After avoiding edges in both assays, the results were almost identical.

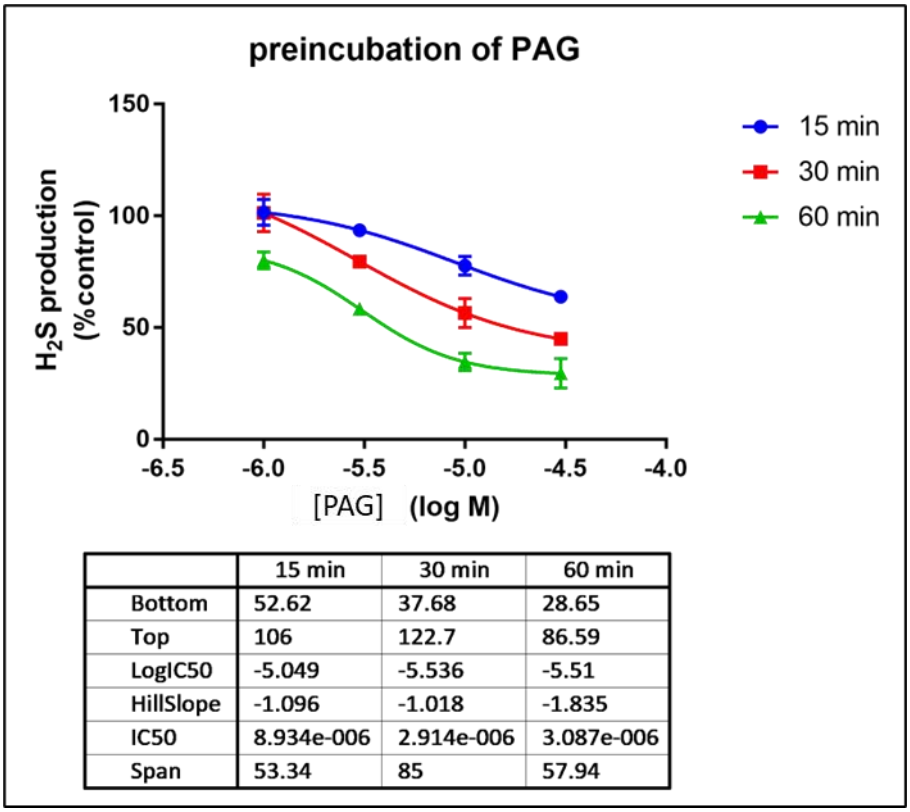
5.1.3.1. *Pre-incubation periods*

The results showed concentration-dependant inhibition of H_2S production via the CSE/CBS pathway using either AOAA (Figure 51) or PAG (Figure 52). The pre-incubation times were tested in one rat cytosol sample for 15, 30 and 60 minutes on the hot plate at 37°. Two-way ANOVA analysis was conducted and a significant difference (*P*-value was < 0.05) was detected between 60 minutes and the two other pre-incubation times, although tissue blanks and negative controls between each incubation time were not significantly different. The results showed that at 60 minutes pre-incubation, the inhibition of H_2S was significantly higher, so all future assays were incubated at 60 minutes.



	15 min	30 min	60 min
Bottom	18.49	8.208	7.847
Top	75.64	68.4	46.87
LogIC50	-4.688	-4.836	-4.724
HillSlope	-2.01	-2.299	-2.174
IC50	2.052e-005	1.457e-005	1.889e-005
Span	57.16	60.2	39.03

Figure 51 Concentration-inhibition curve of AOAA shows an inhibitory effect on the enzymatic production of H_2S via the CSE/CBS pathway in rat liver cytosol samples (n=1) using a SF7-AM fluorescence probe to detect H_2S. In this figure, three pre-incubation times (15, 30 and 60 minutes) were compared and data are expressed as a percentage of the negative control (no inhibitor). Data sets represents mean ± SEM



	15 min	30 min	60 min
Bottom	52.62	37.68	28.65
Top	106	122.7	86.59
LogIC50	-5.049	-5.536	-5.51
HillSlope	-1.096	-1.018	-1.835
IC50	8.934e-006	2.914e-006	3.087e-006
Span	53.34	85	57.94

Figure 52 Concentration-inhibition curve of PAG shows an inhibitory effect on the enzymatic production of H_2S via the CSE/CBS pathway in rat liver cytosol samples (n=1) using a SF7-AM fluorescence probe to detect H_2S. In this figure, three pre-incubation times (15, 30 and 60 minutes) were compared and data are expressed as a percentage of the negative control (no inhibitor). Data sets represent mean ± SEM

5.1.3.2. Effects of shaking the plate

In order to maximise homogenisation of the reaction mixture, the 96-well plate was put in a shaking incubator (environmental shaking). Initial results showed decreased RFU values all over the plate compared to using the static incubator. To investigate the matter further, a kinetic assay was conducted over 90 minutes at 37°C, and the spectrophotometer was set up to shake the plate before each reading (see Figure 53). The results showed an overall decrease in the RFU values, and the negative control values were not as well distinguished from the tissue blanks as the previous "no-shaking" assays. Interestingly, addition of inhibitors at various concentrations produced values well below the tissue blank (see Figure 54), suggesting a shaking-dependant decrease in SF7-AM, which is more pronounced by adding enzyme inhibitors. Due to the volatile nature of H_2S, the decreased RFU values could be because of the combined effect of shaking the plate and absence of plate lid inside the spectrophotometer, leading to increased release and consecutive loss of H_2S into the atmosphere. The kinetic assay was repeated, but without shaking the plate throughout the experiment, and the RFU values were markedly higher, with distinguishable readings of negatives controls and blanks (see Figure 55). Addition of inhibitors in this assay showed concentration-dependant inhibition of H_2S, but the results did not go below tissue blanks (see Figure 56). Based on these results, no shaking mechanisms were used in future assays and the plates were moved with caution. Most assays were performed using a single rat liver cytosol

preparation, as they were intended for qualitative optimisation rather than quantitative determination of inhibition.

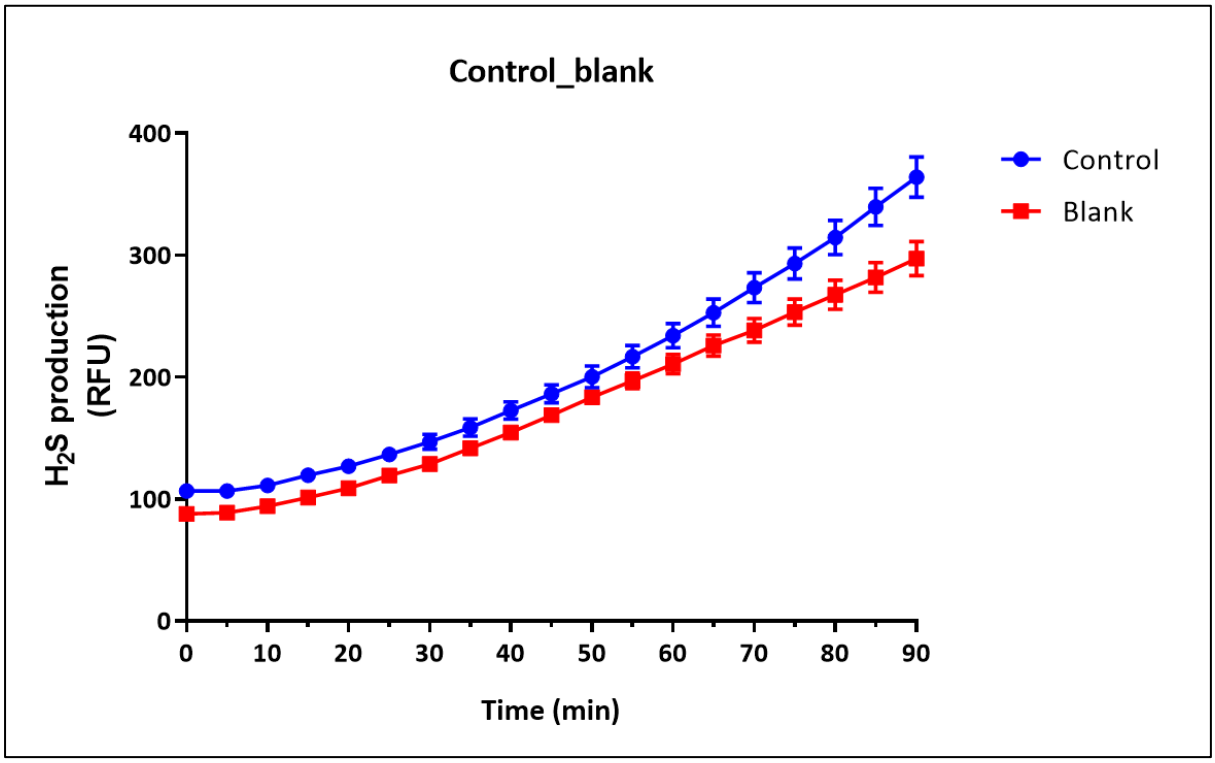


Figure 53 Investigation of the difference between H_2S production (in the CSE/CBS pathway) of the negative control and tissue blank of one (n=1) rat liver cytosol sample, in quadruplicate, over 90 minutes at 37° using H_2S detection assay via SF7-AM fluorescence probe. This kinetic assay was set up to shake the plate before each reading at 5 minutes intervals. Data sets represent mean ± SEM

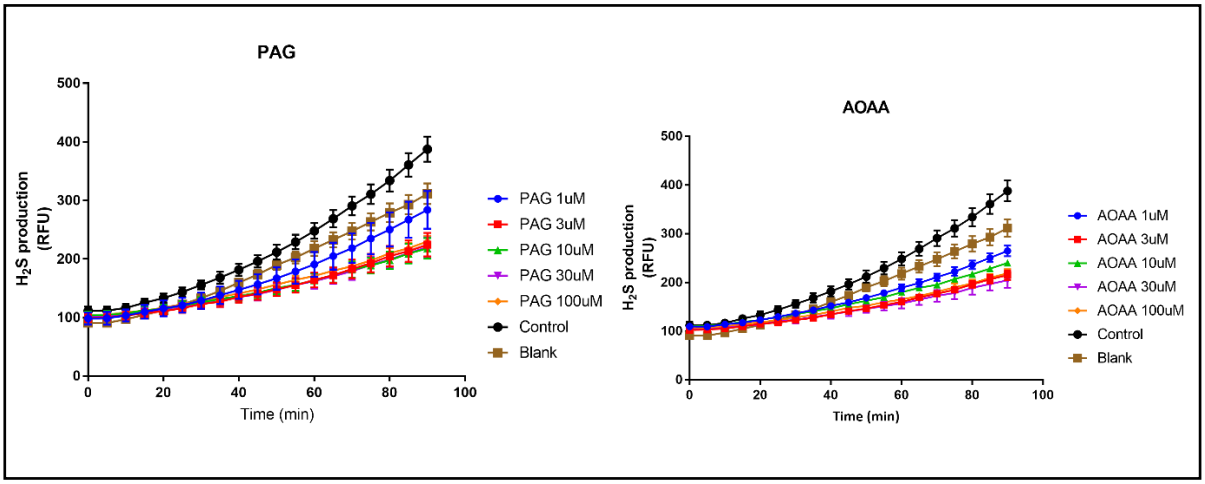


Figure 54 Kinetic assay of the inhibitory effect of AOAA and PAG on the enzymatic production of H_2S via the CSE/CBS pathway in rat liver cytosol samples (n=1) , in quadruplicate, using H_2S detection assay via SF7-AM fluorescence probe over 90 minutes at 37°C. In this figure, data are expressed as relative florescence value (RFU) which correlates with H_2S production. This kinetic assay was set up to shake the plate before each reading at 5-minute intervals. Data sets represent mean ± SEM

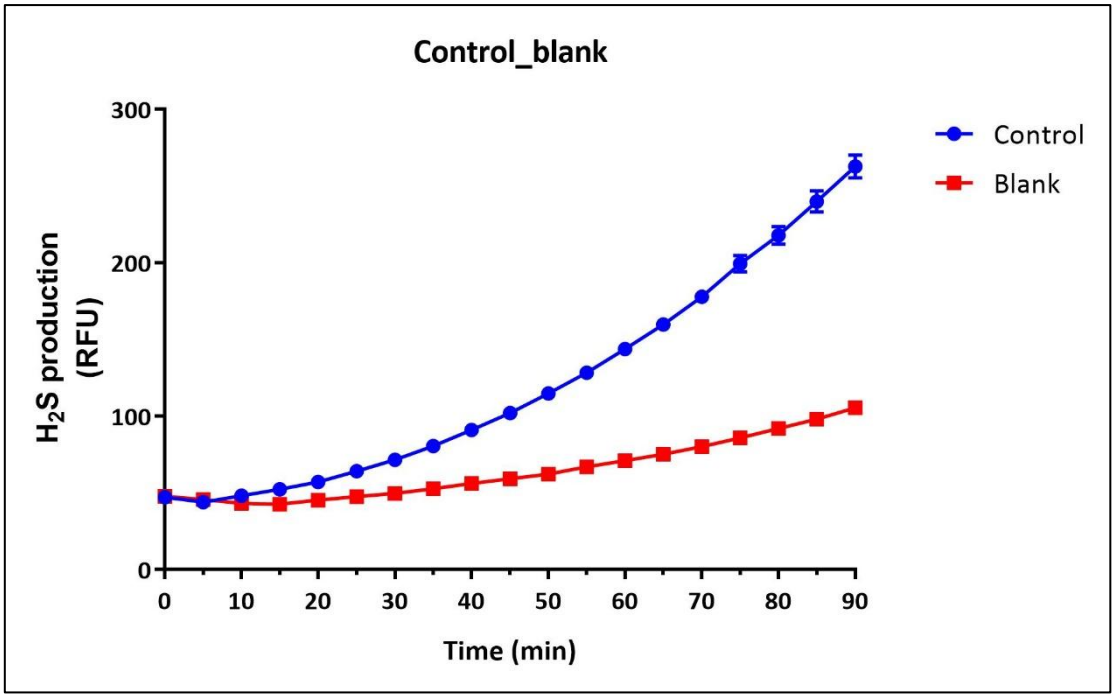


Figure 55 Investigation of the difference between H_2S production (in the CSE/CBS pathway) of the negative control and tissue blank of one (n=1) rat liver cytosol sample, in quadruplicate, over 90 minutes at 37°C using the H_2S detection assay via SF7-AM fluorescence probe. This kinetic assay was set up to not shake the plate. Data sets represent mean ± SEM

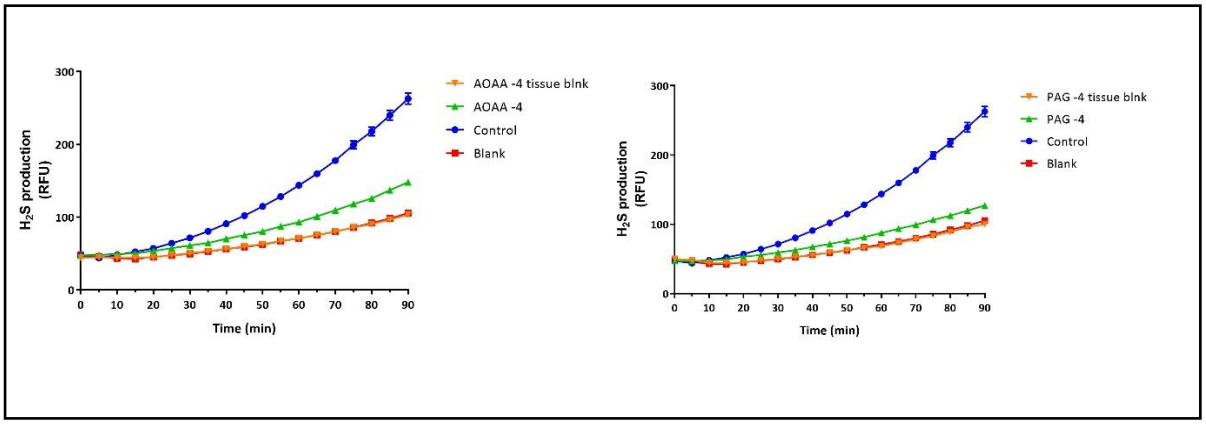


Figure 56 Kinetic assay of the inhibitory effect of AOAA and PAG on the enzymatic production of H_2S via CSE/CBS pathway in rat liver cytosol samples (n=1) , in quadruplicate, using H_2S detection assay via SF7-AM fluorescence probe over 90 minutes at 37°C. In this figure, data are expressed as relative florescence value (RFU) which correlates with H_2S production. This kinetic assay was set up to not shake the plate. Data sets represent mean ± SEM

5.1.3.3. Changing plate type

A side by side comparison of the effects of AOAA on H_2S production in regular transparent and black opaque 96-well plates was performed (see Figure 57). After avoiding pipetting into perimeter wells in both plates, the errors in the data sets were reduced. There was a slightly larger, vertical dynamic range of the black plates compared to the transparent plates but it was not significant enough to warrant continuous use of the more expensive black plates in future assays.

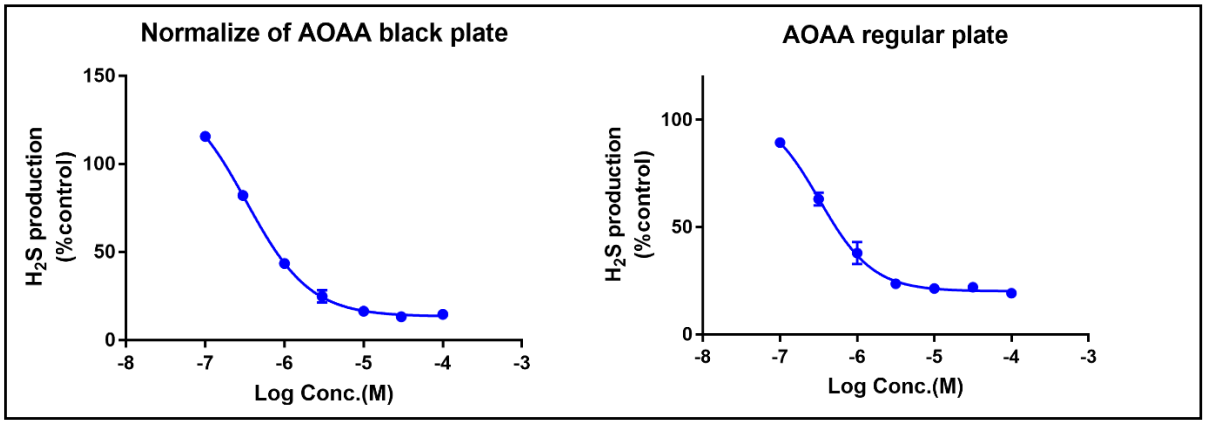


Figure 57 A side-by-side comparison of the effects of AOAA on H_2S production in regular transparent and black opaque 96-well plates. This concentration-inhibition curve of AOAA shows the inhibitory effect on the enzymatic production of H_2S via CSE/CBS pathway in rat liver cytosol samples (n=1) using H_2S detection assay via SF7-AM fluorescence probe. Data are expressed as a percentage of the negative control (no inhibitor). Data sets represent mean ± SEM

5.1.3.4. Substrate concentration

Initial investigations included selection of the optimum mercaptopyruvate concentration to be used in the assays. At low concentration, the absorbance of tissue blanks could not be distinguished from the negative controls (no inhibitor), but they were at 10 mM (Figure 58), thus, for subsequent assays, 10 mM mercaptopyruvate was used.

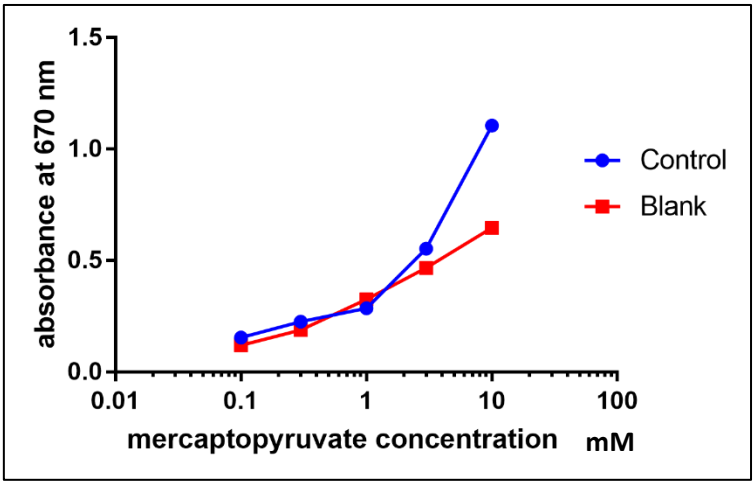


Figure 58 Effect of mercaptopyruvate concentration on the absorbance of methylene blue in one rat liver cytosol sample. Data sets represent mean± SEM

5.1.3.5. Quenching

To ensure that no signal interference occurred during compound screening, control experiments were performed to verify that test compounds did not directly interact with the fluorescent probe independently of enzyme activity. Mercaptopyruvate, the substrate used in the 3MST assays, was monitored over time at a final concentration of 10 mM to assess baseline signal generation. To evaluate the suitability of this system for detecting potential quenching or H_2S scavenging, the lead compound CDS004892 was incubated at 100 µM and 300 µM for 90 minutes in buffer containing 10 mM mercaptopyruvate, and the resulting fluorescence was compared with a blank control containing mercaptopyruvate and buffer alone. No significant differences were observed between the blank and CDS004892-treated samples at any of the measured time points, as shown in Figure 47 and Figure 60, indicating that CDS004892 does not interfere with fluorescence readout under

these conditions. All subsequent compounds tested in this study were subjected to the same control assay at a 60-minute time point to ensure that no direct signal interference was present.

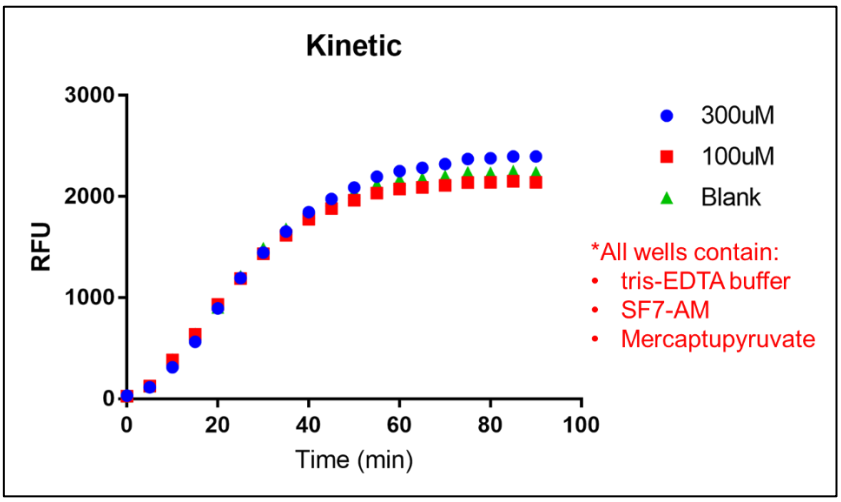


Figure 59 Kinetic assay of CDS004892 in the absence of enzyme over 90 minutes at two concentrations (300 µM and 100 µM). The assay was performed without any enzyme source to assess whether CDS004892 interferes with the fluorescence signal through probe quenching or H_2S scavenging. No significant difference was observed between the fluorescence signal of the blank control (mercaptopyruvate and SF7-AM only) and samples containing CDS004892, indicating that the compound does not directly interfere with signal generation. All wells contained SF7-AM and mercaptopyruvate.

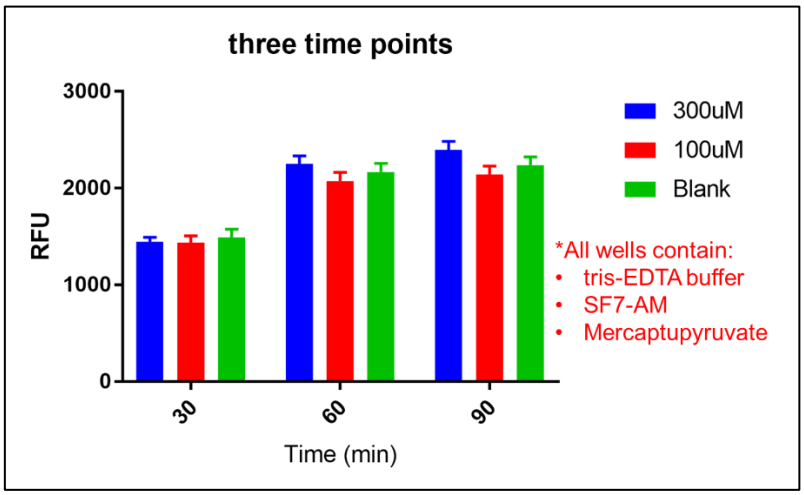


Figure 60 Fluorescence measurements of CDS004892 in the absence of enzyme at three time points (30, 60 and 90 minutes) at concentrations of 300 µM and 100 µM. The assay was performed without any enzyme source to evaluate whether CDS004892 interferes with fluorescence readout through probe quenching or H_2S scavenging. No significant difference was observed between the blank control (mercaptopyruvate and SF7-AM only) and CDS004892-treated samples at any time point, indicating that the compound does not interfere with signal generation. All wells contained SF7-AM and mercaptopyruvate.

5.1.3.6. Evaluation AzMC fluorescence probe for detection of H_2S production through CBS/CSE pathway

In this method, CBS/CSE substrate L-cysteine and pyridoxal phosphate were added to the reaction mixture to stimulate H_2S production. The inhibitor AOAA (100 µM final concentration) was prepared and added to 96-well plates containing 70µL RLC (1/10 dilution in Tris EDTA buffer) and pre-incubated

for 60 minutes at 37°C. After incubation, 10 µL of a mixture containing 100mM L-cysteine and different concentrations of AzMC (10,50 µM final concentration), both dissolved in Tris-EDTA buffer, were added to all wells. Finally, 10µL of Pyridoxal phosphate (100µM final concentration) was added. To detect any interactions between substrates and fluorescence probe, some wells only contained PLP or L-cysteine in combination with either cytosol, cytosol with inhibitor, buffer and buffer with inhibitor. The 96-well plate was then incubated at 37°C for 90 minutes and the fluorescence was measured using a fluorimeter (excitation 365nm and emission at 450nm).

In this assay, to ascertain that H_2S production is CSE/CBS dependent, the effects of PLP addition were tested and observed. The assay was repeated three times using the same rat cytosol sample but with different concentrations of the fluorescence probe (see **Error! Reference source not found.**) and the addition of AOAA (100µM) was tested. At 10 µM concentration of AzMC, AOAA did not exhibit any inhibition of H_2S production, on the contrary, there was an increase of H_2S production compared to the negative controls (with and without PLP). However, the addition of the inhibitor did show some degree of inhibition when AzMC concentration increased. It was also observed that PLP did not produce any significant increase in H_2S production in all three experiments.

These results indicated that the observed increase in H_2S production might not be CSE/CBS dependent. The discrepancies in AOAA inhibitory effects with the change of AzMC concentration indicate that there could be an interfering element.

Detection of H_2S in the CBS/CSE pathway using AzMC fluorescence probe is similar to the previous method where SF7-AM is used. In this method, CBS/CSE substrate L-cysteine and pyridoxal phosphate were added to the reaction mixture to stimulate H_2S production. AOAA (100 µM final concentration) was prepared and 10µL of the inhibitor was added to 96-well plates containing 70µL RLC (1/10 dilution in Tris EDTA buffer) and pre-incubated for 60 minutes at 37°C. After incubation, 10µL of a mixture containing 100mM L-cysteine and different concentrations of AzMC (10,50,100 µM final concentration), both dissolved in Tris-EDTA buffer, were added to all wells. Finally, 10µL of Pyridoxal phosphate (100µM final concentration) was added. The 96-well plate was then incubated at 37°C over 240 minutes, and the fluorescence was measured using a fluorimeter (excitation 365nm and emission at 450nm).

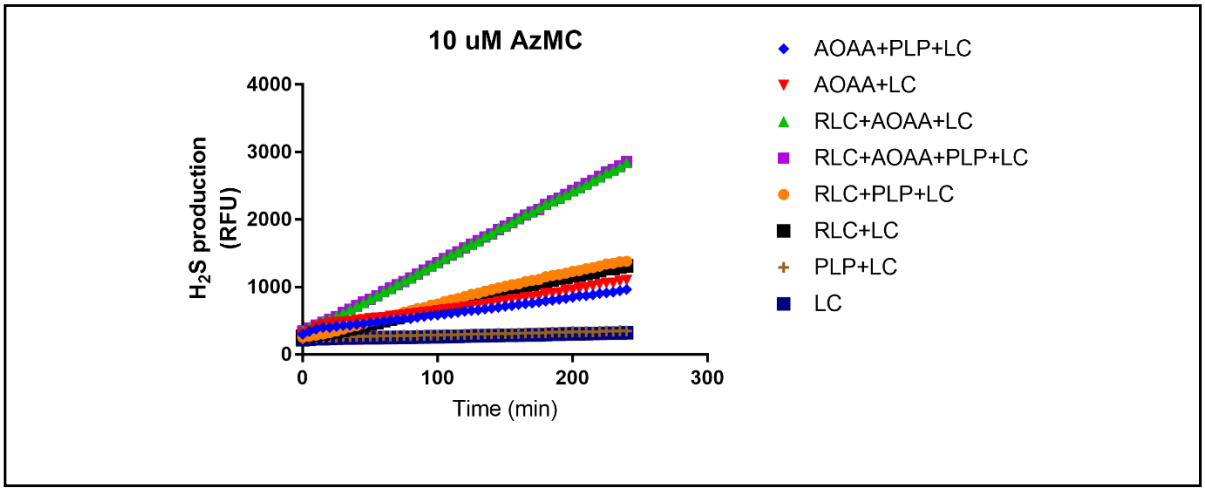


Figure 61 Kinetic assay of the inhibitory effect of AOAA on the enzymatic production of H_2S via the CSE/CBS pathway in rat liver cytosol (RLC) samples (n=1) using H_2S detection assay via AzMC fluorescence probe at three different concentrations (10,50 and 100 µM) over 240 minutes at 37°C. In this figure, data are expressed as relative florescence value (RFU) which correlates with H_2S production. Data sets represent mean ± SEM.

RLC: rat liver cytosol
PLP: pyridoxal phosphate
LC: L-cysteine

5.2 Chemistry Experimental Methods

5.2.1 General Experimental Information

Chemicals and solvents were obtained from commercial suppliers (including Sigma-Aldrich, Alfa Aesar, Fisher Scientific, Acros Organics, and Fluorochem) and were used as supplied unless otherwise stated. Anhydrous solvents were purchased from Sigma-Aldrich and used without additional purification. All synthesized compounds were dried under high vacuum, either at room temperature or in an oven maintained at 40 °C.

^{1}H and ^{13}C nuclear magnetic resonance (NMR) spectra were recorded at ambient temperature using either a Bruker AVANCE III HD 400 spectrometer equipped with a 5 mm BBFO probe, operating at 400.25 MHz for ^{1}H and 100.66 MHz for ^{13}C, or a Bruker AVANCE III 500 spectrometer fitted with a 5 mm dual ^{1}H/^{13}C helium-cooled cryoprobe, operating at 500.13 MHz for ^{1}H and 125.77 MHz for ^{13}C. Samples were prepared in deuterated dimethyl sulfoxide (DMSO-d_6). Spectral processing was carried out using iNMR (version 5.5.7), with chemical shifts (δ) reported in parts per million (ppm) relative to tetramethylsilane (TMS) using residual solvent signals as internal references. Coupling constants (*J*) are reported in hertz (Hz). Further spectral analysis was performed using MestReNova (version 15.1.1).

^{1}H and ^{13}C NMR spectra were recorded on a 400 MHz spectrometer at ambient temperature. Chemical shifts (δ) are reported in parts per million (ppm) relative to tetramethylsilane (TMS) or residual solvent peaks. Coupling constants (J) are reported in hertz (Hz). Multiplicities are denoted as s (singlet), d (doublet), t (triplet), q (quartet), m (multiplet), or br (broad).

Liquid chromatography–mass spectrometry (LC–MS) analyses were performed using a Shimadzu UFLCXR HPLC system coupled to an Applied Biosystems API2000 electrospray ionization mass spectrometer. Mass spectra were recorded using electrospray ionization (ESI) in positive and/or negative ion mode. Purification of compounds was achieved by flash chromatography using an Interchim Puriflash system (Interchim, Montluçon, France) equipped with pre-packed cartridges, operated at a maximum flow rate of 250 mL min^{-1} and a pressure limit of 100 bar.

The compounds described in this chapter were used in biological investigations. Only compounds meeting predefined purity criteria (≥95%) were advanced to biological evaluation.

All reagents and solvents were obtained from commercial suppliers and used as received unless otherwise stated. Reactions were monitored by thin-layer chromatography (TLC) on silica gel plates, visualized under UV light (254 nm) and/or by appropriate staining reagents.

Melting points were determined using a manual melting point apparatus and averages of three readings were recorded.

5.2.1.1. General Synthetic Procedures

A series of twenty structurally related compounds were synthesised to explore the effect of systematic structural modification on biological activity. All compounds were synthesised according to General Procedures A and/or B unless otherwise stated.

5.2.1.1.1. General Procedure A: Synthesis of amide linker compounds

5.2.1.1.1.1. Amide Formation Using EDCI/HOBt

At room temperature, the appropriate carboxylic acid was dissolved in 1 ml DMF then 1 ml DIPEA was added to neutralize the solution, followed by the addition of EDCI (0.3 mmol), HOBt 0.3 mmol , and the chosen amine. The reaction mixture was stirred at room temperature for 2h.

Upon completion, the solvent was evaporated *in vacuo*. The resulting residue was redissolved in methanol and purified by column chromatography using DMF containing 5% methanol as the eluent. Fractions containing the desired product were combined and concentrated under reduced pressure to afford solid product. The product was further dried under vacuum at 40 °C for 1 h to give the final compound.

5.2.1.1.1.2. Amide Formation Using BEP/ in Acetonitrile

For selected compounds, amide bond formation using conventional coupling reagents proved challenging. Optimal yields were achieved using a BEP/NMI-mediated coupling protocol in acetonitrile. The appropriate carboxylic acid and amine were dissolved in acetonitrile, followed by the addition of BEP (0.25 mmol, 1 equiv.) and N-methylimidazole (NMI) (0.87 mmol, 3.5 equiv.). The reaction mixture was stirred at room temperature until completion, as monitored by TLC. The reaction was then quenched, and the product was isolated by filtration or solvent extraction. Removal of the volatile solvent under reduced pressure afforded the crude amide, which was purified as required by flash chromatography. Figure 62.

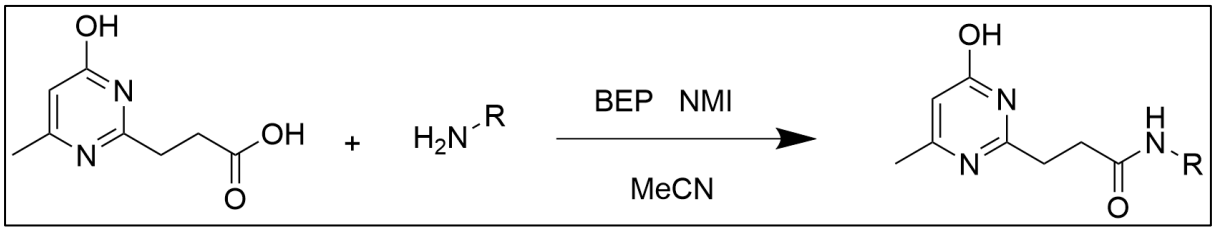


Figure 62 Simplified scheme of amide bond formation

5.2.1.1.2. General Procedure B: Synthesis of mercaptoacetyl-linker Compounds

A suspension of the aryl thiol (1.0 equivalent) in methanol (0.1 M) was prepared, and a solution of KOH (1.0 equivalent, 1 M in methanol) was added dropwise. The mixture was stirred at room temperature for 15 minutes, after which the acyl bromide (1.2 equivalents) was introduced. The reaction was allowed to proceed for 12 hours at room temperature. Afterward, water (in an amount equal to the volume of methanol used) was added to quench the reaction. The resulting product was collected by filtration, washed with diethyl ether, and dried under high vacuum (Figure 21).

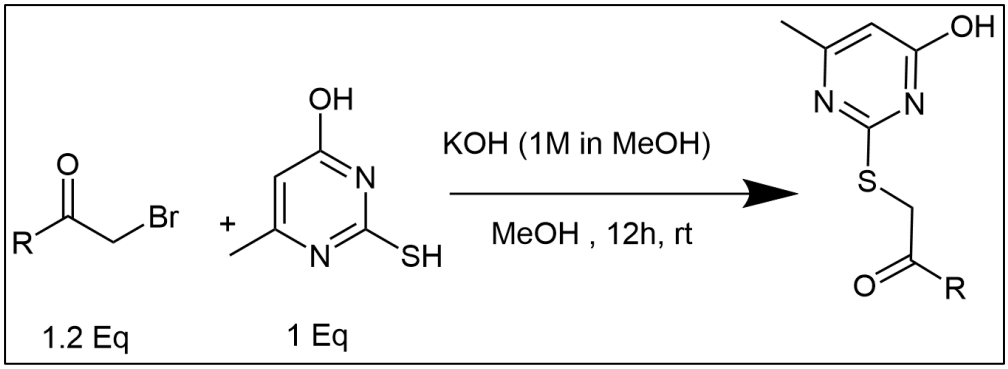


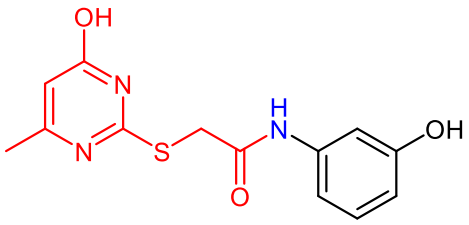
Figure 63 Simplified scheme of mercaptoacetyl linker compound synthesis

5.2.2 Synthesis and Characterization of Target Compounds

5.2.2.1. Individual Compound Data

MNA01

2-[(1,6-dihydro-4-methyl-6-oxo-2-pyrimidinyl)thio]-N-(3-hydroxyphenyl)- acetamide



Appearance: white powder

At room temperature [(4-Methyl-6-oxo-1,6-dihydro-2-pyrimidinyl)sulfanyl]acetic acid (0.05 g, 0.25 mmol, 1 equiv.) was dissolved in 1ml dimethylformamide then neutralized by 1ml *N,N*-di isopropyl ethylamine. Then 0.057g (0.3 mmol) EDCI, 0.04g (0.3 mmol) HOBt and 3-aminophenol (0.027 g, 0.25 mmol, 1 equiv.) were added and mixed for two hours. Solvent was evaporated and the residue dissolved in 0.6 ml methanol then separated using column chromatography (DMF/5%methanol). Elute containing product was evaporated and a white solid was obtained and dried in a vacuum oven at 40° for 1 hour. (yield 60 mg, 82%).

^{1}H NMR (400 MHz, DMSO) δ 12.60 (s, 1H), 10.12 (s, 1H), 9.38 (s, 1H), 7.14 (t, *J* = 2.1 Hz, 1H), 7.07 (t, *J* = 8.1 Hz, 1H), 6.92 (dd, *J* = 8.0, 1.9 Hz, 1H), 6.45 (dd, *J* = 8.1, 2.4 Hz, 1H), 5.99 (s, 1H), 4.04 (s, 2H), 2.13 (s, 3H).

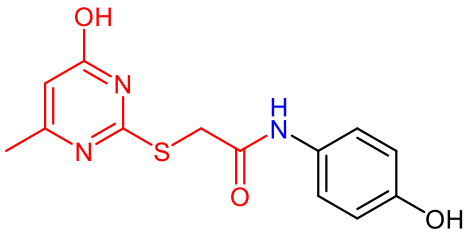
^{13}C NMR (101 MHz, DMSO) δ 165.89, 157.64, 139.90, 129.43, 110.56, 109.89, 106.29, 35.15, 23.15.

MS (ESI^{+}) m/z: $[M+H]^{+}$ 292.0; $[M+Na]^{+}$ 314.1.

Melting point: 212 °C

MNA02

2-((4-hydroxy-6-methylpyrimidin-2-yl)thio)-N-(4-hydroxyphenyl)acetamide



Appearance: white powder

At room temperature [(4-Methyl-6-oxo-1,6-dihydro-2-pyrimidinyl)sulfanyl]acetic acid (0.05 g, 0.25 mmol, 1 equiv.) was dissolved in 1 ml dimethylformamide then neutralized by 1ml *N,N*-di isopropyl ethylamine. Then 0.057g (0.3 mmol) EDCI, 0.04g (0.3 mmol) HOBt and 4-aminophenol (0.027 g, 0.25 mmol, 1 equiv.) were added and mixed for two hours. Solvent was evaporated then the residue

dissolved in 0.6 ml methanol and separated using column chromatography (DMF/5%methanol). Elute containing product was evaporated and a white solid was formed and dried in vacuum over at 40° for 1 hour. (yield 40 mg, 55%).

^{1}H NMR (400 MHz, DMSO) δ 12.55 (s, 1H), 10.00 (s, 1H), 9.20 (s, 1H), 7.37 – 7.29 (m, 2H), 6.73 – 6.65 (m, 2H), 5.98 (s, 1H), 4.01 (s, 2H), 2.62 (s, 1H), 2.14 (s, 3H).

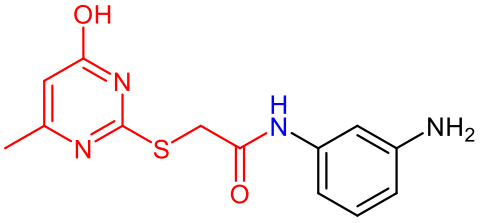
^{13}C NMR (101 MHz, DMSO) δ 165.16, 153.50, 130.51, 120.97, 115.12, 34.99, 23.42.

MS (ESI^{+}) m/z: $[M+H]^{+}$ 295; $[M+Na]^{+}$ 317.

Melting point: 238 °C

MNA03

N-(3-aminophenyl)-2-((4-hydroxy-6-methylpyrimidin-2-yl)thio)acetamide



Appearance: white powder

At room temperature, [(4-methyl-6-oxo-1,6-dihydro-2-pyrimidinyl)sulfanyl]acetic acid (0.05 g, 0.25 mmol, 1 equiv.) was dissolved in 1.0 mL DMF. Then 1 ml DIPEA was added to neutralize the solution, followed by the addition of EDCI (0.057 g, 0.30 mmol), HOBt (0.040 g, 0.30 mmol), and *m*-phenylenediamine (0.108 g, 1mmol, 4 equiv.). The reaction mixture was stirred at room temperature for 2 h. Upon completion, the solvent was removed under reduced pressure. The resulting residue was redissolved in methanol (0.6 mL) and purified by column chromatography using DMF containing 5% methanol as the eluent. Fractions containing the desired product were combined and concentrated under reduced pressure to afford a white solid. The product was further dried under vacuum at 40 °C for 1 h to give the title compound as a white powder. (yield 20 mg, 25%).

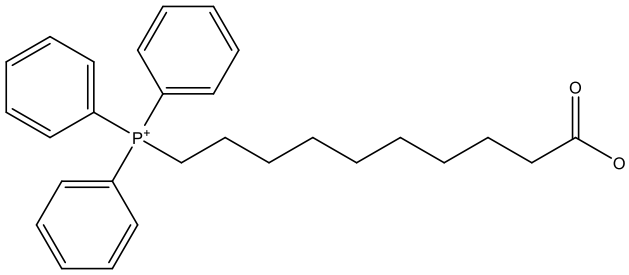
^{1}H NMR (400 MHz, DMSO) δ 9.95 (s, 1H), 6.96 – 6.85 (m, 2H), 6.65 (ddd, *J* = 8.0, 2.1, 1.0 Hz, 1H), 6.25 (ddd, *J* = 7.9, 2.2, 1.0 Hz, 1H), 5.99 (s, 1H), 5.06 (s, 2H), 4.01 (s, 2H), 3.17 (d, *J* = 4.5 Hz, 1H), 2.14 (s, 3H).

MS (ESI^{+}) m/z: $[M+H]^{+}$302 ; $[M+Na]^{+}$3024 .

Melting point: 200°C

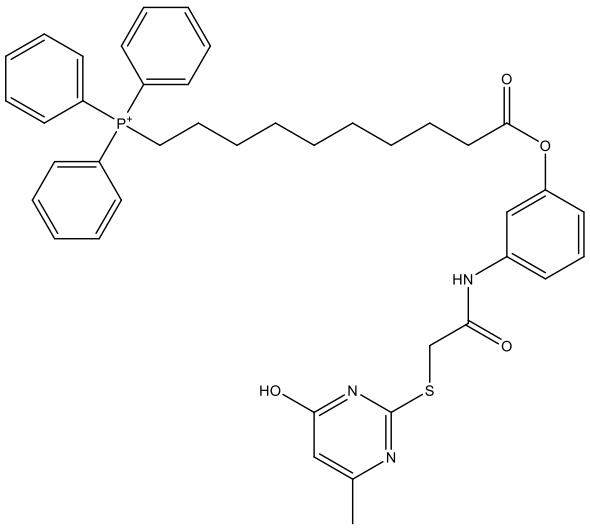
MNA06 (synthesised by Dr Nicholas Kindon)

First preparation of AP219: (9-carboxynonyl)triphenylphosphonium



To produce AP219 salt, a solution of 10-bromodecanoic acid (500 mg, 1.99 mmol) in acetonitrile (5 ml) was added to a stirred solution of triphenylphosphine (522 mg, 1.99 mmol) in acetonitrile (5 ml). The solution was heated at reflux for 70 h, cooled to room temperature then concentrated in vacuo. The resulting material was washed with toluene (2x 10 ml), concentrated in vacuo then dissolved in dichloromethane (30 mE). To this stirred solution was added 5-p-hydroxyphenyl-1 ,2-dithiole- 3-thione (ADT-OH) (456 mg, 1.99 mmol), *N,N*'-dicyclohexylcarbodiimide (431 mg, 2.09 mmol) and 4-dimethylaminopyridine (12 mg, 0.0995 mmol). After 22 h, the resulting suspension was filtered through cotton wool and the filtrate was concentrated in vacuo. Purification by flash column chromatography, loading as a dichloromethane solution and eluting with ethyl acetate then methanol, gave a mixture of the phosphonium salt and silica. Redissolution in dichloromethane, filtration through paper and concentration in vacuo gave the pure phosphonium salt (1.05 g, 73%) as an orange foam.

Second preparation of AP2190MNA001 complex



(10-(3-(2-((4-hydroxy-6-methylpyrimidin-2-yl)thio)acetamido)phenoxy)-10-oxodecyl)triphenylphosphonium

AP219 (30 mg, approximately 0.064 mmol, 1.0 equiv.) and MNA001 (20 mg, 0.0687 mmol, 1.07 equiv.) were dissolved in anhydrous dichloromethane (DCM, 1 mL) in a vial under a nitrogen atmosphere. 4-Dimethylaminopyridine (DMAP, 8.4 mg, 0.0687 mmol, 1.0 equiv.) was added and the mixture was stirred at room temperature for 5 minutes. N,N'-Dicyclohexylcarbodiimide (DCC, 14.2 mg, 0.0687 mmol, 1.0 equiv.) was then added in a single portion, and the reaction was allowed to proceed at 20–25 °C under nitrogen for 24–48 hours. Upon completion, the reaction mixture was filtered to remove the precipitated dicyclohexylurea (DCU), which was rinsed with dichloromethane (2 × 1 mL). The combined organic phases were washed successively with 1 M HCl (2 × 2 mL), saturated aqueous sodium bicarbonate (2 × 2 mL), and brine (1 × 2 mL). The organic layer was dried,

filtered, and concentrated under reduced pressure at temperatures below 30 °C. The crude product was purified by reverse-phase flash chromatography on C18 silica using a 70% water and 30% acetonitrile mobile phase. Fractions containing the desired product were combined and dried under vacuum. (Yield 22mg, 40%)

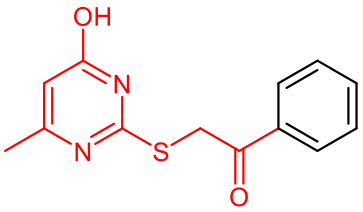
^{1}H NMR (300 MHz, CDC13):ö=7.95-7.65 (m, 17H; 3xPh and Ar 2- and 6-H), 7.42 (s, 1H; =CH), 7.23 (d, J=8.0 Hz, 2H; Ar 3-and 5-H), 3.90-3.79 (m, 2H; CH2CrrrO), 2.58 (t, J=8.5 Hz, 2H; CH2P), 1.80-1.55 (m, 4H; 2xCH2), 1.42-1.19 ppm (m, 1OH; 5xCH2)

3'P NMR (121 MHz, CDC13): ö=25.7 ppm; HRMS (ESI) calculated for C37H3802P53 [M-13r] requires 641.1766. found 641.1751.

Melting point: 200 °C

MNA07

2-((4-hydroxy-6-methylpyrimidin-2-yl)thio)-1-phenylethan-1-one



Appearance: white powder

A suspension of 2-mercapto-6-methylpyrimidin-4-ol (0.05 g, 0.35 mmol, 1 equiv.) in 5 ml methanol was prepared, and a solution of 0.35 ml KOH (1.0 equivalent, 1 M in methanol) was added dropwise. The mixture was stirred at room temperature for 15 minutes, after which the 2-bromo-1-phenylethan-1-one (0.08 g, 0.422 mmol, 1.2 equiv.) was introduced. The reaction was allowed to proceed for 12 hours at room temperature. Afterward, water (in an amount equal to the volume of methanol used) was added to quench the reaction. The resulting product was collected by filtration, washed with diethyl ether, and dried under high vacuum. The resulting residue was redissolved in 0.3 ml DMSO and purified by column chromatography using DMF containing 5% methanol as the eluent. Fractions containing the desired product were combined and dried in vacuo to produce a white solid, further dried under vacuum at 40 °C for 1 h to give the final compound as a white powder. (yield 45 mg, 50%).

^{1}H NMR (400 MHz, DMSO) δ 8.07 – 8.00 (m, 2H), 7.72 – 7.60 (m, 1H), 7.56 (dd, *J* = 8.4, 7.0 Hz, 2H), 5.94 (d, *J* = 10.0 Hz, 1H), 4.74 (s, 2H), 1.95 (s, 3H).

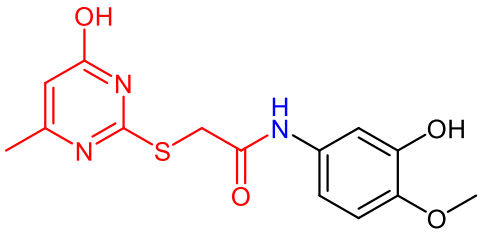
^{13}C NMR (101 MHz, DMSO) δ 194.07, 136.40, 133.77, 129.03, 128.49, 124.62, 37.64, 23.14.

MS (ESI^{+}) m/z: $[M+H]^{+}$ 261; $[M+Na]^{+}$ 282.

Melting point: 185 °C

MNA08

2-((4-hydroxy-6-methylpyrimidin-2-yl)thio)-N-(4-methoxy-3-methylphenyl)acetamide



Appearance: brown powder

At room temperature 2-((4-hydroxy-6-methylpyrimidin-2-yl)thio)acetic acid (0.05 g, 0.25 mmol, 1 equiv.) was dissolved in 3 ml MeCN. BEP (0.06 g, 0.25 mmol, 1 equiv.) was added to activate the carboxylic acid, forming a reactive acyl benzotriazole intermediate, then NMI (0.07 g, 0.87 mmol, 3.5 equiv.) and 5-amino-2-methoxyphenol (0.035 g, 0.25 mmol, 1 equiv.) were added and mixed for 24 hours. Product was evaporated in vacuo to remove MeCN, then dissolved in 0.6ml methanol and separated using column chromatography (DMF/5%methanol). Elute containing product was evaporated and the formed solid dried in vacuum over at 40° for 1 hour. (yield 45 mg, 62%).
^{1}H NMR (400 MHz, DMSO) δ 12.54 (s, 1H), 10.61 (s, 1H), 8.28 (t, *J* = 2.0 Hz, 1H), 7.79 (ddd, *J* = 8.1, 2.3, 1.1 Hz, 1H), 7.65 (dt, *J* = 7.7, 1.4 Hz, 1H), 7.46 (t, *J* = 7.9 Hz, 1H), 5.97 (s, 1H), 4.05 (s, 2H), 3.85 (s, 3H), 2.10 (s, 3H).

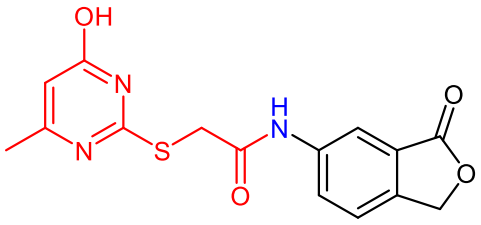
^{13}C NMR (101 MHz, DMSO) δ 165.33, 146.44, 143.92, 132.49, 112.51, 109.90, 107.70, 55.87, 35.05, 23.16.

MS (ESI^{+}) m/z: $[M+H]^{+}$ 312.9; $[M+Na]^{+}$ 344.0.

Melting point: 230 °C

MNA09

2-((4-hydroxy-6-methylpyrimidin-2-yl)thio)-N-(3-oxo-1,3-dihydroisobenzofuran-5-yl)acetamide



Appearance: yellow powder

At room temperature 2-((4-hydroxy-6-methylpyrimidin-2-yl)thio)acetic acid (0.05 g, 0.25 mmol, 1 equiv.) was dissolved in 3 ml MeCN. BEP (0.06 g, 0.25 mmol, 1 equiv.) was added to activate the carboxylic acid, forming a reactive acyl benzotriazole intermediate, then NMI (0.07 g, 0.87 mmol, 3.5 equiv.) and 6-aminoisobenzofuran-1(3H)-one (0.037 g, 0.25 mmol, 1 equiv.) were added and mixed for 24 hours. Product was evaporated in vacuo to remove MeCN, then dissolved in 0.6ml methanol and separated using column chromatography (DMF/5%methanol). Elute containing product was evaporated and the formed solid dried in vacuum over at 40° for 1 hour. (yield 20 mg, 25%).

^{1}H NMR (400 MHz, DMSO) δ 12.56 (s, 1H), 10.64 (s, 1H), 8.16 (s, 1H), 7.82 (dd, *J* = 8.2, 1.9 Hz, 1H), 7.63 (d, *J* = 8.3 Hz, 1H), 5.99 (s, 1H), 5.37 (s, 2H), 4.10 (s, 2H), 2.11 (s, 3H).

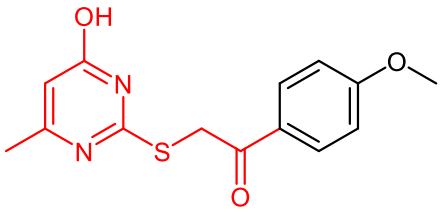
^{13}C NMR (101 MHz, DMSO) δ 170.57, 166.58, 141.96, 139.62, 125.55, 125.28, 123.46, 114.12, 69.82, 35.14, 23.14.

MS (ESI^{+}) m/z: $[M+H]^{+}$ 332; $[M+Na]^{+}$ 353.8.

Melting point: 242 °C

MNA10

2-((4-hydroxy-6-methylpyrimidin-2-yl)thio)-1-(4-methoxyphenyl)ethan-1-one



Appearance: white powder

A suspension of 2-mercapto-6-methylpyrimidin-4-ol (0.05 g, 0.35 mmol, 1 equiv.) in 5 ml methanol was prepared, and a solution of 0.35 ml KOH (1.0 equivalent, 1 M in methanol) was added dropwise. The mixture was stirred at room temperature for 15 minutes, after which the 2-bromo-1-(4-methoxyphenyl)ethan-1-one (0.09 g, 0.422 mmol, 1.2 equiv.) was introduced. The reaction was allowed to proceed for 12 hours at room temperature. Afterward, water (in an amount equal to the volume of methanol used) was added to quench the reaction. The resulting product was collected by filtration, washed with diethyl ether, and dried under high vacuum. The resulting residue was redissolved in 0.3 ml DMSO and purified by column chromatography using DMF containing 5% methanol as the eluent. Fractions containing the desired product were combined and dried in vacuo to produce a white solid, further dried under vacuum at 40 °C for 1 h to give the final compound as a white powder. (yield 40 mg, 40%)

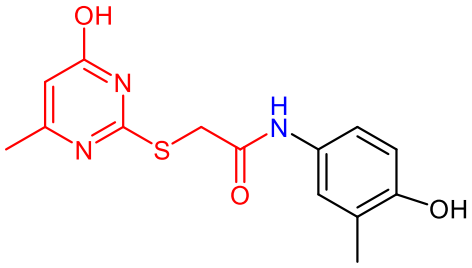
^{1}H NMR (400 MHz, MeOD) δ 5.76 (s, 1H), 3.92 (s, 1H), 3.33 (s, 2H), 2.18 (s, 1H), 2.17 – 2.05 (m, 2H).

^{13}C NMR (101 MHz, DMSO) δ 192.40, 163.85, 131.11, 129.35, 114.37, 55.97, 48.41, 48.09 (d, *J* = 21.3 Hz), 47.77, 47.57, 37.59.

MS (ESI^{+}) m/z: $[M+H]^{+}$ 291; $[M+Na]^{+}$ 313.1.

Melting point: 180 °C

MNA11N-(4-hydroxy-3-methylphenyl)-2-((4-hydroxy-6-methylpyrimidin-2-yl)thio)acetamid



Appearance: white powder

At room temperature 2-((4-hydroxy-6-methylpyrimidin-2-yl)thio)acetic acid (0.1 g, 0.5 mmol, 1 equiv.) was dissolved in 3 ml MeCN. BEP (0.13 g, 0.5 mmol, 1 equiv.) was added to activate the carboxylic acid, forming a reactive acyl benzotriazole intermediate, then NMI (0.14 g, 1.7 mmol, 3.5 equiv.) and 4-amino-2-methylphenol (0.06 g, 0.5 mmol, 1 equiv.) were added and mixed for 24 hours. Product was evaporated in vacuo to remove MeCN, then dissolved in 0.6ml methanol and separated using column chromatography (DMF/5%methanol). Elute containing product was evaporated and the formed solid dried in vacuum over at 40° for 1 hour. (yield 30 mg, 20%)

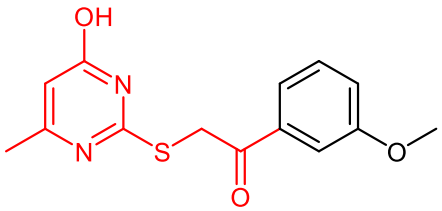
^{1}H NMR (400 MHz, DMSO) δ 12.51 (s, 1H), 10.17 (s, 1H), 9.30 (s, 1H), 7.19 (d, *J* = 2.1 Hz, 1H), 6.94 (d, *J* = 8.1 Hz, 1H), 6.82 (dd, *J* = 8.0, 2.1 Hz, 1H), 5.95 (s, 1H), 3.98 (s, 2H), 2.12 (s, 3H), 2.04 (s, 3H).

MS (ESI$^+$) m/z: $[M+H]^+$ 306.4; $[M+Na]^+$ 328.

Melting point: 220 °C

MNA13

2-((4-hydroxy-6-methylpyrimidin-2-yl)thio)-1-(3-methoxyphenyl)ethan-1-one



Appearance: white powder

A suspension of 2-mercapto-6-methylpyrimidin-4-ol (0.05 g, 0.35 mmol, 1 equiv.) in 5 ml methanol was prepared, and a solution of 0.35 ml KOH (1.0 equivalent, 1 M in methanol) was added dropwise. The mixture was stirred at room temperature for 15 minutes, after which the 2-bromo-1-(3-methoxyphenyl)ethan-1-one (0.09 g, 0.422 mmol, 1.2 equiv.) was introduced. The reaction was allowed to proceed for 12 hours at room temperature. Afterward, water (in an amount equal to the volume of methanol used) was added to quench the reaction. The resulting product was collected by filtration, washed with diethyl ether, and dried under high vacuum. The resulting residue was redissolved in 0.3 ml DMSO and purified by column chromatography using DMF containing 5% methanol as the eluent. Fractions containing the desired product were combined and dried in vacuo to produce a white solid, further dried under vacuum at 40 °C for 1 h to give the final compound as a white powder. (yield 92 mg, 90%)

^{1}H NMR (400 MHz, DMSO) δ 12.56 (s, 1H), 7.64 (dd, *J* = 7.7, 1.5 Hz, 1H), 7.53 – 7.44 (m, 2H), 7.28 – 7.21 (m, 1H), 5.93 (d, *J* = 9.4 Hz, 1H), 4.73 (s, 2H), 3.83 (d, *J* = 1.1 Hz, 3H), 1.97 (s, 3H).

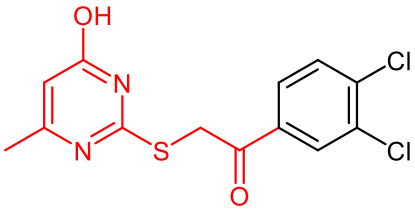
^{13}C NMR (101 MHz, DMSO) δ 193.52, 159.37, 137.60, 129.93, 120.74, 119.37, 112.80, 110.62, 55.38, 37.51, 23.09.

Melting point: 190 °C

MS (ESI^{+}) m/z: [M+H]$^{+}$ 291.1; [M+Na]$^{+}$ 313.4.

MNA14

1-(3,4-dichlorophenyl)-2-((4-hydroxy-6-methylpyrimidin-2-yl)thio)ethan-1-one



Appearance: white powder

A suspension of 2-mercapto-6-methylpyrimidin-4-ol (0.5 g, 3.5 mmol, 1 equiv.) in 5 ml methanol was prepared, and a solution of 0.35 ml KOH (1.0 equivalent, 1 M in methanol) was added dropwise. The mixture was stirred at room temperature for 15 minutes, after which the 2-bromo-1-(3,4-dichlorophenyl)ethan-1-one (1.1 g, 4.22 mmol, 1.2 equiv.) was introduced. The reaction was allowed to proceed for 12 hours at room temperature. Afterward, water (in an amount equal to the volume of methanol used) was added to quench the reaction. The resulting product was collected by filtration, washed with diethyl ether, and dried under high vacuum. The resulting residue was redissolved in 0.3 ml DMSO and purified by column chromatography using DMF containing 5% methanol as the eluent. Fractions containing the desired product were combined and dried in vacuo to produce a white solid, further dried under vacuum at 40 °C for 1 h to give the final compound as a white powder. (yield 0.7g, 70%)

^{1}H NMR (400 MHz, DMSO) δ 8.26 (s, 1H), 7.97 (s, 1H), 7.83 (s, 1H), 7.68 (s, 1H), 5.91 (s, 1H), 4.66 (s, 2H), 2.11 (s, 1H), 1.92 (s, 3H).

14a

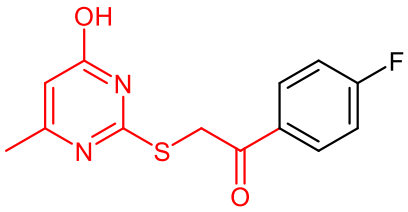
^{1}H NMR (400 MHz, DMSO) δ 8.28 (s, 1H), 8.00 (d, *J* = 7.9 Hz, 1H), 7.85 (d, *J* = 8.4 Hz, 1H), 5.97 – 5.92 (m, 1H), 4.72 – 4.67 (m, 2H), 3.66 (s, 0H), 2.14 (s, 1H), 1.94 (s, 4H).

MS (ESI^{+}) m/z: [M+H]$^{+}$ 306.4; [M+Na]$^{+}$ 328.

Melting point: 195 °C

MNA15

1-(4-fluorophenyl)-2-((4-hydroxy-6-methylpyrimidin-2-yl)thio)ethan-1-one



Appearance: white powder

1-(4-fluorophenyl)-2-((4-hydroxy-6-methylpyrimidin-2-yl)thio)ethan-1-one

A suspension of 2-mercapto-6-methylpyrimidin-4-ol (0.05 g, 0.35 mmol, 1 equiv.) in 5 ml methanol was prepared, and a solution of 0.35 ml KOH (1.0 equivalent, 1 M in methanol) was added dropwise. The mixture was stirred at room temperature for 15 minutes, after which the 2-bromo-1-(4-fluorophenyl)ethan-1-one (0.09 g, 0.422 mmol, 1.2 equiv.) was introduced. The reaction was allowed to proceed for 12 hours at room temperature. Afterward, water (in an amount equal to the volume of methanol used) was added to quench the reaction. The resulting product was collected by filtration, washed with diethyl ether, and dried under high vacuum. The resulting residue was redissolved in 0.3 ml DMSO and purified by column chromatography using DMF containing 5% methanol as the eluent. Fractions containing the desired product were combined and dried in vacuo to produce a white solid, further dried under vacuum at 40 °C for 1 h to give the final compound as a white powder. (yield 30mg, 30%)

^{1}H NMR (400 MHz, DMSO) δ 12.56 (s, 1H), 8.19 – 8.09 (m, 2H), 7.45 – 7.34 (m, 2H), 5.95 (s, 1H), 4.72 (s, 2H), 1.96 (s, 3H).

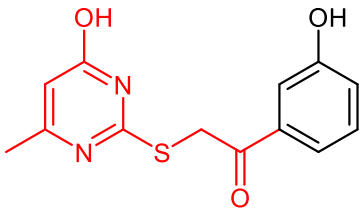
^{13}C NMR (101 MHz, DMSO) δ 192.50, 166.44, 163.94, 133.04, 131.40, 131.30, 115.90, 115.68, 47.84, 47.63, 47.42, 47.22, 22.89.

MS (ESI^{+}) m/z: $[M+H]^{+}$ 279.1; $[M+Na]^{+}$ 300.9.

Melting point: 181 °C

MNA16

2-((4-hydroxy-6-methylpyrimidin-2-yl)thio)-1-(3-hydroxyphenyl)ethan-1-one



Appearance: white powder

A suspension of 2-mercapto-6-methylpyrimidin-4-ol (0.05 g, 0.35 mmol, 1 equiv.) in 5 ml methanol was prepared, and a solution of 0.35 ml KOH (1.0 equivalent, 1 M in methanol) was added dropwise. The mixture was stirred at room temperature for 15 minutes, after which the 2-bromo-1-(3-hydroxyphenyl)ethan-1-one (0.09 g, 0.422 mmol, 1.2 equiv.) was introduced. The reaction was allowed to proceed for 12 hours at room temperature. Afterward, water (in an amount equal to the volume of methanol used) was added to quench the reaction. The resulting product was collected by filtration, washed with diethyl ether, and dried under high vacuum. The resulting residue was redissolved in 0.3 ml DMSO and purified by column chromatography using DMF containing 5% methanol as the eluent. Fractions containing the desired product were combined and dried in vacuo to produce a white solid, further dried under vacuum at 40 °C for 1 h to give the final compound as a white powder. (yield 53mg, 55%)

^{1}H NMR (400 MHz, MeOD) δ 7.55 (d, *J* = 7.7 Hz, 1H), 7.44 (t, *J* = 2.1 Hz, 1H), 7.35 (t, *J* = 7.9 Hz, 1H), 7.06 (dd, *J* = 8.0, 2.6 Hz, 1H), 6.80 (s, 1H), 5.95 (s, 1H), 2.26 (s, 1H), 2.09 (s, 3H).

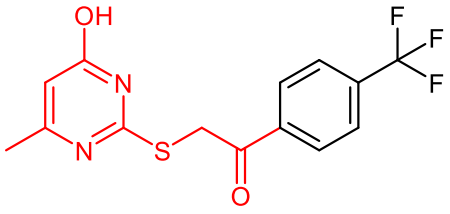
^{13}C NMR (101 MHz, DMSO) δ 129.05, 119.84, 118.76, 113.74, 47.62, 47.41, 47.19, 46.98, 46.77, 46.56, 46.35, 38.51, 38.30, 38.09, 37.88, 37.67, 37.46, 37.25.

MS (ESI^{+}) m/z: [M+H]$^{+}$ 276.9; [M+Na]$^{+}$ 299.1.

Melting point: 216 °C

MNA17

2-((4-hydroxy-6-methylpyrimidin-2-yl)thio)-1-(4-(trifluoromethyl)phenyl)ethan-1-one



Appearance: white crystals

A suspension of 2-mercapto-6-methylpyrimidin-4-ol (0.05 g, 0.35 mmol, 1 equiv.) in 5 ml methanol was prepared, and a solution of 0.35 ml KOH (1.0 equivalent, 1 M in methanol) was added dropwise. The mixture was stirred at room temperature for 15 minutes, after which the 2-bromo-1-(4-(trifluoromethyl)phenyl)ethan-1-one (0.11 g, 0.422 mmol, 1.2 equiv.) was introduced. The reaction

was allowed to proceed for 12 hours at room temperature. Afterward, water (in an amount equal to the volume of methanol used) was added to quench the reaction. The resulting product was collected by filtration, washed with diethyl ether, and dried under high vacuum. The resulting residue was redissolved in 0.3 ml DMSO and purified by column chromatography using DMF containing 5% methanol as the eluent. Fractions containing the desired product were combined and dried in vacuo to produce a white solid, further dried under vacuum at 40 °C for 1 h to give the final compound as white crystals. (yield 25mg, 21%)

^{1}H NMR (400 MHz, DMSO) δ 12.58 (s, 1H), 8.23 (d, *J* = 8.1 Hz, 2H), 7.95 (d, *J* = 7.8 Hz, 3H), 7.74 (d, *J* = 8.0 Hz, 1H), 7.64 (d, *J* = 7.7 Hz, 1H), 5.94 (d, *J* = 9.1 Hz, 1H), 4.75 (s, 2H), 3.60 (q, *J* = 12.5 Hz, 1H), 2.17 (s, 1H), 1.92 (s, 3H).

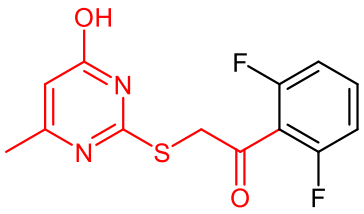
^{13}C NMR (101 MHz, DMSO) δ 139.66, 129.06, 125.74, 125.70, 125.61, 125.15, 108.44, 41.57, 37.53, 22.94.

MS (ESI^{+}) m/z: $[M+H]^{+}$ 329.2; $[M+Na]^{+}$ 350.8 .

Melting point: 149 °C

MNA18

1-(2,6-difluorophenyl)-2-((4-hydroxy-6-methylpyrimidin-2-yl)thio)ethan-1-one



Appearance: yellow powder

A suspension of 2-mercapto-6-methylpyrimidin-4-ol (0.05 g, 0.35 mmol, 1 equiv.) in 5 ml methanol was prepared, and a solution of 0.35 ml KOH (1.0 equivalent, 1 M in methanol) was added dropwise. The mixture was stirred at room temperature for 15 minutes, after which the 2-bromo-1-(2,6-difluorophenyl)ethan-1-one (0.1 g, 0.422 mmol, 1.2 equiv.) was introduced. The reaction was allowed to proceed for 12 hours at room temperature. Afterward, water (in an amount equal to the volume of methanol used) was added to quench the reaction. The resulting product was collected by filtration, washed with diethyl ether, and dried under high vacuum. The resulting residue was redissolved in 0.3 ml DMSO and purified by column chromatography using DMF containing 5% methanol as the eluent. Fractions containing the desired product were combined and dried in vacuo to produce a white solid, further dried under vacuum at 40 °C for 1 h to give the final compound as a white powder. (yield 20mg, 20%)

^{1}H NMR (400 MHz, DMSO) δ 12.64 (s, 1H), 7.63 (tt, *J* = 8.4, 6.6 Hz, 1H), 7.24 (t, *J* = 8.5 Hz, 2H), 4.44 (s, 2H), 2.00 (s, 3H).

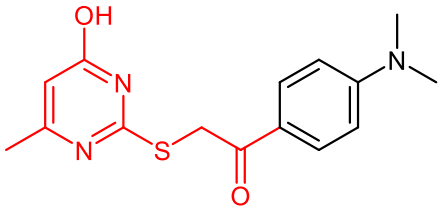
^{13}C NMR (101 MHz, DMSO) δ 111.68, 111.44, 47.66, 47.45, 47.24, 47.03, 46.82, 46.60, 46.39, 38.67, 38.46, 38.25, 38.04, 37.83, 37.62, 37.41.

MS (ESI^{+}) m/z: $[M+H]^{+}$ 297.4; $[M+Na]^{+}$ 318.9.

Melting point: 164 °C

MNA19

1-(4-(dimethylamino)phenyl)-2-((4-hydroxy-6-methylpyrimidin-2-yl)thio)ethan-1-one



Appearance: yellow powder

A suspension of 2-mercapto-6-methylpyrimidin-4-ol (0.05 g, 0.35 mmol, 1 equiv.) in 5 ml methanol was prepared, and a solution of 0.35 ml KOH (1.0 equivalent, 1 M in methanol) was added dropwise. The mixture was stirred at room temperature for 15 minutes, after which the 2-bromo-1-(4-(dimethylamino)phenyl)ethan-1-one (0.1 g, 0.422 mmol, 1.2 equiv.) was introduced. The reaction was allowed to proceed for 12 hours at room temperature. Afterward, water (in an amount equal to the volume of methanol used) was added to quench the reaction. The resulting product was collected by filtration, washed with diethyl ether, and dried under high vacuum. The resulting residue was redissolved in 0.3 ml DMSO and purified by column chromatography using DMF containing 5% methanol as the eluent. Fractions containing the desired product were combined and dried in vacuo to produce a solid, further dried under vacuum at 40 °C for 1 h to give the final compound as a yellow powder. (yield 26mg, 25%)

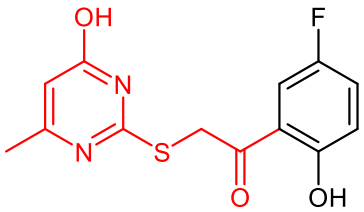
^{1}H NMR (400 MHz, DMSO) δ 12.52 (s, 1H), 7.70 (d, J = 8.8 Hz, 2H), 6.68 (d, J = 8.8 Hz, 2H), 5.93 (s, 1H), 4.16 (s, 2H), 2.94 (s, 6H), 2.08 (s, 3H).

MS (ESI^{+}) m/z: $[M+H]^{+}$ 304; $[M+Na]^{+}$ 326.

Melting point: 109 °C

MNA20

1-(5-fluoro-2-hydroxyphenyl)-2-((4-hydroxy-6-methylpyrimidin-2-yl)thio)ethan-1-one



Appearance: white powder

A suspension of 2-mercapto-6-methylpyrimidin-4-ol (0.05 g, 0.35 mmol, 1 equiv.) in 5 ml methanol was prepared, and a solution of 0.35 ml KOH (1.0 equivalent, 1 M in methanol) was added dropwise. The mixture was stirred at room temperature for 15 minutes, after which 2-bromo-1-(5-fluoro-2-hydroxyphenyl)ethan-1-one (0.098 g, 0.422 mmol, 1.2 equiv.) was introduced. The reaction was allowed to proceed for 12 hours at room temperature. Afterward, water (in an amount equal to the volume of methanol used) was added to quench the reaction. The resulting product was collected by filtration, washed with diethyl ether, and dried under high vacuum. The resulting residue was redissolved in 0.3 ml DMSO and purified by column chromatography using DMF containing 5% methanol as the eluent. Fractions containing the desired product were combined and dried in vacuo to produce a white solid, further dried under vacuum at 40 °C for 1 h to give the final compound as a white powder. (yield 85mg, 80%)

^{1}H NMR (400 MHz, DMSO) δ 11.11 (s, 1H), 7.61 (dd, *J* = 9.4, 3.2 Hz, 1H), 7.39 (td, *J* = 8.5, 3.1 Hz, 1H), 7.03 (dd, *J* = 9.1, 4.5 Hz, 1H), 5.95 (s, 1H), 4.70 (s, 2H), 2.11 (s, 1H), 1.98 (s, 3H).

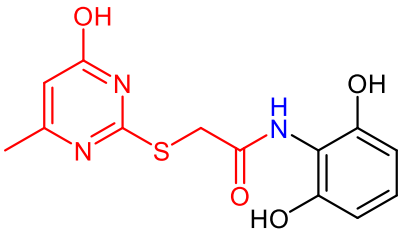
^{13}C NMR (101 MHz, DMSO) δ 156.08, 155.24, 122.58, 122.34, 118.99, 115.67, 115.42, 47.85, 47.64, 47.43, 23.07, 22.80.

MS (ESI^{+}) m/z: $[M+H]^{+}$ 295.0; $[M+Na]^{+}$ 316.9.

Melting point: 197°C

MNA21

N-(2,6-dihydroxyphenyl)-2-((4-hydroxy-6-methylpyrimidin-2-yl)thio)acetamide



Appearance: white powder

At room temperature 2-((4-hydroxy-6-methylpyrimidin-2-yl)thio)acetic acid (0.05 g, 0.25 mmol, 1 equiv.) was dissolved in 3 ml MeCN. BEP (0.06 g, 0.25 mmol, 1 equiv.) was added to activate the carboxylic acid, forming a reactive acyl benzotriazole intermediate, then NMI (0.07 g, 0.87 mmol, 3.5 equiv.) and 2-aminobenzene-1,3-diol (0.031 g, 0.25 mmol, 1 equiv.) were added and mixed for 24 hours. Product was evaporated in vacuo to remove MeCN, then dissolved in 0.6ml methanol and separated using column chromatography (DMF/5%methanol). Elute containing product was evaporated and the formed solid dried in vacuum over at 40° for 1 hour. (yield 30mg, 40%)

^{1}H NMR (400 MHz, DMSO) δ 9.49 (s, 1H), 6.87 (t, *J* = 8.1 Hz, 1H), 6.33 (dd, *J* = 8.1, 1.0 Hz, 2H), 6.01 (s, 1H), 4.12 (s, 2H), 2.19 (s, 3H).

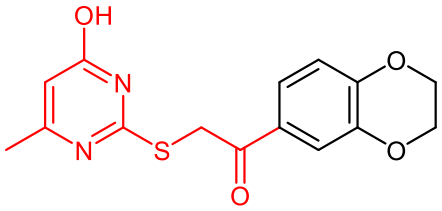
^{13}C NMR (101 MHz, DMSO) δ 167.60, 152.35, 126.93, 113.24, 107.31, 34.05.

MS (ESI^{+}) m/z: $[M+H]^{+}$ 308.1; $[M+Na]^{+}$ 330.0.

Melting point: 245 °C

MNA22

1-(2,3-dihydrobenzo[b][1,4]dioxin-6-yl)-2-((4-hydroxy-6-methylpyrimidin-2-yl)thio)ethan-1-one



Appearance: white powder

A suspension of 2-mercapto-6-methylpyrimidin-4-ol (0.05 g, 0.35 mmol, 1 equiv.) in 5 ml methanol was prepared, and a solution of 0.35 ml KOH (1.0 equivalent, 1 M in methanol) was added dropwise. The mixture was stirred at room temperature for 15 minutes, after which 2-bromo-1-(2,3-dihydrobenzo[b][1,4]dioxin-6-yl)ethan-1-one (0.1 g, 0.422 mmol, 1.2 equiv.) was introduced. The reaction was allowed to proceed for 12 hours at room temperature. Afterward, water (in an amount equal to the volume of methanol used) was added to quench the reaction. The resulting product was collected by filtration, washed with diethyl ether, and dried under high vacuum. The resulting residue was redissolved in 0.3 ml DMSO and purified by column chromatography using DMF containing 5% methanol as the eluent. Fractions containing the desired product were combined and dried in vacuo to produce a white solid, further dried under vacuum at 40 °C for 1 h to give the final compound as a white powder. (yield 17mg, 15%)

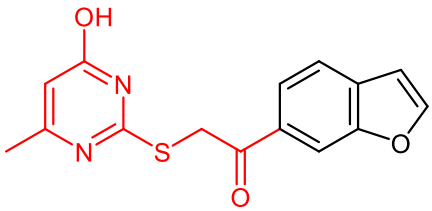
^{13}C NMR (101 MHz, DMSO) δ 189.93, 148.43, 143.23, 127.73, 122.36, 117.46, 117.30, 64.60, 63.92, 47.30.

MS (ESI$^+$) m/z: $[M+H]^+$ 319.0; $[M+Na]^+$ 341.1

Melting point: 185 °C

MNA23

1-(benzofuran-6-yl)-2-((4-hydroxy-6-methylpyrimidin-2-yl)thio)ethan-1-one



Appearance: white powder

A suspension of 2-mercapto-6-methylpyrimidin-4-ol (0.05 g, 0.35 mmol, 1 equiv.) in 5 ml methanol was prepared, and a solution of 0.35 ml KOH (1.0 equivalent, 1 M in methanol) was added dropwise.

The mixture was stirred at room temperature for 15 minutes, after which 1-(benzofuran-6-yl)-2-bromoethan-1-one (0.1 g, 0.422 mmol, 1.2 equiv.) was introduced. The reaction was allowed to proceed for 12 hours at room temperature. Afterward, water (in an amount equal to the volume of methanol used) was added to quench the reaction. The resulting product was collected by filtration, washed with diethyl ether, and dried under high vacuum. The resulting residue was redissolved in 0.3 ml DMSO and purified by column chromatography using DMF containing 5% methanol as the eluent. Fractions containing the desired product were combined and dried in vacuo to produce a white solid, further dried under vacuum at 40 °C for 1 h to give the final compound as a white powder. (yield 25mg, 23%)

^{1}H NMR (400 MHz, DMSO) δ 12.65 (s, 1H), 8.46 (d, *J* = 1.8 Hz, 1H), 8.15 (t, *J* = 1.6 Hz, 1H), 8.02 (dt, *J* = 8.8, 1.5 Hz, 1H), 7.76 (d, *J* = 8.7 Hz, 1H), 7.14 (dd, *J* = 2.2, 1.1 Hz, 1H), 5.94 (s, 1H), 4.82 (s, 2H), 1.97 (s, 3H).

^{13}C NMR (101 MHz, DMSO) δ 193.06, 156.87, 147.73, 131.69, 127.40, 124.90, 122.85, 111.56, 107.51, 37.61, 23.13.

MS (ESI^{+}) m/z: $[M+H]^{+}$ 301.2; $[M+Na]^{+}$ 323.1.

Melting point: 206 °C

5.3 Computational Studies

5.3.1 Source of Compounds for High-Throughput Screening and Computational Studies

Compounds used for high-throughput biochemical screening and in silico studies were sourced from the University of Nottingham Managed Chemical Compound Collection, housed within the Biodiscovery Institute. This fully automated facility maintains a curated library of over 85,000 structurally diverse, drug-like small molecules that largely comply with Lipinski's rule-of-five criteria and provide broad coverage of pharmacophore space.

Library compounds are stored as 10 mM stock solutions in dimethyl sulfoxide (DMSO) and are supported by dedicated infrastructure for quality control, automated handling, and transfer into screening plates. Compound purity is routinely verified using an in-house LC–MS system. Screening-ready samples were tested directly in biochemical assays at a final concentration of 100 µM.

A centralized digital database containing structural and physicochemical information for all library compounds was used to support computational screening and compound selection.

Sequence Comparison and Domain Analysis of 3MST

The amino acid sequences for mouse (*Mus musculus*) and rat (*Rattus norvegicus*) 3-mercaptopyruvate sulfurtransferase (3MST) were retrieved from the NCBI Protein database (Accessions: Q99J99 and Q5XI73, respectively) (Sayers et al., 2023). Pairwise sequence alignment and calculation of percentage identity were performed using the BLASTP algorithm (Johnson et al., 2008) via the NCBI web server (https://blast.ncbi.nlm.nih.gov/), employing default parameters. Conserved protein domains were identified using the NCBI's Conserved Domain Database (CDD) search tool (Lu et al., 2020).

The primary sequence of rat 3MST exhibited 95.27% identity with its mouse counterpart. Conserved domain analysis confirmed that both sequences contain the definitive sulfurtransferase domain (COG2897, E-value = 4.28×10^{-104}) with a perfectly conserved Cys-Gly-Ser (CGS) catalytic motif, as identified by CDD search (Lu et al., 2020).

5.3.2 Molecular Docking Studies

The crystal structure of the target protein was obtained from the Protein Data Bank (PDB ID: 5WQJ) and used as the receptor for molecular docking studies. The binding site was defined based on the position of the co-crystallized ligand present in the crystal structure. This was selected for docking studies as it was, at the time of this work, the only published and publicly available structure containing a co-crystallized ligand (inhibitor) and was of sufficient structural quality for computational analysis.

Protein preparation was performed using UCSF Chimera, including removal of crystallographic water molecules, addition of hydrogen atoms, assignment of appropriate protonation states, and energy minimization. Ligand structures were prepared in UCSF Chimera, energy-minimized, and converted to PDBQT format prior to docking.

Molecular docking was carried out using AutoDock Vina. The docking grid was cantered at coordinates (x = 21, y = 21, z = 21) with grid dimensions of 27 × 27 × 27 Å, fully encompassing the defined binding pocket. Default Vina parameters were employed unless otherwise stated.

For each ligand, multiple binding poses were generated, and the pose with the lowest predicted binding free energy was selected for further analysis. Docking results were visualized and analysed using UCSF Chimera, and predicted binding affinities were recorded as Vina scores (kcal·mol^{-1}).

An initial virtual screening study was conducted by Dr Barrie Kellam using LigandScout (Inte:Ligand GmbH, Vienna, Austria), based on the available crystal structure of the target protein. The resulting prioritized compounds were subsequently re-evaluated in this work by reproducing the docking studies using UCSF Chimera and AutoDock Vina under the conditions described above. Docking poses and predicted binding affinities were recorded and compared to confirm consistency with the initial screening results.

A second, focused virtual screening of sulphonamide-containing compounds was carried out manually as part of this study using AutoDock Vina. These compounds were docked individually into the defined binding site, and the resulting binding poses and predicted affinities were analysed and recorded.

5.3.3 Analysis of Virtual Screening Results

5.3.4 Data warrior

Docking results were compiled and analyzed in DataWarrior, where compounds were classified based on qualitative fit within the binding pocket, associated Vina scores, and chemical similarity calculated using FragFP. Biological activity data were added retrospectively for compounds selected for experimental testing.

Docking outputs were collated and analysed using DataWarrior. For each compound evaluated in the virtual screening, docking results were recorded and categorized based on qualitative assessment of the predicted binding pose. Compounds were classified based on whether the docked pose was compatible with the defined binding pocket (“fit”) or incompatible (“no fit”). A pose was considered a “fit” if it satisfied one or more of the following interactions: a sulfur–carbonyl interaction with Cysteine 248, direct or water-mediated hydrogen bonds with Arginine 188, or water-mediated hydrogen bonds with Arginine 197 and Glutamic acid 196. Poses not meeting these criteria were classified as “no fit.”

Predicted binding affinities obtained from AutoDock Vina were recorded as Vina scores (kcal·mol^{-1}) for each compound. In addition, chemical similarity to the reference structure from literature (Hanaoka compound 1) was calculated using the FragFP (fragment-based fingerprint) method implemented in DataWarrior. In addition, molecular descriptors including molecular weight, calculated log P, and the number of hydrogen bond donors and acceptors were generated in DataWarrior and used to examine trends and patterns across the dataset.

For compounds that progressed to experimental biological evaluation, assay outcomes were subsequently incorporated into the dataset and annotated as active or inactive at 10µM. These

combined criteria were used to support compound prioritization and retrospective analysis of the virtual screening results.

The compounds used in the sulphonamide screening are listed in the Appendix, together with their corresponding AutoDock Vina scores and binding-pocket fit assessments. Each compound is identified by its Nottingham library code (ID), and the associated SMILES strings are provided. In addition, calculated physicochemical descriptors, including hydrogen bond donors and acceptors, cLogP, and molecular weight, are reported to support interpretation of the screening results.

6. References

Abe, K. and Kimura, H. (1996) 'The possible role of hydrogen sulfide as an endogenous neuromodulator', *Journal of Neuroscience*, 16, pp. 1066–1071.

Adánez-Rubio, I., Millera, Á., Bilbao, R. and Alzueta, M. (2020) 'Effect of H_2S on the S-PAH formation during ethylene pyrolysis', *Fuel*, 276, 118033. https://doi.org/10.1016/j.fuel.2020.118033

Ahmad, A. and Szabó, C. (2016) 'Both the H_2S biosynthesis inhibitor aminooxyacetic acid and the mitochondrially targeted H_2S donor AP39 exert protective effects in a mouse model of burn injury', *Pharmacological Research*, 113, pp. 348–355.

Ahmad, A., Gerö, D., Olah, G. and Szabó, C. (2016a) 'Effect of endotoxemia in mice genetically deficient in cystathionine-γ-lyase, cystathionine-β-synthase or 3-mercaptopyruvate sulfurtransferase', *International Journal of Molecular Medicine*, 38, pp. 1683–1692.

Ahmad, A., Olah, G., Szczesny, B., Wood, M.E., Whiteman, M. and Szabó, C. (2016b) 'AP39, a mitochondrially-targeted hydrogen sulfide donor, exerts protective effects in renal epithelial cells subjected to oxidative stress in vitro and in acute renal injury in vivo', *Shock*, 45, p. 88.

Aitken, S.M. and Kirsch, J.F. (2005) 'The enzymology of cystathionine biosynthesis: strategies for the control of substrate and reaction specificity', *Archives of Biochemistry and Biophysics*, 433, pp. 166–175.

Al-Hazmi, G. (2024) 'New green chemistry approach of synthesis and antifungal activities', *Polish Journal of Environmental Studies*, 33(5), pp. 5549–5556. https://doi.org/10.15244/pjoes/183851

Almehaize, M. (2017) *Screening for inhibitors of hydrogen sulfide synthesising enzymes*. Unpublished Master's thesis, University of Nottingham.

Andreadou, I., Iliodromitis, E.K., Rassaf, T., Schulz, R., Papapetropoulos, A. and Ferdinandy, P. (2015) 'The role of gasotransmitters NO, H_2S and CO in myocardial ischaemia/reperfusion injury and cardioprotection by preconditioning, postconditioning and remote conditioning', *British Journal of Pharmacology*, 172, pp. 1587–1606.

Asimakopoulou, A., Panopoulos, P., Chasapis, C.T., Coletta, C., Zhou, Z., Cirino, G., Giannis, A., Szabó, C., Spyroulias, G.A. and Papapetropoulos, A. (2013) 'Selectivity of commonly used pharmacological inhibitors for cystathionine β-synthase (CBS) and cystathionine γ-lyase (CSE)', *British Journal of Pharmacology*, 169, pp. 922–932.

Aslami, H., Schultz, M.J. and Juffermans, N.P. (2009) 'Potential applications of hydrogen sulfide-induced suspended animation', *Current Medicinal Chemistry*, 16, pp. 1295–1303.

Augsburger, F. and Szabó, C. (2020) 'Potential role of the 3-mercaptopyruvate sulfurtransferase (3-MST)–hydrogen sulfide (H_2S) pathway in cancer cells', *Pharmacological Research*, 154, 104083. https://doi.org/10.1016/j.phrs.2018.11.034

Augsburger, F., Randi, E., Jendly, M., Ascenção, K., Dilek, N. and Szabó, C. (2020) 'Role of 3-mercaptopyruvate sulfurtransferase in the regulation of proliferation, migration, and bioenergetics in murine colon cancer cells', *Biomolecules*, 10(3), 447. https://doi.org/10.3390/biom10030447

Bantzi, M., Augsburger, F., Loup, J., Berset, Y., Vasilakaki, S., Myrianthopoulos, V., Mikros, E., Szabó, C. and Bochet, C.G. (2021) 'Novel aryl-substituted pyrimidones as inhibitors of 3-mercaptopyruvate sulfurtransferase with antiproliferative efficacy in colon cancer', *Journal of Medicinal Chemistry*, 64(9), pp. 6221–6240. https://doi.org/10.1021/acs.jmedchem.1c00260

Baron, R. and Vellore, N. (2012) 'LSD1/CoREST is an allosteric nanoscale clamp regulated by H3-histone-tail molecular recognition', *Proceedings of the National Academy of Sciences*, 109(31), pp. 12509–12514. https://doi.org/10.1073/pnas.1207892109

Battin, E.E. and Brumaghim, J.L. (2009) 'Antioxidant activity of sulfur and selenium: a review of reactive oxygen species scavenging, glutathione peroxidase and metal-binding antioxidant mechanisms', *Cell Biochemistry and Biophysics*, 55(1), pp. 1–23. https://doi.org/10.1007/s12013-009-9054-7

Bełtowski, J. (2015) 'Hydrogen sulfide in pharmacology and medicine – An update', *Pharmacological Reports*, 67, pp. 647–658.

Beutner, G.L. *et al.* (2018) *TCFH–NMI: direct access to N-acyl imidazoliums for challenging amide bond formations*, **Organic Letters**, 20(21), pp. 4218–4222.
Baldwin, O.W.M. *et al.* (2022) *Facile amide bond formation with TCFH–NMI in an organic laboratory course*, **Journal of Chemical Education**, 99(11), pp. 3747–3751.

Bhatia, M. (2005) 'Hydrogen sulfide as a vasodilator', *IUBMB Life*, 57, pp. 603–606.

Bordo, D. and Bork, P. (2002) 'The rhodanese/Cdc25 phosphatase superfamily: sequence–structure–function relations', *EMBO Reports*, 3, pp. 741–746.

Brancaleone, V., Vellecco, V., Matassa, D., Di Villa Bianca, R.D.E., Sorrentino, R., Ianaro, A., Bucci, M., Esposito, F. and Cirino, G. (2015) 'Crucial role of androgen receptor in vascular H_2S biosynthesis induced by testosterone', *British Journal of Pharmacology*, 172, pp. 1505–1515.

Cai, W.-J., Wang, M.-J., Moore, P.K., Jin, H.-M., Yao, T. and Zhu, Y.-C. (2007) 'The novel proangiogenic effect of hydrogen sulfide is dependent on Akt phosphorylation', *Cardiovascular Research*, 76, pp. 29–40.

Caliendo, G., Cirino, G., Santagada, V. and Wallace, J.L. (2010) 'Synthesis and biological effects of hydrogen sulfide (H_2S): development of H_2S-releasing drugs as pharmaceuticals', *Journal of Medicinal Chemistry*, 53, pp. 6275–6286.

Casili, G., Randi, E., Panagaki, T., Zuhra, K., Petrosino, M. and Szabó, C. (2022) 'Inhibition of the 3-mercaptopyruvate sulfurtransferase–hydrogen sulfide system promotes cellular lipid accumulation', *GeroScience*, 44(4), pp. 2271–2289. https://doi.org/10.1007/s11357-022-00600-9

Chatzianastasiou, A., Bibli, S.I., Andreadou, I., Efentakis, P., Kaludercic, N., Wood, M.E., Whiteman, M., Di Lisa, F., Daiber, A., Manolopoulos, V.G., Szabó, C. and Papapetropoulos, A. (2016) 'Cardioprotection by H_2S donors: nitric oxide-dependent and -independent mechanisms', *Journal of Pharmacology and Experimental Therapeutics*, 358, pp. 431–440.

Chen, L., McBranch, D.W., Wang, H.-L., Helgeson, R., Wudl, F. and Whitten, D.G. (1999) 'Highly sensitive biological and chemical sensors based on reversible fluorescence quenching in a conjugated polymer', *Proceedings of the National Academy of Sciences of the United States of America*, 96(22), pp. 12287–12292. https://doi.org/10.1073/pnas.96.22.12287

Chen, X., Jhee, K.-H. and Kruger, W.D. (2004) 'Production of the neuromodulator H_2S by cystathionine β-synthase via the condensation of cysteine and homocysteine', *Journal of Biological Chemistry*, 279, pp. 52082–52086.

Chi, Z., Liu, R., Yang, H., Shen, H. and Wang, J. (2011) 'Binding of tetracycline and chlortetracycline to the enzyme trypsin: spectroscopic and molecular modeling investigations', *PLOS ONE*, 6(12), e28361. https://doi.org/10.1371/journal.pone.0028361

Clausen, T., Huber, R., Messerschmidt, A., Pohlenz, H.-D. and Laber, B. (1997) 'Slow-binding inhibition of *Escherichia coli* cystathionine β-lyase by L-aminoethoxyvinylglycine: a kinetic and X-ray study', *Biochemistry*, 36, pp. 12633–12643.

Cuevasanta, E., Denicola, A., Alvarez, B. and Möller, M.N. (2012) 'Solubility and permeation of hydrogen sulfide in lipid membranes', *PLOS ONE*, 7, e34562.

Esechie, A., Kiss, L., Olah, G., Horváth, E.M., Hawkins, H., Szabó, C. and Traber, D.L. (2008) 'Protective effect of hydrogen sulfide in a murine model of acute lung injury induced by combined burn and smoke inhalation', *Clinical Science*, 115, pp. 91–97.

Flannigan, K.L., McCoy, K.D. and Wallace, J.L. (2011) 'Eukaryotic and prokaryotic contributions to colonic hydrogen sulfide synthesis', *American Journal of Physiology – Gastrointestinal and Liver Physiology*, 301, pp. G188–G193.

Fräsdorf, B., Radon, C. and Leimkühler, S. (2014) 'Characterization and interaction studies of two isoforms of the dual localized 3-mercaptopyruvate sulfurtransferase TUM1 from humans', *Journal of Biological Chemistry*, 289, pp. 34543–34556.

Frendo, J. and Wróbel, M. (1997) 'The activity of 3-mercaptopyruvate sulfurtransferase in erythrocytes from patients with polycythemia vera', *Acta Biochimica Polonica*, 44, pp. 771–773.

Gerö, D., Torregrossa, R., Perry, A., Waters, A., Le-Trionnaire, S., Whatmore, J.L., Wood, M.E. and Whiteman, M. (2016) 'The novel mitochondria-targeted hydrogen sulfide donors AP123 and AP39

protect against hyperglycemic injury in microvascular endothelial cells in vitro', *Pharmacological Research*, 113, pp. 186–198.

Gil, V., Gallego, D. and Jiménez, M. (2011) 'Effects of inhibitors of hydrogen sulphide synthesis on rat colonic motility', *British Journal of Pharmacology*, 164(2B), pp. 485–498. https://doi.org/10.1111/j.1476-5381.2011.01431.x

Hajna, Z., Sághy, É., Payrits, M., Aubdool, A.A., Szőke, É., Pozsgai, G., Bátai, I.Z., Nagy, L., Filotás, D. and Helyes, Z. (2016) 'Capsaicin-sensitive sensory nerves mediate the cellular and microvascular effects of H_2S via TRPA1 receptor activation and neuropeptide release', *Journal of Molecular Neuroscience*, 60, pp. 157–170.

Hanaoka, K., Sasakura, K., Suwanai, Y., Toma-Fukai, S., Shimamoto, K., Takano, Y., Shibuya, N., Terai, T., Komatsu, T., Ueno, T. and Nagano, T. (2017) 'Discovery and mechanistic characterization of selective inhibitors of H_2S-producing enzyme: 3-mercaptopyruvate sulfurtransferase (3MST) targeting active-site cysteine persulfide', *Scientific Reports*, 7, 40227. https://doi.org/10.1038/srep40227

Jacob, C. and Anwar, A. (2008) 'The chemistry behind redox regulation with a focus on sulfur redox systems', *Physiologia Plantarum*, 133(3), pp. 469–480. https://doi.org/10.1111/j.1399-3054.2008.01080.x

Johnson, M., Zaretskaya, I., Raytselis, Y., Merezhuk, Y., McGinnis, S. and Madden, T.L., 2008. NCBI BLAST: a better web interface. *Nucleic Acids Research*, 36(Web Server issue), pp.W5-W9. Available at: https://doi.org/10.1093/nar/gkn201

Jurkowska, H., Placha, W., Nagahara, N. and Wróbel, M. (2011) 'The expression and activity of cystathionine-γ-lyase and 3-mercaptopyruvate sulfurtransferase in human neoplastic cell lines', *Amino Acids*, 41, pp. 151–158.

Kabil, O. and Banerjee, R. (2010) 'Redox biochemistry of hydrogen sulfide', *Journal of Biological Chemistry*, 285, pp. 21903–21907.

Karwi, Q.G., Whiteman, M., Wood, M.E., Torregrossa, R. and Baxter, G.F. (2016) 'Pharmacological postconditioning against myocardial infarction with a slow-releasing hydrogen sulfide donor, GYY4137', *Pharmacological Research*, 111, pp. 442–451. https://doi.org/10.1016/j.phrs.2016.06.028

Katsouda, A., Peleli, M., Asimakopoulou, A., Papapetropoulos, A. and Beis, D. (2020) 'Generation and characterisation of a CRISPR/Cas9-induced 3-mst-deficient zebrafish', *Biomolecules*, 10(2), 317. https://doi.org/10.3390/biom10020317

Kimura, H. (2011) 'Hydrogen sulfide: its production, release and functions', *Amino Acids*, 41, pp. 113–121.

Kimura, Y., Koike, S., Shibuya, N., Lefer, D., Ogasawara, Y. and Kimura, H. (2017) '3-mercaptopyruvate sulfurtransferase produces potential redox regulators cysteine- and glutathione-persulfide (Cys-SSH and GSSH) together with signaling molecules H_2S_2, H_2S_3 and H_2S', *Scientific Reports*, 7, 11004. https://doi.org/10.1038/s41598-017-11004-7

Lin, V.S., Lippert, A.R. and Chang, C.J. (2013) 'Cell-trappable fluorescent probes for endogenous hydrogen sulfide signaling and imaging H_2O_2-dependent H_2S production', *Proceedings of the National Academy of Sciences of the United States of America*, 110, pp. 7131–7135.

Loiselle, J., Yang, G. and Wu, L. (2018) 'Hydrogen sulfide and hepatic lipid metabolism: a critical pairing for liver health', *British Journal of Pharmacology*, 177(4), pp. 757–768. https://doi.org/10.1111/bph.14556

Lu, S., Wang, J., Chitsaz, F., Derbyshire, M.K., Geer, R.C., Gonzales, N.R., Gwadz, M., Hurwitz, D.I., Marchler, G.H., Song, J.S., Thanki, N., Yamashita, R.A., Yang, M., Zhang, D., Zheng, C., Lanczycki, C.J. and Marchler-Bauer, A., 2020. CDD/SPARCLE: the conserved domain database in 2020. *Nucleic Acids Research*, 48(D1), pp.D265-D268. Available at: https://doi.org/10.1093/nar/gkz991

Mikami, Y., Shibuya, N., Kimura, Y., Nagahara, N., Ogasawara, Y. and Kimura, H. (2011) 'Thioredoxin and dihydrolipoic acid are required for 3-mercaptopyruvate sulfurtransferase to produce hydrogen sulfide', *Biochemical Journal*, 439, pp. 479–485.

Möller, M. and Denicola, A. (2002) 'Protein tryptophan accessibility studied by fluorescence quenching', *Biochemistry and Molecular Biology Education*, 30(3), pp. 175–178. https://doi.org/10.1002/bmb.2002.494030030035

Nagahara, N., Nagano, M., Ito, T., Shimamura, K., Akimoto, T. and Suzuki, H. (2013) 'Antioxidant enzyme, 3-mercaptopyruvate sulfurtransferase-knockout mice exhibit increased anxiety-like behaviors: a model for human mercaptolactate–cysteine disulfiduria', *Scientific Reports*, 3, 1986. https://doi.org/10.1038/srep01986

Pinzi, L. and Rastelli, G. (2019) 'Molecular docking: shifting paradigms in drug discovery', *International Journal of Molecular Sciences*, 20(18), 4331. https://doi.org/10.3390/ijms20184331

Rao, S., Dobariya, P., Bellamkonda, H. and More, S. (2023) 'Role of 3-mercaptopyruvate sulfurtransferase (3-MST) in physiology and disease', *Antioxidants*, 12(3), 603. https://doi.org/10.3390/antiox12030603

Riahi, S. and Rowley, C.N. (2014) 'Why can hydrogen sulfide permeate cell membranes?', *Journal of the American Chemical Society*, 136, pp. 15111–15113.

Santos, S., Rodrigues, L., Martins, V., Petrosino, M., Zuhra, K., Ascenção, K. and Szabó, C. (2023) 'Role of cystathionine β-synthase and 3-mercaptopyruvate sulfurtransferase in the regulation of proliferation, migration and bioenergetics of murine breast cancer cells', *Antioxidants*, 12(3), 647. https://doi.org/10.3390/antiox12030647

Sayers, E.W., Cavanaugh, M., Clark, K., Ostell, J., Pruitt, K.D. and Karsch-Mizrachi, I., 2023. Database resources of the National Center for Biotechnology Information. *Nucleic Acids Research*, 51(D1), pp.D29-D38. Available at: https://doi.org/10.1093/nar/gkac1032

Shibuya, N., Koike, S., Tanaka, M., Ishigami-Yuasa, M., Kimura, Y., Ogasawara, Y., Fukui, K., Nagahara, N. and Kimura, H. (2013) 'A novel pathway for the production of hydrogen sulfide from D-cysteine in mammalian cells', *Nature Communications*, 4, 1366.

Shibuya, N., Mikami, Y., Kimura, Y., Nagahara, N. and Kimura, H. (2009) 'Vascular endothelium expresses 3-mercaptopyruvate sulfurtransferase and produces hydrogen sulfide', *Journal of Biochemistry*, 146, pp. 623–626.

Shibuya, N., Tanaka, M., Yoshida, M., Ogasawara, Y., Togawa, T., Ishii, K. and Kimura, H. (2009) '3-Mercaptopyruvate sulfurtransferase produces hydrogen sulfide and bound sulfane sulfur in the brain', *Antioxidants & Redox Signaling*, 11, pp. 703–714.

Sun, H., Wu, Z., Nie, X., Wang, X. and Bian, J. (2021) 'Implications of hydrogen sulfide in liver pathophysiology: mechanistic insights and therapeutic potential', *Journal of Advanced Research*, 27, pp. 127–135. https://doi.org/10.1016/j.jare.2020.05.010

Szabó, C. (2018) 'A timeline of hydrogen sulfide (H_2S) research: from environmental toxin to biological mediator', *Biochemical Pharmacology*, 149, pp. 5–19.

Szabó, C. and Papapetropoulos, A. (2017) 'International Union of Basic and Clinical Pharmacology. CII: Pharmacological modulation of H_2S levels: H_2S donors and H_2S biosynthesis inhibitors', *Pharmacological Reviews*, 69, pp. 497–564.

Takano, Y., Echizen, H. and Hanaoka, K. (2017) 'Fluorescent probes and selective inhibitors for biological studies of hydrogen sulfide- and polysulfide-mediated signaling', *Antioxidants & Redox Signaling*, 27, pp. 669–683.

Thomas Sander, Joel Freyss, Modest von Korff, Christian Rufener. DataWarrior: An Open-Source Program For Chemistry Aware Data Visualization And Analysis. *J Chem Inf Model* **2015**, *55*, 460-473, doi 10.1021/ci500588j

Whiteman, M., Armstrong, J.S., Chu, S.H., Jia-Ling, S., Wong, B.S., Cheung, N.S., Halliwell, B. and Moore, P.K. (2004) 'The novel neuromodulator hydrogen sulfide: an endogenous peroxynitrite "scavenger"?', *Journal of Neurochemistry*, 90, pp. 765–768.

Wróbel, M., Jurkowska, H., Śliwa, L. and Srebro, Z. (2004) 'Sulfurtransferases and cyanide detoxification in mouse liver, kidney, and brain', *Toxicology Mechanisms and Methods*, 14, pp. 331–337.

Xie, L., Feng, H., Li, S., Meng, G., Liu, S., Tang, X., Ma, Y., Han, Y., Xiao, Y. and Gu, Y. (2016) 'SIRT3 mediates the antioxidant effect of hydrogen sulfide in endothelial cells', *Antioxidants & Redox Signaling*, 24, pp. 329–343.

Yang, G., Wu, L., Jiang, B., Yang, W., Qi, J., Cao, K., Meng, Q., Mustafa, A.K., Mu, W. and Zhang, S. (2008) 'H_2S as a physiologic vasorelaxant: hypertension in mice with deletion of cystathionine γ-lyase', *Science*, 322, pp. 587–590.

Zhao, W., Zhang, J., Lu, Y. and Wang, R. (2001) 'The vasorelaxant effect of H_2S as a novel endogenous gaseous KATP channel opener', *The EMBO Journal*, 20, pp. 6008–6016.

7. Appendix

Table A1. Virtual screening results for sulphonamides from the Nottingham compound library, including AutoDock Vina docking scores, SMILES strings, and key physicochemical properties.

MCCC Sample Id	Smiles	vina score	fit	cLogP	H-Acceptors	H-Donors	Total Molweight
NCC-00043152	CC(C(Nc(cc1)ccc1C(C)=O)=O)OC(c(cc1)ccc1NS(c1c(C)ccc(C)c1)(=O)=O)=O	-9.4	Y	3.5824	8	2	494.566
NCC-00052321	CCOC(N(CC1)CCN1C(COC(c1cccc(S(Nc(cc2)ccc2F)(=O)=O)c1)=O)=O)=O	-10.1	Y	2.0673	10	1	493.511
NCC-00016160	CC(C(N(CC1)CCN1S(c1ccccc1)(=O)=O)=O)N(C)Cc(cc1)cc(OC)c1OC(F)F	-7.4	N	2.0388	8	0	497.561
NCC-00073854	CC(C(Nc(cccc1)c1C#N)=O)OC(c(cccc1)c1NS(c1c(C)ccc(C)c1)(=O)=O)=O	-8	N	3.5468	8	2	477.54
NCC-00018484	Cc1c(C(Nc2cccc(S(Nc3cc(C(F)(F)F)ccc3)(=O)=O)c2)=O)[nH]c(C)c1C(OC)=O	-10.1	Y	3.3858	8	3	495.477
NCC-00087261	CN(CC(Nc(cc1)ccc1OC(F)(F)F)=O)C(CNS(c1cc(cccc2)c2cc1)(=O)=O)=O	-9.4	Y	3.221	8	2	495.477
NCC-00036232	CC(C)(C)OC(N(CCC1)CC1C(Nc1cccc(S(Nc(cccc2)c2OC)(=O)=O)c1)=O)=O	-8.5	Y	3.288	9	2	489.591
NCC-00027542	CCN(CC1)CCN1C(C(C)OC(c(cc1)ccc1NS(c1ccc(C(C)O)cc1)(=O)=O)=O)=O	-9.5	Y	1.7553	9	2	489.591
NCC-00035867	CC(C(Nc(cc1)ccc1C(N)=O)=O)OC(c(cc1)ccc1S(Nc1c(C)cccc1)(=O)=O)=O	-10.3	Y	2.4546	9	3	481.528
NCC-00031554	Cc1c(C)[o]c(NC(COC(c2cc(S(Nc3cc(C)ccc3)(=O)=O)c(C)cc2)=O)=O)c1C#N	-8.5	N	3.4154	9	2	481.528
NCC-00036672	Cc(cc1C)cc(C)c1NC(CN(C)C(c(cc1)ccc1S(Nc(cc1)ccc1F)(=O)=O)=O)=O	-7.8	N	3.5889	7	2	483.562
NCC-00017412	Cc(cc(cc1)S(Nc(cc2)ccc2C(NCC(c(cc2)ccc2OC)N(C)C)=O)(=O)=O)c1F	-10.4	Y	2.7705	7	2	485.578
NCC-00030893	Cc(cc1)cc(C)c1S(Nc(cc1)ccc1C(NCC(N(C)Cc1cc(F)ccc1)=O)=O)(=O)=O	-9.9	Y	2.9544	7	2	483.562
NCC-00044740	CC(C)(CNC(Cc(cc1)ccc1NS(c1cc(C(F)(F)F)ccc1)(=O)=O)=O)N1CCOCC1	-10.5	Y	2.6526	7	2	499.552
NCC-00012254	CCN(CCN(C)C)C(c(cc1)cc(NS(c2c(C)cc(C)cc2)(=O)=O)c1N1CCNCC1)=O	-7.1	N	1.9834	8	2	487.667
NCC-00063652	CC(C)C(C(Nc(cc1)cc(S(Nc(cccc2)c2OC)(=O)=O)c1N1CCCC1)=O)NC(N)=O	-7.8	N	1.5766	10	4	489.595

NCC-00054295	CC(C)(C)OC(N1C(COC(c2cccc(NS(c(cccc3)c3OC)(=O)=O)c2)=O)CCC1)=O	-8.6	Y	3.617	9	1	490.575
NCC-00027147	CC(c(cc1)ccc1NC(CCN(c(cc1)ccc1OC)S(c1cc(C)c(C)cc1)(=O)=O)=O)=O	-8.3	N	3.5997	7	1	480.583
NCC-00087795	CC(C)c(cc1C(C)C)cc(C(OCC(N(CC2)CCN2S(c2ccccc2)(=O)=O)=O)=O)c1O	-8.9	Y	3.8985	8	1	488.603
NCC-00036335	Cc1cccc(C)c1NC(COC(c(cc1)ccc1S(N(C)c(cccc1)c1OC)(=O)=O)=O)=O	-7.9	N	3.1871	8	1	482.555
NCC-00070527	Cc1cccc(NS(c2cc(C(NCc(cc3OC)cc(OC)c3OC)=O)c(C)cc2)(=O)=O)c1	-9.9	Y	3.2934	8	2	484.571
NCC-00029229	CC(C(NC(N)=O)=O)OC(CCC(N(CC1)CCN1S(c1cc(cccc2)c2cc1)(=O)=O)=O)=O	-8.1	N	1.0005	11	2	490.535
NCC-00007615	CCCCN(C)C(c(cc(cc1)NS(c2ccc(C(C)(C)C)cc2)(=O)=O)c1N1CCNCC1)=O	-6.3	N	4.0865	7	2	486.679
NCC-00007542	CC(C)CN(CC(C)C)C(c(cc(cc1)NS(c(cccc2)c2F)(=O)=O)c1N1CCNCC1)=O	-6.8	N	3.4483	7	2	490.642
NCC-00063172	CCc(cccc1)c1NC(CNC(CCC(N(CC1)CCN1S(c1ccccc1)(=O)=O)=O)=O)=O	-9.7	Y	2.0066	9	2	486.591
NCC-00007281	CCc(cccc1)c1S(Nc(ccc(N1CCN(CC(NC(C)C)=O)CC1)c1)c1C(O)=O)(=O)=O	-7.6	N	0.9045	9	3	488.607
NCC-00016931	CCCN(CC1)CCN1C(COc(cc1)ccc1N(C)S(c(cc1)ccc1NC(C)=O)(=O)=O)=O	-8.7	N	1.7869	9	1	488.607
NCC-00007029	Cc1c(CCCN(C)c(ccc(C(O)=O)c2)c2NS(c(cc2)ccc2OC)(=O)=O)c(C)n[n]1C	-7.4	N	2.4309	9	2	486.591
NCC-00038334	Cc(ccc(NC(CNC(NCc1ccccc1)=O)=O)c1)c1S(Nc(cc1)ccc1OC)(=O)=O	-8.8	Y	2.1671	9	4	482.559
NCC-00035110	CCN(c1ccccc1)S(c(cc1)cc(NC(c(cc2)nnc2O)=O)c1OCC(F)(F)F)(=O)=O	-7.5	N	2.4682	9	2	496.465
NCC-00069833	CC(N(CC1)CCN1C(c(cc1)cc(S(Nc2cc(OC)cc(OC)c2)(=O)=O)c1OC)=O)=O	-7.8	N	1.5891	10	1	477.536
NCC-00044659	CC(C(N(CC1)CCN1S(c1ccccc1)(=O)=O)=O)OC(c1cc(NS(C)(=O)=O)ccc1)=O	-8.9	Y	1.2782	10	1	495.576
NCC-00044111	Cc(ccc(S(Nc1cc(C(NCC(Cc2ccccc2)N(C)C)=O)ccc1)(=O)=O)c1)c1F	-8.3	N	3.3432	6	2	469.579
NCC-00063301	CC(C(Nc1cccc(S(Nc(cccc2)c2OC)(=O)=O)c1)=O)NC(c1cc(C)ccc1)=O	-9.3	Y	2.8231	8	3	467.545

NCC-00031679	Cc1c(C)c(S(N(C)c(cc2)ccc2OCC(NCC(NC2CC2)=O)=O)(=O)=O)c(C)c(C)c1	-7.9	N	1.8666	8	2	473.592
NCC-00026828	Cc(cc1)ccc1S(N(CC(NC(NCc1ccccc1)=O)=O)c(cccc1)c1OC)(=O)=O	-8.2	N	2.4253	8	2	467.545
NCC-00002546	Cc(cc1)cc(C(c2ccccc2)=O)c1NC(CNC(CNS(c1ccccc1)(=O)=O)=O)=O	-8.7	Y	2.135	8	3	465.529
NCC-00056307	CC(C)(C)c(cc1)ccc1C(Nc(cccc1)c1NS(c1cc(S(N)(=O)=O)ccc1)(=O)=O)=O	-6	N	3.4521	8	3	487.6
NCC-00030345	Cc(ccc(NC(CN(Cc1ccccc1)S(c1ccccc1)(=O)=O)=O)c1)c1S(NC)(=O)=O	-6.8	N	2.558	8	2	487.6
NCC-00085782	CCOc(ccc(S(Nc(cc1)ccc1NC(C)=O)(=O)=O)c1)c1NC(c(cc1)ccc1Cl)=O	-8.6	N	3.7522	8	3	487.963
NCC-00054810	Cc1ccc(CNC(c2c(C)ccc(S(Nc(c(OC)c3)cc(Cl)c3OC)(=O)=O)c2)=O)[n]1C	-8.8	N	2.9327	8	2	491.994
NCC-00049611	CC(C)C(CNC(c1cccc(S(Nc(cc(cc2)Cl)c2OC)(=O)=O)c1)=O)N1CCOCC1	-7.8	Y	2.6343	8	2	496.026
NCC-00002508	CCOC(N(CC1)CCN1C(CN(c(cc1)c(C)cc1Cl)S(c1ccc(C)cc1)(=O)=O)=O)=O	-6.5	N	3.2525	8	0	494.01
NCC-00073815	CCC(C(Nc1n[o]c(C)c1)=O)OC(c1cccc(NS(c(cc2)cc(F)c2F)(=O)=O)c1)=O	-10	Y	2.839	9	2	479.459
NCC-00076441	CCN(CC)C(c(cc1OC)cc(NS(c(cc2)cc(c(C)c3)c2nc3O)(=O)=O)c1OC)=O	-7.6	N	3.0022	9	2	473.548
NCC-00013852	CCOC(N(CC1)CCN1C(CN(c1ccccc1)S(c(cc1)ccc1OCC)(=O)=O)=O)=O	-5.9	N	2.295	9	0	475.564
NCC-00068392	CC(COC)NS(c(cc1)ccc1NC(C(CCCC1)N1S(c1ccccc1)(=O)=O)=O)(=O)=O	-8	N	1.9694	9	2	495.619
NCC-00030058	CC(CCCC1C)N1S(c(cc1)ccc1NS(c(cc1)cc(OC)c1NC(C)=O)(=O)=O)(=O)=O	-8.2	N	2.4486	9	2	495.619
NCC-00081887	CCOc(cc1)ccc1NS(c1cc(C(Nc2cc(CS(N)(=O)=O)ccc2)=O)ccc1)(=O)=O	-9	Y	2.4403	9	3	489.572
NCC-00000876	CC(Nc1c(/C=C\c(cc2)cc(S(Nc(cc3)cc(Cl)c3OC)(=O)=O)c2OC)[o]nc1C)=O	-7.5	N	3.1976	9	2	491.951
NCC-00036148	N#Cc1cccc(NC(COC(c(cc(cc2)S(Nc(cccc3)c3Cl)(=O)=O)c2O)=O)=O)c1	-10<NL>	Y	2.76	9	3	485.903
NCC-00055862	CCOC(N(CC1)CCN1C(c(cc(cc1)S(Nc(cc2)ccc2OCC)(=O)=O)c1Cl)=O)=O	-8.5	N	3.3509	9	1	495.982

NCC-00057350	CC(C)(C)C(N(CC1)CCC1C(Nc(cc(cc1)Cl)c1NS(c(cccc1)c1F)(=O)=O)=O)=O	-7.6	N	3.9539	7	2	496.001
NCC-00012005	CC(C)CCNC(C(C)(CN(CC1=O)S(c2ccccc2)(=O)=O)N1c1cc(C)cc(C)c1)=O	-6.7	N	3.2621	7	1	471.62
NCC-00027552	Cc(cc1)ccc1S(N(C)c(cc1)ccc1OCC(NCC1(CCCCC1)N(C)C)=O)(=O)=O	-6.7	N	2.3687	7	1	473.636
NCC-00014788	CCN(CC)S(c(cc1)cc(NS(c2ccc(C(C)(C)C)cc2)(=O)=O)c1N1CCCC1)(=O)=O	-6.6	N	4.0628	7	1	493.691
NCC-00035158	Cc(cc1)ccc1NC(CN(C)C(CN(c1ccccc1)S(c(cc1)ccc1F)(=O)=O)=O)=O	-7.4	N	2.4512	7	1	469.536
NCC-00070861	CCOc(cc1)ccc1S(Nc(cc1)ccc1C(N(CCC#N)c(cc1)ccc1F)=O)(=O)=O	-7.8	N	3.899	7	1	467.52
NCC-00018876	CCN(CC(NCc1ccc[s]1)=O)C(c(cc1)ccc1S(Nc1c(C)c(C)ccc1)(=O)=O)=O	-8.1	N	3.1265	7	2	485.627
NCC-00027205	CCCCN(C(N)=C(C(N1)=O)N(C)C(CN(C)S(c2cc(cccc3)c3cc2)(=O)=O)=O)C1=O	-7.7	N	1.5979	10	2	473.552
NCC-00056038	Cc(cc(C)c(S(Nc1cc(C(Nc2nccnc2)=O)ccc1)(=O)=O)c1C)c1NS(C)(=O)=O	-7.7	N	1.5362	10	3	489.576
NCC-00002308	Cc(cc1)ccc1S(N(C(c(cc1OC)cc(OC)c1OC)=O)c(cc1)ccc1OC)(=O)=O	-5.7	N	3.4283	8	0	471.529
NCC-00029807	CN(c(cccc1)c1OC)S(c(cc1)cc(C(OCC(c(cc2)ccc2F)=O)=O)c1Cl)(=O)=O	-9.2	N	3.3736	7	0	491.922
NCC-00011189	CCCC(N(c(cc1)cc2c1[o]c(C)c2C(OCC)=O)S(c(cc1)ccc1C(O)=O)(=O)=O)=O	-7	N	3.4833	9	1	473.501
NCC-00084340	CC(C(c1c(C)c(C(OC)=O)c(C)[nH]1)=O)OC(C(CC1)CCN1S(c1ccccc1)(=O)=O)=O	-7.6	N	2.0378	9	1	476.548
NCC-00088803	Cc(cc1)ccc1S(CCC(OCC(N(CC1)CCN1S(c1ccccc1)(=O)=O)=O)=O)(=O)=O	-8.6	Y	1.4061	9	0	494.587
NCC-00080608	CCOc(ccc(NS(c1c(C)c(C)cc(C(O)=O)c1)(=O)=O)c1)c1S(N1CCCCC1)(=O)=O	-7	N	2.6747	9	2	496.603
NCC-00038305	CC(C)CC(Nc(cc1)cc(N(S(c2ccccc2)(=O)=O)S(c2ccccc2)(=O)=O)c1F)=O	-7	N	4.1565	7	1	490.575
NCC-00035787	Cc(cc1)ccc1OCCN(C)C(c(cc1)ccc1S(N(C)c(cccc1)c1OC)(=O)=O)=O	-8.6	Y	3.2681	7	0	468.572
NCC-00062250	Cc(cc1)ccc1C(CCC(Nc1cc(S(Nc(cccc2)c2OC)(=O)=O)c(C)cc1)=O)=O	-9.2	N	3.7426	7	2	466.556

NCC-00073846	Cc(cc1)ccc1NS(c1cc(C(N(C)CCc(cc2)cc(OC)c2OC)=O)ccc1)(=O)=O	-7.9	Y	3.7161	7	1	468.572
NCC-00009428	CC(c1ccccc1)NC(CN(c(cc1)ccc1OC)S(c(cc(C)cc1)c1OC)(=O)=O)=O	-6.4	N	2.8563	7	1	468.572
NCC-00030805	CC(c(cc1)ccc1S(Nc(cc1)ccc1C(N(C)Cc(cc1)cc(F)c1OC)=O)(=O)=O)=O	-10	Y	2.9841	7	1	470.52
NCC-00063142	CC(c1ccc[s]1)NC(COC(c(cccc1)c1NS(c1c(C)cc(C)cc1C)(=O)=O)=O)=O	-7	N	3.5585	7	2	486.611
NCC-00070492	Cc1ccc(C(CC(OC)=O)NC(c2cccc(S(Nc(cc3)ccc3F)(=O)=O)c2)=O)cc1	-9.7	Y	3.153	7	2	470.52
NCC-00070557	Cc1cccc(NS(c(cc2)cc(C(OC(C(N(C)C)=O)c3ccccc3)=O)c2Cl)(=O)=O)c1	-10	N	3.4703	7	1	486.975
NCC-00031483	CCOC(C(CCC1)CN1C(c1cccc(S(Nc2cc(C(F)(F)F)ccc2)(=O)=O)c1)=O)=O	-8.2	N	3.4725	7	1	484.494
NCC-00036434	COc(cc1)ccc1N(CC(N(CC(F)(F)F)Cc1ccc[o]1)=O)S(c1ccccc1)(=O)=O	-6.2	N	2.6415	7	0	482.478
NCC-00019501	CCN(c1ccccc1)S(c(cc1)ccc1C(Nc(cccc1)c1S(C(F)F)(=O)=O)=O)(=O)=O	-6.6	N	3.8374	7	1	494.538
NCC-00015158	CC(c(cc1)ccc1S(Nc(cc1)ccc1C(NCc(cc1)cc(OC)c1OC)=O)(=O)=O)O	-10.3	Y	2.365	8	3	470.544
NCC-00056461	CCOc(cc1)ccc1NS(c1c(C)ccc(NC(CC2(CC(O)=O)CCCC2)=O)c1)(=O)=O	-8.3	N	3.3087	8	3	474.576
NCC-00029936	CC(C)CN(C(CC1)CS1(=O)=O)C(c(cc1)ccc1S(N(C)c(ccc1)c1OC)(=O)=O)=O	-6.6	N	1.9419	8	0	494.631
NCC-00027681	CCOC(c1c(C)cc(NC(c2cccc(S(N(C)c(cc3)ccc3OC)(=O)=O)c2)=O)[s]1)=O	-8.3	Y	3.6608	8	1	488.584
NCC-00035137	COc(ccc(C(NC1CCCCCC1)=O)c1)c1S(Nc(c(OC)c1)cc(Cl)c1OC)(=O)=O	-7.4	N	3.6912	8	2	497.01
NCC-00030170	CC(OCc(cc1)ccc1C(Nc(cc1)cc(S(Nc(cccc2)c2OC)(=O)=O)c1Cl)=O)=O	-9.2	N	3.5295	8	2	488.947
NCC-00015231	CCN(c1ccccc1)S(c(cc1)cc(NC(COC(C2(CCCCC2)O)=O)=O)c1Cl)(=O)=O	-7.5	N	2.6585	8	2	494.994
NCC-00028917	CN(c(cc1)ccc1OC)S(c1cccc(C(OCC(Nc(cccc2)c2Cl)=O)=O)c1)(=O)=O	-8.2	N	3.1053	8	1	488.947
NCC-00036557	Cc(cc1)ccc1S(N(C)c(cc1)ccc1OCC(Nc(cc(cc1)C(O)=O)c1Cl)=O)(=O)=O	-9.5	N	3.0213	8	2	488.947

NCC-00027257	OC(c(cc(cc1)S(Nc2cc(C(Nc3cc(C(F)(F)F)ccc3)=O)ccc2)(=O)=O)c1O)=O	-9.2	N	3.0939	8	4	480.418
NCC-00029718	O=C(COC(c1cccc(S(Nc2cc(C(F)(F)F)ccc2)(=O)=O)c1)=O)NCc1ccc[o]1	-9.5	Y	2.4105	8	2	482.434
NCC-00004673	CC(c1cccc(NC(CN(c2cc(C(F)(F)F)ccc2)S(c2ccccc2)(=O)=O)=O)c1)=O	-7.8	N	3.3758	6	1	476.474
NCC-00079831	Cc(c(NC(C(F)(F)F)(C(F)(F)F)NS(c1ccccc1)(=O)=O)c1O)n[n]1-c1ccccc1	-6.3	N	3.6282	7	3	494.415
NCC-00072025	CC(c1ncccc1)NC(CNC(c(cc1)ccc1NS(c(cc1)ccc1OC)(=O)=O)=O)=O	-9.7	Y	1.1691	9	3	468.533
NCC-00020300	Cc1nc(C)nc(O)c1CCC(Nc(cc1)cc(S(Nc(cc2)ccc2Cl)(=O)=O)c1OC)=O	-8.2	N	3.1685	9	3	490.967
NCC-00019457	CC(Nc(cc1)ccc1S(N(C)c(cc1)ccc1OCC(Nc([s]cc1)c1C#N)=O)(=O)=O)=O	-8.1	N	2.0996	9	2	484.556
NCC-00050552	CC(C)[n]1nccc1NC(COC(c(cccc1)c1NS(c(cc1)c(C)cc1F)(=O)=O)=O)=O	-6.4	N	2.2659	9	2	474.512
NCC-00046943	Cc(ccc(S(Nc(c(OC)c1)cc(Cl)c1OC)(=O)=O)c1)c1C(N(C)Cc1c[n](C)nc1)=O	-6.5	N	1.9543	9	1	492.983
NCC-00085642	CC(C)C[n]1nc(C)c(C(OC(C)C(N(CC2)CCN2S(c2ccccc2)(=O)=O)=O)=O)c1Cl	-8.3	N	2.3218	9	0	497.014
NCC-00078180	CCCN(C(C=C1)=O)N=C1C(Nc(cc1)cc(S(Nc(cc2)ccc2OC)(=O)=O)c1OC)=O	-8.4	N	1.3388	10	2	472.521
NCC-00020610	CCCCc(cc1)ccc1NS(c1cc(C(Nc2c[n](C)c(C(N)=O)c2)=O)c(C)cc1)(=O)=O	-8.8	N	3.115	8	3	468.576
NCC-00035473	CC(NCC(Nc(cc1)cc(S(Nc2cc(C(F)(F)F)ccc2)(=O)=O)c1N1CCCC1)=O)=O	-8.5	N	2.0854	8	3	484.498
NCC-00000064	CCCCCc1nc(C(OCC)=O)c(-c(c2c3cccc2)c[n]3S(c2ccccc2)(=O)=O)[o]1	-8.3	N	4.6583	7	0	466.556
NCC-00007298	CCN(CC)C(CN(C)c(cc1)cc(C(O)=O)c1NS(c1c(C)cc(C)cc1C)(=O)=O)=O	-8	N	2.5347	8	2	461.581
NCC-00055450	CC(C)C(C)(C#N)NC(COC(c1cccc(NS(c2c(C)ccc(F)c2)(=O)=O)c1)=O)=O	-8.8	Y	2.4646	8	2	461.513
NCC-00085030	CC(C)(C)NC(NC(COC(c1cccc(NS(c(cc2)cc(F)c2F)(=O)=O)c1)=O)=O)=O	-10.6	Y	2.0889	9	3	469.464
NCC-00050621	CC(C)CNC(NC(COC(c1cc(S(Nc2cc(C)ccc2)(=O)=O)c(C)cc1)=O)=O)=O	-8.2	Y	2.5079	9	3	461.537

NCC-00029638	CC(C)(C)NC(NC(COC(c1cccc(S(N(C)c2ccc(C)cc2)(=O)=O)c1)=O)=O)=O	-7.2	N	2.1364	9	2	461.537
NCC-00062563	CCCCc(cc1)ccc1NS(c1cc(C(NCC(NC(C)(C)C)=O)=O)c(C)cc1)(=O)=O	-8.1	N	3.6396	7	3	459.609
NCC-00035753	CCN(CC)S(c(cc1)cc(NS(c2c(C(F)(F)F)cccc2)(=O)=O)c1OC(C)C)(=O)=O	-5.8	N	3.5338	7	1	494.554
NCC-00016247	CC(C(NCc(cc1OC)cc(OC)c1OC)=O)NS(c1ccc(C(C)(C)C)cc1)(=O)=O	-6.4	N	3.018	8	2	464.581
NCC-00086883	Cc(ccc(S(Nc1c(C)cccc1)(=O)=O)c1)c1C(NCC(c1ccccc1)N(C)C)=O	-7.6	N	3.0836	6	2	451.589
NCC-00027456	CN(Cc1cnccc1)C(Cc(cc1)ccc1NS(c1cc(C(F)(F)F)ccc1)(=O)=O)=O	-9.7	Y	2.9276	6	1	463.479
NCC-00007093	Cc1n[o]c(C)c1CCN(C)c(ccc(C(O)=O)c1)c1NS(c(cc(cc1)F)c1F)(=O)=O	-7.3	N	2.5961	8	2	465.476
NCC-00054561	Cc(cc1)cnc1NC(c(cc(cc1)S(Nc(c(OC)c2)cc(Cl)c2OC)(=O)=O)c1Cl)=O	-8.3	N	3.8726	8	2	496.37
NCC-00038449	CN(C)C(COc(cc1)ccc1NC(CN(C)S(c1cc(cccc2)c2cc1)(=O)=O)=O)=O	-8.5	N	2.1452	8	1	455.534
NCC-00020612	CC(C)(CNC(c1cc(S(Nc(cccc2)c2OC)(=O)=O)c(C)cc1)=O)N1CCOCC1	-7.7	N	2.0801	8	2	461.581
NCC-00000907	CCOc(cccc1)c1NS(c1c(C)ccc(/C=C\c([o]nc2C)c2NC(C)=O)c1)(=O)=O	-6.7	N	3.4118	8	2	455.534
NCC-00020193	Cc(cc1)ccc1NS(c(cc(cc1)C(NCC(c2ccc[o]2)N(C)C)=O)c1OC)(=O)=O	-7.7	N	1.8584	8	2	457.549
NCC-00029445	CCOC(c1c(C)nc(NC(c2cccc(S(N(C)c3ccc(C)cc3)(=O)=O)c2)=O)[s]1)=O	-8.6	Y	3.78	8	1	473.573
NCC-00084897	CCN(CC)S(c(cc1)ccc1S(Nc(cccc1)c1C(NC1CCCC1)=O)(=O)=O)(=O)=O	-6.3	N	2.6424	8	2	479.62
NCC-00032878	CN(Cc1cnccc1)C(c1cc(S(Nc(cccc2)c2F)(=O)=O)cc(OC)c1OC)=O	-7.6	N	2.042	8	1	459.497
NCC-00030578	Cc1cccc(NS(c(cc2)ccc2C(Nc(cc2)ccc2S(NC)(=O)=O)=O)(=O)=O)c1C	-8.4	Y	2.9194	8	3	473.573
NCC-00036108	CCN(c1ccccc1)S(c1cc(C(OCC(Nc([s]cc2)c2C#N)=O)=O)ccc1)(=O)=O	-7.8	N	2.7852	8	1	469.541
NCC-00050564	CCOc(cc1)ccc1NS(c(cc(cc1)C(NCCC(N2CCCC2)=O)=O)c1Cl)(=O)=O	-8.7	Y	2.9354	8	2	479.983

NCC-00036479	N#CC1(CCCCC1)NC(COC(c(cccc1)c1NS(c(cc1)ccc1Cl)(=O)=O)=O)=O	-8.1	N	2.6607	8	2	475.952
NCC-00007095	CCOC(N(CC1)CCN1c(ccc(C(O)=O)c1)c1NS(c(cc1)cc(F)c1F)(=O)=O)=O	-6.8	N	2.09	9	2	469.464
NCC-00009196	COc(ccc(CCNC(CC(C(NCC1)=O)N1S(c1ccccc1)(=O)=O)=O)c1)c1OC	-7.3	N	1.1574	9	2	461.537
NCC-00047710	CC(C(N(C1(C)C)c(cccc2)c2NC1=O)=O)OC(CCNS(c1ccccc1)(=O)=O)=O	-7.9	Y	1.595	9	2	459.522
NCC-00007060	CCOC(N(CC1)CCN1c(ccc(NS(c1c(C)ccc(C)c1)(=O)=O)c1)c1C(O)=O)=O	-6.9	N	2.5762	9	2	461.537
NCC-00029519	CC(C)(C)c1cc(S(Nc2cc(C(N(CC3)CCC3C(N)=O)=O)ccc2)(=O)=O)c(C)cc1	-7.5	N	3.318	7	2	457.593
NCC-00020489	CCOc(cc1)ccc1NS(c(cc1)ccc1C(NCC1(CCCCC1)N(C)C)=O)(=O)=O	-7	N	2.881	7	2	459.609
NCC-00037641	CCc(cccc1)c1NC(CNC(c(cccc1)c1S(N(C)c1ccccc1)(=O)=O)=O)=O	-6.6	N	2.8546	7	2	451.546
NCC-00071183	CC(CCCC1C)N1C(c(cccc1)c1NS(c1ccc(CCNC(C)=O)cc1)(=O)=O)=O	-7.8	N	3.2896	7	2	457.593
NCC-00031433	CC(C)CC(CNC(c1cccc(S(Nc2ccc(C)cc2)(=O)=O)c1)=O)N1CCOCC1	-9.4	Y	2.8966	7	2	459.609
NCC-00031427	CN(C)Cc1ccc(CNC(c(cc2)ccc2S(Nc(cccc2)c2OC)(=O)=O)=O)cc1	-8.9	Y	2.3685	7	2	453.561
NCC-00020443	CC(C)CC(N(CC1)CCN1C(c(cc1)ccc1NS(c1c(C)ccc(C)c1)(=O)=O)=O)=O	-8.8	N	3.614	7	1	457.593
NCC-00082431	CC(C)CN1CC(CNC(c(cc2)ccc2NS(c2c(C)ccc(C)c2)(=O)=O)=O)OCC1	-8.7	Y	2.7515	7	2	459.609
NCC-00056161	CCC(CCNC(c(cc1)ccc1NS(c1cc(C)c(C)cc1)(=O)=O)=O)N(CCC1)C1=O	-9.2	Y	3.278	7	2	457.593
NCC-00019763	CC(C1)OC(C)CN1C(C)(C)CNC(c(cc1)ccc1S(Nc(cccc1)c1F)(=O)=O)=O	-9	Y	2.5564	7	2	463.572
NCC-00011989	CC(C)CCNC(C(C)(CN(C1)S(c2ccccc2)(=O)=O)N(CCc2ccc[s]2)C1=O)=O	-6.6	N	2.7939	7	1	477.648
NCC-00035799	CC(C)(CNC(c(cc(cc1)S(Nc2cc(C)c(C)cc2)(=O)=O)c1Cl)=O)N1CCOCC1	-10.1	Y	3.1	7	2	480.027
NCC-00072188	CC(c(cccc1)c1Cl)NC(C(CCC(N)=O)NS(c1cc(cccc2)c2cc1)(=O)=O)=O	-8.1	N	2.9679	7	3	473.98

NCC-00069634	CC(C)[n]1nccc1N(CC(N(CCC#N)c1ccccc1)=O)S(c1ccccc1)(=O)=O	-5.7	N	2.1691	8	0	451.55
NCC-00012235	Cc(cccc1)c1S(Nc(cc(cc1)C(N(C)CC(NC)=O)=O)c1N1CCNCC1)(=O)=O	-7.1	N	0.6171	9	3	459.569
NCC-00037077	COc(ccc(CCC(OCC(N(CC1)CCN1S(c1ccccc1)(=O)=O)=O)=O)c1)c1O	-9.1	Y	1.907	9	1	462.521
NCC-00017399	CC(C(N1CCOCC1)=O)OC(c1c(C)ccc(S(Nc(cc2)ccc2OC)(=O)=O)c1)=O	-8.2	N	1.8241	9	1	462.521
NCC-00055513	COC(c1ccc(CNC(c(cc2)ccc2NS(c(cc2)cc(Cl)c2Cl)(=O)=O)=O)cc1)=O	-10.5	Y	3.9406	7	2	493.366
NCC-00018444	Cc(cc1)ccc1N(C)S(c1cc(C(NS(c(cc2)cc(C)c2F)(=O)=O)=O)ccc1)(=O)=O	-10.4	Y	3.2784	7	1	476.548
NCC-00029667	NC(COC(c(cc1)cc(S(N(Cc2ccccc2)c(cc2)ccc2Cl)(=O)=O)c1Cl)=O)=O	-6.5	N	3.1392	7	1	493.366
NCC-00014769	CN(c(c(OC)c1)cc(Cl)c1OC)S(c1cc(C(Nc2cc(F)ccc2)=O)ccc1)(=O)=O	-8.3	N	3.5782	7	1	478.927
NCC-00067035	COc(cc1)cc(NC(CN(c2cc(Cl)cc(Cl)c2)S(c2ccccc2)(=O)=O)=O)c1OC	-6.5	N	3.7283	7	1	495.382
NCC-00031866	CCOc(cc1)ccc1S(Nc1cc(C(NCc(cc2C)cc(C)c2O)=O)ccc1)(=O)=O	-8.6	Y	3.494	7	3	454.545
NCC-00029041	CCOC(C(CC1)CCN1C(c(cccc1)c1NS(c1c(C)cc(C)cc1C)(=O)=O)=O)=O	-7.2	N	3.6559	7	1	458.577
NCC-00015738	CC(C)c(cccc1C)c1NC(COC(CNS(c1cc(cccc2)c2cc1)(=O)=O)=O)=O	-9.1	Y	3.8606	7	2	454.545
NCC-00035138	Cc(ccc(C(N(C)Cc1cc(OC)ccc1)=O)c1)c1S(Nc(cccc1)c1OC)(=O)=O	-8.9	Y	3.286	7	1	454.545
NCC-00032884	Cc(cc1)cc(C)c1S(N(CCC(N(C)Cc1ccc[o]1)=O)c(cc1)ccc1OC)(=O)=O	-6.9	N	2.8931	7	0	456.561
NCC-00029569	CC(CC(C)C1)CN1C(CN(c(cc1)ccc1OC)S(c(cc1)ccc1C(C)=O)(=O)=O)=O	-6.4	N	2.6869	7	0	458.577
NCC-00002662	CCc1cc(C(OCC)=O)c(NC(c(cccc2)c2NS(c2ccc(C)cc2)(=O)=O)=O)[s]1	-7.3	N	4.5851	7	2	472.585
NCC-00044961	CC(CCCC1)C1NC(COC(c1cc(NS(c(cc2)ccc2F)(=O)=O)c(C)cc1)=O)=O	-8.2	N	3.2251	7	2	462.54
NCC-00028930	Cc(cc(c(OC)c1)NC(c2cc(S(N(C)c(cc3)ccc3OC)(=O)=O)ccc2)=O)c1Cl	-9	Y	3.8213	7	1	474.964

NCC-00002589	Cc(cc1)ccc1N(CC(Nc(cccc1)c1Cl)=O)S(c(cc1)cc(OC)c1OC)(=O)=O	-6.6	N	3.4662	7	1	474.964
NCC-00039313	CC(C)Oc(cc1)ccc1C(Nc(cc(cc1)S(Nc(cccc2)c2Cl)(=O)=O)c1OC)=O	-8.1	N	4.3378	7	2	474.964
NCC-00034944	CN(c(cc1)ccc1F)S(c(cc1)cc(C(OCC(NCc2ccc[o]2)=O)=O)c1Cl)(=O)=O	-9.6	Y	2.1742	8	1	480.899
NCC-00002504	CCOc(cc1)ccc1NS(c1c(C)ccc(C(Nc(cccc2)c2C(O)=O)=O)c1)(=O)=O	-7.7	N	3.2715	8	3	454.502
NCC-00074154	CC(C(N(CC1)CCN1S(c1ccccc1)(=O)=O)=O)OC(COc1c(C)cccc1C)=O	-6.8	N	2.4922	8	0	460.549
NCC-00046306	CC(C(N(CC1)CCN1S(c1ccccc1)(=O)=O)=O)OC(Cc(cc1)cc(F)c1OC)=O	-8	N	2.2584	8	0	464.512
NCC-00026753	CN(Cc(cccc1)c1OC)C(Cc(cc1)ccc1NS(c(ccc(Cl)c1)c1F)(=O)=O)=O	-8.9	Y	3.717	6	1	476.955
NCC-00004536	CCOc(cc1)ccc1N(CC(N(C)Cc1ccccc1)=O)S(c1ccc(C)cc1)(=O)=O	-6.1	N	3.3124	6	0	452.573
NCC-00015007	CCCCN(c1ccccc1)S(c1cc(C(Nc2cc(C(C)=O)ccc2)=O)ccc1)(=O)=O	-7.4	N	4.1977	6	1	450.557
NCC-00034969	CC(C(NCc1ccccc1)=O)N(c(cc1)ccc1C(C)=O)S(c1ccc(C)cc1)(=O)=O	-6.5	N	2.9401	6	1	450.557
NCC-00029549	CCOc(cc1)ccc1N(C)S(c1cc(C(NCc(cc2)ccc2F)=O)c(C)cc1)(=O)=O	-9.5	Y	3.5018	6	1	456.537
NCC-00032538	CCN(c1ccccc1)S(c1cc(C(N(C)CCOc(cc2)ccc2F)=O)ccc1)(=O)=O	-7.8	N	3.5013	6	0	456.537
NCC-00038732	CN(Cc(cc1)cc(F)c1OC)C(CN(Cc1ccccc1)S(c1ccccc1)(=O)=O)=O	-6.9	N	3.0954	6	0	456.537
NCC-00018668	CC(C1CC1)N(CC(F)(F)F)C(c(cc1)ccc1S(N(C)c(cccc1)c1OC)(=O)=O)=O	-6.1	N	3.4735	6	0	470.51
NCC-00036417	CC(C1CC1)N(CC(F)(F)F)C(CN(c(cc1)ccc1OC)S(c1ccccc1)(=O)=O)=O	-6	N	3.1184	6	0	470.51
NCC-00016354	CCN(c1ccccc1)S(c(cc1)cc(NC(CSc2ncc[n]2C(C)C)=O)c1Cl)(=O)=O	-5.8	N	3.515	7	1	493.051
NCC-00028450	CC(C)(C)c1cc(S(Nc(cc2)ccc2C(N(C)Cc2c[n](C)nc2)=O)(=O)=O)c(C)cc1	-8.9	Y	3.0702	7	1	454.593
NCC-00007557	CCCNC(c(cc(cc1)NS(c2ccc(CC(C)C)cc2)(=O)=O)c1N1CCNCC1)=O	-7.5	N	3.2159	7	3	458.625

NCC-00007602	CCC(C)NC(c(cc(cc1)NS(c2c(C)cc(C)cc2C)(=O)=O)c1N1CCNCC1)=O	-7.4	N	3.1747	7	3	458.625
NCC-00034895	CCN(c1ccccc1)S(c(cc1)cc(NC(CN(C)C2CCN(C)CC2)=O)c1Cl)(=O)=O	-8.4	N	2.3745	7	1	479.043
NCC-00013187	CCN(c1ccccc1)S(c(cc1)ccc1NC(c(nc(nc1)S(C)(=O)=O)c1Cl)=O)(=O)=O	-6.7	N	1.7586	9	1	494.979
NCC-00014345	CCOc(cc1)ccc1NC(C(NCCN(CC1)CCN1S(c1ccccc1)(=O)=O)=O)=O	-8.5	N	1.0242	9	2	460.553
NCC-00017032	CC(C)[n]1nccc1N(CC(Nc(cccc1)c1C(OC)=O)=O)S(c1ccccc1)(=O)=O	-5.7	N	1.7264	9	1	456.522
NCC-00020190	Cc1cc(NC(CN(C)C(c2c(C)ccc(S(Nc(cccc3)c3F)(=O)=O)c2)=O)=O)n[o]1	-8.4	N	2.0607	9	2	460.485
NCC-00050947	CC(C(Nc(ccc(NS(c(cc1)cc(Cl)c1OC)(=O)=O)c1)c1Cl)=O)[n]1nc(C)cc1C	-9.9	Y	3.0883	8	2	497.402
NCC-00017495	Cc(cccc1)c1NS(c(cc1)ccc1C(Nc(cccc1)c1NC(N(C)C)=O)=O)(=O)=O	-8.7	Y	3.1493	8	3	452.534
NCC-00028935	Cc([n](C)nc1C)c1NC(CN(c(cc1)ccc1OC)S(c1c(C)ccc(C)c1)(=O)=O)=O	-6.3	N	2.1322	8	1	456.565
NCC-00069233	O=C(CN(c(cc1)cc(C(F)(F)F)c1Cl)S(c1ccccc1)(=O)=O)Nc1cnccc1	-6.8	N	3.1097	6	1	469.87
NCC-00088991	CC(C)(C)c(cc1C)cc(C)c1S(NC(CC1)CCN1C(Nc1ccccc1)=O)(=O)=O	-6.8	N	5.0502	6	2	443.61
NCC-00063669	Cc(cc1)ccc1N(CCC(Nc(cc1)cc(Cl)c1C#N)=O)S(c1ccccc1)(=O)=O	-7.3	N	3.8962	6	1	453.949
NCC-00068168	CN(C)C(CNC(CN(C)S(c1cc(cccc2)c2cc1)(=O)=O)=O)c1cc(F)ccc1	-7.7	N	2.2554	6	1	443.541
NCC-00030112	Cc1cc(N(CCC(NCc2cnccc2)=O)S(c(cc2)ccc2Cl)(=O)=O)cc(C)c1	-7.4	N	3.113	6	1	457.981
NCC-00069472	Cc(cc(cc1)Cl)c1N(CC(Nc1ccc(CC#N)cc1)=O)S(c1ccccc1)(=O)=O	-7.8	N	3.6113	6	1	453.949
NCC-00038415	CN(C)c(c(F)cc(NC(c1cccc(S(Nc(cccc2)c2F)(=O)=O)c1)=O)c1)c1F	-6.7	N	3.305	6	2	449.452
NCC-00019787	Cc1n[o]c(C)c1CC(Nc(cc1)cc(NS(c(cc2)cc(Cl)c2Cl)(=O)=O)c1OC)=O	-7.9	N	3.4524	8	2	484.359
NCC-00027947	Cc1cccc(NS(c2c(C)ccc(NC(Cc([s]3)ccc3S(N)(=O)=O)=O)c2)(=O)=O)c1	-9.8	Y	2.6274	8	3	479.601

NCC-00034535	CCN(CC)S(c(cc1)cc(NS(c(cccc2)c2Cl)(=O)=O)c1N1CCOCC1)(=O)=O	-6.7	N	2.2649	8	1	488.027
NCC-00083384	CC(C(Nc(ncc(Cl)c1)c1Cl)=O)OC(C(CC1)CCN1S(c1ccccc1)(=O)=O)=O	-9.1	Y	3.0015	8	1	486.375
NCC-00031562	CCOc(cc1)ccc1N(C)S(c1cc(C(OCc(nn[s]2)c2Cl)=O)c(C)cc1)(=O)=O	-8.4	N	3.6707	8	0	481.98
NCC-00036725	O=C(COC(c(cc1)ccc1S(Nc1ccccc1)(=O)=O)=O)Nc(ncc(Cl)c1)c1Cl	-9.4	Y	3.2266	8	2	480.327
NCC-00007627	CCc(ccc(-c1n[o]c(C(F)(F)F)c1)c1)c1S(Nc(cc1)ccc1S(N)(=O)=O)(=O)=O	-8.8	N	2.545	8	2	475.467
NCC-00086209	COC(c(c(F)c1)cc(NS(c(cc2)ccc2N(C2=O)N=CC(Cl)=C2Cl)(=O)=O)c1F)=O	-8.2	Y	2.8767	8	1	490.269
NCC-00009694	OCC(c1ccccc1)NC(CNC(C(CCC1)CN1S(c1ccccc1)(=O)=O)=O)=O	-8.2	Y	0.6749	8	3	445.538
NCC-00004896	COc(cccc1)c1NC(CCNC(C(CC1)CCN1S(c1ccccc1)(=O)=O)=O)=O	-7.6	Y	1.9899	8	2	445.538
NCC-00019040	Cc(ccc(C(OC)=O)c1)c1S(Nc1cc(NC(Nc2ccccc2)=O)ccc1)(=O)=O	-8	Y	3.357	8	3	439.491
NCC-00012841	CCOc(cc1)ccc1N(C(N(CC(NCCC(C)C)=O)c1c2cccc1)=O)S2(=O)=O	-6.4	N	3.0756	8	1	445.538
NCC-00057954	CC(C)(C)OC(N(CC1)CCN1C(c1cccc(NS(c2ccccc2)(=O)=O)c1)=O)=O	-7.5	N	3.1485	8	1	445.538
NCC-00073388	CCOc(cccc1)c1N(CC(N(CC1)CCC1C(N)=O)=O)S(c1ccccc1)(=O)=O	-6.2	N	1.2786	8	1	445.538
NCC-00005944	Cc(cc(cc1)S(Nc(cc2)ccc2Cl)(=O)=O)c1OCC(NCCN1CCOCC1)=O	-9.5	Y	1.5911	8	2	467.972
NCC-00030642	CC(c1c(C)nc(NC(c(cc2)ccc2S(N(C)c(cccc2)c2OC)(=O)=O)=O)[s]1)=O	-6.9	N	2.918	8	1	459.546
NCC-00087400	CC(c(cc(cc1)OC)c1OC)NC(CN(c1ncc[s]1)S(c1ccccc1)(=O)=O)=O	-6.7	N	2.1377	8	1	461.562
NCC-00028998	Cc1cc(S(Nc(cc2)ccc2C(Nc(cc2)ccc2S(N)(=O)=O)=O)(=O)=O)c(C)cc1	-7.7	N	2.558	8	3	459.546
NCC-00019755	Cc1cccc(NS(c(cc2)ccc2C(N(CC2)CCC2NS(C)(=O)=O)=O)(=O)=O)c1C	-10.2	Y	2.5231	8	2	465.593
NCC-00029983	CN(c(cccc1)c1OC)S(c(cc1)cc(C(N(CC2)CCC2C(N)=O)=O)c1Cl)(=O)=O	-6.8	N	1.8334	8	1	465.957

NCC-00019258	NC(NC(COC(Cc(cc1)ccc1NS(c1cc(cccc2)c2cc1)(=O)=O)=O)=O)=O	-9.4	Y	1.5821	9	3	441.463
NCC-00068307	CC(NCCC(OCC(N(CC1)CCN1S(c1cc(cccc2)c2cc1)(=O)=O)=O)=O)=O	-7.5	N	1.1589	9	1	447.511
NCC-00017461	CCOc(ccc(NC(C)=O)c1)c1S(N(C1)c(cccc2)c2OC1C(N(C)C)=O)(=O)=O	-6.3	N	1.3378	9	1	447.511
NCC-00005985	CCOC(N(CC1)CCN1C(c(cccc1)c1NS(c(cc1)ccc1OC)(=O)=O)=O)=O	-7	N	2.3386	9	1	447.511
NCC-00031435	CC(C1)C1C(NCC(Nc(cc1)cc(S(Nc(cc2)ccc2OC)(=O)=O)c1OC)=O)=O	-7.8	N	1.1935	9	3	447.511
NCC-00014740	Cc1cc(NC(COC(c(cc(cc2)S(N(C)c3ccccc3)(=O)=O)c2Cl)=O)=O)n[o]1	-8.3	N	2.3349	9	1	463.897
NCC-00014576	Cc(ccc(S(Nc1cc(C(N2CCOCC2)=O)ccc1)(=O)=O)c1C)c1NS(C)(=O)=O	-6.8	Y	1.3695	9	2	467.565
NCC-00035112	CCNc(ccc(S(N(CC)CC)(=O)=O)c1)c1NS(c(cc1)cc2c1OCCO2)(=O)=O	-7.1	N	2.022	9	2	469.581
NCC-00015346	COc(cc(cc1C(Nc(cc2)cnc2O)=O)S(Nc(cccc2)c2F)(=O)=O)c1OC	-7.4	N	2.0718	9	3	447.442
NCC-00019029	Cc1n[o]c(C)c1CSCC(Nc1cc(S(Nc(cc2)ccc2Cl)(=O)=O)c(C)cc1)=O	-7.7	N	3.4518	7	2	480.008
NCC-00019926	CC(C)(C)c1cc(S(Nc(cc2)ccc2C(NCC(NC2CC2)=O)=O)(=O)=O)c(C)cc1	-9	Y	2.9367	7	3	443.566
NCC-00038611	Cc(c(C)c1C)c(C)c(C)c1S(Nc(cc1)ccc1NC(CN1CCOCC1)=O)(=O)=O	-8.7	Y	2.6444	7	2	445.582
NCC-00009423	CN(c(cc1)ccc1C(Nc1ccc(CC#N)cc1)=O)S(c(cc1)ccc1OC)(=O)=O	-8.7	N	2.9465	7	1	435.503
NCC-00034827	CC(C)CCN(CC(Nc(cc1)ccc1N1CCOCC1)=O)S(c1ccccc1)(=O)=O	-6.8	N	2.873	7	1	445.582
NCC-00029006	Cc(cc1)ccc1S(N(C)c(cc1)ccc1OCC(NCCc1ncccc1)=O)(=O)=O	-8.2	N	2.1228	7	1	439.535
NCC-00067802	CCc(cccc1)c1N(CC(Nc(cccc1)c1C(N)=O)=O)S(c1ccccc1)(=O)=O	-7.3	N	2.5031	7	2	437.519
NCC-00007063	CCCN(CC1)CCN1c(ccc(NS(c1c(C)cc(C)cc1C)(=O)=O)c1)c1C(O)=O	-7.6	N	2.1881	7	2	445.582
NCC-00044974	CCCNC(CN(CCC)C(C(CC1)CCN1S(c1cc(CCC2)c2cc1)(=O)=O)=O)=O	-7.5	N	2.6995	7	1	449.614

NCC-00012317	CS(c(cc1)nnc1-c1cccc(NS(c(cc2)cc(C(F)(F)F)c2F)(=O)=O)c1)(=O)=O	-7.8	N	1.9276	7	1	475.442
NCC-00031423	CCCN(CCC)C(c1cc(O)nc(cc2)c1cc2S(Nc(cc1)ccc1F)(=O)=O)=O	-6.3	N	3.8079	7	2	445.514
NCC-00036304	CN(c(cc1)ccc1OCC(Nc1cc(C#N)ccc1)=O)S(c(cccc1)c1F)(=O)=O	-9.5	Y	2.5227	7	1	439.466
NCC-00030021	CN(CCc1ncccc1)C(c(cc1)cc(S(Nc(cc2)ccc2OC)(=O)=O)c1Cl)=O	-9.2	Y	3.1013	7	1	459.953
NCC-00020614	CSc1nnc[n]1-c1cccc(NS(c(cc2)ccc2C(NCC(F)(F)F)=O)(=O)=O)c1	-8.8	N	2.2397	8	2	471.483
NCC-00080812	CCOC(c1c(C)nc(NC(Nc2c(C)nc(NS(c3ccccc3)(=O)=O)[s]2)=O)[s]1)=O	-8.6	Y	3.7376	10	3	481.577
NCC-00010206	CC(C)C1OC(c2cccc(NS(c(cc(cc3)OC)c3OC)(=O)=O)c2)OCC1(C)C	-6.8	N	3.1146	7	1	449.566
NCC-00012265	Cc1c(-c(cc2)cc(S(Nc(cc3OC)cc(OC)c3OC)(=O)=O)c2OC)[o]nc1C	-7.5	N	2.581	9	1	448.495
NCC-00009739	CC(C)(CS(N1c(cc2)cc(C)c2S(Nc2cc(C(OC)=O)ccc2)(=O)=O)(=O)=O)C1=O	-8.5	N	1.0732	9	1	466.534
NCC-00035643	CCOC(c1c(C)cc(NC(c2cccc(S(Nc(cccc3)c3F)(=O)=O)c2)=O)[s]1)=O	-7.8	N	3.9264	7	2	462.521
NCC-00027568	OC(CC1(CC(Nc(cc2)cc(S(Nc(cccc3)c3Cl)(=O)=O)c2Cl)=O)CCCC1)=O	-7.9	N	3.8405	7	3	485.387
NCC-00033490	CN(c1ccccc1)S(c1cc(NC(Cc(ccc(OC)c2)c2OC)=O)ccc1)(=O)=O	-8.7	Y	2.8695	7	1	440.519
NCC-00033455	Cc(cc1)ccc1S(N(C)c(cc1)ccc1C(OC(C(N)=O)c1ccccc1)=O)(=O)=O	-8.5	N	2.1515	7	1	438.503
NCC-00047771	CN(CC(NC(CC(OC)=O)c1ccccc1)=O)S(c1cc(cccc2)c2cc1)(=O)=O	-8.1	Y	2.4671	7	1	440.519
NCC-00036186	CN(c(cc1)ccc1OC)S(c1cc(C(OCc(cc2)ccc2C#N)=O)ccc1)(=O)=O	-8.7	N	2.9606	7	0	436.487
NCC-00088597	CN(Cc(ccc(OC)c1)c1OC)C(c(cc1)ccc1NS(c1ccccc1)(=O)=O)=O	-9.8	Y	2.9421	7	1	440.519
NCC-00007065	CC(c(cc1)ccc1S(Nc(cc(cc1)C(O)=O)c1N(C)Cc1ccccc1)(=O)=O)=O	-5.9	N	2.6295	7	2	438.503
NCC-00017087	Cc(cc1)ccc1S(N(C)c(cc1)ccc1C(OCC(N1CCCCCC1)=O)=O)(=O)=O	-8.7	Y	2.946	7	0	444.55

NCC-00038160	CC(C)(C)NC(COC(c(cc(cc1)S(N(CCC2)c3c2cccc3)(=O)=O)c1Cl)=O)=O	-7.2	N	3.3671	7	1	464.969
NCC-00056623	CC(C)(C)c(cc1C)cc(C)c1S(Nc(cccc1)c1S(N1CCOCC1)(=O)=O)(=O)=O	-6.4	N	3.2712	7	1	466.621
NCC-00038654	CCOC(C(CCC1)CN1C(c1cccc(S(N(C)c2cccc(Cl)c2)(=O)=O)c1)=O)=O	-8	N	3.1354	7	0	464.969
NCC-00004634	COC(c(cccc1)c1NC(CN(c1ccccc1)S(c(cc1)ccc1Cl)(=O)=O)=O)=O	-7.1	N	3.1753	7	1	458.921
NCC-00036498	O=C(COC(c(cc1)ccc1NS(c(cc1)cc(F)c1F)(=O)=O)=O)NCC1OCCC1	-9.9	Y	1.4568	8	2	454.449
NCC-00067039	COC(c1cc(NS(c(cc2)cc(Nc3ccc[s]3)c2Cl)(=O)=O)cc(C(OC)=O)c1)=O	-7.9	N	3.8951	8	2	480.948
NCC-00018604	COc(cc1)ccc1NS(c(cc1)ccc1C(OC(C(N)=O)c1ccccc1)=O)(=O)=O	-9.2	Y	1.8324	8	2	440.475
NCC-00007696	CC(N(CCOc1c2)c1cc(C)c2S(N(CC(OC)=O)c1cc(C)cc(C)c1)(=O)=O)=O	-6.5	N	2.297	8	0	446.522
NCC-00030604	COc(cc1)ccc1NS(c(cc1)cc(OC)c1NC(OCc1ccccc1)=O)(=O)=O	-8.6	Y	3.1437	8	2	442.491
NCC-00035320	COc(cccc1)c1NS(c(cc1)ccc1C(OCC(N1CCCCCC1)=O)=O)(=O)=O	-8.4	Y	2.6269	8	1	446.522
NCC-00084882	CCOc(ccc(S(N1CCOCC1)(=O)=O)c1)c1NS(c1ccc(C(C)C)cc1)(=O)=O	-7.4	N	2.5248	8	1	468.593
NCC-00034421	COc(cc(cc1C(NCCc2ccc[o]2)=O)S(Nc(cccc2)c2F)(=O)=O)c1OC	-7.2	N	2.3952	8	2	448.47
NCC-00007028	CCOC(C(CC1)CCN1c(ccc(NS(c(cccc1)c1Cl)(=O)=O)c1)c1C(O)=O)=O	-8.1	N	2.71	8	2	466.941
NCC-00035979	Cc(cccc1)c1N(CC(Nc(cc1)ccc1OC(F)F)=O)S(c1ccccc1)(=O)=O	-6.8	N	3.1696	6	1	446.473
NCC-00085573	CC(C)c(cccc1)c1NC(c(cc1)ccc1NS(c(cc1)ccc1C(C)=O)(=O)=O)=O	-9.7	Y	4.1644	6	2	436.531
NCC-00030962	CCN(C(c1c(C)ccc(S(N(C)c(cccc2)c2OC)(=O)=O)c1)=O)c1ccccc1	-6.1	N	3.941	6	0	438.546
NCC-00069271	CCc(cccc1)c1NC(CN(c(cccc1)c1OCC)S(c1ccccc1)(=O)=O)=O	-6.1	N	3.7521	6	1	438.546
NCC-00006126	CCN(c1ccccc1)S(c(cc1)ccc1NC(COc1c(C)ccc(C)c1)=O)(=O)=O	-7.5	Y	3.6804	6	1	438.546

NCC-00029968	CN(Cc1cc(F)ccc1)C(c(cc1)ccc1S(N(C)c(cccc1)c1OC)(=O)=O)=O	-6.6	N	3.0181	6	0	442.51
NCC-00035957	O=C(c1cccc(S(Nc(cccc2)c2F)(=O)=O)c1)NCc(cccc1)c1OC(F)F	-9.5	Y	3.0858	6	2	450.436
NCC-00056293	CN(CC(Nc(cccc1)c1OCC(F)(F)F)=O)S(c1cc(cccc2)c2cc1)(=O)=O	-8.4	Y	3.6856	6	1	452.452
NCC-00035479	CCc1nnc(NC(CCN(c2cc(C)cc(C)c2)S(c(cc2)ccc2Cl)(=O)=O)=O)[s]1	-7.5	N	4.007	7	1	479.024
NCC-00038229	CN(CC1)CCN1c(cc1)ccc1NS(c(cc1)ccc1C(NCC(F)(F)F)=O)(=O)=O	-8.3	N	2.0665	7	2	456.488
NCC-00015923	Cc([n](C)nc1C)c1NC(c(cc1)ccc1S(Nc1cc(C(F)(F)F)ccc1)(=O)=O)=O	-9.9	Y	2.8126	7	2	452.456
NCC-00006011	O=S(c(cc1)ccc1OC(F)(F)F)(Nc(cc1)ccc1S(Nc1ncccn1)(=O)=O)=O	-8	N	2.1631	9	2	474.439
NCC-00056909	CC(C(N(CC1)CCN1S(c1ccccc1)(=O)=O)=O)Sc1nc(O)nc(C)c1C(C)=O	-7.4	N	1.7586	9	1	464.566
NCC-00034941	CC(NCC(Nc(cc(cc1)S(Nc(cccc2)c2Cl)(=O)=O)c1N1CCOCC1)=O)=O	-8.3	N	1.0211	9	3	466.945
NCC-00027158	CC(Nc(ccc(S(Nc1cc(S(NC2=NCCC2)(=O)=O)ccc1)(=O)=O)c1)c1OC)=O	-8.4	N	0.8163	10	3	466.538
NCC-00037299	CCN(c1ccccc1)S(c(cc(cc1)NC(CSc2nc(O)ccn2)=O)c1Cl)(=O)=O	-7.2	N	2.9211	8	2	478.98
NCC-00042398	COc(cccc1)c1N(CCC#N)C(CN(CC1)CCN1S(c1ccccc1)(=O)=O)=O	-6.2	N	1.8899	8	0	442.538
NCC-00007075	CCC[n]1nc(C)cc1CN(C)c(ccc(NS(c1ccccc1)(=O)=O)c1)c1C(O)=O	-8.5	Y	1.9829	8	2	442.538
NCC-00047123	Cc1nc(SC)nc(O)c1CCC(Nc(cccc1)c1NS(c1ccccc1)(=O)=O)=O	-7	N	3.1184	8	3	458.562
NCC-00038353	CCN(CC)CCNC(c(cc1)ccc1NS(c(cc(C(O)=O)c(Cl)c1)c1Cl)(=O)=O)=O	-8	N	1.4932	8	3	488.391
NCC-00064713	CC(C)(C)OC(CN(CCN(C)C)C(C(CCC1)CN1S(c1ccccc1)(=O)=O)=O)=O	-5.4	N	1.4835	8	0	453.602
NCC-00034971	CC(C)(C)C(COC(c1cc(S(Nc(cccc2)c2F)(=O)=O)cc(OC)c1OC)=O)=O	-6.9	N	2.8787	8	1	453.486
NCC-00019447	CC(C(OC)=O)NC(c(cc(cc1)S(Nc(c(OC)c2)cc(Cl)c2OC)(=O)=O)c1Cl)=O	-7.7	N	2.3867	9	2	491.347

NCC-00034850	CC(C)N(C(C)C)C(COC(c(cccc1)c1NS(c(cc(cc1)Cl)c1Cl)(=O)=O)=O)=O	-7.5	N	3.9651	7	1	487.403
NCC-00035906	CCN(c1ccccc1)S(c(cc1)cc(C(OCC(NC(C)C)C=O)=O)=O)c1Cl)(=O)=O	-9	Y	2.6023	8	1	466.941
NCC-00030438	CN(c(cccc1)c1OC)S(c(cc1)ccc1C(OCC(NCC(F)(F)F)=O)=O)(=O)=O	-8	N	1.6812	8	1	460.428
NCC-00018948	CC(C)CC(C(N(C)C)=O)NC(c(cc1)ccc1S(Nc1ccc(C)cc1)(=O)=O)=O	-9.2	Y	2.578	7	2	431.555
NCC-00036645	CCN(CC)C(CN(C)C(c1cccc(NS(c2c(C)ccc(C)c2)(=O)=O)c1)=O)=O	-7.7	N	2.5146	7	1	431.555
NCC-00013712	CCN(c1ccc(C(C(F)(F)F)(C(OCC)=O)O)cc1)S(c1ccc(C)cc1)(=O)=O	-6.9	N	2.9322	6	1	445.457
NCC-00036524	CCOc(cc1)ccc1NS(c1cc(C(OCC(C(C)(C)C)=O)=O)c(C)cc1)(=O)=O	-7.4	N	3.5981	7	1	433.523
NCC-00077964	CC(C)C(C(OC(C)C(N(C)C(CC1)CS1(=O)=O)=O)=O)NS(c1ccccc1)(=O)=O	-6.4	N	0.4481	9	1	460.57
NCC-00030430	Cc(ccc(F)c1)c1S(Nc1cc(C(OCC(NCC(F)(F)F)=O)=O)ccc1)(=O)=O	-9.3	Y	2.2907	7	2	448.392
NCC-00036679	CC(C)CC(C(OC)=O)NC(c(cc1)cc(S(N(C)c2ccccc2)(=O)=O)c1Cl)=O	-6.5	N	2.953	7	1	452.958
NCC-00016396	CCC(C)(C)NC(c1cccc(S(N(C)c(c(OC)c2)cc(Cl)c2OC)(=O)=O)c1)=O	-6.2	N	3.3693	7	1	454.973
NCC-00018710	CCN(Cc1cccc(NS(c2cc(C(O)=O)c(C)cc2)(=O)=O)c1)C(C(F)(F)F)=O	-8.2	N	2.3579	7	2	444.429
NCC-00014612	COC(C(C(F)(F)F)(Nc1ccc(C(F)(F)F)cc1)NS(c1ccccc1)(=O)=O)=O	-5.7	N	3.5714	6	2	456.362
NCC-00035804	CC(C(NCC(F)(F)F)=O)N(c(cccc1)c1OC)S(c(cc1)cc(Cl)c1Cl)(=O)=O	-6	N	3.3395	6	1	485.309
NCC-00035832	Cc(cc1C)cc(C)c1S(N(CC(NCC(F)(F)F)=O)c(cc1)ccc1OC)(=O)=O	-5.7	N	2.7999	6	1	444.473
NCC-00009690	CCOc(ccc(N(C(CC1)=O)S1(=O)=O)c1)c1S(Nc(cccc1)c1C(N)=O)(=O)=O	-8.2	N	-0.3609	10	2	453.495
NCC-00027087	Cc1nc(-c2cccc(NS(c(cc3)ccc3C(NCC(F)(F)F)=O)(=O)=O)c2)c[s]1	-8.8	N	3.2123	6	2	455.48
NCC-00034441	CN(CCNC(c(cc1)ccc1S(N(C)c1ccccc1)(=O)=O)=O)c1ccccc1	-8.5	Y	2.6941	6	1	423.536

NCC-00036704	CC(C)(CNC(c(cc1)ccc1S(Nc1c(C)cccc1)(=O)=O)=O)N1CCCCC1	-9.2	Y	3.3141	6	2	429.583
NCC-00009381	Cc(cc1)ccc1S(N(CC(NCc1ncccc1)=O)c1cc(C)c(C)cc1)(=O)=O	-7.2	N	2.4505	6	1	423.536
NCC-00000796	CC(C)NC(c(cc1)cnc1Sc(cc1)ccc1NS(c1c(C)cccc1)(=O)=O)=O	-9.1	Y	3.4246	6	2	441.575
NCC-00029859	CN(C1CCN(C)CC1)C(c(cc1)cc(S(Nc(cc(cc2)Cl)c2Cl)(=O)=O)c1Cl)=O	-7.7	N	3.9831	6	1	490.838
NCC-00015172	COc(ccc(S(Nc(cccc1)c1Cl)(=O)=O)c1)c1NS(N1CCCCCC1)(=O)=O	-7.4	N	2.7313	8	2	474.001
NCC-00033697	CCOc(cc1)ccc1NS(c(cc1)cc(c(C(NC(C)C)=O)c2)c1nc2O)(=O)=O	-7.3	N	2.8211	8	3	429.496
NCC-00036039	CCN(CC)CCNC(c(cc1)ccc1NS(c(cc1)cc2c1OCCO2)(=O)=O)=O	-9.6	Y	1.8887	8	2	433.527
NCC-00036145	CCOc(cc1)ccc1NS(c(cc1)cc(OC)c1NC(c1cnccc1)=O)(=O)=O	-8.5	Y	2.3716	8	2	427.48
NCC-00016758	CC(Nc(ccc(S(Nc(cccc1)c1C(N1CCCCC1)=O)(=O)=O)c1)c1OC)=O	-6.3	N	2.4307	8	2	431.512
NCC-00003843	CCCCC(N(c(cc1)ccc1OC)S(c(cc1)cc(N2C)c1N(C)C2=O)(=O)=O)=O	-6.8	N	2.8221	8	0	431.512
NCC-00007664	COc1c(CN(CCS(N2CCNCC2)(=O)=O)S(c2ccccc2)(=O)=O)cccc1	-6.5	N	1.4609	8	1	453.582
NCC-00034787	CCOC(c1c(C)c(C(CN(c2ncc[s]2)S(c2ccccc2)(=O)=O)=O)c(C)[nH]1)=O	-7.2	N	2.2867	8	1	447.535
NCC-00012373	CCS(c(cc1)nnc1-c1cccc(NS(c(cc(C)cc2)c2OC)(=O)=O)c1)(=O)=O	-7.9	Y	1.7494	8	1	447.535
NCC-00032452	CCOC(c(cc1)cc(Br)c1S(Nc(cc1)c(C)cc1Oc1nccnc1)(=O)=O)=O	-8.9	Y	3.0923	8	1	492.349
NCC-00011445	Cc(nn1)cc(Cc(cc2)ccc2S(Nc(c(OC)cc(OC)c2)c2Cl)(=O)=O)c1O	-8.3	Y	2.8144	8	2	449.914
NCC-00033607	COc(c(NS(c(cc1)cc(C(NC2=NCCS2)=O)c1Cl)(=O)=O)c1)cc(OC)c1Cl	-7.1	N	2.6739	8	2	490.387
NCC-00038135	COCC(Nc(cc1)cc(S(Nc(cc2)ccc2OC)(=O)=O)c1N1CCOCC1)=O	-7.1	N	0.7626	9	2	435.5
NCC-00030199	OC(c1cccc(S(Nc2cccc(S(NC3=NCCCCC3)(=O)=O)c2)(=O)=O)c1)=O	-8.3	N	1.2927	9	3	451.523

NCC-00016889	CC(Nc(cc1)cc(S(Nc(cc2)cc(Cl)c2Sc2ncccc2)(=O)=O)c1OC)=O	-7.8	Y	3.116	7	2	463.965
NCC-00079165	O=C(CN(c(ccc(Cl)c1)c1Cl)S(c1ccccc1)(=O)=O)NCCN1CCOCC1	-6.4	N	1.8284	7	1	472.392
NCC-00029604	O=C(c(cc(cc1)S(Nc2cc(C(F)(F)F)ccc2)(=O)=O)c1Cl)NN1CCOCC1	-8.8	N	1.6609	7	2	463.863
NCC-00007132	CCC(N(CCC1)c2c1ccc(NS(c(cc1)ccc1NC(C(C)C)=O)(=O)=O)c2)=O	-8.4	N	3.222	7	2	429.539
NCC-00036925	CC(CNC(c(cc1)ccc1S(Nc(cc1)ccc1OC)(=O)=O)=O)CN1CCCC1	-8.7	Y	2.491	7	2	431.555
NCC-00013872	CCOc(cc1)ccc1S(N(CC(NCc1cnccc1)=O)c1ccccc1)(=O)=O	-5.9	N	1.7011	7	1	425.508
NCC-00057887	CC(C(Nc1cc(NS(c2ccccc2)(=O)=O)c(C)cc1)=O)NC(C1CCCC1)=O	-7.6	N	2.4514	7	3	429.539
NCC-00035095	Cc(ccc(S(Nc(cc1)ccc1OC)(=O)=O)c1)c1NC(c(cc1)ccc1C#N)=O	-8.9	N	3.2157	7	2	421.476
NCC-00034794	Cc(ccc(S(N(C)c(cccc1)c1OC)(=O)=O)c1)c1C(NCc1nccc1)=O	-7.4	N	1.9938	7	1	425.508
NCC-00046571	CNC(C(c1ccccc1)NC(c1cccc(NS(c2ccccc2)(=O)=O)c1)=O)=O	-9.3	Y	1.7797	7	3	423.492
NCC-00029788	Cc(cc1)ccc1NS(c(cc(cc1)C(N(C)Cc2cnccc2)=O)c1OC)(=O)=O	-7.9	N	2.3551	7	1	425.508
NCC-00020253	CNC(C1(CCCCC1)NC(c(cc1)ccc1NS(c(cc1)ccc1F)(=O)=O)=O)=O	-9.1	N	2.0294	7	3	433.503
NCC-00027578	CCC(Nc1nc(-c2cccc(N(C(CC)=O)S(c3ccccc3)(=O)=O)c2)c[s]1)=O	-6.8	N	3.9086	7	1	443.547
NCC-00013672	Cc1cc(C)n[n]1S(c1c(C)c(N(C)S(c2ccc(C)cc2)(=O)=O)c(C)cc1)(=O)=O	-6.6	N	2.292	7	0	447.579
NCC-00006016	Cc(cc(cc1)S(Nc(cc2)ccc2F)(=O)=O)c1OCC(NCc1ncccc1)=O	-10	Y	1.8883	7	2	429.471
NCC-00004848	Cc(cc1)ccc1S(N(CC(N1CCN(C)CC1)=O)c(cc(cc1)Cl)c1OC)(=O)=O	-6.1	N	2.1724	7	0	451.973
NCC-00035007	COc(cc1)ccc1N(CCC(Nc1cnccc1)=O)S(c1cccc(Cl)c1)(=O)=O	-6.8	N	2.6458	7	1	445.926
NCC-00016753	Cc1ccc(C(Nc(cc2)cc(S(Nc(cc(C)cc3)c3Br)(=O)=O)c2OC)=O)[n]1C	-7.2	N	3.4125	7	2	492.393

NCC-00001957	CCNc1cc(C)nc(Nc(cc2)ccc2NS(c(cc2)ccc2OCC)(=O)=O)n1	-7.1	N	3.4343	8	3	427.528
NCC-00004039	Cc(cc(cc1)S(Nc(cc2)ccc2Nc2nc(C)nc(N(C)C)c2)(=O)=O)c1OC	-9	Y	3.0324	8	2	427.528
NCC-00017424	CCC[n]1nnnc1COC(c(cccc1)c1NS(c(cc1)c(C)cc1F)(=O)=O)=O	-7.7	N	2.1265	9	1	433.463
NCC-00065231	CCCC[n]1c(SC(C)C(N(CC2)CCN2S(c2ccccc2)(=O)=O)=O)nnc1O	-7	N	2.2649	9	1	453.586
NCC-00006456	CC(C)Oc(cc1)ccc1NS(c1cccc(S(C(CC2)CS2(=O)=O)(=O)=O)c1)(=O)=O	-8.5	Y	1.0918	8	1	473.59
NCC-00034538	CN(c(cc1)ccc1OCc([o]cc1)c1C(OC)=O)S(c(cc1)ccc1OC)(=O)=O	-8.4	Y	2.2437	8	0	431.464
NCC-00031421	CCN(c1ccccc1)S(c1cc(C(OCC(c2ccccc2)=O)=O)ccc1)(=O)=O	-8.1	Y	3.1431	6	0	423.488
NCC-00035738	Cc1cccc(S(N(Cc(cc2)ccc2C(OC)=O)c(cccc2)c2OC)(=O)=O)c1	-5.8	N	3.4689	6	0	425.504
NCC-00013616	Cc(cc1)ccc1OCC(CN(c(cccc1)c1OC)S(c1ccccc1)(=O)=O)O	-6.7	N	2.9954	6	1	427.52
NCC-00036466	CC(c(cc1)ccc1S(N(CCOc1ccccc1)c(cc1)ccc1OC)(=O)=O)=O	-6.4	N	3.0901	6	0	425.504
NCC-00035461	CC(C(c1ccccc1)=O)OC(c(cc1)ccc1S(Nc(cccc1)c1F)(=O)=O)=O	-9.1	Y	3.2917	6	1	427.451
NCC-00017051	CN(c1ccccc1)S(c(cccc1)c1C(OCc(cc1)cc(F)c1OC)=O)(=O)=O	-7.4	N	3.2258	6	0	429.467
NCC-00036795	COc(cc1)ccc1N(C(CC1)CS1(=O)=O)S(c1cc(OC(F)(F)F)ccc1)(=O)=O	-6.9	N	2.2566	7	0	465.468
NCC-00004025	Cc(cc(cc1)N(C(CC2)=O)S2(=O)=O)c1S(Nc(cc(cc1)C(OC)=O)c1Cl)(=O)=O	-6.6	N	1.0784	9	1	472.925
NCC-00010513	O=C(C1)NCC1c(cc1)ccc1S(Nc1cc(C(F)(F)F)cc(C(F)(F)F)c1)(=O)=O	-8.8	N	3.5764	5	2	452.374
NCC-00000900	CN(c1c(C(NCc2ccc(C(F)(F)F)cc2)=O)[s]cc1)S(c1ccccc1)(=O)=O	-8	N	3.4357	5	1	454.492
NCC-00030829	CN(CC(Nc(ccc(C(F)(F)F)c1)c1Cl)=O)S(c1cc(cccc2)c2cc1)(=O)=O	-9.7	Y	4.3193	5	1	456.871
NCC-00035751	CCN(c1ccccc1)S(c1cc(C(NCC(C)c2ccccc2)=O)ccc1)(=O)=O	-8.1	N	3.9847	5	1	422.547

NCC-00019858	Cc1ccc(CN(C)C(c2c(C)ccc(S(Nc(cccc3)c3F)(=O)=O)c2)=O)cc1	-7.7	N	3.8707	5	1	426.511
NCC-00016549	CCN(c1ccccc1)S(c(cc1)ccc1C(N(CCC1)CC1C(F)(F)F)=O)(=O)=O	-7	N	3.8621	5	0	440.485
NCC-00016184	Oc1nc(ccc(S(Nc(cc(C(F)(F)F)cc2)c2OCC(F)(F)F)(=O)=O)c2)c2[o]1	-6.9	N	3.6632	7	2	456.318
NCC-00004063	Cc1cc(N(C(CC2)=O)S2(=O)=O)cc(C)c1S(Nc1cc(C(F)(F)F)ccc1)(=O)=O	-7.2	N	1.7516	7	1	462.468
NCC-00016408	CN(c(cccc1)c1OC)S(c(cc1)ccc1C(Nc(cccc1)c1OC)=O)(=O)=O	-6.8	N	2.8714	7	1	426.492
NCC-00028991	CCN(CC)C(COC(c1cccc(S(N(C(C)C2)c3c2cccc3)(=O)=O)c1)=O)=O	-6.5	N	2.6767	7	0	430.523
NCC-00030486	CCOc(cc1)ccc1NS(c(cc(cc1)NC(CC2CCCC2)=O)c1OC)(=O)=O	-7.9	N	3.3852	7	2	432.539
NCC-00043949	CC(C(N(C)c1ccccc1)=O)OC(CNS(c1cc(cccc2)c2cc1)(=O)=O)=O	-9.3	Y	2.9384	7	1	426.492
NCC-00030989	CC[n](c(C)c1)c(C)c1C(COC(C(CC1)CCN1S(c1ccccc1)(=O)=O)=O)=O	-8.6	Y	2.1543	7	0	432.539
NCC-00029431	CCN(c1ccccc1)S(c(cc1)cc(NC(CCc2ccc[o]2)=O)c1OC)(=O)=O	-7.3	N	2.9889	7	1	428.508
NCC-00079982	OC(c(cccc1)c1NC(CN(c(cccc1)c1F)S(c1ccccc1)(=O)=O)=O)=O	-7.2	N	2.2422	7	2	428.439
NCC-00010739	CC(CC(C)C1)CN1S(c(cc1)cc(N(C)S(c2ccccc2)(=O)=O)c1OC)(=O)=O	-5.7	N	2.5393	7	0	452.594
NCC-00027492	O=C(COC(CNS(c1cc(cccc2)c2cc1)(=O)=O)=O)NCc1cccc(Cl)c1	-9.7	Y	2.6451	7	2	446.91
NCC-00035858	Cc1cccc(N(CC(NCC(F)(F)F)=O)S(c(cc2)cc3c2OCCO3)(=O)=O)c1	-6.6	N	2.1609	7	1	444.429
NCC-00001180	CCOC(c1n[o]c(-c(cc2)cc(S(Nc(ccc(Cl)c3)c3F)(=O)=O)c2OC)c1)=O	-8.2	N	3.1293	8	1	454.861
NCC-00004273	CN(c(cc1)ccc1C(NCC1OCCC1)=O)S(c(cc1)cc(OC)c1OC)(=O)=O	-8.1	N	1.4625	8	1	434.511
NCC-00001183	CCN(c1ccccc1)S(c(cc(cc1)-c2cc(C(OCC)=O)n[o]2)c1OC)(=O)=O	-7.2	N	2.734	8	0	430.48
NCC-00031298	CC(C1)OC(C)CN1C(c(cccc1)c1NS(c1c(C)ccc(C(O)=O)c1)(=O)=O)=O	-6.8	N	2.1114	8	2	432.496

NCC-00028320	CCCNC(C(C1)Oc(cccc2)c2N1S(c(cc1)ccc1C(OCC)=O)(=O)=O)=O	-6.9	N	2.2113	8	1	432.496
NCC-00029696	CN(CCC1)CC1OC(c(cccc1)c1NS(c(cc1)cc(OC)c1OC)(=O)=O)=O	-8.5	N	2.2328	8	1	434.511
NCC-00036167	CN(c1ccccc1)S(c(cc1)cc(C(OCC(N2CCOCC2)=O)=O)c1Cl)(=O)=O	-7.2	N	1.7021	8	0	452.914
NCC-00008439	Cc1cc(N(CCCC2)S2(=O)=O)cc(C)c1S(Nc(ccc(OC)c1)c1OC)(=O)=O	-6.6	N	1.6715	8	1	454.566
NCC-00076443	CCOC(C(N(CC1)S(c2ccccc2)(=O)=O)OCC)N1S(c1ccccc1)(=O)=O	-6.4	N	2.6482	8	0	454.566
NCC-00026963	CN(Cc([s]1)ccc1Cl)C(c(cc1)ccc1S(N(C)c(cccc1)c1OC)(=O)=O)=O	-7.7	Y	3.5946	6	0	464.993
NCC-00014754	Cc(ccc(NC(CCC(c1ccc[s]1)=O)=O)c1)c1S(Nc(cccc1)c1Cl)(=O)=O	-7.5	N	3.9413	6	2	462.977
NCC-00013909	O=C(CN(c(cc(C(F)(F)F)cc1)c1Cl)S(c1ccccc1)(=O)=O)N1CCOCC1	-6.5	N	2.6374	6	0	462.875
NCC-00037799	CN(C)CC(CCCC1)C1OC(c(cc1)ccc1S(N(C)c1ccccc1)(=O)=O)=O	-7.1	N	2.8954	6	0	430.567
NCC-00009391	Cc(cc1)ccc1NS(c(cc1)ccc1OCC(N(C)Cc1ccccc1)=O)(=O)=O	-9.2	Y	3.0009	6	1	424.52
NCC-00082364	Cc(ccc(NC(COc1c(C)cccc1C)=O)c1)c1NS(c1ccccc1)(=O)=O	-8.3	Y	3.7128	6	2	424.52
NCC-00019097	Cc(ccc(NC(CCc(cc1)ccc1OC)=O)c1)c1NS(c1ccccc1)(=O)=O	-9	Y	3.8326	6	2	424.52
NCC-00019549	CCN(c1ccccc1)S(c(cc1)ccc1OCC(N(C)C1CCCCC1)=O)(=O)=O	-7.7	N	3.1061	6	0	430.567
NCC-00014196	CCN(c1ccccc1)S(c(cc1)ccc1NC(C(C)Oc1ccccc1)=O)(=O)=O	-8	N	3.3519	6	1	424.52
NCC-00010132	COC(CNC(c1ccccc1)c(cc(cc1)Br)c1NS(c1ccccc1)(=O)=O)=O	-6	N	3.314	6	2	489.389
NCC-00037520	COC(c(cccc1)c1S(Nc(cc(C(F)(F)F)cc1)c1N1CCCCC1)(=O)=O)=O	-6	N	3.553	6	1	442.457
NCC-00030005	CCCCc1nnc(NC(c(cc(cc2)S(N(C)c3ccccc3)(=O)=O)c2Cl)=O)[s]1	-7.5	N	4.1287	7	1	464.997
NCC-00028680	CC(C)[C@@H](C(NCc1c(C[n]2cncc2)cccc1)=O)NS(c1ccccc1)(=O)=O	-6.9	N	1.9693	7	2	426.539

NCC-00000734	Cc(cc1)ccc1S(Nc(cc(cc1)C(NCCN(C)C)=O)c1N1CCCC1)(=O)=O	-7	N	1.9322	7	2	430.571
NCC-00012274	CC(C)CNC(c(cc1)cc(NS(c2ccc(C)cc2)(=O)=O)c1N1CCNCC1)=O	-7.3	N	2.3459	7	3	430.571
NCC-00018251	Cc1nc(SC)nc(C)c1CCC(N(CC1)CCC1NS(c1ccccc1)(=O)=O)=O	-7.8	Y	3.191	7	1	448.61
NCC-00035368	CCC(CC)c1nnc(NC(c(cc2)ccc2S(N(C)c2ccccc2)(=O)=O)=O)[s]1	-6.6	Y	3.9502	7	1	444.579
NCC-00012306	CCC(C)NC(c(cc1)cc(NS(c(cccc2)c2F)(=O)=O)c1N1CCNCC1)=O	-7.1	N	2.2438	7	3	434.534
NCC-00037709	N#CCCN(CCC#N)C(c(cc1)cc(S(N(CC2)c3c2cccc3)(=O)=O)c1Cl)=O	-7.8	N	2.8001	7	0	442.926
NCC-00061769	Cc([n](C)nc1C)c1NC(CC(c(cc1)ccc1Cl)NS(c1ccccc1)(=O)=O)=O	-7.2	N	2.7944	7	2	446.958
NCC-00019158	CN(c1ccccc1)S(c1cc(NC(CCN(C(C=C2)=O)NC2=O)=O)ccc1)(=O)=O	-8.5	N	-0.8362	9	2	428.468
NCC-00015854	CN(C(CC1)=O)N=C1C(Nc(cc1)cc(NS(c(cc2)ccc2F)(=O)=O)c1OC)=O	-8.5	N	0.9243	9	2	434.447
NCC-00062320	CC(Nc1nc(C(OCC(N(CC2)CCN2S(c2ccccc2)(=O)=O)=O)=O)c[s]1)=O	-8.5	Y	1.2532	10	1	452.511
NCC-00065281	Cc1ccc(CNC(CCC(N(CC2)CCN2S(c2ccccc2)(=O)=O)=O)=O)[n]1C	-8.6	Y	1.18	8	1	432.543
NCC-00035490	Cc(cc1)cc(C)c1S(Nc(cc1)ccc1S(Nc1nc(C)cc(C)n1)(=O)=O)(=O)=O	-9.1	Y	2.5477	8	2	446.551
NCC-00029707	CCc1nnc(NC(COc(cc2)ccc2N(C)S(c2ccc(C)cc2)(=O)=O)=O)[s]1	-7.7	N	2.5327	8	1	446.551
NCC-00017999	CCOc(cc1)ccc1NS(c1cc(C(Nc2nnc(C(C)C)[s]2)=O)ccc1)(=O)=O	-8.9	Y	3.4725	8	2	446.551
NCC-00007083	N#CCCN(CC1)CCN1c(ccc(C(O)=O)c1)c1NS(c(cc1)ccc1F)(=O)=O	-6.6	N	0.5028	8	2	432.475
NCC-00012251	CN(C)C(c(cc1)cc(NS(c(cc(cc2)Cl)c2OC)(=O)=O)c1N1CCNCC1)=O	-6.6	N	1.7255	8	2	452.961
NCC-00015833	OC(CCc(cc1)ccc1S(Nc(cc(C(F)(F)F)cc1)c1-[n]1ncnc1)(=O)=O)=O	-7.7	N	1.7897	8	2	440.401
NCC-00027469	CN(c(cc1)ccc1Cl)S(c(cc(cc1)C(NCc2ccncc2)=O)c1Cl)(=O)=O	-7.6	N	2.9319	6	1	450.345

NCC-00069213	CCN(CC1)CCN1C(CN(c(cc(cc1)Cl)c1Cl)S(c1ccccc1)(=O)=O)=O	-6	N	2.9108	6	0	456.393
NCC-00030497	CCN(c1ccccc1)S(c1cc(C(C(c2ncccc2)C#N)=O)ccc1)(=O)=O	-7.2	N	2.3095	6	0	405.477
NCC-00074237	CC(C(NCC(C)(C)N(CC1)Cc2c1cccc2)=O)NS(c1ccccc1)(=O)=O	-7.7	N	2.1816	6	2	415.556
NCC-00017991	CCN(CC)CCNC(c(cc1)ccc1S(N(CCC1)c2c1cccc2)(=O)=O)=O	-6.6	N	2.5694	6	1	415.556
NCC-00087558	CC(c1cnccc1)NC(CN(Cc1ccccc1)S(c1ccccc1)(=O)=O)=O	-6.8	N	2.0839	6	1	409.509
NCC-00083066	CC(C)N(C(C)C)C(CN(c1nc(cccc2)c2[s]1)S(c1ccccc1)(=O)=O)=O	-6.4	N	3.5477	6	0	431.58
NCC-00007425	CC(C)Sc(cc(c(N1C)c2)N(C)C1=O)c2NS(c1c(C)cc(C)c(C)c1)(=O)=O	-6.9	N	3.9793	6	1	433.595
NCC-00035623	CCN(Cc1ccncc1)C(c(cccc1)c1NS(c(cc1)ccc1Br)(=O)=O)=O	-7	N	3.2127	6	1	474.378
NCC-00033951	O=C(c1cnc(C(F)(F)F)cc1)Nc1cccc(NS(c2ccccc2)(=O)=O)c1	-9	Y	3.0076	6	2	421.398
NCC-00011109	CN(C)c1ccc(C(N(CC2)C(C(F)(F)F)=O)N2S(c2ccccc2)(=O)=O)cc1	-6.2	N	2.5405	6	0	427.446
NCC-00028214	CNC(c(cc1)ccc1S(Nc(cc(C(F)(F)F)cc1)c1-[n]1cccc1)(=O)=O)=O	-7.2	N	2.4307	6	2	423.414
NCC-00056730	NC(COc(cccc1)c1C(N(CC1)CCC1NS(c1ccccc1)(=O)=O)=O)=O	-7.8	N	1.4488	8	2	417.485
NCC-00015918	Cc(cc1)c(C)cc1S(N(C)c(cc1)ccc1OCC(N(CCN1)C1=O)=O)(=O)=O	-7.9	Y	1.6709	8	1	417.485
NCC-00003610	Cc(ccc(-c(cc1)nnc1O)c1)c1S(N(C)c(ccc(OC)c1)c1OC)(=O)=O	-7.2	N	1.9939	8	1	415.469
NCC-00019558	CCc1n[o]c(C)c1C(Nc1cccc(S(Nc(cc2)ccc2OC)(=O)=O)c1)=O	-8.1	N	2.6579	8	2	415.469
NCC-00007042	CCN(CC1)CCN1c(ccc(C(O)=O)c1)c1NS(c(cc1)ccc1OC)(=O)=O	-6.6	N	0.632	8	2	419.501
NCC-00019994	CCCNC(CSc1nc(cc(cc2)S(Nc(cccc3)c3OC)(=O)=O)c2[o]1)=O	-8	Y	2.6549	8	2	435.524
NCC-00002101	CCc1nc(-c2cc(S(Nc(c(OC)c3)cc(Cl)c3OC)(=O)=O)c(C)cc2)n[o]1	-8	N	3.3472	8	1	437.903

NCC-00068694	Cc1n[o]c(COC(CCC(N(CC2)CCN2S(c2ccccc2)(=O)=O)=O)=O)c1	-8.4	Y	1.2092	9	0	421.473
NCC-00036144	COc(ccc(S(Nc(cccc1)c1C(NN1CCOCC1)=O)(=O)=O)c1)c1OC	-6.9	N	0.0666	9	2	421.473
NCC-00003375	CN(c(c(N(C)C1=O)c2)cc(NS(c(cc(cc3)OC)c3OC)(=O)=O)c2Cl)C1=O	-6.6	N	0.8871	9	1	439.875
NCC-00044106	CC(C)(C)c(cc1)ccc1S(NCc1c(C)[n](Cc2ccccc2)nc1C)(=O)=O	-8.1	N	4.0006	5	1	411.568
NCC-00018697	CCN(CC1)CCN1c(cccc1)c1NS(c(cc(cc1C(O)=O)Br)c1F)(=O)=O	-6.6	N	1.528	7	2	486.361
NCC-00003331	CN(c(c(N(C)C1=O)c2)cc(C(F)(F)F)c2NS(c(cc2)ccc2Cl)(=O)=O)C1=O	-6.7	N	1.8754	7	1	447.82
NCC-00030903	CN(c1ccccc1)S(c1cc(C(NCCC(N2CCCC2)=O)=O)ccc1)(=O)=O	-8.1	N	1.8983	7	1	415.513
NCC-00010201	Cc1cc(NC(CC(CN(C)S(c2ccccc2)(=O)=O)c2ccccc2)=O)n[o]1	-6.5	N	3.154	7	1	413.497
NCC-00031228	CC(C)(C)NC(c(cc1)ccc1NS(c(cc1)cc(CC2)c1N2C(C)=O)(=O)=O)=O	-9.6	Y	2.6342	7	2	415.513
NCC-00035608	Cc(ccc(S(N(C)c(cccc1)c1OC)(=O)=O)c1)c1C(N1CCN(C)CC1)=O	-6.4	N	1.9215	7	0	417.528
NCC-00038028	CCOc(cc1)ccc1S(N(C)c(cc1)ccc1Oc1nc(C)nc(C)c1)(=O)=O	-8.2	Y	3.0153	7	0	413.497
NCC-00035969	CCOc(cc1)ccc1S(N(C)c(cc1)ccc1Oc(cc1)ncc1C#N)(=O)=O	-7.2	N	2.7819	7	0	409.465
NCC-00012831	CCN(CC)C(CN(c(cccc1)c1S(N1c2c(C)cccc2C)(=O)=O)C1=O)=O	-6.1	N	2.9728	7	0	415.513
NCC-00016800	CC(c1ccncc1)NC(c1cccc(S(Nc(cccc2)c2OC)(=O)=O)c1)=O	-7.5	N	2.0314	7	2	411.481
NCC-00020755	Cc1n[o]c(C)c1CC(Nc1cccc(NS(c2cc(C)c(C)cc2)(=O)=O)c1)=O	-9.9	Y	2.9982	7	2	413.497
NCC-00005996	Cc(cc(cc1)S(Nc(cc2)ccc2Cl)(=O)=O)c1OCC(N1CCN(C)CC1)=O	-7.9	Y	2.2672	7	1	437.947
NCC-00016239	Cc(cc1)ccc1S(N(CCC(Nc1ncc[s]1)=O)c(cccc1)c1OC)(=O)=O	-6.1	N	3.0099	7	1	431.536
NCC-00037754	O=C(c1cccc(S(Nc(cc(C(F)(F)F)cc2)c2Cl)(=O)=O)c1)N[n]1cnnc1	-9.3	N	2.425	8	2	445.808

NCC-00001954	Cc1cc(S(Nc(cc2)ccc2Nc2nc(N(C)C)cc(C)n2)(=O)=O)c(C)cc1	-9.3	Y	3.6289	7	2	411.529
NCC-00018870	CCN(CC)S(c(cc1)cc(NS(c2c3nsnc3ccc2)(=O)=O)c1NC)(=O)=O	-6.9	N	2.1535	9	2	455.583
NCC-00005950	CC(C)C(N(CC1)C(CSc2nnc(C)c(O)n2)=O)N1S(c1ccccc1)(=O)=O	-7.1	N	1.9357	9	1	437.544
NCC-00027244	CCOC(c(c1c2ccc(O)c1C(O)=O)c(C)[n]2S(c1ccc(C)cc1)(=O)=O)=O	-6.2	N	2.1507	8	2	417.437
NCC-00036172	CCOc(ccc(Br)c1)c1S(Nc(cccc1)c1C(OC(CCO1)C1=O)=O)(=O)=O	-6.7	N	2.4167	8	1	484.322
NCC-00034521	OC(c(cc1OCCCOc1c1)c1NS(c(cccc1)c1OC(F)(F)F)(=O)=O)=O	-8.8	N	2.8636	8	2	433.358
NCC-00017069	CN(c1ccccc1)S(c(cccc1)c1C(OCC(c([s]1)ccc1Cl)=O)=O)(=O)=O	-7.3	N	3.4141	6	0	449.934
NCC-00076884	CCOC(c1c(C)[o]c(cc2)c1cc2N(CC(C)C)S(c1ccccc1)(=O)=O)=O	-6.6	N	4.1117	6	0	415.509
NCC-00002517	CCOc(cc1)ccc1S(Nc(cc1)cc2c1[o]c(C)c2C(OC(C)C)=O)(=O)=O	-7.8	N	3.8231	7	1	417.481
NCC-00030815	CCN(c1ccccc1)S(c(cc1)ccc1OCc1ccc(C(OC)=O)[o]1)(=O)=O	-7.4	N	2.774	7	0	415.465
NCC-00034156	CC(CC1)Sc(ccc(C(F)(F)F)c2)c2N1S(c(cc1)ccc1S(C)(=O)=O)(=O)=O	-7	N	2.5153	5	0	465.536
NCC-00030945	CCN(c1ccccc1)S(c(cc1)ccc1OCC(c(cccc1)c1F)=O)(=O)=O	-8.1	N	3.2609	5	0	413.468
NCC-00013344	CCOC(CN(c(ccc(S(Nc(cc(C)cc1)c1OC)(=O)=O)c1)c1O1)C1=O)=O	-8.2	N	1.9971	9	1	420.441
NCC-00004086	CC(CS(N1c(cc2)ccc2S(Nc(ccc(OC)c2)c2OC)(=O)=O)(=O)=O)C1=O	-7.8	N	0.3448	9	1	440.496
NCC-00017004	Cc(cc1)ccc1S(N(CC(N(C)Cc([s]1)ccc1Cl)=O)c1ccccc1)(=O)=O	-5.8	N	3.6534	5	0	448.994
NCC-00018185	O=C1N(Cc(cc2)ccc2NS(c(cc2)cc(C(F)(F)F)c2Cl)(=O)=O)C=CC=C1	-9.5	Y	3.0598	5	1	442.844
NCC-00035903	COc(ccc(S(Nc(cccc1)c1Cl)(=O)=O)c1)c1NS(c([s]1)ccc1Cl)(=O)=O	-6.8	N	3.5936	7	2	493.411
NCC-00028735	Cc(ccc(S(Nc(cccc1)c1N1CCCCC1)(=O)=O)c1C)c1OCC(O)=O	-6.6	N	2.5395	7	2	418.512

NCC-00018771	CC(CCCC1)N1C(COC(c1cccc(NS(c2ccccc2)(=O)=O)c1)=O)=O	-7	N	2.6796	7	1	416.497
NCC-00018427	Cc(cc(c(OC)c1)OC)c1S(Nc1ccc(CN(C=CC=C2)C2=O)cc1)(=O)=O	-6.7	N	1.8094	7	1	414.481
NCC-00036513	Cc(cc1)ccc1NS(c1cc(C(OCC(N2CCCC2)=O)=O)c(C)cc1)(=O)=O	-8.7	Y	2.7007	7	1	416.497
NCC-00010779	CCOc(cc1)cc(NS(c(c2c3nccc2)ccc3OCC)(=O)=O)c1OCC	-6.7	N	3.2836	7	1	416.497
NCC-00071731	CCOC(c1c(NC(C(CCC2)N2S(c2ccccc2)(=O)=O)=O)[s]c(C)c1C)=O	-6.5	N	3.2985	7	1	436.552
NCC-00087040	CS(CCC(C(NC(CC1)c2c1cccc2)=O)NS(c1ccccc1)(=O)=O)(=O)=O	-6.8	N	1.4631	7	2	436.552
NCC-00012299	CCOC(CCN(c1ccccc1)S(c(cc1)cc(N2)c1SCCC2=O)(=O)=O)=O	-6.1	N	1.1085	7	1	434.536
NCC-00007153	CCCS(N(CCC1)c(cc2)c1cc2NS(c(cc(C)cc1)c1OC)(=O)=O)(=O)=O	-7	N	2.8922	7	1	438.567
NCC-00008034	COc(c(S(Nc(cc1)ccc1C(c1ccncc1)=O)(=O)=O)c1)cc(Cl)c1OC	-7.8	N	2.5538	7	1	432.883
NCC-00029967	CC(c(cc1)ccc1N(CC(N1CCOCC1)=O)S(c(cc1)ccc1Cl)(=O)=O)=O	-6.9	N	1.6603	7	0	436.915
NCC-00007249	COc(ccc(Cl)c1)c1S(Nc(ccc(N1CCCCCC1)c1)c1C(O)=O)(=O)=O	-7.8	N	3.1548	7	2	438.931
NCC-00031191	Cc1n[o]c(C)c1CN(c(cccc1)c1Cl)S(c(cccc1)c1C(OC)=O)(=O)=O	-6.7	N	3.0071	7	0	434.899
NCC-00012646	CCc(ccc(-c1cc(C)n[o]1)c1)c1S(Nc(c(OC)cc(OC)c1)c1Cl)(=O)=O	-6.7	N	3.7426	7	1	436.915
NCC-00020460	O=C(C1=COCCO1)Nc1cccc(S(Nc2cc(C(F)(F)F)ccc2)(=O)=O)c1	-9	N	1.667	7	2	428.386
NCC-00003876	Cc(cc1C)cc(Cl)c1NS(c(cc(cc1)N(C(CC2)=O)S2(=O)=O)c1OC)(=O)=O	-6.3	N	1.4393	8	1	458.942
NCC-00018597	Cc1cccc(C(N2CCCC2)=O)c1NS(c(cc(cc1)C(O)=O)c1OC)(=O)=O	-6	N	2.214	8	2	418.469
NCC-00013320	CCOc(cc1)ccc1NS(c(cc1)cc(CC2)c1N2C(CCC(O)=O)=O)(=O)=O	-8.3	N	2.018	8	2	418.469
NCC-00018541	COc(ccc(C(O)=O)c1)c1S(Nc1ccc(CN(C=CC=C2)C2=O)cc1)(=O)=O	7.6	N	1.0206	8	2	414.437

NCC-00001514	CCOC(c1cccc(NC(C(CCC2=O)N2S(c2ccccc2)(=O)=O)=O)c1)=O	-7.6	N	1.9883	8	1	416.453
NCC-00058192	O=C(COC(C(CCCC1)N1S(c1ccccc1)(=O)=O)=O)NC(c1ccc[s]1)=O	-7.5	N	1.7935	8	1	436.508
NCC-00027247	CCOC(c(cccc1)c1NS(c(cc1)ccc1S(N1CCCC1)(=O)=O)(=O)=O)=O	-7.8	N	2.1428	8	1	438.524
NCC-00007122	CCOC(c(cccc1)c1NS(c(cc1)ccc1N(CCCC1)S1(=O)=O)(=O)=O)=O	-8.6	N	1.443	8	1	438.524
NCC-00011743	CC(N(CCOc1c2)c1cc(C)c2S(Nc(c(OC)c1)cc(Cl)c1OC)(=O)=O)=O	-7.4	N	2.6121	8	1	440.903
NCC-00011766	CCOC(c1cccc(NS(c(cc2OCCN(C(C)=O)c2c2)c2Cl)(=O)=O)c1)=O	-8.2	N	2.7275	8	1	438.887
NCC-00036325	COc(ccc(NS(c1cccc(Cl)c1Cl)(=O)=O)c1)c1S(N1CCOCC1)(=O)=O	-7.3	N	2.1435	8	1	481.376
NCC-00013821	Cc(cc(C)c(S(N1CCCCC1)(=O)=O)c1)c1N(C)S(c(cc1)ccc1Cl)(=O)=O	-6.2	N	3.3645	6	0	457.013
NCC-00011748	CC(N(CCOc1c2)c1cc(C)c2S(Nc(cc1)cc(C(F)(F)F)c1Cl)(=O)=O)=O	-8.2	N	3.6004	6	1	448.848
NCC-00020530	O=C(c1ccc[o]1)Nc1cccc(NS(c(cc2)c(C(F)(F)F)cc2Cl)(=O)=O)c1	-9.3	Y	3.7492	6	2	444.816
NCC-00083155	CC(C)OCc(cc1)ccc1C(N(CC1)CCC1NS(c1ccccc1)(=O)=O)=O	-8.2	Y	3.3828	6	1	416.54
NCC-00029074	CC(CCCC1)C1NC(c1cccc(S(N(C)c(cc2)ccc2OC)(=O)=O)c1)=O	-7	N	3.0577	6	1	416.54
NCC-00032420	Cc(ccc(NC(c1cc(OC)c(C)cc1)=O)c1)c1NS(c1ccccc1)(=O)=O	-8.5	N	3.724	6	2	410.493
NCC-00027145	OC(CCc(cc1)ccc1S(Nc1cc(/C=C/c2ncccc2)ccc1)(=O)=O)=O	-8.9	Y	3.1564	6	2	408.477
NCC-00019080	CN(C)C(COc(cc1)ccc1NS(c1ccc(C2CCCCC2)cc1)(=O)=O)=O	-7.8	N	3.3757	6	1	416.54
NCC-00017679	Cc(ccc(S(Nc(cc1)ccc1OC)(=O)=O)c1)c1C(N(C)Cc1ccc[s]1)=O	-7.5	N	3.2226	6	1	430.548
NCC-00019441	CC(NCc(cc1)ccc1S(N(Cc1ccc[s]1)c(cc1)ccc1OC)(=O)=O)=O	-5.9	N	2.4917	6	1	430.548
NCC-00033228	CC(C1CC1)NC(CCN(c(cc1)ccc1OC)S(c1cccc(Cl)c1)(=O)=O)=O	-6.5	N	3.0217	6	1	436.959

NCC-00038072	CC(CNC(c(cc1)ccc1S(Nc1ccc(C)cc1)(=O)=O)=O)C[n]1cncc1	-8.6	Y	2.0518	7	2	412.513
NCC-00027309	CC(C)[n]1nccc1N(CC(N(C)C1CCCCC1)=O)S(c1ccccc1)(=O)=O	-6.6	N	1.9269	7	0	418.56
NCC-00035345	N#Cc(cccc1)c1NC(Nc1cccc(S(Nc(cccc2)c2F)(=O)=O)c1)=O	-8	N	3.0365	7	3	410.428
NCC-00049770	CC(C)C(C(Nc1nnc(C(C)C)[s]1)=O)NS(c1cc(cccc2)c2cc1)(=O)=O	-7.8	Y	3.8338	7	2	432.568
NCC-00033837	CC[n]1c(NC(C(CCSC)NS(c2ccccc2)(=O)=O)=O)nc2c1cccc2	-6.8	N	2.8982	7	2	432.568
NCC-00032954	CC(C(N(CC1)CCN1S(c1ccccc1)(=O)=O)=O)OC(c1ncc(C)nc1)=O	-8.5	Y	0.6796	9	0	418.473
NCC-00000823	CCOC(CCNC(Nc1nc(CCN(C2)S(c3ccccc3)(=O)=O)c2[s]1)=O)=O	-7.8	Y	1.8601	9	2	438.528
NCC-00064673	CC(C)(C)c(cc1C)cc(C)c1S(NC(c1n[nH]c(C)n1)c1ccccc1)(=O)=O	-6.4	N	4.0814	6	2	412.556
NCC-00077510	CCN(Cc1nc(-c2ccccc2)n[o]1)C(CN(C)S(c1ccccc1)(=O)=O)=O	-8	N	1.8719	8	0	414.485
NCC-00014987	Cc(cc1)cc(C)c1NS(c1c(C)ccc(NC(C(CC2)=NNC2=O)=O)c1)(=O)=O	-8.8	N	1.9075	8	3	414.485
NCC-00077377	CC[n]1nc(C)c(S(Nc(cc2)ccc2NS(c2ccc(C)cc2)(=O)=O)(=O)=O)c1	-9.2	Y	1.3179	8	2	434.54
NCC-00007942	Cc([n](C)nc1C(Nc(cc2)ccc2S(Nc(cccc2)c2OC)(=O)=O)=O)c1Cl	-8.1	Y	2.1564	8	2	434.903
NCC-00034721	CC(C)C(C(OC(C)C(Nc([s]cc1)c1C#N)=O)=O)NS(c1ccccc1)(=O)=O	-7.4	N	2.3362	8	2	435.524
NCC-00016304	CC(NCC(OCC(Nc1cccc(S(N(C)c2ccccc2)(=O)=O)c1)=O)=O)=O	-7.6	N	0.2092	9	2	419.457
NCC-00063758	CC(C)(C)C(COC(CCN(c1ccc(C)cc1)S(c1ccccc1)(=O)=O)=O)=O	-6.4	N	3.2663	6	0	417.524
NCC-00029855	CC(C)(C)OC(COC(c1cccc(S(N(C)c2cccc(Cl)c2)(=O)=O)c1)=O)=O	-7.9	N	3.087	7	0	439.915
NCC-00073619	CC(C)C(C(OC(C(N(C)C)=O)c1ccccc1)=O)NS(c1ccccc1)(=O)=O	-6.6	N	2.0236	7	1	418.512
NCC-00030622	CCN(CC)S(c(cc1)ccc1S(Nc(cc(cc1)Cl)c1C(OC)=O)(=O)=O)(=O)=O	-5.9	N	2.5089	8	1	460.958

NCC-00035755	CC(C)N(C(C)C)C(CN(c(cccc1)c1OC)S(c(cc1)ccc1Cl)(=O)=O)=O	-5.4	N	3.2813	6	0	438.974
NCC-00030475	CC(C(Nc1cccc(S(Nc2cc(C(F)(F)F)ccc2)(=O)=O)c1)=O)NC(N)=O	-8.8	N	1.3312	8	4	430.406
NCC-00088129	CC(C)c(cc1)ccc1S(NCCC(NCc(cc1)ccc1N(C)C)=O)(=O)=O	-8.2	Y	2.8246	6	2	403.545
NCC-00036013	CC(C)C(CNC(c1cccc(S(Nc(cc2)ccc2Br)(=O)=O)c1)=O)N(C)C	-8.5	Y	2.8545	6	2	468.414
NCC-00009522	Cc(cc1)ccc1S(N(CC(NCCN(C)C)=O)c1c(C)ccc(Cl)c1)(=O)=O	-6	N	1.9412	6	1	423.963
NCC-00034959	CC(NCCC(Nc(cc1)cc(NS(c(cc2)ccc2F)(=O)=O)c1OC)=O)=O	-7	N	1.2313	8	3	409.437
NCC-00077632	NC(NC(C(c1ccccc1)OC(CCNS(c1ccccc1)(=O)=O)=O)=O)=O	-7.4	N	0.6137	9	3	405.43
NCC-00015580	CC(C)NC(CNC(c1cccc(NS(c(cc(cc2)Cl)c2Cl)(=O)=O)c1)=O)=O	-9.1	Y	2.4588	7	3	444.338
NCC-00019750	CC(C)c(cc1)ccc1S(NCCC(NCc(c(C)cc(C)n1)c1O)=O)(=O)=O	-8.4	Y	2.6748	7	3	405.517
NCC-00029840	Cc1cc(S(Nc(c(C(OC)=O)cc(OC)c2OC)c2OC)(=O)=O)c(C)cc1	-5.6	N	2.3495	8	1	409.458
NCC-00077436	CCOC(c1cc(NS(c2cc(C)c(C)cc2)(=O)=O)cc(C(OCC)=O)c1)=O	-6.6	N	3.2851	7	1	405.47
NCC-00035732	Cc(cc(cc1)F)c1S(Nc(cc(c(OC)c1)OC(F)F)c1C(OC)=O)(=O)=O	-6.3	N	2.4158	7	1	419.375
NCC-00016257	COC(c(cc(c(OC)c1)OC)c1NS(c1c(C(F)(F)F)cccc1)(=O)=O)=O	-5.9	N	2.58	7	1	419.375
NCC-00005308	COC(C(CC(c1ccccc1)=C)(C(F)(F)F)NS(c1ccccc1)(=O)=O)=O	-6	N	3.6272	5	1	413.415
NCC-00029038	CC(C)CNC(COC(c(cc1)ccc1S(Nc1c(C)cccc1)(=O)=O)=O)=O	-8.6	N	2.3783	7	2	404.486
NCC-00030987	CC(C)(C)c(cc1)ccc1S(NCc(cc1)ccc1C(OCC(N)=O)=O)(=O)=O	-8.7	N	2.4302	7	2	404.486
NCC-00037920	CC(C)(C)OC(Nc(ccc(NS(c1c(C)ccc(C)c1)(=O)=O)c1)c1OC)=O	-6.4	N	3.6296	7	2	406.501
NCC-00007302	CCCCN(C)c(cc1)cc(C(O)=O)c1NS(c(cc1)ccc1OCC)(=O)=O	-8	N	2.9916	7	2	406.501

NCC-00011350	CC(C)(CO)NS(c1cc(N(C)S(c2ccccc2)(=O)=O)c(C)cc1C)(=O)=O	-6.5	N	1.8966	7	2	426.556
NCC-00047629	CC(C)c(cc1)ccc1S(NCCC(OC(C)C(N1CCOCC1)=O)=O)(=O)=O	-7.6	N	1.6628	8	1	412.505
NCC-00030022	CN(c(cc1)ccc1OCC(NCC(F)(F)F)=O)S(c(cc1)ccc1Cl)(=O)=O	-8.6	N	2.3742	6	1	436.837
NCC-00004518	CCOc(cc1)ccc1N(CC(NC(C)(C)C)=O)S(c1ccc(C)cc1)(=O)=O	-5.9	N	2.774	6	1	404.529
NCC-00007094	CCN(CC)c(ccc(NS(c1ccc(C(C)(C)C)cc1)(=O)=O)c1)c1C(O)=O	-6.5	N	3.7347	6	2	404.529
NCC-00036799	CC(C(Nc1cccc(S(N(C)c2ccccc2)(=O)=O)c1)=O)OCC(F)(F)F	-7.7	N	2.3187	6	1	416.419
NCC-00036011	CCN(c1ccccc1)S(c(cc1)cc(NC(CC(F)(F)F)=O)c1OC)(=O)=O	-6.5	N	2.8426	6	1	416.419
NCC-00026665	COc(ccc(NC(CNC(N)=O)=O)c1)c1NS(c(cc1)cc(Cl)c1Cl)(=O)=O	-7.3	N	1.2656	9	4	447.298
NCC-00081891	CCCC(C(Nc1cc(NS(c2ccccc2)(=O)=O)c(C)cc1)=O)NC(N)=O	-6.5	N	1.7356	8	4	404.49
NCC-00063380	O=C(CN(c1ncc[s]1)S(c1ccccc1)(=O)=O)NCCc1cccc(Cl)c1	-6.7	N	3.0271	6	1	435.955
NCC-00081732	CC[n](c(C)c1)c(C)c1C(CN(c1ccncc1)S(c1ccccc1)(=O)=O)=O	-5.6	N	1.73	6	0	397.498
NCC-00085915	CC(C)C(C(Nc1ncc(C)cc1)=O)NS(c1cc(cccc2)c2cc1)(=O)=O	-7.9	N	3.4982	6	2	397.498
NCC-00028944	Cc(cc1)c(C)cc1NC(CN(c1ccncc1)S(c1ccccc1)(=O)=O)=O	-6.8	N	2.3432	6	1	395.482
NCC-00015668	CC(CC1)CCN1C(CN(c1ccccc1)S(c(cccc1)c1C#N)(=O)=O)=O	-6	N	2.452	6	0	397.498
NCC-00038407	CCN(c1ccccc1)S(c1cc(C(NC2CCN(C)CC2)=O)ccc1)(=O)=O	-6.4	N	2.2101	6	1	401.529
NCC-00011393	CCN(c1cc(C)ccc1)S(c1ccc(Cc(cc(C)nn2)c2O)cc1)(=O)=O	-7.6	N	3.0038	6	1	397.498
NCC-00017318	CC(c1ccncc1)NC(c(cc1)ccc1NS(c(cc1)ccc1F)(=O)=O)=O	-10	Y	2.2022	6	2	399.445
NCC-00007250	CC(C)(C)c(cc1)ccc1S(Nc1cc(C)c2nc(NC(C)=O)[s]c2c1)(=O)=O	-6.9	N	4.3906	6	2	417.553

NCC-00028757	O=C(CN(c1ccncc1)S(c1ccccc1)(=O)=O)NCc(cccc1)c1F	-6	N	1.4656	6	1	399.445
NCC-00034544	N#CC(C(c1cccc(S(Nc(cc2)ccc2F)(=O)=O)c1)=O)c1ncccc1	-8	N	2.0988	6	1	395.413
NCC-00062447	Cc(cc1)ccc1S(Nc(cc(cc1)Cl)c1C(NCc1ccncc1)=O)(=O)=O	-7.1	N	2.7646	6	2	415.9
NCC-00017677	Cc1cccc(NS(c2c(C)ccc(NC(c3cc(Br)cnc3)=O)c2)(=O)=O)c1	-8	N	3.5183	6	2	460.351
NCC-00033664	O=C(c(cccn1)c1SC(F)F)N(CC1)CCC1NS(c1ccccc1)(=O)=O	-7.9	N	3.778	6	1	427.495
NCC-00033597	Cc(cc(cc1)Oc2nccnc2)c1NS(c1cc(C(F)(F)F)ccc1)(=O)=O	-9.2	N	2.8961	6	1	409.387
NCC-00074357	Cc(cc1)ccc1S(Nc(cc1)ccc1Oc1nc(C(F)(F)F)ccn1)(=O)=O	-9.8	Y	3.4068	6	1	409.387
NCC-00001542	COc(cc1)nnc1-c(cc1)ccc1NS(c1cc(C(F)(F)F)ccc1)(=O)=O	-10.2	Y	3.0088	6	1	409.387
NCC-00057234	Cc(ccc(C(OC)=O)c1)c1S(Nc(cc1)ccc1Oc1nccnc1)(=O)=O	-8.1	Y	1.9608	8	1	399.426
NCC-00082380	COc(cc1)ccc1Oc(nccc1)c1NS(c(cc1)ccc1C(N)=O)(=O)=O	-7.3	N	1.7221	8	2	399.426
NCC-00027476	NC(CCS(CCN(CC1)CCN1S(c1cc(CCC2)c2cc1)(=O)=O)(=O)=O)=O	-7.7	N	-0.0133	8	1	429.56
NCC-00015026	Cc1c(C(OCC(N(CC2)CCN2S(c2ccccc2)(=O)=O)=O)=O)[s]c(C)n1	-8	Y	1.5243	8	0	423.513
NCC-00011880	Cc(c(S(Nc(cc1)ccc1OC(F)(F)F)(=O)=O)c1)cc(nc2O)c1nc2O	-8.4	N	2.8506	8	3	415.347
NCC-00013715	OC(c(cc1)ccc1S(Nc(cc1)ccc1S(Nc1cnc[s]1)(=O)=O)(=O)=O)=O	-9	Y	0.7098	9	3	439.492
NCC-00038040	CN(CC(C1)C(OCC(N(CC2)CCN2S(c2ccccc2)(=O)=O)=O)=O)C1=O	-8.4	Y	-0.1923	9	0	409.462
NCC-00007082	CN(CC1)CCN1c(ccc(NS(c(cc1)cc(Cl)c1Cl)(=O)=O)c1)c1C(O)=O	-7.2	N	1.5077	7	2	444.338
NCC-00072217	COc1ncc(CNC(CCNS(c2cc(cccc3)c3cc2)(=O)=O)=O)cc1	-9.2	Y	2.2161	7	2	399.47
NCC-00001032	CCOC(c1cccc(NS(c2c(C)ccc(-c3n[nH]c(C)c3)c2)(=O)=O)c1)=O	-8.7	N	2.6636	7	2	399.47

NCC-00019450	Cc1cccc(NS(c2cc(C(N(C)CC(NC3CC3)=O)=O)ccc2)(=O)=O)c1	-7.7	N	1.6213	7	2	401.486
NCC-00029165	CC(c1cccc(NCC(N(CC2)CCN2S(c2ccccc2)(=O)=O)=O)c1)=O	-8.7	Y	1.4754	7	1	401.486
NCC-00004119	CCCc1n[o]c(-c(cc(cc2)S(N(CC)c3ccccc3)(=O)=O)c2OC)n1	-7.4	N	3.2332	7	0	401.486
NCC-00069515	CN(CC1)CCN1C(CN(c1cc(OC)ccc1)S(c1ccccc1)(=O)=O)=O	-6.3	N	1.2225	7	0	403.501
NCC-00007597	CC(Nc(ccc(C)c1)c1S(Nc1ccc(C2(CC2)C(NC)=O)cc1)(=O)=O)=O	-7.9	N	1.5665	7	3	401.486
NCC-00012813	CC(C)NC(CN(c(cccc1)c1S(N1c2c(C)cccc2C)(=O)=O)C1=O)=O	-6	N	2.6593	7	1	401.486
NCC-00001507	Cc1cc(S(Nc2cc(-c(cc3)nnc3OC)ccc2)(=O)=O)c(C)cc1OC	-7.5	N	2.7783	7	1	399.47
NCC-00058229	CC(C(N(C)C)=O)NC(C(CC1)CCN1S(c1cc(CCC2)c2cc1)(=O)=O)=O	-8.1	Y	1.3374	7	1	407.533
NCC-00017020	Cc(cc1)ccc1S(N(C)c(cc1)ccc1C(Nc1ncccc1O)=O)(=O)=O	-8.2	Y	2.3601	7	2	397.454
NCC-00011378	CCOc(cccc1)c1NS(c1ccc(Cc(cc(C)nn2)c2O)cc1)(=O)=O	-8.4	Y	2.6847	7	2	399.47
NCC-00012792	CCC(C)NC(CN(c(cccc1)c1S(N1c(cc2)ccc2F)(=O)=O)C1=O)=O	-6.6	N	2.5267	7	1	405.449
NCC-00020473	CCCNS(c(cc1)ccc1NS(c1cccc2c1ncc(C)c2)(=O)=O)(=O)=O	7.7	N	2.6047	7	2	419.525
NCC-00004722	Cc(cc1)ccc1S(Nc(cccc1)c1NC(CSc1nnc(N)[s]1)=O)(=O)=O	-7.2	N	2.3233	8	3	435.552
NCC-00018041	COc(c(S(Nc(cccc1)c1-[n]1ncc(C#N)c1N)(=O)=O)cc(Cl)c1)c1Br	-5.3	N	1.8984	8	2	482.745
NCC-00033859	O=C(CSCc1cccc(Cl)c1)Nc1n[nH]c(NS(c2ccccc2)(=O)=O)n1	-9.8	Y	2.4107	8	3	437.931
NCC-00056613	CC(C)C(C(Nc(cc1)ccc1-[n]1ncnc1)=O)NS(c1ccccc1)(=O)=O	-7.3	N	1.6545	8	2	399.474
NCC-00035556	CC(Nc1cc(C)n[n]1-c(cc1)ccc1NS(c1cc(C#N)ccc1)(=O)=O)=O	-9.3	Y	1.4161	8	2	395.442
NCC-00062024	CCCc1n[nH]c(SC(C)C(N(CC2)CCN2S(c2ccccc2)(=O)=O)=O)n1	-7.8	N	2.0469	8	1	423.56

NCC-00032924	CCN(c1ccccc1)S(c(cc1)ccc1C(OC(CCCC1)C1=O)=O)(=O)=O	-7.7	N	3.0305	6	0	401.482
NCC-00056752	CCOc1c(COC(C(CCCC2)N2S(c2ccccc2)(=O)=O)=O)cccc1	-6.6	N	3.0971	6	0	403.498
NCC-00085012	COC(c([s]cc1)c1N(S(c1ccccc1)(=O)=O)S(c1ccccc1)(=O)=O)=O	-6.2	N	3.0045	7	0	437.516
NCC-00005521	O=S(C(CC1)CS1(=O)=O)(c1cc(S(Nc(c(F)ccc2)c2F)(=O)=O)ccc1)=O	-8.8	Y	0.5978	7	1	451.49
NCC-00019209	CCN(c1ccccc1)S(c1c(C)ccc(C(OC(CCO2)C2=O)=O)c1)(=O)=O	-6.9	N	2.0106	7	0	403.454
NCC-00033072	O=C(CC(c(cc1)ccc1Cl)NS(c1ccccc1)(=O)=O)OC(CCO1)C1=O	-6.5	N	2.1853	7	1	423.872
NCC-00031469	COCc1cc(NS(c(cc2)ccc2OC(F)(F)F)(=O)=O)cc2c1OCOC2	-7.6	N	2.3832	7	1	419.375
NCC-00001877	COc1cc(NS(c(cc(c(N2)c3)OCC2=O)c3Cl)(=O)=O)cc(OC)c1OC	-7.8	N	1.217	9	2	428.848
NCC-00068580	CC(c(cc1)cc(F)c1F)NC(C(CCCC1)N1S(c1ccccc1)(=O)=O)=O	-6.9	N	2.7749	5	1	408.468
NCC-00019583	CN(C(c(cc1)ccc1NS(c(cc1)cc(F)c1F)(=O)=O)=O)c1ccccc1	-9.8	Y	3.5572	5	1	402.42
NCC-00000884	CN(c1c(C(NCCc(cc2)ccc2Cl)=O)[s]cc1)S(c1ccccc1)(=O)=O	-7.3	N	3.6235	5	1	434.967
NCC-00004533	O=C(CN(c1cc(Cl)cc(Cl)c1)S(c1ccccc1)(=O)=O)N1CCCCCC1	-5.8	N	3.9011	5	0	441.378
NCC-00010790	CCOc(c1c2cccn1)ccc2S(Nc(cc1)cc(C(F)(F)F)c1Cl)(=O)=O	-8.9	N	4.0653	5	1	430.833
NCC-00009548	Cc1cc(O)nc(c(C)c2)c1cc2S(Nc(cc1)cc(C(F)(F)F)c1F)(=O)=O	-8.2	N	3.9173	5	2	414.378
NCC-00037615	CCN(c1ccccc1)S(c(cc1)ccc1OCc(cccc1)c1C#N)(=O)=O	-8.1	N	3.4539	5	0	392.478
NCC-00082540	CC(C)(C)c(cc1)ccc1S(Nc(c(C)ccc1)c1C(N1CCCC1)=O)(=O)=O	-6	N	4.3808	5	1	400.541
NCC-00036649	CCN(c1ccccc1)S(c(cc1)ccc1C(N(C)C1CCCCC1)=O)(=O)=O	-6.3	N	3.5312	5	0	400.541
NCC-00019083	CN(C)C(c1cccc(S(N(Cc2ccccc2)c2ccccc2)(=O)=O)c1)=O	-6.7	N	2.9873	5	0	394.494

NCC-00057240	Cc(ccc(NC(CCCc1ccc[s]1)=O)c1)c1NS(c1ccccc1)(=O)=O	-7.4	N	4.2236	5	2	414.549
NCC-00001015	CC(CC1)Sc(ccc(S(Nc2c(C)cc(C)cc2C)(=O)=O)c2)c2N1C(C)=O	-6.5	N	3.4697	5	1	418.58
NCC-00031103	Cc(cc1)cc(C)c1S(Nc(cc(C(F)(F)F)cc1)c1N1CCOCC1)(=O)=O	-7.1	N	3.1638	5	1	414.447
NCC-00012278	CC(CSc(ccc(S(Nc(c(OC)cc(OC)c1)c1Cl)(=O)=O)c1)c1N1)C1=O	-7.7	N	1.52	7	2	442.943
NCC-00055123	Cc(ccc(C(O)=O)c1)c1S(Nc1cc(OCc2ncccc2)ccc1)(=O)=O	-8.8	Y	2.1889	7	2	398.438
NCC-00055981	CC(C)(c(cc1)cc2c1OCCO2)NC(CN(C)S(c1ccccc1)(=O)=O)=O	-8.6	N	2.232	7	1	404.486
NCC-00081506	COc(cccc1)c1N(CC(CN1CCOCC1)O)S(c1ccccc1)(=O)=O	-5.6	N	0.8953	7	1	406.501
NCC-00001925	CCOc(cc1)cc(NS(c(cc2)ccc2-c2c[o]c(C)n2)(=O)=O)c1OCC	-7.2	N	3.1873	7	1	402.47
NCC-00003075	CCOC(c1cccc(NS(c(cc2)cc(CCC3)c2N3C(C)=O)(=O)=O)c1)=O	-8.3	Y	2.7105	7	1	402.47
NCC-00007040	CC(C)c(cc1)ccc1S(Nc(cc(cc1)C(O)=O)c1N1CCOCC1)(=O)=O	-6.7	N	2.2998	7	2	404.486
NCC-00000404	CCOc(cc1)ccc1N(C)S(c(cc(cc1)-c2cnc(C)[o]2)c1OC)(=O)=O	-7.6	N	2.6862	7	0	402.47
NCC-00006348	Cc1cc(O)nc(c(OC)c2)c1c(OC)c2S(Nc1c(C)c(F)ccc1)(=O)=O	-6.9	N	2.929	7	2	406.433
NCC-00003441	CCC(N(CCc1c2)c1cc(S(Nc(ccc(OC)c1)c1OC)(=O)=O)c2Br)=O	-7.7	N	3.0888	7	1	469.355
NCC-00011953	CC(C1)N(C(C)=O)c(cc2)c1cc2S(Nc(c(OC)cc(OC)c1)c1Cl)(=O)=O	-7.1	N	2.8399	7	1	424.904
NCC-00018931	CSc(cc(cc1)C(O)=O)c1NS(c(cc1)ccc1S(NC1CC1)(=O)=O)(=O)=O	-7.6	N	1.5761	8	3	442.536
NCC-00007099	COc(ccc(N(CCC1)S1(=O)=O)c1)c1NS(c(cc1)cc(F)c1OC)(=O)=O	-7.6	N	0.7425	8	1	430.476
NCC-00007175	COc(cc1)cc(S(Nc(cc2)cc(N(CCC3)S3(=O)=O)c2Cl)(=O)=O)c1OC	-8.4	Y	1.2477	8	1	446.931
NCC-00011648	CC(N1c(cc(cc2)S(N(C)c(cc(cc3)OC)c3OC)(=O)=O)c2OCC1)=O	-7.2	N	1.5674	8	0	406.458

NCC-00033709	CC(Nc(cc(cc1)S(N(CC2)c(cc3)c2cc3C(OC)=O)(=O)=O)c1OC)=O	-8.7	N	1.8229	8	1	404.442
NCC-00029266	Cc1nc(ccc(NS(c(cc(cc2)C(OC)=O)c2C(OC)=O)(=O)=O)c2)c2[s]1	-7.8	N	2.1358	8	1	420.465
NCC-00035632	CCOC(CSc1nc(cc(cc2)S(Nc(cc3)ccc3OC)(=O)=O)c2[o]1)=O	-8.3	Y	2.6747	8	1	422.481
NCC-00020752	O=C(c1cc(OC(F)F)ccc1)N(CC1)CCC1NS(c1ccccc1)(=O)=O	-7.9	N	2.956	6	1	410.44
NCC-00034267	Cc1cc(Cl)c(C)c(S(Nc(cc2)ccc2NC(C2OCCC2)=O)(=O)=O)c1Cl	-7.2	N	3.4557	6	2	443.35
NCC-00011728	CC(N1c(cc(cc2)S(Nc(cc3)ccc3OC(F)(F)F)(=O)=O)c2SCC1)=O	-8.3	N	2.5229	6	1	432.442
NCC-00036891	CN(c1ccccc1)S(c1cc(NC(COC2CCCCC2)=O)ccc1)(=O)=O	-8.1	N	2.6245	6	1	402.513
NCC-00012626	CCc(ccc(-c1cc(C)n[o]1)c1)c1S(N(C)c(cc1)ccc1OCC)(=O)=O	-7.1	N	3.5181	6	0	400.498
NCC-00089000	CC(CCc1ccc[o]1)NC(CN(C)S(c1cc(cccc2)c2cc1)(=O)=O)=O	-9	Y	3.0069	6	1	400.498
NCC-00073736	CCCN(CC(Nc(cccc1)c1OC)=O)S(c1cc(CCC2)c2cc1)(=O)=O	-6.5	N	3.2761	6	1	402.513
NCC-00012857	CC(C)(C)C(CN(c(cccc1)c1S(N1c2cc(C)cc(C)c2)(=O)=O)C1=O)=O	-7.1	N	3.8562	6	0	400.498
NCC-00008105	Cc(cc1)ccc1S(N(CC(N1CCOCC1)=O)c1c(C)c(C)ccc1)(=O)=O	-6	N	2.2148	6	0	402.513
NCC-00071700	CCCCN(Cc1cc(cc(cc2)OC)c2nc1O)S(c1ccccc1)(=O)=O	-7.2	N	3.8631	6	1	400.498
NCC-00012625	CCc(cccc1)c1N(C)S(c(cc(cc1)-c2c(C)c(C)n[o]2)c1OC)(=O)=O	-7.3	N	3.4557	6	0	400.498
NCC-00088798	Cc1ccc(C(CCC(N(CC2)CCC2NS(c2ccccc2)(=O)=O)=O)=O)[s]1	-8.3	Y	3.0979	6	1	420.553
NCC-00020483	Cc1c(C)c(S(N(CC2)c(cc3)c2cc3S(N(C)C)(=O)=O)(=O)=O)c(C)c(C)c1	7.2	N	2.8704	6	0	422.568
NCC-00013681	Cc(cc1)ccc1S(N(C)c1c(C)ccc(S(N2CCCC2)(=O)=O)c1C)(=O)=O	-6	N	2.7604	6	0	422.568
NCC-00057028	Cc1cc(OCC(CN(c2ncc[s]2)S(c2ccccc2)(=O)=O)O)c(C)cc1	-6.5	N	3.0346	6	1	418.537

NCC-00034664	Cc(ccc(C(NC(CC1)CCC1O)=O)c1)c1NS(c(cc1)ccc1F)(=O)=O	-8.1	N	2.5458	6	3	406.477
NCC-00036504	CCN(c1ccccc1)S(c(cc1)cc(C(NCC2OCCC2)=O)c1Cl)(=O)=O	-8.5	Y	2.6148	6	1	422.932
NCC-00076419	COC(C(C(F)(F)F)(c1c[nH]c2c1cccc2)NS(c1ccccc1)(=O)=O)=O	-6.4	N	2.7516	6	2	412.387
NCC-00035521	Cc(ccc(S(N1CCCCC1)(=O)=O)c1)c1NS(c(ccc(F)c1)c1F)(=O)=O	-7.1	N	2.711	6	1	430.495
NCC-00062395	N#Cc(ccc(NC(CN(c1ncc[s]1)S(c1ccccc1)(=O)=O)=O)c1)c1Cl	-7	N	2.7232	7	1	432.911
NCC-00038673	CN(C)c(cc1)ncc1NC(CCNS(c1cc(cccc2)c2cc1)(=O)=O)=O	-9.3	Y	2.4731	7	2	398.486
NCC-00009295	CC(CC(N(CC1)CCN1S(c1ccccc1)(=O)=O)=O)[n]1nc(C)c(Cl)c1C	-8.1	Y	2.2128	7	0	424.952
NCC-00035411	COc(cccc1)c1NS(c1cc(NC(C(CC2)=NNC2=O)=O)ccc1)(=O)=O	-8.1	Y	0.8058	9	3	402.43
NCC-00075874	CN(C(NC(C1(C(F)(F)F)NS(c2ccccc2)(=O)=O)=O)=C1C(N1C)=O)C1=O	-6.4	N	0.5178	9	2	418.351
NCC-00080826	COc(ccc(CCN1CN=C(NS(c2ccccc2)(=O)=O)NC1)c1)c1OC	-8.2	Y	2.4425	8	2	404.49
NCC-00011963	CN(c1cc(C(NCCN2CCOCC2)=O)ncc1)S(c1ccccc1)(=O)=O	-7.2	N	0.0246	8	1	404.49
NCC-00033935	Cc(cc(c(OC)c1)OC)c1S(Nc(cc1)ccc1Sc1nnc[n]1C)(=O)=O	-7.3	Y	2.1285	8	1	420.513
NCC-00005976	COc1cccc(C(NCCc2nnc(NS(c3ccccc3)(=O)=O)[s]2)=O)c1	-8.5	Y	2.0187	8	2	418.497
NCC-00016182	NC(Cc1c[s]c(NC(c(cc2)ccc2NS(c2ccccc2)(=O)=O)=O)n1)=O	-9.4	Y	1.8709	8	3	416.481
NCC-00038049	Cc1c(C(Nc2cc(S(Nc(cc3)ccc3Br)(=O)=O)c(C)cc2)=O)[s]cn1	-8.2	N	3.4327	6	2	466.379
NCC-00001550	CCOc(cc1)nnc1-c1cccc(NS(c(cc(cc2)F)c2F)(=O)=O)c1	-8.2	N	2.7684	6	1	391.397
NCC-00007616	CC(Nc1nc(cc(cc2)NS(c3cc(C(F)(F)F)ccc3)(=O)=O)c2[s]1)=O	-10.4	Y	3.3131	6	2	415.415
NCC-00003629	CCN(c1cc(C)ccc1)S(c1c(C)ccc(-c(cc2)nnc2O)c1)(=O)=O	-7.6	N	2.8841	6	1	383.471

NCC-00043008	CC(C)(C)c(cc1C)cc(C)c1S(Nc1c[n](CC2OCCC2)nc1)(=O)=O	-6.6	N	2.4402	6	1	391.534
NCC-00004337	CCN(CC(NCc1cnccc1)=O)S(c1cc(cccc2)c2cc1)(=O)=O	-6.5	N	1.9798	6	1	383.471
NCC-00067828	CCN(CC1)CCN1C(c(cccc1)c1N(C)S(c1ccccc1)(=O)=O)=O	-5.8	N	2.0539	6	0	387.503
NCC-00014730	CN(c1ccccc1)S(c(cc1)ccc1C(Nc([s]cc1)c1C#N)=O)(=O)=O	-6.9	N	2.821	6	1	397.478
NCC-00012247	CC(C1)Sc(ccc(S(Nc2cc(N(C)C)c(C)cc2)(=O)=O)c2)c2NC1=O	-7.1	N	1.6971	6	2	405.542
NCC-00035296	CCCc1nc(SC(CCCC2)C2NS(c2ccccc2)(=O)=O)nc(O)c1	-6.9	N	4.0055	6	2	407.558
NCC-00031085	CN(c1ccccc1)S(c1cccc(NC(c2cc(Br)cnc2)=O)c1)(=O)=O	-7.3	N	2.7357	6	1	446.324
NCC-00066982	CC(C)(C)c(cc1)ccc1S(Nc(cc(c(N1C)c2)N(C)C1=O)c2Br)(=O)=O	-6.2	N	3.8741	6	1	452.372
NCC-00011430	Cc(cc(cc1)NS(c2ccc(Cc(cc(C)nn3)c3O)cc2)(=O)=O)c1Br	-8.5	Y	3.4175	6	2	448.34
NCC-00036601	O=C(C1)NCCN1S(c1cccc(NS(c(cccc2)c2Cl)(=O)=O)c1)(=O)=O	-8	N	0.8978	8	2	429.904
NCC-00010282	Cc(ccc(S(N(C1)c(cccc2)c2NC1=O)(=O)=O)c1C)c1NS(C)(=O)=O	-6.9	N	0.6492	8	2	409.486
NCC-00037080	COCC[n]1ncc(cc2)c1cc2NS(c(cc1)ccc1S(C)(=O)=O)(=O)=O	-7.7	N	0.0971	8	1	409.486
NCC-00004062	CN(C)c(cc1)ccc1NS(c(cc1)ccc1N(C(CC1)=O)S1(=O)=O)(=O)=O	-7.5	N	0.1119	8	1	409.486
NCC-00003363	CN(c(ccc(NS(c(cc1)cc(Cl)c1OC)(=O)=O)c1)c1N(C)C1=O)C1=O	-7.2	N	0.9571	8	1	409.849
NCC-00007268	CCC(Nc1nc(ccc(NS(c(cc(cc2)Cl)c2OC)(=O)=O)c2)c2[s]1)=O	-7	N	3.4552	7	2	425.916
NCC-00003384	Cc(cc(cc1)S(Nc(cc(c(N(C)C2=O)c3)N(C)C2=O)c3Cl)(=O)=O)c1F	-7.2	N	1.4718	7	1	411.84
NCC-00061406	NC(c1cccc(NC(C(CCCC2)N2S(c2ccccc2)(=O)=O)=O)c1)=O	-7.5	N	1.6645	7	2	387.459
NCC-00079513	Cc(cc1)cc(NC(N(CC2)CCN2S(c2ccccc2)(=O)=O)=O)c1OC	-6.2	N	2.5801	7	1	389.475

NCC-00001092	Cc(cc1C)cc(C)c1S(Nc(cc1)cc(N(C)C2=O)c1N(C)C2=O)(=O)=O	-7.2	N	1.4528	7	1	387.459
NCC-00011918	Cc1cccc(N(C)S(c(cc2N(C)C3=O)c(C)cc2N(C)C3=O)(=O)=O)c1	-6.2	N	1.0141	7	0	387.459
NCC-00011862	CCc(cccc1)c1NS(c(cc1N(C)C2=O)c(C)cc1N(C)C2=O)(=O)=O	-8.8	Y	1.5245	7	1	387.459
NCC-00013395	CCN(c(ccc(S(Nc1ccc(C)cc1)(=O)=O)c1)c1N(CC)C1=O)C1=O	-7.4	N	1.5776	7	1	387.459
NCC-00017045	Cc(cc1)ccc1S(N(C)c(cc1)ccc1C(N(CCN1)CC1=O)=O)(=O)=O	-7.8	Y	1.1724	7	1	387.459
NCC-00004126	CCCc1n[o]c(-c(cc(cc2)S(Nc(cc3)ccc3Cl)(=O)=O)c2OC)n1	-9	Y	3.5277	7	1	407.877
NCC-00005476	O=C(CC(C(NCC1)=O)N1S(c1ccccc1)(=O)=O)NCCc1ccc[s]1	-6.8	N	1.164	7	2	407.514
NCC-00035078	CN(c(cc1)ccc1OC)S(c1cc(C(NC2=NCCS2)=O)ccc1)(=O)=O	-6.7	N	1.4371	7	1	405.498
NCC-00007316	CCc(cccc1)c1S(Nc1cc(OC)c2nc(NC(C)=O)[s]c2c1)(=O)=O	-6.4	N	3.1543	7	2	405.498
NCC-00016834	CC(Nc(ccc(S(Nc(cc1)ccc1-c1ncc[s]1)(=O)=O)c1)c1OC)=O	-7.1	Y	2.2475	7	2	403.482
NCC-00009142	O=C(CC(C(NCC1)=O)N1S(c1ccccc1)(=O)=O)Nc1cccc(Cl)c1	-7.2	N	1.7639	7	2	407.877
NCC-00011870	Cc(c(S(Nc1cc(C(F)(F)F)ccc1)(=O)=O)c1)cc(nc2O)c1nc2O	-10	Y	2.5999	7	3	399.348
NCC-00068854	CC(C)c1n[o]c(CN(c2ccn[n]2C(C)C)S(c2ccccc2)(=O)=O)n1	-6.1	N	1.6917	8	0	389.479
NCC-00061699	CC(C)[n]1nccc1NC(CN(c1ncc[s]1)S(c1ccccc1)(=O)=O)=O	-5.9	N	1.4387	8	1	405.502
NCC-00027250	Nc([n](C(c1cccc(S(Nc2cccc(Cl)c2)(=O)=O)c1)=O)nc1)c1C#N	-8.8	N	1.8906	8	2	401.833
NCC-00009031	OC(c1cccc(Oc(cc2)ccc2S(Nc(cc2)ccc2F)(=O)=O)c1)=O	-8.1	N	2.9402	6	2	387.386
NCC-00028645	COc(ccc(C(O)=O)c1)c1S(N(Cc1ccc[o]1)c1ccccc1)(=O)=O	-5.9	N	1.8858	7	1	387.411
NCC-00016977	CCOc(cc(CC(C)O1)c1c1)c1NS(c(cc1)cc(C(O)=O)c1Cl)(=O)=O	-7.3	N	2.9366	7	2	411.861

NCC-00002268	COCc1c(C(OC)=O)c(cc(cc2)NS(c(cc3)ccc3Cl)(=O)=O)c2[o]1	-8.5	Y	2.8139	7	1	409.845
NCC-00034545	COC(c(cc1)cc(CC2)c1N2S(c(cc1)cc(C(F)(F)F)c1Cl)(=O)=O)=O	-8.7	N	3.6435	5	0	419.806
NCC-00034618	O=S(c1cc(C(F)(F)F)ccc1)(Nc1cc(OCC2OCCC2)ccc1)=O	-9.4	Y	3.0368	5	1	401.404
NCC-00012245	CCCN(c(cccc1)c1F)S(c(cc1)cc(N2)c1SC(C)CC2=O)(=O)=O	-6.2	N	2.3235	5	1	408.517
NCC-00085780	Cc(cc1)ccc1S(Nc1c(CNc(cc2)ccc2OC)cccc1)(=O)=O	-7	N	3.2977	5	2	382.483
NCC-00009759	Cc(cc1)ccc1N(CC(CN1CCCC1)O)S(c1ccc(C)cc1)(=O)=O	-5.9	N	2.4751	5	1	388.53
NCC-00012614	CCCN(c(cccc1)c1F)S(c(cc1)cc(C2(C)C)c1N(C)C2=O)(=O)=O	-6.2	N	2.744	5	0	390.478
NCC-00011760	CCN(c1cc(C)ccc1)S(c(cc1)cc2c1SC(C)CN2C(C)=O)(=O)=O	-6.6	N	2.7514	5	0	404.554
NCC-00003853	CCCC(C)NC(c(cc1)cc(CC2)c1N2S(c(cc1)ccc1Br)(=O)=O)=O	-7.9	Y	4.1146	5	1	451.384
NCC-00084507	Cc(cc1C)cc(Cl)c1NC(C(CCCC1)N1S(c1ccccc1)(=O)=O)=O	-5.4	N	3.871	5	1	406.933
NCC-00034995	CC(CC1)CCN1C(c1cccc(S(Nc(cc(C)cc2)c2Br)(=O)=O)c1)=O	-8.2	N	4.1354	5	1	451.384
NCC-00030365	O=C(c(cc1)ccc1S(Nc1cc(CCC2)c2cc1)(=O)=O)NCC(F)(F)F	-8.7	Y	3.1029	5	2	398.404
NCC-00038169	O=C(Cc1ccc[s]1)Nc(cc1)cc(S(Nc(cc2)ccc2Cl)(=O)=O)c1Cl	-7.8	N	4.1829	5	2	441.358
NCC-00000931	CC(N(CC1)c(cc2)c1cc2S(N(CC(O)=O)c1ccc(C)cc1)(=O)=O)=O	-6.9	N	1.4283	7	1	388.443
NCC-00007600	CNC(C1(CC1)c(cc1)ccc1NS(c(cc(cc1)OC)c1OC)(=O)=O)=O	-7.6	N	1.3789	7	2	390.459
NCC-00030053	O=C(COC(CNS(c1ccccc1)(=O)=O)=O)Nc1cc(CCC2)c2cc1	-8.5	Y	1.9501	7	2	388.443
NCC-00037563	CCOC(c(cc1)ccc1S(Nc(cc1)ccc1N1CCOCC1)(=O)=O)=O	-8.4	Y	1.947	7	1	390.459
NCC-00027056	Cc(ccc(S(Nc(cc1)ccc1OC)(=O)=O)c1)c1NC(C1OCCC1)=O	-8.2	N	1.8298	7	2	390.459

NCC-00009706	CC(C)(CS(N1c(cc2)ccc2S(N(C)c2ccccc2)(=O)=O)(=O)=O)C1=O	-7.5	N	0.7215	7	0	408.498
NCC-00003896	CCN(c1ccccc1)S(c1c(C)ccc(N(C(CC2)=O)S2(=O)=O)c1)(=O)=O	-6.9	N	0.8709	7	0	408.498
NCC-00086812	COC(c1ccc(NC(C(CCC2)CN2S(c2ccccc2)(=O)=O)=O)[s]1)=O	-8.4	N	2.491	7	1	408.498
NCC-00004026	CCN(c1ccccc1)S(c(cc1)ccc1N(C(C(C)C1)=O)S1(=O)=O)(=O)=O	-6.1	N	0.7963	7	0	408.498
NCC-00012477	COc(c(NS(c(cc1)cc(CCC2)c1NC2=O)(=O)=O)c1)cc(OC)c1Cl	-7.5	N	2.218	7	2	410.877
NCC-00033194	COC(c(cc(cc1)Br)c1NS(c(cc1)ccc1N(CCC1)C1=O)(=O)=O)=O	-7.9	N	2.5217	7	1	453.312
NCC-00031765	NC(C(C1)Oc(cccc2)c2N1S(c(cccc1)c1OC(F)(F)F)(=O)=O)=O	-6.4	N	1.7788	7	1	402.348
NCC-00011726	Cc(cc(c(OC1)c2)NC1=O)c2S(N(C)c(ccc(OC)c1)c1OC)(=O)=O	-7	N	0.9301	8	1	392.431
NCC-00006315	Cc(cc(c(OC1)c2)NC1=O)c2S(Nc1ccc(CCC(O)=O)cc1)(=O)=O	-8.8	N	1.1025	8	3	390.415
NCC-00018646	Cc1cc(cccc2S(Nc(cc3)cc(OC(F)F)c3OC)(=O)=O)c2nc1	-7.1	N	2.718	6	1	394.397
NCC-00007162	CCCS(Nc(cc1)cc(CCC2)c1N2S(c(cc1)ccc1F)(=O)=O)(=O)=O	-7.9	N	2.7191	6	1	412.505
NCC-00007144	CCS(N(CCC1)c2c1ccc(NS(c(cc1)c(C)cc1F)(=O)=O)c2)(=O)=O	-6.9	N	2.6086	6	1	412.505
NCC-00035344	CN(c(cc1)ccc1Cl)S(c(cc(cc1)C(N2CCOCC2)=O)c1Cl)(=O)=O	-7.6	N	2.7502	6	0	429.323
NCC-00050669	COc(c(CN(c1ncc[s]1)S(c1ccccc1)(=O)=O)c1)cc(Br)c1OC	-6.4	N	3.4925	6	0	469.379
NCC-00012301	CCOc(cccc1)c1NS(c1c(C)ccc(-c2c(C)c(C)n[o]2)c1)(=O)=O	-8.1	Y	3.5412	6	1	386.471
NCC-00001765	CCN(c(cc1)ccc1OC)S(c(cc1)cc(CCC2)c1N2C(C)=O)(=O)=O	-7.4	N	2.6327	6	0	388.487
NCC-00020501	Cc(cc1)ccc1NS(c1cc(C(NCC2OCCC2)=O)c(C)cc1)(=O)=O	-9.6	Y	2.3851	6	2	388.487
NCC-00013116	CCOc(cc1)ccc1NC(C(CC1)=CCN1S(c1ccccc1)(=O)=O)=O	-7.7	N	2.7536	6	1	386.471

NCC-00008710	O=C(CN(CCc1ccccc1)S(c1ccccc1)(=O)=O)N1CCOCC1	-6.8	N	2.0456	6	0	388.487
NCC-00069736	Cc1cc(C(CN(Cc2ccc[o]2)S(c2ccccc2)(=O)=O)=O)c(C)[n]1C	-5.6	N	2.096	6	0	386.471
NCC-00005400	COc(ccc(S(Nc1ccc(Cc2ccncc2)cc1)(=O)=O)c1)c1OC	-8.3	Y	2.6337	6	1	384.455
NCC-00069706	COc(cccc1)c1N(CC(N1CCCCC1)=O)S(c1ccccc1)(=O)=O	-5.8	N	2.2771	6	0	388.487
NCC-00000620	Cc(cc1)ccc1S(Nc(cc(cc1)C(OC)=O)c1N1CCCCC1)(=O)=O	-6.9	N	3.0486	6	1	388.487
NCC-00007317	CC(CCC1)CN1c(cc1)cc(C(O)=O)c1NS(c1c(C)cccc1)(=O)=O	-8.5	N	2.89	6	2	388.487
NCC-00012260	CCOc(cc1)ccc1N(C)S(c(cc1)cc(N2)c1SC(C)CC2=O)(=O)=O	-8	N	1.6983	6	1	406.526
NCC-00057828	Cc([o]cc1)c1C(Nc(cc(cc1)NS(c2ccc(C)cc2)(=O)=O)c1F)=O	-9.6	Y	3.0835	6	2	388.418
NCC-00007058	CC(CCC1)CN1c(ccc(C(O)=O)c1)c1NS(c1cc(F)ccc1)(=O)=O	-6.4	N	2.6469	6	2	392.45
NCC-00017067	CCOc(ccc(NS(c1cc(NC(C2C(C)C2)=O)ccc1)(=O)=O)c1)c1Br	-7.3	N	3.3113	6	2	453.356
NCC-00011140	COc(cc1)ccc1N(C(c1cnccc1)=O)S(c(cc1)ccc1Cl)(=O)=O	-6	N	2.8995	6	0	402.857
NCC-00011668	CCCN(c(cccc1)c1Br)S(c(cc1)cc2c1OCCN2C(C)=O)(=O)=O	-6.3	N	3.2933	6	0	453.356
NCC-00049681	CN(CC(Nc1cc(C[n]2nccc2)ccc1)=O)S(c1ccccc1)(=O)=O	-8.3	Y	1.0904	7	1	384.459
NCC-00062825	Cc1c[n](CC(Nc2cc(NS(c3ccccc3)(=O)=O)c(C)cc2)=O)nc1	-8.4	Y	1.3509	7	2	384.459
NCC-00033609	C[n]1c(-c(cc2)ccc2NS(c(cc2)ccc2OC(F)(F)F)(=O)=O)nnc1	-7.4	N	2.6034	7	1	398.364
NCC-00016521	CC(C)(C)c(cc1)ccc1S(Nc(cc1)ccc1Sc1nnc[n]1C)(=O)=O	-8.9	Y	3.5065	6	1	402.542
NCC-00030147	CN(c1ccccc1)S(c1cc(NC(c(cc2)nnc2O)=O)ccc1)(=O)=O	-8.1	N	1.2413	8	2	384.415
NCC-00071172	Cc1nc(O)nc(O)c1S(Nc1cc(CCc2ncccc2)ccc1)(=O)=O	-8.4	N	2.0774	8	3	386.431

NCC-00003343	CC(Nc(cc1)cc(C)c1S(Nc(cc1)cc(N2C)c1N(C)C2=O)(=O)=O)=O	-8.2	N	1.6146	8	2	388.447
NCC-00036627	Cc(ccc(C(Nc1nnc[s]1)=O)c1)c1S(Nc(cc1)ccc1OC)(=O)=O	-8	N	2.1703	8	2	404.47
NCC-00034281	CC(C)NC(Nc(cccc1)c1NS(c(c(C)c(cc1C)Cl)c1Cl)(=O)=O)=O	-6.5	N	4.0568	6	3	430.355
NCC-00036085	Cc(c(Cl)c(NC(COC(CNS(c1ccccc1)(=O)=O)=O)=O)nc1)c1Cl	-8.1	Y	2.0417	8	2	432.283
NCC-00032046	CNC(CN(c(cccc1)c1C(NC)=O)S(c(cc1)ccc1OC)(=O)=O)=O	-5.8	N	0.3164	8	2	391.447
NCC-00061101	CCNc(ccc(C(OCC)=O)c1)c1NS(c(cc1)ccc1C(N)=O)(=O)=O	-6.8	N	1.4186	8	3	391.447
NCC-00058416	Cc(cc1C(O)=O)cc(S(Nc(cc(C(OC)=O)c(F)c2)c2F)(=O)=O)c1O	-6.6	N	1.5566	8	3	401.341
NCC-00006136	CCOC(c(cc1)ccc1NS(c(cc(C(C)C)c(C)c1)c1OC)(=O)=O)=O	-7.5	N	3.7389	6	1	391.486
NCC-00068479	CC(C)C(C(OC(C)C(c1ccccc1)=O)=O)NS(c1ccccc1)(=O)=O	-6.1	N	2.6941	6	1	389.471
NCC-00008729	Cc(cc1C)cc(C)c1S(Nc(cc(cc1)C(OC)=O)c1C(OC)=O)(=O)=O	-6.4	N	2.8164	7	1	391.443
NCC-00031661	Cc(cc1C)cc(C)c1S(N(CC(N)=O)c1cc(C(F)(F)F)ccc1)(=O)=O	-6.2	N	2.4761	5	1	400.42
NCC-00055782	CN(CC(Nc(cc(C(OC)=O)c(F)c1)c1F)=O)S(c1ccccc1)(=O)=O	-8.1	Y	1.7852	7	1	398.385
NCC-00014011	Cc(cc1)cc(C)c1NS(c(cc1)ccc1NC(CCC(OC)=O)=O)(=O)=O	-8.2	Y	2.4106	7	2	390.459
NCC-00006105	Cc(cc1C)cc(C)c1NS(c(cc1)ccc1NC(CCC(O)=O)=O)(=O)=O	-7.2	N	2.3266	7	3	390.459
NCC-00015904	Cc(cc1C)cc(C)c1NS(c(cc1)cc(N(C)S(C)(=O)=O)c1OC)(=O)=O	-6.1	N	1.8743	7	1	412.53
NCC-00056492	CCNc(ccc(C(OCC)=O)c1)c1NS(c(cc1)cc(Br)c1OC)(=O)=O	-6.2	N	2.9865	7	2	457.344
NCC-00030859	CC(C)NS(c(cc1)ccc1NS(c(cc(cc1)C(O)=O)c1Cl)(=O)=O)(=O)=O	-8.1	Y	1.9408	8	3	432.904
NCC-00030463	CC(c1c(C)[nH]c(C(COC(CNS(c2ccccc2)(=O)=O)=O)=O)c1C)=O	-7.9	Y	0.6923	8	2	392.431

NCC-00018639	O=C(COC(CCNS(c1ccccc1)(=O)=O)=O)NC(c1ccccc1)=O	-9	Y	1.3815	8	2	390.415
NCC-00029781	CC(Nc(cc1)cc(NS(c(cc(C(F)(F)F)cc2)c2Cl)(=O)=O)c1OC)=O	-7	N	3.0467	6	2	422.81
NCC-00019740	CC(C)(C)c(cc1C)cc(C)c1S(Nc1cc(OCC(N)=O)ccc1)(=O)=O	-7.4	N	2.8906	6	2	390.502
NCC-00014782	CC(C)CCNC(c(cc1)cc(S(Nc(cccc2)c2OC)(=O)=O)c1F)=O	-6.9	N	2.9617	6	2	394.466
NCC-00035582	CN(CCC#N)C(c(cc(cc1)S(Nc(cc2)ccc2Cl)(=O)=O)c1Cl)=O	-6.8	N	2.9823	6	1	412.296
NCC-00034283	CC(C)NC(Nc(cccc1)c1NS(c1cc(C(O)=O)ccc1)(=O)=O)=O	-7	N	1.6421	8	4	377.42
NCC-00019404	CCOC(c(cc1)ccc1S(Nc(cc(cc1)NC(N)=O)c1Cl)(=O)=O)=O	-7.7	Y	1.9652	8	3	397.838
NCC-00033626	CS(c(cc1)cc(NS(c2ccc(CCC(O)=O)cc2)(=O)=O)c1F)(=O)=O	-7.7	N	0.9991	7	2	401.434
NCC-00045148	CCC(C(OC)=O)OC(c1cccc(NS(c2ccccc2)(=O)=O)c1)=O	-8.6	Y	2.2433	7	1	377.416
NCC-00033815	CC(C)OC(c(cc1)ccc1NS(c(cc1)cc(OC)c1OC)(=O)=O)=O	-7.4	N	2.4973	7	1	379.432
NCC-00015408	CC(C)c(cc1)ccc1S(Nc(cc(c(OC)c1)OC)c1C(O)=O)(=O)=O	-6.5	N	2.4908	7	2	379.432
NCC-00063830	Cc(ccc(S(C)(=O)=O)c1)c1NS(c1c(C)c(C)cc(C(O)=O)c1)(=O)=O	-8	N	1.4775	7	2	397.471
NCC-00069547	CCS(c(cc1)ccc1NS(c(cc1OC)c(C)cc1OC)(=O)=O)(=O)=O	-6.4	N	1.6616	7	1	399.487
NCC-00035762	Cc(ccc(NS(c(cc(cc1)C(OC)=O)c1C(OC)=O)(=O)=O)c1)c1Cl	-7.1	N	2.7346	7	1	397.834
NCC-00013725	CCOC(C(C1(C(F)(F)F)NS(c2ccccc2)(=O)=O)=C(C)OC1=O)=O	-6.2	N	1.4505	7	1	393.337
NCC-00037975	CC(C)(C)c(cc1)ccc1S(N(CC(OC)=O)c1c(C)cccc1)(=O)=O	-6.5	N	3.3476	5	0	375.487
NCC-00017085	CCC(C)(C)NC(c(cc1)cc(NS(c(cc2)ccc2F)(=O)=O)c1Cl)=O	-7	N	3.7049	5	2	398.885
NCC-00013862	CNC(CN(c(cc(C(F)(F)F)cc1)c1Cl)S(c1ccccc1)(=O)=O)=O	-6.1	N	2.4019	5	1	406.811

NCC-00019046	CCCC(C)NC(c1c(C)ccc(S(Nc2c(C)cccc2)(=O)=O)c1)=O	-7.4	N	3.7597	5	2	374.503
NCC-00018719	CN(C)C(COC(c(cccc1)c1S(N(C)c1ccccc1)(=O)=O)=O)=O	-5.9	N	1.1271	7	0	376.432
NCC-00029507	CC(C(N)=O)OC(c(ccc(Cl)c1)c1NS(c1ccc(C)cc1)(=O)=O)=O	-6.9	N	1.9131	7	2	396.85
NCC-00033074	CCN(c1ccccc1)S(c(cc(C(OCC#N)=O)c(Cl)c1)c1Cl)(=O)=O	-6	N	3.0471	6	0	413.28
NCC-00007046	CCCCN(C)c(ccc(NS(c1cc(C)ccc1)(=O)=O)c1)c1C(O)=O	-6.6	N	2.9992	6	2	376.476
NCC-00064591	CC(c1ccc(C)[o]1)NC(C(CCSC)NS(c1ccccc1)(=O)=O)=O	-5.9	N	2.123	6	2	396.531
NCC-00090267	NC(COc(c(F)cc(SCCNS(c1ccccc1)(=O)=O)c1)c1F)=O	-7.3	N	1.7117	6	2	402.441
NCC-00061390	Cc1cc(NC(CN(C)C(CN(C)S(c2ccccc2)(=O)=O)=O)=O)n[o]1	-6.8	N	0.1804	9	1	380.424
NCC-00036473	NC(NCC(Nc(cc1)cc(S(Nc(cc2)ccc2Cl)(=O)=O)c1Cl)=O)=O	-8	N	1.3356	8	4	417.272
NCC-00019432	CC(NCc(cc1)ccc1S(Nc(cc1)cc2c1nc(SC)[s]2)(=O)=O)=O	-8.9	Y	2.3509	6	2	407.538
NCC-00036567	CN(c1ccccc1)S(c1cccc(C(Nc([s]2)ncc2Br)=O)c1)(=O)=O	-7.3	N	3.5666	6	1	452.352
NCC-00037914	O=S(c(cc(cc1)Cl)c1Cl)(Nc1cc(OCC[n]2nccc2)ccc1)=O	-8.1	Y	2.5077	6	1	412.296
NCC-00017502	Cc(cc1)ccc1S(Nc(cc1)ccc1Oc1nc(C)nc(C)c1)(=O)=O	-7.8	N	3.1177	6	1	369.444
NCC-00002155	CCc1nc(-c2cc(S(N(C)c3ccc(C)cc3)(=O)=O)c(C)cc2)n[o]1	-7.2	N	3.1303	6	0	371.46
NCC-00015585	Cc(cccc1)c1NS(c(cc1)ccc1C(NN1CCCCC1)=O)(=O)=O	-8.5	Y	1.7145	6	2	373.476
NCC-00004309	CC(C)C(N(CC1)C(Nc2ccccc2)=O)N1S(c1ccccc1)(=O)=O	-5.9	N	3.4632	6	1	373.476
NCC-00013101	CCN1C(CNC(C(CC2)=CCN2S(c2ccccc2)(=O)=O)=O)CCC1	-8.6	Y	1.5241	6	1	377.507
NCC-00045955	CC(C)(C)c(cc1)ccc1S(Nc(cc1)ccc1-[n]1c(O)ncc1)(=O)=O	-8.1	N	3.187	6	2	371.46

NCC-00012320	CC(C)CC(Nc(cc1)cc2c1nc(NS(c1ccccc1)(=O)=O)[s]2)=O	-6.5	N	3.5919	6	2	389.499
NCC-00007541	CCC(Nc1nc(cc(cc2)NS(c3c(C)ccc(C)c3)(=O)=O)c2[s]1)=O	-6.6	N	3.607	6	2	389.499
NCC-00064645	CC(c1cccc(S(Nc2cc(Sc3ncccc3)ncc2)(=O)=O)c1)=O	-8	N	1.844	6	1	385.467
NCC-00076687	CCNC(CCSc1nc(cccc2)c2[n]1S(c1ccccc1)(=O)=O)=O	-6.2	N	2.2648	6	1	389.499
NCC-00010845	CC1SC(N(c2ccccc2)S(c(cc2)ccc2NC(C)=O)(=O)=O)=NC1	-6.2	N	2.4441	6	1	389.499
NCC-00003552	Cc(ccc(-c(cc1)nnc1O)c1)c1S(Nc1cc(Cl)c(C)cc1)(=O)=O	-8.4	N	3.1786	6	2	389.862
NCC-00031591	CCc1nnc(COC(C(CCCC2)N2S(c2ccccc2)(=O)=O)=O)[o]1	-6.6	N	1.4814	8	0	379.436
NCC-00011887	CCOc(cccc1)c1NS(c(c(C)c1)cc(nc2O)c1nc2O)(=O)=O	-7.5	N	2.0879	8	3	375.404
NCC-00011161	CCCN(c(cccc1)c1C(O)=O)S(c(cc1)cc2c1[nH]c(O)n2)(=O)=O	-6.6	N	1.6627	8	3	375.404
NCC-00011879	CC(c(cc1)ccc1NS(c(c(C)c1)cc(nc2O)c1nc2O)(=O)=O)=O	-8.3	N	1.6228	8	3	373.388
NCC-00011900	Cc(c(S(Nc(cc1)cc(Cl)c1OC)(=O)=O)c1)cc(nc2O)c1nc2O	-7.9	N	2.2876	8	3	395.822
NCC-00033393	CCCc(cc1)ccc1S(Nc(cc1)ccc1-c1nc(C)ncc1)(=O)=O	-9.7	Y	3.593	5	1	367.472
NCC-00034661	CC(C)(C)c(cc1)ccc1S(Nc1cc(C[n]2nccc2)ccc1)(=O)=O	-8	Y	2.9604	5	1	369.488
NCC-00081468	Cc(cc1)ccc1S(Nc1c(CNc(cc2)ncc2Br)cccc1)(=O)=O	-6.7	N	3.4434	5	2	432.341
NCC-00027260	CC(C)[n]1nccc1N(Cc(cc1)ccc1Br)S(c1ccccc1)(=O)=O	-5.9	N	3.1643	5	0	434.357
NCC-00033504	O=S(c1ccc(C(F)(F)F)cc1)(Nc1c(C[n]2nccc2)cccc1)=O	-7.2	N	2.2268	5	1	381.377
NCC-00001726	CC(c(cc1)ccc1NS(c1c(C)ccc(-c2nc(C)n[o]2)c1)(=O)=O)=O	-9.2	Y	2.3368	7	1	371.416
NCC-00066267	Cc(ccc(S(Nc1cc(C[n]2nccc2)ccc1)(=O)=O)c1)c1C(O)=O	-10	Y	1.2075	7	2	371.416

NCC-00016896	CCOc(cc1)ccc1S(Nc(cccc1)c1-[n]1c(O)ncc1C)(=O)=O	-6.8	N	2.3393	7	2	373.432
NCC-00009360	Cc1cccc(C)c1NS(c(cc1)cc(C(N2C)=O)c1N(C)C2=O)(=O)=O	-7.8	N	2.1101	7	1	373.432
NCC-00066277	Oc(cc1)ncc1C(NCC(CC1)CCN1S(c1ccccc1)(=O)=O)=O	-9.1	Y	1.668	7	2	375.448
NCC-00004500	CC(Nc(cc1)cc(S(Nc(cc2)cc3c2nc(C)[s]3)(=O)=O)c1OC)=O	-8	N	1.9435	7	2	391.471
NCC-00009460	Cc(cc1C)cc(NS(c(cc(c(N2C)c3)OC2=O)c3Cl)(=O)=O)c1C#N	-7	N	2.8884	7	1	391.834
NCC-00004283	Cc1nc(C)n[n]1CCC(N(CC1)CCN1S(c1ccccc1)(=O)=O)=O	-6.7	Y	0.6667	8	0	377.468
NCC-00031448	Cc(cc(cc1)S(Nc(cc2)ccc2C(Nc2n[nH]cn2)=O)(=O)=O)c1F	-10.7	Y	1.6903	8	3	375.383
NCC-00016898	Cc1nnn[n]1-c1c(C)ccc(NS(c(cc(cc2)Br)c2OC)(=O)=O)c1	-7.5	N	2.0898	8	1	438.305
NCC-00035977	C[n]1nnnc1-c(cc1)cc(S(Nc(cccc2)c2OC)(=O)=O)c1OC	-7.6	N	1.2538	9	1	375.408
NCC-00027687	Cc1cc(C(O)=O)cc(S(Nc2cc(-c3n[nH]nn3)ccc2)(=O)=O)c1C	-8.1	N	1.398	9	3	373.392
NCC-00029037	COc(cc1)ccc1N(Cc([s]1)ccc1Cl)S(c(cc1)ccc1F)(=O)=O	-5.9	N	3.9901	4	0	411.904
NCC-00004624	COc(cc1)c(C(F)(F)F)cc1S(N(CCCC1)c2c1cccc2)(=O)=O	-6.5	N	3.7385	4	0	385.405
NCC-00033398	CN(c1ccccc1)S(c1cc(C(OCC2OCCC2)=O)ccc1)(=O)=O	-8.3	Y	2.0767	6	0	375.444
NCC-00008154	CC(c(c1c2)c(C)[o]c1cc(C)c2NS(c(cc1)ccc1OC)(=O)=O)=O	-7.4	N	2.9533	6	1	373.428
NCC-00035285	O=C(c1cccc(S(Nc(cc2)ccc2F)(=O)=O)c1)OC(CCO1)C1=O	-9.2	Y	1.456	7	1	379.363
NCC-00015317	O=S(c(cc(C(F)(F)F)cc1)c1Cl)(Nc(cc1OCCOc1c1)c1Cl)=O	-8.2	N	3.9978	5	1	428.213
NCC-00056472	OC(c(cc1)cc(NS(c2ccc(C3CCCCC3)cc2)(=O)=O)c1F)=O	-8	Y	3.6814	5	2	377.435
NCC-00031910	CN(CC(Nc(cc1)cnc1-[n]1ncnc1)=O)S(c1ccccc1)(=O)=O	-8.1	Y	1.1548	9	1	372.408

NCC-00031161	Cc(cc1)c(C)cc1NS(c(cc1)ccc1C(Nc1n[nH]nn1)=O)(=O)=O	-10	Y	1.7869	9	3	372.408
NCC-00003461	CC(Cc1c2)N(C(C)=O)c1cc(S(Nc1c(C)c(Cl)ccc1)(=O)=O)c2Br	-7.9	N	4.049	5	1	457.775
NCC-00007123	CC(C)(C)C(Nc1cc(N(CCC2)S(c3ccccc3)(=O)=O)c2cc1)=O	-6.8	N	3.5604	5	1	372.488
NCC-00003759	CCC(C)NC(CN(c(ccc(CC)c1)c1-c1c2cccc1)S2(=O)=O)=O	-8.3	N	3.3645	5	1	372.488
NCC-00013896	CC(C)(C=C(C)c1c2cccc1)N2S(c(cc1)ccc1NC(C)=O)(=O)=O	-6.9	N	2.859	5	1	370.472
NCC-00007274	CCN(C(CC1)=O)c(cc2)c1cc2NS(c1ccc(C(C)C)cc1)(=O)=O	-7.5	N	3.3616	5	1	372.488
NCC-00003301	CCC(N(CC1)c(cc2)c1cc2S(Nc1c(CC)cccc1C)(=O)=O)=O	-7.7	N	3.607	5	1	372.488
NCC-00012621	CCc(cccc1)c1N(C)S(c(cc1)cc(C2(C)C)c1N(C)C2=O)(=O)=O	-6.5	N	2.542	5	0	372.488
NCC-00018669	CCc1c(C)cc(C(N(CC2)CCC2NS(c2ccccc2)(=O)=O)=O)[s]1	-5.8	N	3.8388	5	1	392.543
NCC-00086071	CC(c(c(F)ccc1)c1N(CC1)CCC1NS(c1ccccc1)(=O)=O)=O	-6.6	N	2.7533	5	1	376.451
NCC-00087463	CN(Cc1ccc[s]1)C(CN(C)S(c1cc(cccc2)c2cc1)(=O)=O)=O	-7.4	Y	2.7075	5	0	388.511
NCC-00027117	Cc1cc(S(N(Cc2c[s]cn2)c(cc2)ccc2OC)(=O)=O)c(C)cc1	-5.2	N	2.7311	5	0	388.511
NCC-00011765	CCc(cc1)ccc1NS(c(cc1)cc2c1SC(C)CN2C(C)=O)(=O)=O	-9.3	Y	2.8555	5	1	390.527
NCC-00012027	CCC1Sc(ccc(S(Nc2c(C)cc(C)cc2C)(=O)=O)c2)c2NC1=O	-6.5	N	2.6009	5	2	390.527
NCC-00014045	Cc1cccc(Cl)c1NS(c1c(C)c(N(CCC2)C2=O)c(C)cc1)(=O)=O	-5.9	N	3.5212	5	1	392.906
NCC-00056859	Cc1n[o]c(COC(c2cccc(NS(c3ccccc3)(=O)=O)c2)=O)c1	-7.5	N	2.152	7	1	372.4
NCC-00032180	CN(c(cccc1)c1C(OC)=O)S(c(cc1)cc(C2)c1N(C)C2=O)(=O)=O	-5.9	N	1.2445	7	0	374.416
NCC-00012681	COc1cc(NS(c(cc2)ccc2N(CCC2)C2=O)(=O)=O)cc(OC)c1	-7.2	Y	1.7435	7	1	376.432

NCC-00000433	CCCN(c(ccc(NS(c(cc(cc1)Cl)c1OC)(=O)=O)c1)c1O1)C1=O	-7.1	N	3.1557	7	1	396.85
NCC-00016133	NS(c(cc1)cc(CC2)c1N2S(c(cc(cc1)C(O)=O)c1Br)(=O)=O)(=O)=O	-8.2	N	1.2505	8	2	461.312
NCC-00038279	O=S(c1ccccc1)(N(Cc1cc(C(F)(F)F)ccc1)c1ncc[s]1)=O	-5.9	N	3.7556	4	0	398.428
NCC-00038230	Cc1c[s]c(Sc(cc2)ccc2NS(c2cc(C(O)=O)ccc2)(=O)=O)n1	-8.8	Y	2.9876	6	2	406.506
NCC-00037979	Cc(cc1)cc(Br)c1S(N(CCC1)c2c1c(NS(C)(=O)=O)ccc2)(=O)=O	-6.6	N	2.736	6	1	459.384
NCC-00007271	CCN(C(C1)=O)c(cc2)c1cc2NS(c(cc(C)c(C)c1)c1OC)(=O)=O	-8.6	Y	2.4504	6	1	374.46
NCC-00000415	CCCN(c(ccc(NS(c1c(C)c(C)cc(C)c1)(=O)=O)c1)c1O1)C1=O	-7.3	N	3.6514	6	1	374.46
NCC-00011727	CCCCN(c1ccccc1)S(c(cc1OC2)c(C)cc1NC2=O)(=O)=O	-6.5	N	2.3852	6	1	374.46
NCC-00028952	CN(c(cc1)ccc1OCC(c1ccc[nH]1)=O)S(c1ccccc1)(=O)=O	-8.1	Y	1.5303	6	1	370.428
NCC-00032022	CC(Nc(cc(cc1)S(N(CCC2)c3c2cccc3C)(=O)=O)c1OC)=O	-6.1	N	2.5958	6	1	374.46
NCC-00027229	CCN(c1ccccc1)S(c(cc1)ccc1C(N1CCOCC1)=O)(=O)=O	-6.4	N	1.9445	6	0	374.46
NCC-00057415	OC(CN(CC1)CCN1S(c1ccccc1)(=O)=O)COCc1ccc[s]1	-7.3	Y	1.4366	6	1	396.531
NCC-00065323	COC(c1ccc(CN(c2ncc[s]2)S(c2ccccc2)(=O)=O)cc1)=O	-6.5	N	2.8203	6	0	388.467
NCC-00007116	Cc(c(C)c1)cc(C)c1S(Nc1cccc(N(CCC2)S2(=O)=O)c1)(=O)=O	-8.3	N	1.8134	6	1	394.515
NCC-00019332	COc(cccc1)c1NS(c(cc(cc1)NC(C2CCC2)=O)c1Cl)(=O)=O	-7.4	N	2.8585	6	2	394.878
NCC-00001723	CC(N(CCC1)c(cc2)c1cc2S(Nc(cc(cc1)Cl)c1OC)(=O)=O)=O	-7.2	N	2.9272	6	1	394.878
NCC-00028026	CN(C)c(c(NS(c1c(CCC2)c2cc(C(O)=O)c1)(=O)=O)ccc1)c1Cl	-6.4	N	2.761	6	2	394.878
NCC-00034264	O=C1OCCN1c1cccc(NS(c2ccc(C(F)(F)F)cc2)(=O)=O)c1	-8	N	2.4895	6	1	386.349

NCC-00056033	Cc1cc(C)n[n]1CC(N(CC1)CCC1NS(c1ccccc1)(=O)=O)=O	-7.7	N	1.1393	7	1	376.48
NCC-00067354	CC(NCCc1nc(cc(cc2)NS(c3ccccc3)(=O)=O)c2[n]1C)=O	-8.9	Y	1.4238	7	2	372.448
NCC-00043390	O=C(CCNS(c1ccccc1)(=O)=O)NCC[n]1c(cccc2)c2nc1	-7.9	Y	1.4002	7	2	372.448
NCC-00027825	Cc(cc1)c[n]2c1nc(CNC(CCNS(c1ccccc1)(=O)=O)=O)c2	-8.3	Y	1.0816	7	2	372.448
NCC-00030293	CN(C)c(ccc(C(F)(F)F)c1)c1NS(c1c2nsnc2ccc1)(=O)=O	-6.8	N	3.22	6	1	402.42
NCC-00085537	CC(C)(C)c(cc1)ccc1S(Nc(cc1)ccc1-c1nnc[n]1C)(=O)=O	-8.7	Y	3.0863	6	1	370.476
NCC-00057523	NC(c(cc1)ccc1S(Nc1cnc(-c2cc(O)ccc2)nc1)(=O)=O)=O	-9.5	Y	0.7801	8	3	370.388
NCC-00064465	CC(C)(C)NC(N(CC1)CCN1S(c1cc(CCC2)c2cc1)(=O)=O)=O	-7.4	N	2.5585	6	1	365.496
NCC-00013121	O=C(C(CC1)=CCN1S(c1ccccc1)(=O)=O)NCc1cnccc1	-8.1	Y	1.1258	6	1	357.433
NCC-00007525	CCC(Nc(cc1)ccc1S(N1c(cccc2)c2N(C)CC1)(=O)=O)=O	-6.7	N	1.9953	6	1	359.449
NCC-00007520	CC(Nc(ccc(C)c1)c1S(N1c(cccc2)c2N(C)CC1)(=O)=O)=O	-6.2	N	1.8848	6	1	359.449
NCC-00062151	O=C(c1cc(Br)cnc1)N(CC1)CCC1NS(c1ccccc1)(=O)=O	-7.3	N	2.5109	6	1	424.318
NCC-00033977	CN(c(cccc1)c1C(N)=O)S(c(cc1)cc(N2)c1OCC2=O)(=O)=O	-6.2	N	-0.1865	8	2	361.377
NCC-00010527	N#Cc(cc(c(N(CC1)CCN1S(c1ccccc1)(=O)=O)c1)F)c1Cl	-7.2	N	2.8494	5	0	379.842
NCC-00068483	CC(C)(C)c(cc1)ccc1S(NCCc1c[n](CCCC2)c2n1)(=O)=O	-8.3	Y	4.0068	5	1	361.508
NCC-00029800	N#Cc1cccc(S(Nc(cc(cc2)Cl)c2N2CCCCC2)(=O)=O)c1	-6.4	N	3.2333	5	1	375.879
NCC-00004586	CC(C)c1ncc[n]1-c(cc1)ccc1NS(c(cc1)ccc1Br)(=O)=O	-8.3	Y	3.383	5	1	420.33
NCC-00031212	Cc1cc(NC(CCNS(c2cc(cccc3)c3cc2)(=O)=O)=O)n[o]1	-9.9	Y	2.3858	7	2	359.405

NCC-00037318	Cc1cccc(N(C)S(c(cc2)cc(C(N3)=O)c2NC3=O)(=O)=O)c1C	-7.7	N	1.4041	7	2	359.405
NCC-00011869	Cc(cc1)ccc1N(C)S(c(c(C)c1)cc(nc2O)c1nc2O)(=O)=O	6.8	N	2.0007	7	2	359.405
NCC-00011868	COc1cc(NS(c(cc2)ccc2-[n]2nccc2)(=O)=O)cc(OC)c1	-6.9	N	0.9875	7	1	359.405
NCC-00009498	Cc(c(F)ccc1)c1NS(c(cc1)cc(C(N2C)=O)c1NC2=O)(=O)=O	-10.3	Y	1.5087	7	2	363.368
NCC-00009619	CN(c(c(O1)c2)cc(Cl)c2S(Nc2ccc(CC#N)cc2)(=O)=O)C1=O	-8.1	N	2.3701	7	1	377.807
NCC-00003351	CN(c(c(N1C)c2)cc(NS(c(cccc3)c3Cl)(=O)=O)c2OC)C1=O	-7.1	N	2.103	7	1	381.839
NCC-00011905	Cc(cc1)cc(Br)c1NS(c(c(C)c1)cc(nc2O)c1nc2O)(=O)=O	-7.8	N	2.8207	7	3	424.274
NCC-00016440	Nc1nnc[n]1C(c(cccc1)c1NS(c(cc1)ccc1Br)(=O)=O)=O	-7.1	N	2.0327	8	2	422.262
NCC-00011198	CCc(cc1)ccc1S(Nc(cc1)cc2c1[o]c(C)c2C(O)=O)(=O)=O	-10.6	Y	3.0528	6	2	359.401
NCC-00031374	COc(ccc(NS(c1cc(CCC2)c2cc1)(=O)=O)c1)c1OCCO	-7.3	N	2.1131	6	2	363.433
NCC-00076955	COc1cccc(N(C(C2)C=CS2(=O)=O)S(c2ccccc2)(=O)=O)c1	-5.7	N	1.2564	6	0	379.456
NCC-00013882	Cc(ccc(C(OC)=O)c1)c1NS(c(cc1)cc2c1OCCO2)(=O)=O	-8.4	Y	2.1944	7	1	363.389
NCC-00004639	OC(CN(c(cc1)ccc1F)S(c(cc1)cc2c1OCCO2)(=O)=O)=O	6.5	N	1.0735	7	1	367.352
NCC-00010731	Cc(cc1)ccc1S(N(C(C1)C=CS1(=O)=O)c(cc1)ccc1Br)(=O)=O	-6.1	N	2.3955	5	0	442.353
NCC-00006313	Cc(c(OC)c1C)c(C)c(OC)c1S(N(CC1)c2c1cccc2)(=O)=O	-6.1	N	3.1679	5	0	361.461
NCC-00003010	CC(CCc(cc1)c2cc1F)N2S(c(cc(cc1)OC)c1OC)(=O)=O	-6.2	N	2.9037	5	0	365.424
NCC-00057947	CCCC[n]1nnnc1CN(c1ncc[s]1)S(c1ccccc1)(=O)=O	-6.5	N	1.7537	8	0	378.48
NCC-00033247	O=S(c1ccccc1)(N(CCOc1cccc(Cl)c1)c1ncc[s]1)=O	-5.6	N	3.5202	5	0	394.902

NCC-00019949	O=C(C1)Nc(cc2)c1cc2S(Nc(cc1)cc(C(F)(F)F)c1Cl)(=O)=O	-10.6	Y	2.5223	5	2	390.768
NCC-00006220	CC(C)(C)c(cc(cc1)S([n]2c(cccc3)c3nc2C)(=O)=O)c1OC	-6.7	N	3.2557	5	0	358.461
NCC-00012624	Cc(cc1)c(C)cc1N(C)S(c(cc1)cc(CCC2)c1NC2=O)(=O)=O	-8.7	Y	2.345	5	1	358.461
NCC-00011811	CC(C)(c(cc(cc1)S(Nc2cc(C)cc(C)c2)(=O)=O)c1N1C)C1=O	-7.9	N	2.5651	5	1	358.461
NCC-00007257	Cc1c(C)c(S(Nc(cc2)cc(CC3)c2NC3=O)(=O)=O)c(C)c(C)c1	-8.5	N	2.7856	5	2	358.461
NCC-00012191	CC(C)c(cc1)ccc1NS(c(cc1)cc(C2(C)C)c1NC2=O)(=O)=O	-7.6	N	2.706	5	2	358.461
NCC-00007258	CC(C)(C)c(cc1)ccc1S(Nc(cc1)cc(CC2)c1NC2=O)(=O)=O	-8.7	N	2.9919	5	2	358.461
NCC-00056589	Cc1cc(C(CN(C)S(c2cc(cccc3)c3cc2)(=O)=O)=O)c(C)[nH]1	-8.1	N	2.5508	5	1	356.445
NCC-00012302	CC(CSc(ccc(S(Nc1c(C)cc(C)cc1)(=O)=O)c1)c1N1)C1=O	-8.7	Y	1.7418	5	2	376.5
NCC-00012283	CC(CSc(ccc(S(N(C)c1cc(C)ccc1)(=O)=O)c1)c1N1)C1=O	-7.1	N	1.3031	5	1	376.5
NCC-00000811	Cc1nc(-c(cc2)cc(S(Nc3c(C)cccc3)(=O)=O)c2OC)c[s]1	-7.9	N	3.1568	5	1	374.484
NCC-00012515	CCc(cccc1C)c1NS(c(cc1)cc(N2)c1SCCC2=O)(=O)=O	-6.3	N	1.8881	5	2	376.5
NCC-00002903	CC(N(CCc1c2)c1cc(S(Nc1c(C)cc(C)cc1)(=O)=O)c2Br)=O	-7.9	N	3.4622	5	1	423.33
NCC-00031471	CN(C)C(c(ccc(Cl)c1)c1NS(c1cc(CCC2)c2cc1)(=O)=O)=O	-7.2	N	3.0848	5	1	378.879
NCC-00003740	CC(C)CNC(CN(c(ccc(Br)c1)c1-c1c2cccc1)S2(=O)=O)=O	-6.5	N	3.1892	5	1	423.33
NCC-00032464	O=C(C1CC1)Nc(cc(cc1)NS(c(ccc(Br)c2)c2Cl)(=O)=O)c1F	-7.6	N	3.4125	5	2	447.711
NCC-00013857	O=C(C(F)(F)F)Nc(cc1)ccc1S(N(CC1)c2c1cccc2)(=O)=O	-7.5	N	2.4642	5	1	370.35
NCC-00035079	O=S(c(c(F)cc(F)c1)c1Br)(Nc(cccc1)c1N1CCOCC1)=O	-6.1	N	2.5545	5	1	433.272

NCC-00000394	CCN(c(ccc(NS(c(cc1)ccc1OCC)(=O)=O)c1)c1O1)C1=O	-9.6	Y	2.5016	7	1	362.405
NCC-00069936	Cc1cccc(NS(c(cc2)cc(c(C(O)=O)c3)c2nc3O)(=O)=O)c1	-9.6	Y	1.939	7	3	358.373
NCC-00086336	Cc1nc(cc(cc2)NS(c3c(C)c(C)cc(C(O)=O)c3)(=O)=O)c2[o]1	-8.1	N	2.3768	7	2	360.389
NCC-00009368	Cc(ccc(S(Nc(cc1)cc2c1OCCO2)(=O)=O)c1)c1C(NC)=O	-9.8	Y	1.7202	7	2	362.405
NCC-00037561	NC(COC(c1cccc(S(N(CC2)c3c2cccc3)(=O)=O)c1)=O)=O	-8.3	N	0.9214	7	1	360.389
NCC-00027646	[O-]C(c1cc(O)nc(cc2)c1cc2S(Nc(cc1)ccc1F)(=O)=O)=O	-8.1	Y	-0.3801	7	2	361.328
NCC-00016406	COC(Nc(cc1)ccc1S(Nc(cc1)cc2c1OCCO2)(=O)=O)=O	-8.1	Y	1.8444	8	2	364.377
NCC-00013748	Cc1nc(cc(cc2)NS(c(cc3)cc(C(F)(F)F)c3Cl)(=O)=O)c2[s]1	-10	Y	3.7641	4	1	406.835
NCC-00031238	Cc1cc(C(O)=O)cc(S(Nc2cccc3c2nccc3)(=O)=O)c1C	-9.8	Y	2.4476	6	2	356.401
NCC-00052723	CN(CC(NC(C1)COc2c1cccc2)=O)S(c1ccccc1)(=O)=O	-7.4	N	1.693	6	1	360.433
NCC-00015063	CC(Cc1c2cccc1)N2S(c(cc1)cc(OC)c1NC(C)=O)(=O)=O	-7.1	Y	2.2346	6	1	360.433
NCC-00015521	CNC(c(cc1)ccc1S(N(CCC1)c(cc2)c1cc2OC)(=O)=O)=O	-7.3	Y	1.987	6	1	360.433
NCC-00000790	CC(c(cc1)ccc1S(Nc1cc(C(N2)SCC2=O)ccc1)(=O)=O)=O	-9	Y	1.1751	6	2	376.456
NCC-00008081	CCOC(CSc1nc(cccc2)c2[n]1S(c1ccccc1)(=O)=O)=O	-6.1	N	2.2846	6	0	376.456
NCC-00061639	Cc(nc1)cnc1C(N(CC1)CCC1NS(c1ccccc1)(=O)=O)=O	-8.6	Y	1.2367	7	1	360.437
NCC-00083153	CNC(c(cc1)cnc1N(CC1)CCN1S(c1ccccc1)(=O)=O)=O	-8.4	Y	1.0963	7	1	360.437
NCC-00046280	Cc(ccc(NC(c1n[nH]cc1)=O)c1)c1NS(c1ccccc1)(=O)=O	-7.5	N	1.3977	7	3	356.405
NCC-00074236	N#Cc1cccc(S(Nc2cc(Oc3ncccn3)ccc2)(=O)=O)c1	-8.5	Y	1.9962	7	1	352.373

NCC-00031008	CC(Nc1nc(CN(CC2)CCN2S(c2ccccc2)(=O)=O)c[s]1)=O	-8.2	N	1.6129	7	1	380.492
NCC-00031607	Cc1nc(-c(cccc2)c2NS(c(cc(cc2)Br)c2OC)(=O)=O)n[nH]1	-6.5	N	2.2602	7	2	423.29
NCC-00088539	CC(C)c(cc1)ccc1S(Nc1cc(-c2n[nH]c(C)n2)ccc1)(=O)=O	-10	Y	2.792	6	2	356.449
NCC-00076491	O=C(CC(C(NCC1)=O)N1S(c1ccccc1)(=O)=O)Nc1ncc[s]1	-6.3	N	0.7832	8	2	380.448
NCC-00020634	CC(C)c(cc1)ccc1S(NCCC(Nc1nccc(C)c1)=O)(=O)=O	-9	Y	2.9132	6	2	361.465
NCC-00038560	CC(C)(C)c(cc1)ccc1S(NCCC(Nc1ncc(C)[s]1)=O)(=O)=O	-7.6	Y	3.6651	6	2	381.52
NCC-00016558	Cc1cc(C(O)=O)cc(S(Nc(cccc2)c2OC(F)F)(=O)=O)c1C	-8.5	Y	2.301	6	2	371.359
NCC-00028835	Cc1cc(OC)cc(C)c1S(Nc(cc1)cc(C(OC)=O)c1Cl)(=O)=O	-6.9	N	3.0955	6	1	383.851
NCC-00017857	COC(c1cccc(S(Nc(cccc2)c2OC(F)(F)F)(=O)=O)c1)=O	-6.3	N	2.9707	6	1	375.322
NCC-00016100	CN(c(cccc1)c1C(OC)=O)S(c(cc(cc1)OC)c1OC)(=O)=O	-5.9	N	1.6369	7	0	365.405
NCC-00045184	CC(c1cccc(S(Nc(cc2OC)cc(OC)c2OC)(=O)=O)c1)=O	-7.1	N	1.6199	7	1	365.405
NCC-00038158	CCOC(c(cc1)ccc1S(Nc(cc(cc1)C(O)=O)c1Cl)(=O)=O)=O	-7.3	N	2.3691	7	2	383.807
NCC-00018261	CC(C)(C)c(cc1)ccc1S(N(C)c(cccc1)c1C(OC)=O)(=O)=O	-6.1	N	3.3588	5	0	361.461
NCC-00058419	CCN(c1cc(C(OCC)=O)ccc1)S(c1c(C)ccc(F)c1)(=O)=O	-5.5	N	3.0342	5	0	365.424
NCC-00015351	CN(c(cccc1)c1C(OC)=O)S(c1c(C(F)(F)F)cccc1)(=O)=O	-6.2	N	2.6252	5	0	373.35
NCC-00085735	CCCNC(CN(c1cc(Cl)cc(Cl)c1)S(c1ccccc1)(=O)=O)=O	-5.8	N	3.0203	5	1	401.313
NCC-00017670	CC(Nc1cccc(NS(c(cc2)c(C(F)(F)F)cc2Cl)(=O)=O)c1)=O	-9	Y	3.1167	5	2	392.784
NCC-00036701	Cc(cc1)ccc1S(Nc(cc1)ccc1C(NCC(OC)=O)=O)(=O)=O	-9	Y	1.2993	7	2	362.405

NCC-00016732	COc1cccc(N(CCC#N)S(c2cc(C(O)=O)ccc2)(=O)=O)c1	-6.2	N	1.3853	7	1	360.389
NCC-00028719	COc(cc1C(O)=O)cc(OC)c1NS(c(cc1)ccc1C#N)(=O)=O	-6.8	N	1.1394	8	2	362.361
NCC-00010004	CCOC(NCCc(cc1)ccc1S(N(C)c1ccccc1)(=O)=O)=O	-7	N	2.3166	6	1	362.449
NCC-00034796	CCN(c1ccccc1)S(c(cc(CNC(C)=O)cc1)c1OC)(=O)=O	-6	N	1.6133	6	1	362.449
NCC-00061185	CC(C)(C)c(cc1)ccc1S(NCCC(Nc1n[n](C)cc1)=O)(=O)=O	-7.3	N	2.0274	7	2	364.469
NCC-00083244	CCNC(NC(C(C)N(c1ncc[s]1)S(c1ccccc1)(=O)=O)=O)=O	-5.6	N	1.1242	8	2	382.464
NCC-00057551	CC(c1c(C)nc(C)[s]1)NC(CCNS(c1ccccc1)(=O)=O)=O	-7	N	1.682	6	2	367.493
NCC-00051283	CN(CC(NCc1cc(OC)ncc1)=O)S(c1ccccc1)(=O)=O	-6.8	N	0.6605	7	1	349.41
NCC-00042963	Cc(cc(cc1)OC)c1S(Nc(cc(C(O)=O)c(F)c1)c1F)(=O)=O	-8.5	Y	1.9193	6	2	357.332
NCC-00081793	CC(C)OCC(N(c(cc1)ccc1O)S(c1ccccc1)(=O)=O)=O	-5.8	N	1.8417	6	1	349.406
NCC-00014547	CC(c(cc(c(OC)c1)OC)c1NS(c1ccc(C)cc1)(=O)=O)O	-6.1	N	1.852	6	2	351.422
NCC-00028891	Cc(cc1)cc(C(O)=O)c1NS(c(cc1C)c(C)cc1OC)(=O)=O	-8.3	Y	2.4055	6	2	349.406
NCC-00035502	CCOC(COc1cccc(NS(c2cccc(Cl)c2)(=O)=O)c1)=O	-7.7	Y	2.4589	6	1	369.824
NCC-00045734	CCOC(c(cc(cc1)NS(c(ccc(C)c2)c2Cl)(=O)=O)c1Cl)=O	-8.3	Y	3.8339	5	1	388.27
NCC-00010223	CCOC(CC(c1ccc(C)cc1)NS(c1ccccc1)(=O)=O)=O	-5.6	N	2.846	5	1	347.434
NCC-00004656	CC(C)c(cc1)ccc1N(CC(O)=O)S(c1ccc(C)cc1)(=O)=O	-6.1	N	2.5248	5	1	347.434
NCC-00019815	Cc1cc(Cl)c(C)c(S(N(C)c(cccc2)c2C(N)=O)(=O)=O)c1Cl	-6.2	N	2.851	5	1	387.286
NCC-00031295	CCC(C)c(cc1)ccc1S(N(C)c(cccc1)c1C(N)=O)(=O)=O	-6.4	N	2.5926	5	1	346.45

NCC-00013861	CCNC(CN(c1c(C)c(C)ccc1)S(c1ccccc1)(=O)=O)=O	-5.8	N	2.0417	5	1	346.45
NCC-00067030	COc(ccc(N(CC(N)=O)S(c1ccccc1)(=O)=O)c1)c1OC	-5.8	N	0.4561	7	1	350.394
NCC-00032691	COC(c(cc(cc1)S(Nc(cccc2)c2C(N)=O)(=O)=O)c1O)=O	-8.3	Y	0.6133	8	3	350.35
NCC-00061494	COC(c(c(F)c1)cc(NS(c(cccc2)c2C#N)(=O)=O)c1F)=O	-7.6	N	1.9089	6	1	352.316
NCC-00006323	CC(Nc(cc1)ccc1NS(c(cc(c(OC)c1)Cl)c1Cl)(=O)=O)=O	-7.3	Y	2.8044	6	2	389.258
NCC-00036036	CCOCC(Nc1cccc(S(Nc(cc2)ccc2Cl)(=O)=O)c1)=O	-8.3	Y	2.1759	6	2	368.84
NCC-00008033	CCOc(ccc(S(Nc1c(C)c(F)ccc1)(=O)=O)c1)c1C(N)=O	-6.9	N	1.827	6	2	352.385
NCC-00028066	CC(Nc(ccc(S(Nc(cc(C)cc1)c1F)(=O)=O)c1)c1OC)=O	-7.2	N	2.0371	6	2	352.385
NCC-00035574	NC(c(cccc1)c1NS(c(cc1)cc(Cl)c1OC(F)F)(=O)=O)=O	-9.5	Y	1.8214	6	2	376.766
NCC-00043341	CNC(NC(CCN(c1ncc[s]1)S(c1ccccc1)(=O)=O)=O)=O	-6.1	N	0.813	8	2	368.437
NCC-00039377	C[n]1c(C(CN(CC2)CCN2S(c2ccccc2)(=O)=O)=O)ccc1	-6.5	N	0.681	6	0	347.438
NCC-00039571	CC(c1ccc[n]1CC1)N1C(CN(C)S(c1ccccc1)(=O)=O)=O	-6.3	N	1.8843	6	0	347.438
NCC-00000412	Cc(cc1)ccc1S(Nc(cc1N2C)c(C)cc1N(C)C2=O)(=O)=O	-6.8	N	2.2548	6	1	345.422
NCC-00039787	CC(c1cccc(S(Nc2cc(-c3n[nH]cc3)ccc2)(=O)=O)c1)=O	-10.3	Y	1.4737	6	2	341.39
NCC-00012197	COc(cc1)ccc1NS(c(cc1)cc2c1N=CNS2(=O)=O)(=O)=O	-9.1	Y	0.4095	8	2	367.405
NCC-00052401	CC(C)c1nc(CN(c2ncc[s]2)S(c2ccccc2)(=O)=O)c[s]1	-5.6	N	2.9784	5	0	379.528
NCC-00019271	O=S(c(cc(C(F)(F)F)cc1)c1Cl)(Nc(cc1)cc2c1[nH]nc2)=O	-10	Y	2.6235	5	2	375.757
NCC-00011863	CCc(cccc1C)c1NS(c(cc1)ccc1-[n]1nccc1)(=O)=O	-6.8	N	2.2309	5	1	341.434

NCC-00010565	CC(C)c(cc1)ccc1S(NCCc1ncc2[n]1cccc2)(=O)=O	-8.8	Y	2.8079	5	1	343.45
NCC-00001900	Cc(cc(c(OC1)c2)NC1=O)c2S(Nc1cc(C#N)ccc1)(=O)=O	-8.4	Y	1.0005	7	2	343.362
NCC-00050241	Oc(cc1)ncc1C(N(CC1)CCN1S(c1ccccc1)(=O)=O)=O	-7.3	N	1.3171	7	1	347.394
NCC-00003009	CCc(cc1)ccc1NS(c(cc1)cc(nc2O)c1nc2O)(=O)=O	-10	Y	2.1672	7	3	345.378
NCC-00028714	Cc(cc1C)cc(C(O)=O)c1NS(c1c2nsnc2ccc1)(=O)=O	-6.6	N	2.6482	7	2	363.417
NCC-00005265	CCN(c(cccc1)c1C(O)=O)S(c1c2nsnc2ccc1)(=O)=O	-6.3	N	2.2719	7	1	363.417
NCC-00069148	C[n]1c(SCC(N(CC2)CN2S(c2ccccc2)(=O)=O)=O)nnc1	-6.9	N	0.8025	8	0	367.453
NCC-00010250	Cc1cc(-[n]2nnnc2)cc(C)c1S(N(C)c1ccccc1)(=O)=O	-6.6	N	1.4503	7	0	343.41
NCC-00004448	Cc(cc1)ccc1S(Nc1c(CN[n]2cnnc2)cccc1)(=O)=O	-7.7	N	1.2322	7	2	343.41
NCC-00010973	CC(C)c1cc(S(N(CC2)c3c2cccc3)(=O)=O)c(C)cc1OC	-6.3	N	3.7371	4	0	345.462
NCC-00026743	Cc(cc1)c(C)cc1S(N(Cc1ccc[o]1)c1ccccc1)(=O)=O	-6.4	N	3.1585	4	0	341.43
NCC-00066275	CN(CCOc(cc1)ccc1F)S(c1cc(CCC2)c2cc1)(=O)=O	-8	Y	3.2188	4	0	349.425
NCC-00048050	Oc(cc1)ccc1N(C(c1ccc[o]1)=O)S(c1ccccc1)(=O)=O	-6.6	Y	2.2074	6	1	343.358
NCC-00028269	Cc(cc1C(O)=O)cc(S(N(CCC2)c3c2cccc3)(=O)=O)c1O	-6.7	N	2.1015	6	2	347.39
NCC-00066548	COC(c(cc(cc1)NS(c(cc2)cc3c2OCC3)(=O)=O)c1Cl)=O	-7.8	N	2.7035	6	1	367.808
NCC-00035237	O=S(c(cc1)cc(C(F)(F)F)c1Cl)(N1c(cccc2)c2SCC1)=O	-6.4	N	3.1052	3	0	393.836
NCC-00029704	CC(C)(C=C(C)c1c2ccc(C)c1)N2S(c(cc1)ccc1F)(=O)=O	-6.6	N	3.6	3	0	345.437
NCC-00028853	OC(c(c(F)ccc1)c1NS(c1cc(CCCC2)c2cc1)(=O)=O)=O	-7.9	N	2.7014	5	2	349.381

NCC-00058431	COC(c1cccc2c1CCCN2S(c(cccc1)c1Cl)(=O)=O)=O	-6.9	N	3.1372	5	0	365.836
NCC-00009996	CCOc(cc1)c(C)cc1S([n]1c(cc(C)c(C)c2)c2nc1)(=O)=O	-9	Y	2.8784	5	0	344.434
NCC-00012284	Cc1n[o]c(-c2cc(S(Nc3cc(C)ccc3)(=O)=O)c(C)cc2)c1	-8	N	3.2049	5	1	342.418
NCC-00064758	Cc1n[o]c(CN(c2c(C)cccc2)S(c2ccccc2)(=O)=O)c1	-6	N	2.4881	5	0	342.418
NCC-00004666	CCC(N(CC1)C(c2ccccc2)N1S(c1ccccc1)(=O)=O)=O	-5.4	N	2.6142	5	0	344.434
NCC-00000443	Cc1ncc(-c(cc2)ccc2S(N(C)c2cc(C)ccc2)(=O)=O)[o]1	-7.2	N	2.7638	5	0	342.418
NCC-00012877	CCCCN(c(cccc1)c1S(N1c(cc2)ccc2Cl)(=O)=O)C1=O	-6.3	N	4.0433	5	0	364.852
NCC-00002045	Cc(cc1)ccc1S(N(C)c(cc1)cc2c1[s]c(C(N)=O)c2)(=O)=O	-7.9	Y	2.2163	5	1	360.457
NCC-00000405	Cc1ncc(-c2cc(S(Nc(cccc3)c3Cl)(=O)=O)c(C)cc2)[o]1	-8.7	N	3.4646	5	1	362.836
NCC-00015365	Oc1nc(ccc(S(Nc(cc2)ccc2OC(F)F)(=O)=O)c2)c2[o]1	-10.1	Y	2.1637	7	2	356.304
NCC-00012910	CN(c(cccc1)c1S(N1c2cc(OC)cc(OC)c2)(=O)=O)C1=O	-6.4	N	1.9822	7	0	348.378
NCC-00033173	O=C(C(CCC1)N1S(c1ccccc1)(=O)=O)NC(CC1)CS1(=O)=O	-6.6	N	-0.1098	7	1	372.465
NCC-00014330	CN(c(ccc(S(Nc(cc1)ccc1C(O)=O)(=O)=O)c1)c1O1)C1=O	-9.3	N	1.2441	8	2	348.334
NCC-00027686	Cc(cc1)ccc1S(N(Cc1ccc[n]1C)c1ccccc1)(=O)=O	-6	N	2.5352	4	0	340.446
NCC-00042066	COC(c1ccc[n]1C(CC1)CCN1S(c1ccccc1)(=O)=O)=O	-8.5	Y	2.1401	6	0	348.422
NCC-00011724	Cc(cc1N(C)CCOc1c1)c1S(Nc1cc(OC)ccc1)(=O)=O	-7	Y	2.0194	6	1	348.422
NCC-00015698	O=C(CCc1ccc[o]1)N(CC1)CCN1S(c1ccccc1)(=O)=O	-7.5	N	1.9535	6	0	348.422
NCC-00016393	COC(Nc(cc1)ccc1S(Nc1cc(CCC2)c2cc1)(=O)=O)=O	-8.2	Y	2.6804	6	2	346.406

NCC-00053294	O=C(C1COCC1)Nc(cccc1)c1NS(c1ccccc1)(=O)=O	-6.3	N	1.5005	6	2	346.406
NCC-00058081	OC(c(cc1)ccc1NS(c(c1c2nccc1)ccc2F)(=O)=O)=O	-8.6	Y	1.8606	6	2	346.337
NCC-00012466	COc1cc(NS(c(cc2)cc3c2SCCN3)(=O)=O)cc(OC)c1	-7.1	Y	0.8689	6	2	366.461
NCC-00001724	COc(ccc(NS(c(cc1)cc(cc2)c1nc2O)(=O)=O)c1)c1Cl	-9.5	Y	2.8164	6	2	364.808
NCC-00084666	COc1ccnc(N(CC2)CCC2NS(c2ccccc2)(=O)=O)n1	-9.2	Y	1.869	7	1	348.426
NCC-00031708	CN(CC(Nc1cccc2c[nH]nc12)=O)S(c1ccccc1)(=O)=O	-8.5	Y	0.8811	7	2	344.394
NCC-00002852	CN(c(ccc(NS(c1cc(C#N)ccc1)(=O)=O)c1)c1N1C)C1=O	-9.2	Y	1.4026	7	1	342.378
NCC-00000858	CNC(Nc(cc1)cc2c1[s]c(NS(c1ccccc1)(=O)=O)n2)=O	-7.2	N	2.1938	7	3	362.433
NCC-00057040	CC(Nc1cccc(NS(c2c3nsnc3ccc2)(=O)=O)c1C)=O	-8.9	Y	2.5229	7	2	362.433
NCC-00034591	C[n]1c(Sc(cccc2)c2NS(c(cccc2)c2Cl)(=O)=O)nnc1	-6	N	2.5306	6	1	380.879
NCC-00041714	N#Cc1c(N(CC2)CCC2NS(c2ccccc2)(=O)=O)[s]nc1Cl	-7.5	Y	2.7856	6	1	382.895
NCC-00036968	Cc(cc1C)cc(C)c1S(Nc(cccc1)c1-[n]1nncc1)(=O)=O	-6.8	N	1.8048	6	1	342.422
NCC-00061123	CC(C)c(cc1)ccc1S(Nc1cnc2[n](C)nc(C)c2c1)(=O)=O	-7.7	N	2.2048	6	1	344.438
NCC-00035970	O=S(c(cc(cc1)Br)c1Br)(Nc(cc1)ccc1Sc1n[nH]cn1)=O	-8.1	Y	3.2422	6	2	490.199
NCC-00072678	Cc(c1c2)n[n](C)c1ncc2S(Nc1cc(C(O)=O)ccc1)(=O)=O	-7.8	N	0.5029	8	2	346.366
NCC-00032931	Cc(cc(c(OC)c1)NS(c2c3nsnc3ccc2)(=O)=O)c1Cl	-7.5	N	3.3552	6	1	369.852
NCC-00005959	Cc(cc(cc1)S(Nc(cc2[nH]c(O)nc2c2)c2Br)(=O)=O)c1F	-7.9	Y	2.752	6	3	400.227
NCC-00006542	Cc1cc(C)n[n]1C(C(CCC1)N1S(c1ccccc1)(=O)=O)=O	-5.9	N	1.4188	6	0	333.411

NCC-00038541	OC(CN(CC1)CCN1S(c1ccccc1)(=O)=O)c1ccc[nH]1	-7.5	Y	0.3664	6	2	335.427
NCC-00074435	C[n]1c(C(N(CC2)CCN2S(c2ccccc2)(=O)=O)=O)ccc1	-6.3	N	1.2216	6	0	333.411
NCC-00034993	Nc1nc(-c(cc2)ccc2NS(c(cc2)ccc2Cl)(=O)=O)c[s]1	-9.3	Y	3.2629	5	2	365.864
NCC-00076576	Nc([n](cc1-c2ccccc2)S(c2ccccc2)(=O)=O)c1C#N	-8	Y	1.8022	5	1	323.375
NCC-00011922	Cc(cc1)ccc1N(C)S(c(cc1)ccc1-[n]1nccc1)(=O)=O	-7.6	Y	1.3766	5	0	327.407
NCC-00056677	N#CCCN(c1nc(cccc2)c2[s]1)S(c1ccccc1)(=O)=O	-5.9	N	2.7726	5	0	343.43
NCC-00017997	OC(c(cc1)cc(NS(c2c3nsnc3ccc2)(=O)=O)c1F)=O	-8.8	Y	2.0612	7	2	353.354
NCC-00084896	COC(c1cccc(NS(c2c3nsnc3ccc2)(=O)=O)c1)=O	-7.5	Y	2.3883	7	1	349.39
NCC-00008934	O=C(CSc1c[nH]nn1)N(CC1)CN1S(c1ccccc1)(=O)=O	-8	N	0.2943	8	1	353.426
NCC-00013911	CCC(c(c1c2cccc1)c[n]2S(c1ccc(C)cc1)(=O)=O)=O	-6.5	Y	2.6197	4	0	327.403
NCC-00016407	Cc(cc1C)cc(C)c1S(N(CCCc1ccc2)c1c2O)(=O)=O	-6.1	N	3.3042	4	1	331.435
NCC-00052847	Cc(ccc(S(Nc(cc1)cc2c1OCC2)(=O)=O)c1)c1C(O)=O	-10	Y	2.0135	6	2	333.363
NCC-00004558	Cc(cc1OCOc1c1)c1NS(c(cc(cc1)F)c1OC)(=O)=O	-7.8	N	2.4448	6	1	339.342
NCC-00012766	COc(cc1)cc(OC)c1N(S(c1c2cccc1)(=O)=O)S2(=O)=O	-6	N	1.6036	7	0	355.39
NCC-00002489	CC(CC1(C)C)c(cccc2)c2N1S(c1ccc(C)cc1)(=O)=O	6.5	N	4.2638	3	0	329.463
NCC-00012907	CC(C)NC(c(cc1)cc(-c2c3cccc2)c1N(C)S3(=O)=O)=O	-6.3	N	2.5057	5	1	330.407
NCC-00003792	Cc(cc1)ccc1S(N(CC1)c(cc2)c1cc2C(NC)=O)(=O)=O	-9	Y	2.0589	5	1	330.407
NCC-00003758	CC(C)c(cc1)cc(-c2c3cccc2)c1N(CC(N)=O)S3(=O)=O	-6.9	N	2.2205	5	1	330.407

NCC-00068896	CCOc(cc1)ccc1S(Nc(cc1)cc2c1[nH]c(C)c2)(=O)=O	-7.4	N	2.7323	5	2	330.407
NCC-00013609	CCOc(cc1)ccc1S(Nc1cc(cccc2)c2nc1)(=O)=O	-7.8	N	2.611	5	1	328.391
NCC-00064373	CC(c1cccc(S(Nc2cccc3c2nccc3)(=O)=O)c1)=O	-9.9	Y	2.1459	5	1	326.375
NCC-00005559	Cc1cccc(NS(c(c2c3cccc2)ccc3OC)(=O)=O)n1	-8.1	Y	2.8315	5	1	328.391
NCC-00010607	CCOc(cc(cc1)S([n]2c(cccc3)c3nc2C)(=O)=O)c1F	-6.6	N	2.1809	5	0	334.37
NCC-00003739	CN(C)C(CN(c(ccc(Br)c1)c1-c1c2cccc1)S2(=O)=O)=O	-6.4	N	2.3767	5	0	395.276
NCC-00017603	NC(c(cc1)ccc1S(Nc(cc1OCOc1c1)c1Cl)(=O)=O)=O	-8.6	Y	1.7634	7	2	354.769
NCC-00031416	N#Cc(cc1)ccc1S(N(CCC1)c(cc2F)c1cc2F)(=O)=O	-9	Y	2.6554	4	0	334.345
NCC-00047070	O=S(c1ccccc1)(N(Cc(cccc1)c1F)c1ncc[s]1)=O	-5.8	N	3.0081	4	0	348.421
NCC-00007674	CC1Sc(ccc(S(Nc(cc2)c(C)cc2Cl)(=O)=O)c2)c2NC1	8.5	Y	2.6309	4	2	368.908
NCC-00032222	N#Cc(cc(cc1)NS(c2cc(CCCC3)c3cc2)(=O)=O)c1Cl	-8.2	N	3.5571	4	1	346.837
NCC-00031237	OCCN(c1ccccc1)S(c(cc1)cc(C2)c1NC2=O)(=O)=O	-8.4	Y	0.4528	6	2	332.379
NCC-00037216	COC(N(CC1)CCC1NS(c1cc(CCC2)c2cc1)(=O)=O)=O	-8.9	Y	2.3608	6	1	338.427
NCC-00017417	NC(C(C1)Oc(cccc2)c2N1S(c1cccc(Cl)c1)(=O)=O)=O	-6.7	N	1.2858	6	1	352.797
NCC-00040694	Cc(cc1)cc(S(Nc(cc2)ccc2-[n]2ncnc2)(=O)=O)c1O	-9.3	Y	1.002	7	2	330.367
NCC-00067461	C[n]1c(SC(CCCC2)C2NS(c2ccccc2)(=O)=O)nnc1	-6.1	N	2.1978	6	1	352.482
NCC-00010582	O=S(c1ccccc1)(NC1=NCN(CCc2ccc[s]2)CN1)=O	-8.2	Y	2.4491	6	2	350.466
NCC-00071748	Cc1nc(O)nc(O)c1S(Nc1cc(cccc2)c2nc1)(=O)=O	-8.7	Y	1.1389	8	3	332.339

NCC-00016415	COC(Nc(cc1)ccc1S([n]1nnc2c1cccc2)(=O)=O)=O	-9.9	Y	1.2521	8	1	332.339
NCC-00063919	Oc(nccc1)c1-c1nnc(CNS(c2ccccc2)(=O)=O)[o]1	-8.7	Y	0.9225	8	2	332.339
NCC-00067449	CC(NC(C1(C(F)(F)F)NS(c2ccccc2)(=O)=O)=O)=C1C#N	-6.1	N	0.9947	6	2	345.3
NCC-00028366	Cc(cc1C(O)=O)cc(S(Nc(cc2)cc(Cl)c2F)(=O)=O)c1O	-7	N	2.1488	6	3	359.76
NCC-00047277	CCc1cccc(NS(c(cc(C)cc2C(O)=O)c2O)(=O)=O)c1	-8.6	Y	2.2015	6	3	335.379
NCC-00049398	Cc(ccc(C(O)=O)c1)c1S(Nc1c(C)c(O)c(C)cc1)(=O)=O	-8.1	Y	2.1298	6	3	335.379
NCC-00028283	Cc(cc1C(O)=O)cc(S(N(C)c(cc2)ccc2F)(=O)=O)c1O	-8.3	Y	1.448	6	2	339.342
NCC-00009637	CCOc(cc1)ccc1S(Nc(cc1)cc(O)c1C(O)=O)(=O)=O	-6.6	N	1.4344	7	3	337.351
NCC-00035119	CCOC(c(cccc1)c1NS(c(cc1)cc(Cl)c1F)(=O)=O)=O	-9	Y	2.9848	5	1	357.788
NCC-00034887	CC(c(cc1)ccc1S(Nc(cccc1)c1OC(F)F)(=O)=O)=O	-8.8	Y	1.9993	5	1	341.333
NCC-00032902	Cc(cc1)cc(Cl)c1S(N(C)c(cccc1)c1C(OC)=O)(=O)=O	-5.5	N	2.7268	5	0	353.825
NCC-00010274	Cc1cccc(C)c1NS(c(c(OC)c1)cc(OC)c1Cl)(=O)=O	-5.7	N	3.1125	5	1	355.841
NCC-00028452	CCOc(ccc(Br)c1)c1S(Nc(cc1)cc(C#N)c1Cl)(=O)=O	-6.5	N	3.4618	5	1	415.694
NCC-00040612	CCc1ccc(CNC([C@H](C)NS(c2ccccc2)(=O)=O)=O)[s]1	-6.7	N	2.3544	5	2	352.478
NCC-00066181	O=C1N(CCNS(c2ccccc2)(=O)=O)C=CC=C1C(F)(F)F	-9.4	Y	1.4332	5	1	346.328
NCC-00042597	Cc(ccc(S(Nc(cccc1)c1C(N)=O)(=O)=O)c1)c1C(O)=O	-10.4	Y	0.875	7	3	334.351
NCC-00015128	Cc(ccc(C(OC)=O)c1)c1NS(c(cc1)ccc1C#N)(=O)=O	-7.4	N	2.0512	6	1	330.363
NCC-00075567	CC(c1nc(C)n[o]1)NS(c1ccc(C(C)(C)C)cc1)(=O)=O	-7.7	Y	2.4812	6	1	323.416

NCC-00071697	Cc1nc(O)nc(O)c1S(Nc1cc(C(O)=O)ccc1)(=O)=O	-9.2	Y	-0.0328	9	4	325.3
NCC-00064347	CNC(c(cc1)ccc1S(Nc(cc1)cnc1OC)(=O)=O)=O	-9	Y	0.678	7	2	321.356
NCC-00019985	CCN(c1c(C)ccc(O)c1)S(c1cccc(Cl)c1Cl)(=O)=O	-5.8	N	3.4804	4	1	360.26
NCC-00008134	COc(cccc1)c1NS(c(cc1)cc(C(O)=O)c1O)(=O)=O	-5.9	N	1.0281	7	3	323.324
NCC-00008085	CCc(cc1)ccc1N(CC(O)=O)S(c1ccccc1)(=O)=O	-6	Y	1.7534	5	1	319.38
NCC-00006219	Cc(c(N(CC(O)=O)S(c1ccccc1)(=O)=O)ccc1)c1Cl	-6.2	N	1.9438	5	1	339.798
NCC-00033917	Cc1cccc(C(OC)=O)c1NS(c1cc(F)ccc1)(=O)=O	-6.1	N	2.3164	5	1	323.343
NCC-00030427	COC(c(cccc1)c1S(Nc(cc1)cnc1OC)(=O)=O)=O	-6.8	N	1.1522	7	1	322.34
NCC-00066285	NC(COC(C(CCCC1)N1S(c1ccccc1)(=O)=O)=O)=O	-5.8	N	0.0749	7	1	326.372
NCC-00032329	CCN(c(cc1)ccc1F)S(c(cc(cc1)Cl)c1C#N)(=O)=O	-6.2	N	2.8126	4	0	338.789
NCC-00000076	O=S(c1ccccc1)([n]1c(ccc(Br)c2)c2c2c1CCC2)=O	-6.4	N	3.5442	3	0	376.273
NCC-00005064	Cc1nc(cc(cc2)NS(c(cc3)ccc3OC)(=O)=O)c2[nH]1	-9.5	Y	1.7217	6	2	317.368
NCC-00013424	Cc(cc1)ccc1-c(cc1N)n[n]1S(c1ccccc1)(=O)=O	-8.8	Y	2.0284	5	1	313.38
NCC-00030133	Cc(cc1)c(C)cc1S(Nc1ncnc2c1cccc2)(=O)=O	-8.3	N	2.7516	5	1	313.38
NCC-00060385	C[n](cc1)nc1NS(c(cc1)cc(nc2O)c1nc2O)(=O)=O	-9	Y	-0.1786	9	3	321.316
NCC-00014662	CC(C)c(cc1)ccc1S(N1c(cccc2)c2SCC1)(=O)=O	-6.6	N	2.8379	3	0	333.475
NCC-00065740	OC(C(Cc1c(C2)cccc1)N2S(c1ccccc1)(=O)=O)=O	-6	N	1.2957	5	1	317.364
NCC-00003322	Cc([n](C)nc1-[n]2cnnc2)c1NS(c1ccccc1)(=O)=O	-6.3	N	1.0912	8	1	318.36

NCC-00004956	O=C1Nc(cc(cc2)S(Nc(cccc3)c3Cl)(=O)=O)c2SC1	-6.8	N	1.0487	5	2	354.837
NCC-00069176	O=C(c1ccccc1)N(CC1)CN1S(c1ccccc1)(=O)=O	-8.5	Y	2.4449	5	0	316.38
NCC-00080041	O=S(c1ccccc1)(N(CC1OCCCC1)c1ncc[s]1)=O	-6.1	N	2.131	5	0	338.451
NCC-00012827	Cc(ccc(Cl)c1)c1N(C(N(C)c1c2cccc1)=O)S2(=O)=O	-6.3	N	3.0721	5	0	336.798
NCC-00012455	Cc(cc1)ccc1N(C)S(c(cc1)cc2c1SCCN2)(=O)=O	-7.7	Y	1.258	4	1	334.463
NCC-00031283	N#Cc(cccc1)c1S(N(CCCc1ccc2)c1c2F)(=O)=O	-6.6	N	2.5546	4	0	316.355
NCC-00018467	Cc(cc1)ccc1S(Nc1cc(-c2ncc[s]2)ccc1)(=O)=O	-7.1	N	2.9577	4	1	330.431
NCC-00049432	OC(c1cccc(S(Nc2c(cc[nH]3)c3ccc2)(=O)=O)c1)=O	-9.4	Y	1.4832	6	3	316.336
NCC-00035093	O=S(c1ccccc1)(Nc(cc1)nnc1N1CCOCC1)=O	-8.9	Y	0.5007	7	1	320.372
NCC-00081951	CC[n]1ncc(NS(c2cccc3c2ncc(C)c3)(=O)=O)c1	-8.2	N	0.9369	6	1	316.384
NCC-00072739	CC(c1nnc2[n]1CCCCC2)NS(c1ccccc1)(=O)=O	-9.2	Y	2.0687	6	1	320.416
NCC-00066196	O=S(c1ccccc1)(N(CC[n]1nccc1)c1ncc[s]1)=O	-5.6	N	0.8962	6	0	334.423
NCC-00034949	OC(c1cccc(NS(c(cc2)cc3c2[nH]nn3)(=O)=O)c1)=O	-10.7	Y	0.4224	8	3	318.312
NCC-00008015	O=S(c(cc1)cc(Cl)c1F)(Nc1c2nc[nH]c2ccc1)=O	-9.4	Y	2.2651	5	2	325.75
NCC-00001757	Cc1c[s]c2nc(CCNS(c3ccccc3)(=O)=O)c[n]12	-7.1	N	2.1583	5	1	321.424
NCC-00004474	CC(N(C1)S(c2ccccc2)(=O)=O)OC1c1ccccc1	-8.5	Y	2.7029	4	0	303.381
NCC-00052244	CN(Cc([s]1)ccc1Cl)S(c1cc(CCC2)c2cc1)(=O)=O	-8.4	Y	3.7884	3	0	341.882
NCC-00035122	CC(Cc1c2cccc1)N2S(c(cc1)cc(Cl)c1Cl)(=O)=O	-9.3	Y	3.8129	3	0	342.245

NCC-00006085	Cc1cc(Cl)c(C)cc1S(N(CC1)c2c1cccc2)(=O)=O	-9.1	Y	3.57	3	0	321.827
NCC-00012818	Cc(cc(cc1)N(S(c2c3cccc2)(=O)=O)S3(=O)=O)c1Br	-6.6	N	2.8127	5	0	388.261
NCC-00002425	Cc(cc1)ccc1S(N(c(ccc(Cl)c1)c1O1)C1=O)(=O)=O	-9.4	Y	2.9926	5	0	323.755
NCC-00012765	Cc1cc(N(C(Nc2c3cccc2)=O)S3(=O)=O)c(C)cc1	-6.3	N	2.4517	5	1	302.353
NCC-00012809	CCc(cc1)ccc1N(C(Nc1c2cccc1)=O)S2(=O)=O	-7.2	N	2.5234	5	1	302.353
NCC-00012812	Cc(ccc(N(C(Nc1c2cccc1)=O)S2(=O)=O)c1)c1F	-6.4	N	2.2086	5	1	306.316
NCC-00002439	CCc(cc1)ccc1S([n]1c(cccc2)c2nc1C)(=O)=O	-8.4	Y	2.5033	4	0	300.381
NCC-00026792	[O-]C(c(cc1)cc(S(Nc(cc2)ccc2Br)(=O)=O)c1Cl)=O	-6.9	N	0.699	5	1	389.633
NCC-00090509	CNc1cc(NS(c(cc2)ccc2N)(=O)=O)nc(NC)n1	-10	Y	0.0845	8	4	308.365
NCC-00048274	COc(nccc1)c1NS(c1cc(C(O)=O)ccc1)(=O)=O	-8.4	Y	0.7243	7	2	308.313
NCC-00048192	Cc(ccc(S(Nc(cncc1)c1O)(=O)=O)c1)c1C(O)=O	-8.7	Y	0.2707	7	3	308.313
NCC-00010149	Cc1nc(N(C)S(c2ccccc2)(=O)=O)nc(OC)c1	-7.2	N	1.3495	6	0	293.346
NCC-00065032	Cc(ccc(S(Nc1cnccc1)(=O)=O)c1)c1C(N)=O	-9.2	Y	0.389	6	2	291.33
NCC-00014519	OC(CN(Cc1ccc[o]1)S(c1ccccc1)(=O)=O)=O	-6.9	N	0.615	6	1	295.314
NCC-00073156	CCC(CN(c1ncc[s]1)S(c1ccccc1)(=O)=O)=O	-6.4	N	1.7513	5	0	310.397
NCC-00043285	Cc(cc(cc1)S(Nc(cc2)ncc2Cl)(=O)=O)c1OC	-9.1	Y	2.1891	5	1	312.776
NCC-00065029	Cc(c1c2)n[o]c1ncc2S(Nc1cnccc1)(=O)=O	-9	Y	0.3649	7	1	290.302
NCC-00057119	O=S(c1ccccc1)(NCc1c[n](cc[s]2)c2n1)=O	-8.3	Y	1.3303	5	1	293.37

NCC-00069237	O=S(c1ccccc1)(N(CCC1)c2c1cccc2)=O	-7.2	N	2.6182	3	0	273.355
NCC-00082450	NC(CN(c1ncc[s]1)S(c1ccccc1)(=O)=O)=O	-6.3	N	0.2214	6	1	297.358
NCC-00000118	Cc(cc1)ccc1S(Nc(cc1)ccc1OC)(=O)=O	-8.7<NL>	Y	2.2326	4	1	277.343
Hanaoka compound 5	OC(c1cccc(NS(c2ccccc2)(=O)=O)c1)=O	-8.7	Y	1.4438	5	2	277.299
NCC-00013925	Nc(cc1O)n[n]1S(c1ccccc1)(=O)=O	-7.7	N	-0.06	6	2	239.254